The Faculty of Health and Medical Sciences, School and Discipline of Medicine
The University of Adelaide
South Australia, Australia

Aus der Medizinischen Universitätsklinik, Abteilung Innere Medizin I
(Hämatologie, Onkologie und Stammzelltransplantation)
der Albert-Ludwigs-Universität Freiburg Im Breisgau
Freiburg Im Breisgau, Deutschland

The Combined Treatment Efficacy of Anti-CD123 CAR T cells with Azacitidine for the Treatment of Acute Myeloid Leukaemia.

A thesis submitted to the University of Adelaide and Albert-Ludwigs-Universität in fulfilment for the JOINTLY AWARDED DEGREE of

DOCTOR OF PHILOSOPHY in MEDICINE

Nadia El Khawanky
February 2021
Born (Geboren) in Sydney, Australia

For my dearest uncle,

James Chen...

~

For the one who will always have my heart,

Joel McLennon...

~

We are only falling stars,
Fleeting sparks that arc
Across the vast forever of time
Through others' nights,
Only to return as dust to our maker.

And the most we can hope,
In our one brief moment,
Is to brighten their night,
Lead them on their way,
Or just perhaps to grant their wish.

~

Declaration

I, Nadia El Khawanky, certify that this work contains no material which has been accepted for the award of any other degree or diploma in my name, in any university or other tertiary institution and, to the best of my knowledge and belief, contains no material previously published or written by another person, except where due reference has been made in the text.

In addition, I certify that no part of this work will, in the future, be used in a submission in my name, for any other degree or diploma in any university or other tertiary institution without the prior approval of the University of Adelaide and where applicable, any partner institution responsible for the joint-award of this degree.

I acknowledge that copyright of published works contained within this thesis resides with the copyright holder(s) of those works. I also give permission for the digital version of my thesis to be made available on the web, via the University's digital research repository, the Library Search and also through web search engines, unless permission has been granted by the University to restrict access for a period of time.

I acknowledge the support I have received for my research through the provision of an Australian Government Research Training Program Scholarship, the Beacon Scholarship, and the Betty Hartmann Leukaemia Research Scholarship (Faculty of Health and Medical Sciences, Adelaide).

Nadia El Khawanky

February 2021

Acknowledgements

To my ever-patient supervisors, Prof. Deborah White, Associate Prof. Agnes Yong, Dr. Amy Hughes, and Prof. Dr. Robert Zeiser, thank you. As a naive 23-year-old, I embarked on the most challenging journey of my life. A journey that would surely test my patience, perseverance, and will to overcome all the small and big failures that come with pursuing a career in medical research. Throughout the years, you have all supported, mentored, and guided me through all the pitfalls with this project. You all provided me with encouragement, reassurance, and belief in me as well as celebrating the small achievements when it was necessary. Thank you for all the opportunities you have presented me with, from attending local and international conferences, entrusting me to mentor junior students, and critically reviewing papers for journals. Because of all of you, I have become a scientist for the people and not for the grace or the prestige. Because of all of you, I have become a scientist that realises the gravity of what we do and that the sacrifices we make will one day be rewarded knowing that somewhere in the world someone has more time to live and be with their loved ones. I will continue my career to be the scientist you have moulded me to be, a scientist you won't have regretted teaching. Words will never be able to express my appreciation and gratitude for everything you have done for me.

To the members of the Leukaemia lab (Adelaide) past and present, thank you for all the friendships I have formed over the years. It has been an absolute pleasure getting to know and work with all of you. At SAHMRI, I was known as the crazy lady running up and down the lab trying to fit multiple bits of work into a single day but none of you ever complained. Thank you for all the laughs in the tissue culture, at the student's corner where there was endless supplies of chocolate and cake and afternoons where we'd complain about all things science. It was a short and sweet 18-months with you all but it was the best. To all of AG Zeiser, thank you for all your support, acceptance, and welcoming of a foreign person into your lab and greeting with warmth and smiles from day one. I have never eaten so much cake so frequently in my life but I wouldn't change that at all. Thanks for all the food, laughter, gossips, and support you have given me during my time in the lab. It has been a pleasure to work with all of you and to grow as a scientist from all the expertise and knowledge I have been able to learn from each and every one of you.

To my fellow children in AG Zeiser and my joint caretaker of the children, my meme family, my second family, for someone who came to a foreign land from a land where everything runs the opposite way and life is upside down, you have made it an absolute blast. For someone who was raised an only child, I feel like I will leave the lab with lifelong siblings. Because of all of you, I come to work every day with a smile on my face knowing at some point the whole floor will hear me cackling with laughter (which you know you will all miss when I'm gone). Meemaw/boss ma'am, Melon, Jennybean/Sweetloaf, Schmiddo, and Erica, memes, jokes, and bullying aside, I am forever grateful to have met all of you. These will forever be some of the fondest memories of my youth and in 40 or 50 years-time when I'm basically in the grave and you're all still partying in your forever youths, just remember Meanpie will be smiling down on you all and wreaking havoc from above.

To the other lifelong friends, I have made:

Shimu, my moon, my twin, words can't express how much I love you and am so grateful to have you in my life. Wise beyond your years, I will always appreciate the pep talks you've given me over the years (even though you think I don't listen most of the time). Habibti, you will go on to do amazing things with your life and be a woman totally out of this world and I cannot wait to see all that you achieve. Here's to many years of friendship!

To my Vroni, my precious baby face Riri, where do I even begin with you...there simply are no words…I was an introverted little pup when I first started in the ZTZ, but you welcomed me into your life with the warmest smile and the biggest of hugs. You quickly became one of my best gal pals and now…I couldn't do life without you in it. When I need it, you always give things to me straight…no sparkles..no fluff..and I'm so grateful for that. As much as you don't beat around the bush, you are such an empathetic and loving soul who is always there for her nearest and dearest. In the time I've known you, I have learnt so much about life from you and I know I will continue to learn from you for a lifetime. Thank you for always being the understanding one, my ray of sunshine, the one I can always count on without a fault. You will become one of the most treasured, well respected, and successful doctors I will ever come across.

To a lifelong friendship that will not alter no matter where in the world we are! To my longest and dearest friend Emma, what a rollercoaster of a 13 years it's been! 3 different states and then 2 different continents apart, countless of tears and laughs, many university degrees later (mostly me), I am finally saying goodbye to education and you're getting married! Through all these years, I can't thank you enough for being proud of me. You're always the first one to congratulate me and tell me how happy you are that I chose the career that I have. Even though we've been worlds away from each other for most of our friendship, even when were both extremely pre-occupied with adult life, even when we go months without having a good proper conversation, it feels like no time has passed when we catch up. Thank you for your undying support, your endless encouragement, your faith and unconditional love for our friendship. Without you, I think I would have quit this PhD a long time ago.

To my family..mum, dad, nana, It's been a long 27 years with me. I am far from the perfect daughter and granddaughter. I am also far from being the perfect person. But, I hope I have grown to become a person you are proud of. We may not always agree on a lot of things but I cannot thank you enough for shaping me into the woman I am today. I can't thank you enough for giving me the opportunities to flourish under your wings as well as independently. I can't thank you enough for preparing me for life outside of school, letting me make my mistakes, and teaching me to learn from them. I can't thank you enough for feeling my frustrations with me during this PhD, feeling my pain with me, and expressing your joy when I was happy. No words can ever describe the love, respect, and appreciation I have for the three of you. No matter where I end up in the world, no matter where I am at a given time…home isn't Australia for me…home is wherever you are. Mum, dad, nana…I love you.

To the children, patients, and families that I have met during my community service days…thank you for sharing your stories. Thank you for putting your trust in me. Thank you for having faith in me and placing your hope in scientists like me to do the best we can to find ways to give you a better life. This is for all of you.

List of Publications

1. **El Khawanky N** *et. al.* Demethylating therapy prevents CTLA-4 induction in anti-CD123 CAR T cells directed against acute myeloid leukemia. *Nature Communications (2021)* [Re-submitted]

2. Czech M*, **El Khawanky N*,** Schneider S* *et al.* Lipocalin 2 expression identifies an immune-regulatory neutrophil population during late GvHD**.** *(2021)* [Manuscript under Preparation]

3. Paccielli-Freire P, Marques A.H.C, Crispim Baiocchi G, Schmike L.F, Foncesca D.L.M, Salgado R.C, Filgueiras I.S, da Silva Napoleao S.M, Placa D.R, Akashi K.T, Hirata T.D.C, **El Khawanky N** *et al.* Specific immune-regulatory transcriptional signatures reveal sex and age differences in SARS-Cov-2 infected patients. *JCI Insight (2021)*

4. Filgueiras I.S, De Carvalho A.T, Cunha D.P, Da Fonseca D.L.M, **El Khawanky N** *et al.* Neuroinflammation induced by Zika virus infection and its association with severe outcomes. *PLOS Neglected Tropical Diseases (2021)*

5. Kappas L, Amer R.L, Sommerlatte S, Bashir G, Plattfaut C, Gieseler F, Gemoll T, Busch H, Altahrawi A, Al-Sbiei A, Haneefa S.M, Arafat K, Chimke L.F, **El Khawanky N** *et al.* Ambrisentan, an endothelin receptor type A-selective antagonist, inhibits cancer cell migration, invasion, and metastasis. *Scientific Reports (2020)*

6. Mathew N.R*, Vinnakota J.M*, Apostolova P, Erny D, Hamarsheh S, Andrieux G, Kim J.S, Hanke K, Goldmann T, Chappell-Maor L, **El Khawanky N** *et. al.* Graft-versus-host disease of the CNS is mediated by TNF regulation in microglia. *Journal of Clinical Investigation. (2020)*

7. Akbar N, Khan S.N, Amin M.U, Ishfq M, Cabral-Marques O, Schimke L.F, Iqbal A, Ullah I, Hussain M, Ali I, Khan N, **El Khawanky N** *et. al.* Novel nonsense IL-12Rβ1 mutation associated with recurrent tuberculosis. *Immunologic Research. (2019)*

8. Cabral-Marques O, Schimke L.F, Oliveira Jr E.B, **El Khawanky N,** *et. al.* Flow cytometry contributions for the diagnosis and immunopathological characterization of primary immunodeficiency disease with immune dysregulation. *Frontiers in Immunology. (2019)*

9. Martin S.K, Fitter S, **El Khawanky N,** *et. al.* mTORC1 plays an important role in osteblastic regulation of B-lymphopoiesis. *Scientific Reports. (2018)*

*Joint first co-author

Conference Abstracts

1. **El Khawanky N**, Hughes A, Yu W, Taromi S, Aumann K, Clarson J, Lopez A, Brown M.P, Duyster J, Hughes T.P, White D.L, Yong A.S.M & Zeiser R. Azacitidine sensitizes AML cells for effective elimination by CD123 CAR T cells. *SAIG Department of Hematology and Oncology (Internal Medicine I) Freiburg Conference,* March 2020, Lenzkirch-Saig Baden-Württemberg. Poster Presentation.
2. **El Khawanky N**, Hughes A, Yu W, Taromi S, Aumann K, Clarson J, Lopez A, Brown M.P, Duyster J, Hughes T.P, White D.L, Yong A.S.M & Zeiser R. Azacitidine sensitizes AML cells for effective elimination by CD123 CAR T cells. *American Association of Hematology (ASH) 61st Annual Meeting Exposition.* December 2019. Orlando, FL, The United States of America. Poster Presentation. Blood (2019) 134 (Supplement_1): 3904.
3. **El Khawanky N,** Hughes A, Yu W, Taromi S, Clarson J, Lopez A, Brown M, Hughes T.P, Zeiser R, White D.L & Yong A.S.M. Third generation anti-CD23 CAR T cells for the treatment of relapsed/refractory AML: Pre-clinical evaluation for use as single or combinatorial therapy. *SAIG Department of Hematology and Oncology (Internal Medicine I) Freiburg Conference,* March 2019, Lenzkirch-Saig Baden-Württemberg. Poster Presentation.
4. **El Khawanky N,** Hughes A, Yu W, Clarson J, Lopez A, Brown M, Hughes T.P, White D.L. & Yong A.S.M. Anti-CD123 Chimeric Antigen Receptor (CAR) T cells in chronic and acute myeloid leukemia: Pre-clinical *in vitro* studies. *HAA Annual Scientific Meeting*, October 2017, Sydney NSW. Oral Presentation.
5. **El Khawanky N,** Hughes A, Clarson J, Yu W, White D.L & Yong A.S.M. Anti-CD123 Chimeric Antigen Receptor (CAR) T cells in chronic and acute myeloid leukemia: Pre-clinical *in vitro* studies. *Australian Society for Medical Research Scientific Conference.* June 2017 Adelaide, SA. Oral presentation.
6. **El Khawanky N,** Hughes A, Clarson J, White D.L & Yong A.S.M. Advancing chimeric antigen receptor T cell therapy for myeloid leukemias. *Florey Postgraduate Research Conference in the Faculty of Health Sciences,* September 2016 Adelaide, SA. Poster Presentation
7. **El Khawanky, N,** Hughes A, Clarson J, White D.L & Yong A.S.M. Advancing chimeric antigen receptor T cell therapy for myeloid leukemias. *Australian Society for Medical Research Scientific Conference.* June 2016 Adelaide, SA. Poster Presentation.

Scholarships & Awards

1. **Australian Society for Medical Research Scientific Conference Award for Best Poster Presentation, 2016**

Awarded to the candidate with the best poster and presentation at the conference.

2. **Australian Postgraduate Award/Research Training Program Award, Australian Government, 2016-2019**

Support for the educational and professional development of researchers and other professionals undertaking a PhD and is awarded based on academic merit.

3. **The Betty Hartmann Leukemia Research Supplementary Scholarship, The University of Adelaide, 2016-2019**

One scholarship is awarded per annum to applicants in receipt of a major external scholarship based on merit and research proposal in the field of leukemia research.

4. **The Beacon of Enlightment Scholarship, The University of Adelaide, 2019-2020**

Support for the educational and professional development of researchers and other professionals undertaking a PhD and is awarded based on academic merit.

5. **American Association of Hematology (ASH) Conference Abstract Achievement Award, 2019**

Merit-based awards provided to trainees with the top 100-200 high-scoring annual meeting abstracts of which they are the first or senior author and presenter. These merit awards are intended to support the trainees travel costs to the conference.

TABLE OF CONTENTS

DECLARATION I

ACKNOWLEDGEMENTS II

LIST OF PUBLICATIONS VI

CONFERENCE ABSTRACTS VII

SCHOLARSHIPS & AWARDS VIII

ABSTRACT 1
- English Version 1
- German Version 2

CHAPTER 1

INTRODUCTION 6
- 1.1 From Haematopoietic Stem Cells to Leukaemic Stem Cells 6
- 1.2 Acute Myeloid Leukaemia 9
    - 1.2.1 AML Disease Epidemiology & Pathogenesis 9
    - 1.2.2 AML Risk Stratification/Disease Prognosis 14
    - 1.2.3 Standard Treatment Regimen 15
    - 1.2.4 Molecular Targeted Therapies & Other Approved Agents 16
- 1.3 Mechanisms of Immune Escape in AML 20
- 1.4 Immune Therapies for AML 22
    - 1.4.1 Allogeneic Stem Cell Transplantation (allo-hSCT) 22
    - 1.4.2 Monoclonal Antibody Drug Conjugates 22
    - 1.4.3 Bi-specific T cell Engager Antibodies (BiTEs) 23
    - 1.4.4 Immune Checkpoint Inhibitors 24
- 1.5 Chimeric Antigen Receptor (CAR) T cell Therapy 27
    - 1.5.1 Anti-CD19 CAR T cell therapy: The Pioneer of CAR Technology 31
    - 1.5.2 CAR T cells for the Treatment of AML 32
    - 1.5.3 Bench to Bedside Challenges for the Treatment of AML 36

AIMS & SIGNIFICANCE 38

CHAPTER 2

TARGET ANTIGEN EXPRESSION OF CD123 ON PRIMARY AML TUMOUR SAMPLES 42
- 2.1 Introduction 41
- 2.2 Rationale of the Chapter 44
- 2.3 Materials & Methods 45
- 2.4 Results 47
    - 2.4.1 CD123 Expression in AML versus HD BM Primitive Cell Populations 47
    - 2.4.2 CD123 Expression in Bulk AML Myeloid Cells versus HD 51
    - 2.4.3 Association of CD123 Expression with Poor Risk Cytogenetic AML Patients 52
- 2.5 Conclusion & Discussion 53

CHAPTER 3

IN VITRO FUNCTIONAL CHARACTERISATION OF THE THIRD GENERATION CD123 CAR CONSTRUCTS FOR AML 57
- 3.1 Introduction 57
- 3.2 Rationale of the Chapter 60
- 3.3 Materials & Methods 62
- 3.4 Results 79
    - 3.4.1 Generation of the Anti-CD123 CAR Lentiviral Expression Constructs 79
    - 3.4.2 High-yield Production of CAR Lentivirus 81
    - 3.4.3 Achieving High Transduction of Primary T cells 87
    - 3.4.4 Successful Generation and Expansion of Primary Anti-CD123 CAR T Cells 89
    - 3.4.5 Third Generation CD123 CAR T Cells Activate Multiple Effector Functions in the Presence of CD123^{+} Target Cells *in vitro* 91
    - 3.4.6 Immune Exhaustion Profile of the Third Generation CD123 CAR T Cells 96
    - 3.4.7 Third Generation CD123 CAR T Cells Demonstrate Killing Capacity Against CD123^{+} Leukaemia Cells *in vitro,* Mediated by the Secretion of Anti-tumour Related Cytokines 98
    - 3.4.8 Third Generation CD123-CD28-OX4O-SF CAR T Cells Eradicate Primary AML Patient Derived BMMCs, and are Capable of Preventing Colony Formation of Leukaemic Progenitor Cell *in vitro* 104
- 3.5 Conclusion & Discussion 106

CHAPTER 4

COMBINING AZACITIDINE AND CD123 CAR T CELLS FOR THE TREATMENT OF AML *IN VIVO* 112
- 4.1 Introduction 112
- 4.2 Rationale of the Chapter 114
- 4.3 Authorship Consent Form 115
- Manuscript: Demethylating Therapy Prevents CTLA-4 Induction in Anti-CD123 CAR T cells in Acute Myeloid Leukemia 119
- 4.4 Additional Unpublished Materials & Methods 195
- 4.5 Additional Unpublished Results 197
    - 4.5.1 Azacitidine Increases Key Immunogenic Markers in AML 197
    - 4.5.2 CTLA-4$^{\text{negative}}$ CAR T Cells Are Associated with Lower Levels of Regulatory T Cells *in vivo* 200
    - 4.5.3 Direct Application of Azacitidine Does Not Promote an Inhibitory Effect on the CAR T Cells *in vitro* 201

CHAPTER 5

CONCLUSION & FUTURE PERSPECTIVES 205
- 5.1 Thesis Summary & Future Perspectives 205
- 5.2 Conclusion 209

CHAPTER 6

APPENDIX 211
- 6.1 CAR Construct Full DNA Sequences 211
- 6.2 List of All Consumable & Reagents 214
    - 6.2.1 Supplier Details of Specialised Reagents, Reagent Kits, and Consumables 214

6.2.2 Supplier Details of General Consumables Used 217
6.2.3 Fluorochrome-conjugated Flow Cytometry Antibodies 218
6.2.4 Supplier Details of Reagents and Kits Used for CD123 CAR T Cell Cloning........220
6.3 Solutions, Buffers, and Cell Culture Media........221
6.3.1 Recipes of all Solutions, Buffers, and Cell Culture Media Used 221
6.4 General Laboratory Techniques 223
6.4.1 Cryopreservation of Cells........223
6.4.2 Thawing of Cells........223
6.4.3 Lymphoprep Isolation of Peripheral bBlood Mononuclear Cells (PBMNCs) 223
6.4.4 Cell Counts and Viability........224
6.5 Maintenance & Culture of Cell Lines 225
6.5.1 Cell Line Specifications........225
6.5.2 Culture of General Cell Lines........226
6.6 Instruments & Equipment 226
6.6.1 List of Instruments and Equipment Used........226
6.7 Data Analysis Software 227
6.7.1 List of Software Programs Used 227

REFERENCES........228

ABBREVIATIONS 258

LIST OF TABLES 266

LIST OF FIGURES........267

ABSTRACT

English

Chimeric antigen receptor (CAR) T cells have yielded impressive remission rates in treatment-refractory B cell malignancies (B-ALL and B-lymphomas) by targeting CD19, resulting in CAR T cell therapies entering into clinical practice. However, the utility of CAR T cells for acute myeloid leukaemia (AML) remains a challenge. CAR T cells against AML-associated antigens are typically hampered by cytotoxic effects against normal haematopoietic progenitor cells and by CAR T cell exhaustion. Current clinical trials using CAR T cells that target various antigens in AML have resulted in either transient leukaemia cell clearance, or complete clearance of leukaemia at the expense of severe on-target off-tumour toxicities. In this thesis, third-generation anti-CD123 CAR T cells were developed with a humanised binding moiety for CD123 incorporating two intracellular signalling domains. The CAR developed in this project demonstrated strong anti-AML activity without elimination of the healthy haematopoietic system or epithelial tissue damage in mouse xenograft models. However, a sustained and long-term tumour eradication was not observed in the mice. In the clinical setting, this would mean that patients have suboptimal responses to the CAR T cells and may relapse.

The AML microenvironment is immunosuppressive by employing a variety of mechanisms to escape the host immune surveillance, which may hamper the efficacy of CAR T cell therapy. To improve the long-term efficacy of the CAR T cells, combination therapy with DNA methyltransferase inhibitors, such as azacitidine (AZA), was explored. AZA has previously been shown to upregulate the expression of leukaemia-associated antigens on AML thereby inducing more effective T cell responses. AZA was therefore combined with CD123 CAR T cells and evaluated in AML xenograft models. Priming of AML cells with AZA increased the expression of the target antigen, CD123, on the cell surface. CD123 CAR T cells were more effective at eliminating AML cells *in vivo* and induced long term eradication. Interestingly, the combined treatment strategy induced a CTLA-4$^{\text{negative}}$ CD123 CAR T cell population. Functionally, these CTLA-4$^{\text{negative}}$ CD123 CAR T cells exhibited superior cytotoxicity against AML cells with sustained tumour necrosis factor (TNF) production and higher proliferative capacity compared to CTLA-4$^{\text{positive}}$ CD123 CAR T cells. Furthermore, AML xenograft mice treated with CTLA-4$^{\text{negative}}$ CD123 CAR T cells survived longer than CTLA-4$^{\text{positive}}$ CD123 CAR T cell treated mice, and demonstrated recall immunity in secondary AML xenograft recipients. Mechanistically, when AML cells were primed with AZA, the CAR T cells demonstrated increased intracellular retention of CTLA-4 and reduced extracellular expression upon exposure to the AML cells. The decreased expression of extracellular CTLA-4 was associated with decreased numbers of regulatory CAR T cells. Normally, high extracellular CTLA-4 expression prevents the phosphorylation of Lck and Zap70; intracellular molecules required for effective T cell induction and function. In this case, a higher phosphorylation level of these molecules was observed in the CAR T cells exposed to AML cells previously primed with AZA compared to without priming.

The findings in this thesis project indicate that AZA increases the target antigen, CD123, on AML cells, allowing enhanced recognition and elimination by cytotoxic CTLA-4^{negative} CD123 CAR T cells. These novel findings pave the way for a clinical trial combining AZA and CD123 CAR T cells for AML treatment.

German

Chimäre Antigen Rezeptor T-Zellen (CAR T-Zellen) mit Zielantigen CD19 konnten beeindruckende Remissionsraten in therapierefraktären B-Zell Erkrankungen (B-ALL und B-Zell Lymphomen) erzielen, weshalb entsprechende CAR T-Zell Therapien bereits zum Einsatz in der Patientenversorgung kommen. Allerdings stellt die Anwendung von CAR T-Zellen bei der akuten myeloischen Leukämie (AML) weiterhin eine Herausforderung dar. CAR T-Zellen mit AML assoziierten Zielantigenen werden typischerweise von zytotoxischen Effekten normaler hämatopoetischer Vorläuferzellen und der CAR T-Zellerschöpfung in ihrer Wirkung gehemmt. Aktuelle klinische Studien, welche CAR T-Zellen mit verschiedenen AML spezifischen Zielantigenen nutzen, zeigten entweder nur eine zeitweilige Beseitigung leukämischer Zellen, oder die vollständige Beseitigung der Leukämie unter Inkaufnahme schwerwiegender toxischer Nebenwirkungen durch gleichzeitiger Wirkung an nicht leukämischen Zellen mit Ausprägung desselben Zielantigens. In dieser Doktorarbeit wurden anti-CD123 CAR T-Zellen der dritten Generation entwickelt, welche mit einem humanisierten Bindungsstück für CD123 und zwei intrazellulären Signaldomänen ausgestattet sind. Der chimäre Antigen Rezeptor dieser Arbeit zeigte eine ausgeprägte anti-AML Aktivität in Maus Xenograft Modellen ohne dabei das gesunde hämatopoetische System zu unterdrücken oder dem epithelialen Gewebe zu schaden. Allerdings konnte bisher keine nachhaltige und langfristige Tumoreradikation in Maus Modellen beobachtet werden. Für den klinischen Einsatz würde dies bedeuten, dass behandelte Patienten ein suboptimales Ansprechen auf die CAR T-Zellen aufweisen und Rezidive auftreten könnten.

Um der Immunabwehr des Wirtorganismus zu entgehen, verwendet das AML Mikromilieu verschiedene immunsuppressive Mechanismen. Diese Mechanismen behindern wiederum die

Effektivität der CAR T-Zell Therapie. Daher wurde zur Verbesserung der langfristigen Effektivität der CAR T-Zellen eine Kombinationstherapie mit DNA-Methyltransferase Inhibitoren wie Azacitidin (AZA) erforscht. Vorherige Studien zeigten, dass AZA die Expression leukämieassoziierter Antigene der AML hochreguliert und dadurch eine effektivere T-Zell Antwort auslöst. In dieser Arbeit wurde daher AZA mit CD123 CAR T-Zellen als Kombinationstherapie in AML Xenograft Modellen eingesetzt und evaluiert. Die Bahnung und Vorbereitung von AML Zellen durch AZA erhöhte die Expression von CD123, des Zielantigens, auf der Zelloberfläche. CD123 CAR T-Zellen waren effektiver in der Eliminierung von AML Zellen *in vivo* und induzierten eine langfristige Tumoreradikation. Interessanterweise induzierte besagte Kombinationstherapie die Bildung einer CTLA-4$^{\text{negativen}}$ CD123 CAR T-Zellpopulation. Diese CTLA-4$^{\text{negativen}}$ CD123 CAR T-Zellen zeigten, insbesondere im Vergleich mit CTLA-4$^{\text{positiven}}$ CD123 CAR T-Zellen, eine ausgeprägtere Zytotoxizität gegen AML Zellen, nachhaltige TNF Produktion und erhöhtes proliferatives Potential. Des Weiteren überlebten jene AML Xenograft Mäuse länger, welche mit CTLA-4$^{\text{negativen}}$ CD123 CAR T-Zellen behandelt wurden. Zudem wiesen sie ein Immunitätsgedächtnis in sekundären AML Xenograft Empfängern auf. Unter der Behandlung von AML Zellen mit AZA in der Kombinationstherapie zeigten die CAR T-Zellen bei Exposition mit entsprechenden AML Zellen eine verstärkte intrazelluläre Retention und eine erniedrigte extrazelluläre Expression von CTLA-4. Die erniedrigte extrazelluläre Expression von CTLA-4 ging mit einer erniedrigten Anzahl an regulatorischen FOXP3^{+} CAR T-Zellen einher. Normalerweise verhindert eine hohe extrazelluläre Expression von CTLA-4 die Phosphorylierung von Lck und Zap70, intrazellulären Molekülen welche für die effektive T-Zell Induktion und Funktion notwendig sind. In dieser Arbeit konnte beobachtet werden, dass CAR T-Zellen, welche durch die Gabe von AZA vorher gebahnt worden waren, im Vergleich zu CAR T-Zellen ohne verherige AZA Behandlung der AML Zellen, ein erhöhtes Phosphorylierungsniveau dieser Moleküle nach Exposition mit AML Zellen aufwiesen.

Die Ergebnisse dieser Doktorarbeit legen nahe, dass AZA die Expression des Zielantigens CD123 auf AML Zellen erhöht, wodurch die gesteigerte Erkennung und Eliminierung maligner Zellen durch zytotoxische CTLA-4$^{\text{negativen}}$ CD123 CAR T-Zellen ermöglicht wird. Diese neuen Erkenntnisse ebnen den Weg für klinische Studien mit Einsatz von AZA und CD123 CAR T-Zellen in der AML Therapie.

Chapter 1

INTRODUCTION

1.1. From Haematopoietic Stem Cells to Leukaemic Stem Cells

Haematopoietic stem cells (HSCs) are multipotent, self-renewing blood progenitor cells which are found mainly in the bone marrow (BM) of the adult, and constitute approximately 0.2% of the BM composition (Riether et al., 2015). Haematopoietic cells and their mature progeny in the peripheral blood (PB) and tissues have a finite lifespan and must, therefore, be continuously replaced throughout life (Il-Hoan & Kyung-rim, 2010). HSCs infrequently divide, giving rise to transient-amplifying multipotent and lineage-restricted progenitors (MPPs) that proliferate extensively. HSCs are quiescent cells that warrant genomic integrity as frequent chromosomal replications may introduce oncogenic deoxyribonucleic acid (DNA) mutations. Quiescence, therefore, protects the cells from uncontrolled proliferation.

Furthermore, self-renewal is a hallmark and a defining characteristic of HSCs, and this capacity arises from the ability of the HSCs to divide asymmetrically; ensuring one daughter cell remains a HSC. The haematopoietic system is therefore critically dependent on three fundamental cellular processes: survival, proliferation, and differentiation. These processes are tightly regulated by many factors, pathways, and supportive niches of the BM microenvironment to maintain a steady-state level of functional HSCs (Noll et al., 2012) (Jagannathan-Bogdan & Zon, 2013).

HSCs possess non-exhaustive replication and proliferation capacities that can be initiated in stress situations, such as after cytotoxic chemotherapy, irradiation, or during infections. Normal haematopoiesis is impaired when leukaemic cell expansion occurs following neoplastic transformation of immature haematopoietic cells which may have marked morphological, aberrant genetic, and functional heterogeneity (Huntly & Gilliland, 2005) (Reya et al., 2001).

Leukaemic stem cells (LSCs) are the small population of cells within the bulk of leukaemia cells with stem cell characteristics that propagate the disease (Riether et al., 2015). LSCs produce more differentiated and heterogenic leukaemic progeny with a high proliferative potential, failure of terminal differentiation, and inhibition of molecular cues that promote apoptosis, or possess senescence mechanisms which lead to blast accumulation and clinical disease (Seshadri & Qu, 2016). LSCs are thought to originate from HSCs which have undergone leukaemia-initiating events. Conversely, some studies demonstrated that in certain leukaemias, more mature progenitor cell types, or even cells expressing lineage markers can also serve as leukaemia-initiating cells (LIC) that give rise to LSCs *(Figure 1.1)*(Jamieson et al., 2004). This nurtured the idea that the LICs or the stage of haematopoiesis for leukaemic transformation varies between the types of leukaemia.

Much like HSCs, LSCs depend on similar interactions with the BM supportive niche for their survival, persistence, and renewal. Therefore, during leukaemogenesis, LSCs 'hijack' the niche and signalling molecules, consequently suppressing the development of normal HSCs. Colmone and colleagues (Colmone et al., 2008) demonstrated that transplanted leukaemia cells preferentially migrate to C-X-C motif chemokine ligand 12 (CXCL12)-expressing vascular niches. It has been found that the effect of transforming growth factor β (TGF-β) on LSC quiescence, for example, varies in different types of leukaemia. For instance, TGF-β is found to be a crucial regulator of protein kinase B (AKT/PKB) activation thereby maintaining LSCs and inducing the quiescent G_0 state of the cell cycle. In doing so, LSCs become invasive and insensitive to anti-growth and apoptosis signals. It is now widely accepted that the ability of the LSCs and its progeny to evade the immune system is also a fundamental hallmark of leukaemic disease (Hanahan & Weinberg, 2011).

Taken together, it is evident that LSCs depend on similar signals from the same supportive BM niches as HSCs do, although the signals harnessed by the LSCs may differ between the subtypes of leukaemia. One such leukaemia that causes BM failure due to the impairment of normal haematopoiesis is acute myeloid leukaemia (AML).

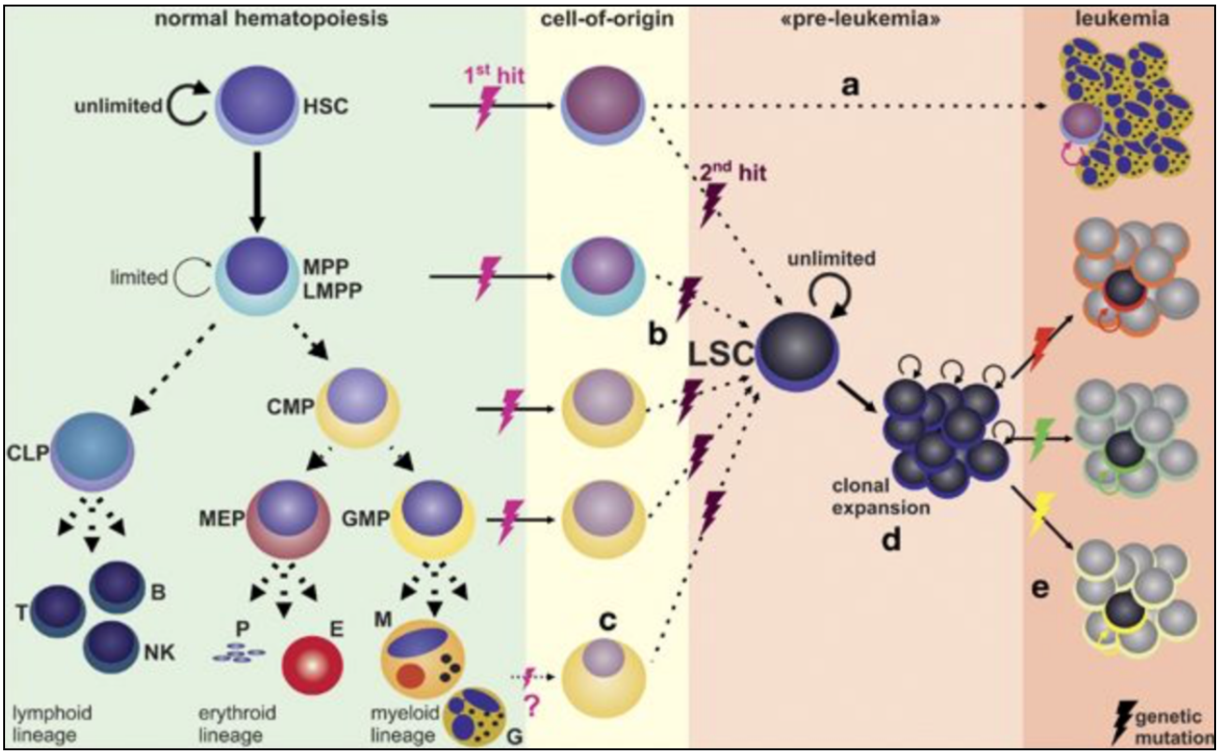
normal hematopoiesis
cell-of-origin
«pre-leukemia»
leukemia
unlimited
HSC
1st hit
a
2nd hit
limited
MPP
LMPP
unlimited
b
LSC
CMP
CLP
MEP
GMP
clonal
expansion
d
e
T
B
NK
P
E
M
c
?
lymphoid
lineage
erythroid
lineage
myeloid
lineage
G
genetic
mutation

Figure 1.1. The aberrant transformation of haematopoietic stem cells to leukaemic stem cells. During normal haematopoiesis, HSCs with unlimited self–renewal capacity differentiate into multipotent progenitors (MPPs) with limited self-renewal capacity. MPPs further differentiate into oligo-potent lineage-restricted (OPPs) progenitors (common lymphoid or myeloid progenitors; CLP and CMP, megakaryocyte-erythrocyte progenitor and granulocyte-macrophage progenitors; MEP and GMP) which have lost self-renewal capacity. These lineage restricted progenitors produce terminally differentiated mature blood cells with intense proliferative capacity e.g. T-, B-, and natural killer (NK) cells of the lymphoid lineage; platelets (P), erythrocytes (E), monocytes (M) and granulocytes (G) of the myeloid lineage. Leukaemic transformation can occur at various stages of the haematopoietic hierarchy. **(A)** For some leukaemias, a genetic chromosomal change can occur from an HSC giving rise to all downstream blood lineages harbouring the same malignant phenotype. **(B)** In other leukaemias, LSCs exhibited immunophenotypes similar to that of MPPs or OPPs suggesting more differentiated cells can also give rise to LSCs after re-acquisition of self-renewal capacity. **(C)** There is increasing evidence suggesting LSCs can arise from mature terminally differentiated blood cells with the ability to also re-acquire self-renewal capacity. **(D)** In the 'pre-leukaemic' phase, genetically unstable LSCs clonally expand and differentiate allowing the accrual of further mutations. **(E)** The accrual of further mutations in the 'pre-leukaemic' phase then leads to the development of different terminally differentiated leukaemic clones. *(Illustration by Riether et al., 2015).*

1.2. Acute Myeloid Leukaemia

1.2.1. AML Disease Epidemiology & Pathogenesis

AML is a heterogeneous clonal disorder characterised by the proliferation and infiltration of aberrantly differentiated immature haematopoietic cells, called AML blasts, into the blood and other peripheral tissues, which consequently causes BM failure. AML represents the most common acute leukaemia in adults, accounting for approximately 80% of cases. The incidence of AML increases with age, from 1.3 per 100,000 population in patients younger than 65 years of age, to 12.2 cases per 100,000 population in patients over 65 (Döhner et al., 2015). The median age of diagnosis is 69 in Australia. AML was incurable up until the last few decades, and is now cured in ~35-40% of patients aged ≤60, and 5-15% of patients aged ≥60 with intensive chemotherapy. AML patients in Australia have a 5-year relative survival of only 26.8% at diagnosis (Australian Institute of Health and Welfare, 2017). The majority of patients present with a combination of leucocytosis and signs of BM failure, of which, anaemia and thrombocytopenia are the most common. In addition, patients often experience symptoms such as fatigue, anorexia, and weight loss. Infection, bleeding, and organ failure are common complications of AML and without prompt medical intervention; death usually ensues within weeks to months of diagnosis (E. H. Estey, 2012). A patient is said to be diagnosed with AML when there is a presence of 20% or more blasts in the BM or PB, or in combination with documented genetic abnormalities (Döhner et al., 2010).

Diagnosis is made through morphologic assessment of BM specimens and blood smears, analysis of cell-surface or cytoplasmic markers by flow cytometry, identification of chromosomal findings by means of conventional cytogenetic testing or fluorescence *in situ* hybridisation (FISH), and screening for selected molecular genetic lesions for disease classification. Under the *World Health Organization (WHO) Classification of Tumours of Hematopoietic and Lymphoid Tissues*, AML is categorised into 7 groups: AML with recurrent genetic abnormalities, AML with myelodysplasia-related changes, prior therapy-related AML, AML not otherwise specified, myeloid sarcoma, Down-syndrome related myeloid proliferations, and undifferentiated/bi-phenotypic acute leukaemia (Döhner et al., 2015).

The pathogenesis of AML is therefore a complex process. Gilliland and colleagues proposed a simplified 'two-hit' model, resulting from two consequent genetic events, for the development of AML (Fröhling et al., 2005)(Kelly & Gilliland, 2002)(Kihara et al., 2014).

The model proposes that a healthy blast can transform to an AML blast by the acquisition of two types of mutations. The first type of genetic mutation consists of constitutively active cell-surface receptors involved in the tyrosine kinase receptor signalling pathways such as Ras, FMS-like tyrosine kinase 3 (FLT3), c-Kit, Janus kinase 2 (JAK2), and tyrosine-protein phosphatase non-receptor type 1 (PTPN1) resulting in the activation of pro-proliferative pathways thereby driving phosphatidylinositol 3-kinase/protein kinase-B (PI3K-Akt), Ras-mitogen activated proten kinase (Ras-MAPK), or signal transducer and activator of transcription (STAT) pathways. Besides cellular proliferation, these mutations can induce anti-apoptotic genes belonging to the B cell lymphoma 2 (Bcl-2) family conferring a survival advantage thereby allowing the expansion of leukaemic blast progenitor cells (Franke et al., 2003)(Bose et al., 2012)(Nosaka, 1999). The second genetic event is exemplified by chromosomal aberrations resulting from the overexpression of homeobox (HOX) genes, the formation of onco-fusion proteins such as runt-related transcription factor 1/ RUNX1 translocation partner 1 (RUNX1/RUNX1T1), promyelocytic leukaemia/retinoic acid receptor alpha (PML-RARA), and molecular changes in transcription factors such as CCAAT/enhancer-binding protein alpha (C/EBPα) and RUNX1 which impair and block normal haematopoietic differentiation (Fröhling et al., 2005).

The understanding of AML has vastly improved within the past decade, with various studies mapping the complex genetic landscape of AML with the advent of next generation sequencing (NGS) (Lindsley et al., 2015)(Marcucci et al., 2011). These studies demonstrated that the presence or absence of specific gene mutations, or changes in gene expression can be correlated with the patients' prognosis. Key molecular abnormalities *(Figure 1.2, Table 1.1)* are now used to predict outcome and help guide treatment regimens for AML patients.

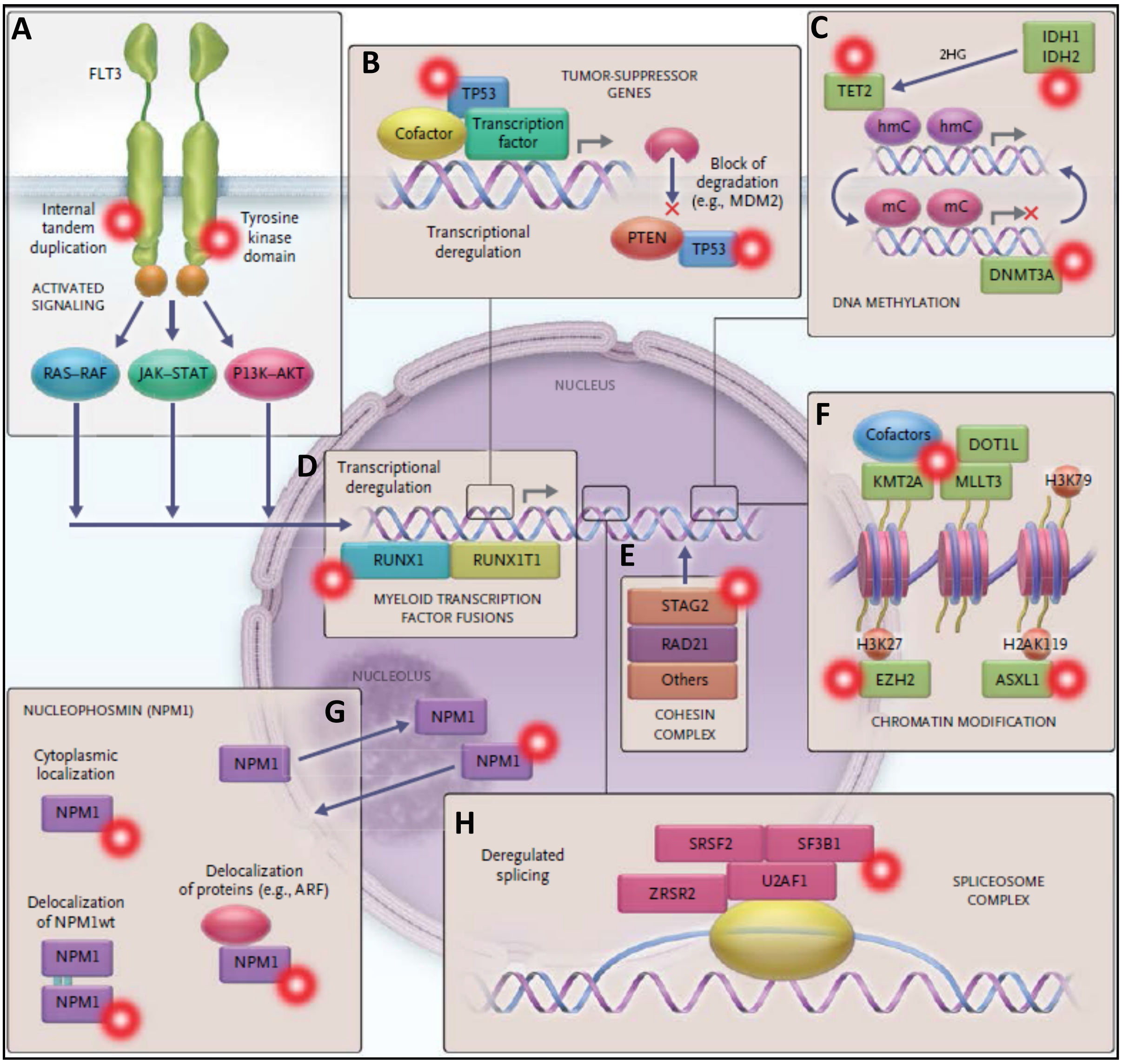
A
FLT3
Internal tandem duplication
Tyrosine kinase domain
ACTIVATED SIGNALING
RAS–RAF
JAK–STAT
P13K–AKT
B
TP53
Cofactor
Transcription factor
TUMOR-SUPPRESSOR GENES
Transcriptional deregulation
Block of degradation (e.g., MDM2)
PTEN
TP53
C
2HG
IDH1
IDH2
TET2
hmC
hmC
mC
mC
DNMT3A
DNA METHYLATION
NUCLEUS
D
Transcriptional deregulation
RUNX1
RUNX1T1
MYELOID TRANSCRIPTION FACTOR FUSIONS
E
STAG2
RAD21
Others
COHESIN COMPLEX
F
Cofactors
DOT1L
KMT2A
MLLT3
H3K79
H3K27
H2AK119
EZH2
ASXL1
CHROMATIN MODIFICATION
NUCLEOLUS
G
NUCLEOPHOSMIN (NPM1)
Cytoplasmic localization
NPM1
Delocalization of NPM1wt
Delocalization of proteins (e.g., ARF)
H
Deregulated splicing
SRSF2
SF3B1
U2AF1
ZRSR2
SPLICEOSOME COMPLEX

Figure 1.2. Functional Categories of Genes Frequently Mutated in Acute Myeloid Leukaemia.
(A) Mutations in the genes of class III tyrosine kinase receptor gene *FLT3* confer a proliferative advantage through aberrant RAS-RAF, JAK-STAT, and PI3K-AKT signalling pathways. **(B)** Tumour suppressor (TP) genes e.g., *TP53* mutations result in transcriptional deregulation and impaired degradation through the mouse double minute 2 homologue (MDM2) and the phosphatase and tensin homologue (PTEN). **(C)** DNA methylation gene mutations such as Tet methylcytosine dioxygenase 2 (*TET2),* DNA methyltransferase 3A *(DNMT3A),* and Isocitrate dehydrogenase 1/2 (*IDH1/2)* (acting through the 2-hydroxyglutarate (2HG) oncometabolite production, leads to the deregulation of DNA methylation (*hmC* 5-hydroxymethyl-cytosine and *mC* 5-methylcytosine). **(D)** Mutations in myeloid transcription factors such as *RUNX1* and transcription factor fusions by chromosomal rearrangements, such as *RUNX1-RUNX1T1* lead to deregulation and impaired haematopoietic differentiation. **(E)** Cohesion complex gene mutations such as stromal antigen-2 (*STAG2)* and double strand break repair protein 21 (*RAD21)* may impair accurate chromosome segregation and transcriptional regulation. **(F)** Additional sex comb-like 1 (*ASXL1)* and enhancer of zeste homolog 2 (*EZH2)* are genes associated with epigenetic homeostasis of cells. Mutations lead to deregulation of chromatin modification e.g. H3 and H2A histone methylation on lysine residues, impairing other methyltransferases such DOT-1 like histone H3K79 methyltransferase (DOT1L). **(G)** The Nucleophosmin 1 *(NPM1)* gene encodes a multifunctional nucleocytoplasmic shuttling protein and mutations result in aberrant cytoplasmic localisation of NPM1 and NPM1-interacting proteins. **(H)** Mutations of spliceosome-complex genes such as SRSF2, SF3B1, U2AF1, and ZRSR2 are involved in deregulated ribonucleic acid (RNA) processing. *(Illustration by Döhner et al., 2015)*

TABLE 1.1. Clinical Significance of Frequent and Recurrent Gene Mutations in AML.

Mutated Gene	Frequency (% of patients)	Clinical Significance
NPM1	25-35	Most frequent in cytogenetically normal AML, often associated with other mutations. In younger patients, it is associated with good prognosis with chemotherapy and there is no benefit from allo-hSCT. Older patients benefit from conventional induction chemotherapy. In cases with other genetic aberrations e.g. Flt3-ITD, patients have poor OS. (Falini et al., 2007) (K. Döhner et al., 2005).
CEBPA	6-10	Most commonly associated with del (9q) mutations. Incidence decreases with age and cytogenetically normal AML. CEBPA bi-allelic mutation or double mutations are found in half of CEPBA cases and confers a higher CR and favourable OS. A favourable outcome can be achieved with conventional induction chemotherapy.
RUNX1	5-15	Incidence increases with age and is often associated with other mutations. This mutation is often present with trisomy 13 or 21 mutations. Mutation often occurs in secondary AML evolving from MDS. *RUNX1* are often predictors of resistance to induction chemotherapy in young and older patients and is often related to poor prognostic outcome.
FLT3-ITD	~20	Strongly expressed in HSCs and drives cellular proliferation and survival through JAK-STAT, MEK/MAPK and PI3K signalling pathways. Associated with a very poor outcome if they have a high mutant-to wild type ITD ratio. ITD in the JM domain or mutations in the second TKD of the *flt3* gene are found in ~25% of cases. These patients may benefit from allo-hSCT in first complete remission however relapse is still frequent. (Kelly & Gilliland, 2002) (Daver et al., 2019)
c-KIT	<5	Mostly associated with core-binding factor AML with t(8;21) and inv(16) and other fusion genes. *cKIT* mutations are shown to confer higher relapse and poor OS. *cKIT* can be targeted using TKIs.
NRAS	~15	Mostly frequent in cytogenetically normal AML, AML with inv(16) and inv(3). Mutant *RAS* may be predictive of sensitivity to cytarabine.
DNMT3A	18-22	Incidence increases with age. Occurs most frequently in cytogenetically normal AML and is associated with *NPM1* and *FLT3-ITD* mutations. Patients with this mutation have a moderate adverse outcome
ASXL1	5-17	Incidence increases with age and is often associated with secondary AML evolving from MDS. *ASXL1* mutations predictive of inferior outcome as it occurs with concurrent mutations (e.g. *RUNX1, SRSF2* and *IDH2*).
IDH1 and IDH2	7-20	Isocitrate dehydrogenases are homodimeric enzymes involved in diverse cellular processes, including adaption to hypoxia, histone demethylation and DNA modification. *IDH1* resides primarily in the cytosol, whereas *IDH2* is primarily mitochondrial. Mutant IDH enzymes have neomorphic activity, catalysing NADPH-dependent reduction of α-KG to an oncometabolite, D-2-hydroxyglutarate (2-HG). 2-HG results in downstream DNA hyper-methylation and a block in myeloid cell differentiation Incidence increases with age and most frequently seen in cytogenetically normal AML. Found in up to 20% of cases and incidence increases with age. IDH2 mutations occur more often than IDH1 mutations. There is an association with *NPM1, DNMT3A and Flt3* mutations. Prognostic significance is dependent on mutational context and whether there are concurrent mutations. Some confer poor prognosis and some confer favourable prognosis. (Reitman et al., 2010) (Losman & Kaelin, 2013) (Fathi et

		al., 2015) (Döhner et al., 2015) (DiNardo et al., 2015) (Figueroa et al., 2010) (Lu et al., 2012)
TET2	7-25	Incidence increases with older age. Tet2 loss leads to increased HSC self-renewal and skewed differentiation towards the monocytic cell lineage. Mutually exclusive of *IDH1* and *IDH2* mutations. Associated with inferior survival among patients with cytogenetically normal AML. Associated with clonal haematopoiesis in healthy elderly persons.
KMT2A-PTD	5	Associated with cytogenetically normal AML and trisomy 11. Translocations associated with the KMT2A gene leads to aggressive acute lymphoid and myeloid leukaemia. Generally has a poor outcome with higher relapse rate and poor OS. However, this is dependent on several factors.
TP53	~8-14	Incidence increases with older age. Predominantly detected in AML with complex aberrant karyotype (e.g. -5 or del(5q), -7 or del(7q)) *TP53* confer very poor outcome and patients are generally resistant to conventional induction therapies and/or relapse following allo-hSCT.

*Abbreviations: OS- overall survival, CR- complete remission, PTD-partial Tandem duplication, MDS-Myelodysplastic syndrome, ITD- Internal tandem duplication, allo-hSCT-allogeneic stem cell transplantation, JM- juxtamembrane, TKD- tyrosine kinase domain, TKI- tyrosine kinase inhibitors, α-KG-alpha ketoglutaric acid. *(Table adapted from Döhner et al., 2015)*

In the majority of cases, AML appears as a *de novo* malignancy. However, genetic mutations have been implicated in the development of AML in more than 97% of these cases. Progression from pre-existing haematopoietic disorders, such as myelodysplastic syndrome (MDS) and aplastic anaemia to AML is also sometimes seen in newly diagnosed AML patients. Additionally, up to 15% of AML patients develop the disorder following cytotoxic treatment for other cancers or diseases with a median latency of 5-10 years. These patients have disease more resistant to intensive chemotherapy than *de novo* AML patients (Sill et al., 2011).

1.2.2. AML Risk Stratification/Disease Prognosis

In 2010, the European LeukemiaNet (ELN) classification scheme was created to standardise risk stratification in adult AML by dividing patients into four risk groups based on their cytogenetic and known molecular abnormalities (Döhner et al., 2010). These risk groups include: favourable, intermediate I, intermediate II, and adverse (poor) (*Table 1.2)*. Patients with favourable prognosis harbour genetic and cytogenetic alterations such as t(15;17)(q22;q12), t(8;21)(q22;q22), inv(16), mutated *NPM1* without Flt-3 ITD, and bi-allelic mutated *CEBPA*. Intermediate I and II categories include mutated *NPM1* with Flt-3 ITD, wild-type *NPM1* with or without Flt-3 ITD and t(9;11). Complex karyotypes, inv(3), -5 or del(5q), -7 or abnormal (17p), and monosomal karyotype are associated with poor survival. In particular, patients with monosomal karyotype have the worst survival prognosis with only a 5-year overall survival (OS) of 4%. Furthermore, patients older than 60 years of age generally have poorer outcomes regardless of their ELN classification (Döhner et al., 2010)(Mrózek et al., 2012)(Medeiros et al., 2010).

TABLE 1. 2. ELN current risk stratification of molecular, genetic and cytogenetic alterations.

Risk Group	**Subsets**
Favourable	t(8;21)(q22;q22); *RUNX1-RUNX1T1*; inv(16)(p13.1q22) or t(16;16)(p13.1;q22); *CBFB-MYH11*; Mutated *NPM1* without *Flt3-ITD* (normal karyotype); Bi-allelic mutated *CEBPA* (normal karyotype)
Intermediate I	Mutated *NPM1* and *Flt3-ITD* (normal karyotype); Wild-type *NPM1* and *Flt3-ITD* (normal karyotype); Wild-type *NPM1* without *Flt3-ITD* (normal karyotype)
Intermediate II	t(9;11)(p22;q23); *MLLT3-KMT2A;* Cytogenetic abnormalities not classified as favourable or adverse
Adverse	Inv(3)(q21q26.2) or t(3;3)(q21;q26.2); *GATA2-MECO (EV11);* t(6;9)(p23;q34); *DEK-NUP214;* t(v;11)(v;q23); *KMT2A* re-arranged; -5 or del(5q); -7; abnormal(17p); complex karyotypes#

#complex karyotype is defined as three or more chromosome abnormalities

1.2.3 Standard Treatment Regimen

The general treatment regimen for AML patients has not changed substantially in the past 40 years. The majority of clinically fit patients will undergo intensive chemotherapy. Chemotherapy is generally curative for AML patients with favourable cytogenetics. The '7+3' regimen of cytarabine and anthracycline, consisting of either daunorubicin or idarubicin, is the standard intensive induction chemotherapy. Complete remission (CR) is achieved in 65%-73% of young *de novo* AML patients but is only 38%-62% in patients over 60 years of age (Cheson et al., 2003)(Döhner et al., 2010). For *de novo* patients who are medically unfit for intensive chemotherapy, DNA hypomethylating agents (HMAs) such as azacitidine (AZA) and decitabine (DEC) are the common off-study agents used for treatment. Patients over the age of 65 treated with AZA demonstrated a longer median survival than patients treated with conventional care regimens (Seymour et al., 2017).

Consolidation therapy is given following induction therapy to prevent disease relapse and to eradicate minimal residual disease (MRD) in the BM (Grimwade & Freeman, 2014)(Kohlmann et al., 2014). There are two main strategies for consolidation therapy; chemotherapy (with or without targeted agents) and allogeneic haematopoietic stem cell transplantation (allo-hSCT). The exact treatment regimen is tailored to the patient taking into consideration several factors, including the risk profile of the AML, the general 'fitness' of the patient, and the availability of a stem cell donor (Döhner et al., 2015). The cumulative incidence of relapse in patients following induction and consolidation therapy approaches 60% in the favourable-risk category and exceeds 85% in the adverse category. Early relapse following treatment (within 6 months after achieving CR) portends a poor overall patient survival. Salvage chemotherapy regimens include a range of different agents (cytarabine, mitoxantrone, idarubicin and fludarabine) and the combination is dependent on the patient's cytogenetic risk profile (Döhner et al., 2015). The likelihood of achieving a second CR is best in younger patients with favourable cytogenetics and a long first remission.

1.2.4. Molecular Targeted Therapies & Other Approved Agents

Despite the standard treatment regimens, over 50% of patients relapse and ultimately will succumb to the disease. The increased understanding of AML pathobiology, classification, and genomic landscape over the years has contributed to the development of novel therapeutic agents. These agents have demonstrated promising clinical activity which has led to Food and Drug Administration (FDA) approval. The most noteworthy and recently approved molecular targeted agents are described below.

FMS-Like Tyrosine Kinase 3 (FLT3) Inhibitors

Patients with FLT3 mutations have a higher relapse rate and are generally more likely to become chemo-refractory. Given the high frequency with which FLT3 mutations occur in AML, FLT3 tyrosine kinase inhibitors (TKIs) have been developed to disrupt the oncogenic signalling initiated by FLT3.

Several first-generation multi-targeted TKIs such as midostaurin and sorafenib have entered clinical practice. Midostaurin is a multi-targeted kinase inhibitor and was FDA approved on the basis of the Phase III RATIFY trial conducted in newly diagnosed young patients <60 years of age with a FLT3 kinase domain mutation (Stone et al., 2017)(Stone et al., 2018). Patients were either treated with midostaurin as front-line therapy or the standard induction and consolidation chemotherapy regimen. The results showed improved OS and event-free survival (EFS), with a 22% reduction in death for those patients treated with midostaurin. This survival benefit persisted in patients who were ineligible for allo-hSCT, highlighting that it is possible to achieve CR and possibly cure patients without transplant. Importantly, 50% of patients in this study survived at a median follow-up of 59 months highlighting the survival benefit of this FLT3 TKI (Stone et al., 2017)(Stone et al., 2018). As a result, midostaurin (in combination with standard induction chemotherapy) was approved by the FDA in 2017 for the treatment of adult patients with newly diagnosed *flt3*-mutated AML.

Sorafenib is used as an off-label agent in combination with AZA for relapsed/refractory (r/r) AML or for older unfit FLT3 AML patients that are ineligible for transplant (Döhner et al., 2017). Randomised trials demonstrated that sorafenib significantly increased EFS and relapse free survival (RFS) but not OS (Röllig et al., 2020). Sorafenib has also shown promise as a maintenance therapy for FLT3-ITD mutant AML patients following allo-hSCT demonstrating improved OS (Brunner et al., 2016).

First-generation TKIs, in general, lack specificity for the mutated FLT3-ITD where acquired resistance-conferring point mutation or gatekeeper mutations commonly occur following a few months of treatment resulting in loss of response. Gilteritinib, a next-generation TKI targeting both of the inactive and active conformational states of the FLT3 kinase domain, was developed to overcome this hurdle (N. Daver et al., 2015).

In a randomised phase III trial (ADMIRAL) (NCT02421939), gilteritinib showed improved survival for patients with r/r AML when compared with standard chemotherapy regimens. Patients treated with giltertinib had a CR rate of 40% compared to those treated with chemotherapy (15.3%). At the final analysis, patients who received gilteritinib were found to have a 36% reduction in risk of death compared to those treated with standard chemotherapy. At 12 months, 37% of patients were alive in the gilteritinib treated arm compared to those treated with chemotherapy (16.7%) (Gorcea et al., 2018)(Perl et al., 2017)(Perl et al., 2019). The survival data combined with gilteritinib's relatively low toxicity resulted in FDA approval in November 2018 as a monotherapy for r/r AML with FLT3 mutations.

Additionally, quizartinib, a more selective and potent inhibitor of FLT3 wildtype (WT) and ITD with significant inhibition of cKIT was investigated for use as a single agent treatment in a large phase II clinical trial on patients with r/r AML. The majority of the patients were FLT3-ITD positive and demonstrated a composite CR (cCR) rate of 50% and CR's were rarely achieved as most patients remained cytopenic. Interestingly, a cCR of >30% was achieved in the patients with FLT3-WT. These promising results allowed 35% of the younger patients to receive allo-hSCT (J. Cortes et al., 2018). In the Phase III QuANTUM-R study, 367 r/r FLT3 ITD$^+$ AML patients were randomised to receive either quizartinib or salvage chemotherapy. Patients receiving quizartinib demonstrated significant but limited improvement of OS (median 6.2 vs 4.7 months). The authors of this study speculate this limited survival benefit may be due to the selection or adaptation of both cell-intrinsic and stroma-mediated resistance to FLT3 inhibition (J. E. Cortes et al., 2019).

Overall, the use of FLT3 inhibitors, compared to previous standard of care prior to their emergence, has demonstrated substantial clinical benefit in r/r AML. This promising treatment strategy offers *flt3* mutated patients an alternative salvage therapy where there was previously none.

Isocitrate Dehydrogenase IDH1/IDH2 Inhibitors

It is well known that AML and other neoplasms can arise from frequent mutations in genes involving DNA methylation and chromatin modifications. One of the most promising new targets is the inhibition of the mutant metabolic enzymes *IDH1* and *IDH2* in AML.

Enasidenib (AG-221) is a selective, oral inhibitor of the IDH2 enzyme approved in 2017 by the FDA following a clinical study (Stein, 2015) demonstrating an overall response rate (ORR) of 40.3% and an average CR rate of approximately 20% in r/r AML. The drug is found to be well tolerated with an average duration of response of about 6 months. However, there are responders with continuous remissions of more than 2 years (Stein et al., 2017). Currently, trials using combination treatment of enasidenib with induction chemotherapy in newly diagnosed AML with mutational IDH2 are ongoing (Stein et al., 2017).

Ivosidenib (AG-120) is a first-in-class potent and reversible inhibitor of IDH1. A phase I dose escalation and expansion study evaluated ivosidenib as a monotherapy for patients with IDH1 mutations with advanced haematologic malignancies (NCT02074839). In this trial where the majority of participants were r/r AML, an ORR was achieved in 36% and CR was achieved in 18% of the cohort. Clearance of the IDH1 mutant was seen in 21% of patients, which equated to a longer duration of remission and longer OS. Ivosidenib was generally well tolerated, although the majority of patients experienced side effects which were alleviated with steroid or hydroxyurea administration. These impressive and promising results led to FDA approval in 2018 for r/r AML and, again, in 2019 for newly diagnosed AML with IDH1 mutations (Nassereddine et al., 2018)(Saygin & Carraway, 2017).

Venetoclax

Venetoclax is an oral and potent inhibitor of BCL-2. In AML, BCL-2 it is a key regulator of the mitochondrial apoptotic pathway leading to the survival of AML blasts (Pan et al., 2014). Inhibition of BCL-2 is thought to overcome chemotherapy resistance while normal HSCs remain unaffected. As a single agent therapy, venetoclax demonstrated little activity with a CR rate of 19% and a median OS of 4.9 months in r/r AML patients (Konopleva et al., 2016). In patients with IDH mutations, a higher rate of CR (33%) was achieved.

In combination with HMAs such as AZA or DEC, an OR was significantly higher in treatment-naïve patients over the age of 65 who were also ineligible for standard induction chemotherapy (NCT02203773). In this study, 67% of patients achieved CR with a median OS of 17.5 months. The results from this trial served as the foundational basis for accelerated approval of this treatment combination by the FDA in November 2018 (DiNardo et al., 2019). Patients in the high-risk subgroups also benefitted from the combination therapy. In particular, a CR of 65% was observed in patients older than 75 years with adverse genetics or in patients with secondary AML. Furthermore, patients harbouring NPM1 or IDH1/2 mutations appeared to have particularly salutary outcomes with CR rates of 91% and 71%, respectively (DiNardo et al., 2019).

In combination with low-dose cytarabine, a CR rate of 54% was observed in newly diagnosed patients with a median response of 8.1 months and a median OS of 10.1 months (NCT02287233). Additionally, 89% of patients with NPM1 mutations achieved CR with venetoclax combination with HMAs. In comparison, patients with more adverse genetics such as *Flt3* and *TP53* mutations had a CR rate of 44% and 30%, respectively (Wei et al., 2019).

CPX-351

CPX-351 is a dual liposomal formulation containing a 1:5 molar ratio of daunorubicin and cytarabine. The dual drug increased synergy between them and promoted leukaemia cell killing in pre-clinical models. Phase I-III trials in AML demonstrated prolonged drug exposure in patient plasma compared to the standard '7+3' induction therapy. Furthermore, the anti-leukaemic effect was superior to the conventional induction therapy due to CPX-351 liposomes accumulating preferentially in the BM relative to other tissues (H. P. Kim et al., 2011)(Tardi et al., 2009). Moreover, CPX-351 conferred a superior OS advantage in older patients with secondary AML (AML evolving from prior haematologic disorders such as MDS) compared to standard induction therapy (Lancet et al., 2018). Patients treated with CPX-351 had a higher median OS of 4 months and a higher CR rate of 12%. However, CPX-351 treatment was associated with increased bleeding events and delayed count recovery but decreases in other side effects including colitis, diarrhoea, and hair loss compared to traditional induction therapy. Nevertheless, CPX-351 has been FDA approved for adults older than 18 years of age with primary or secondary AML, and may replace the conventional induction therapy in the future.

While the inclusion of these new agents into the treatment regimen for AML has vastly improved the outcomes of patients with poor cytogenetic survival outcomes, they are not universal for all AML patients.

1.3. Mechanisms of Immune Escape in AML

In the 1970s, the proposed hypothesis of cancer immunosurveillance was that a healthy immune system could recognise and destroy nascent transformed cells, and that in order for the cancer to develop and thrive, it must learn to evade or shutdown the immune system of the host (Burnet, 1970). Leukaemia and other cancer entities often adapt via one or multiple mechanisms that increase central and peripheral tolerance to evade surveillance of the host's immune system.

Increased understanding in the past decades has demonstrated the critical role the immune system plays in maintaining equilibrium between physiological immune recognition and tumour growth known as 'immunoediting'. Under physiologic conditions, proteins of the human leukocyte antigen (HLA) encoded by the major histocompatibility complex (MHC) play a pivotal role in allowing the adaptive immune system to recognise foreign antigens. Both MHC class I and II proteins present peptides on the surface of nucleated cells for recognition by T cells. Peptides presented by MHC I found on the surface of all cells are recognised by $CD8^+$ cytotoxic T cells, whereas peptides presented by MHC II on the surface of antigen-presenting cells (APCs) such as macrophages, dendritic cells, or B cells are recognised by $CD4^+$ T helper (T_h) cells. Appropriate immune responses are elicited due to the differentiation of T_h effector cells towards T_h1, which augment cytotoxic T lymphocyte responses, or T_h2 cells, which are associated with humoral and allergic responses (Murphy & Reiner, 2002). In doing so, foreign antigens can be eliminated.

Under normal conditions, activated T cells are inactivated by signalling through inhibitory receptors following the clearance of an invading pathogen to prevent unwanted T cell-mediated damage to the host tissues. By contrast, tumour cells 'hijack' the hosts' immune system to its advantage and upregulate the expression of immunosuppressive molecules to avoid elimination by cytotoxic T cells (Blank et al., 2005).

The genetic instability of AML cells or other tumour cells allows for immune evasion from T cells by downregulating or altering its surface MHC molecules (Algarra et al., 1997). Diminished MHC I expression on the tumour cell can be attributed to the regulatory defects affecting downregulation of genes encoding MHC I complex along with the components of antigen processing and presentation, or due to structural defects of the MHC I complex as a result of chromosomal aberrations (del Campo et al., 2012). Furthermore, the loss of mismatched HLA haplotype in relapsed AML patients during transplantation settings is found to be an immune escape mechanism employed by the leukaemic cells in order to avoid killing by the immune cells from the graft (Vago et al., 2009)(Villalobos et al., 2010)(Toffalori et al., 2019).

Tumour cells have also been shown to release factors such as interleukin(IL)-6, IL-1β IL-10, TGF-β, and prostaglandin E_2 (PGE_2) in order to drive the accumulation and inhibitory function of myeloid derived suppressor cells (MDSCs) to the tumour microenvironment thereby polarising the immune response away from T_h1 cells leading to an ineffective immune (and often tumour promoting) response (Rosenberg, 2001)(Movahedi et al., 2008)(Ostrand-Rosenberg & Fenselau, 2018).

In a wide variety of cancers, including leukaemia, T_h17 cells have also been shown to promote tumour growth by releasing the immunosuppressive compound adenosine, or converting to T regulatory (T_{reg}) cells (Gagliani et al., 2015). Furthermore, the increased release of indolamine 2,3, dioxygenase (IDO) as well as the upregulated expression of inducible T cell co-stimulator ligand (ICOSL) on AML blasts stimulates T cells through the inducible T cell co-stimulator (ICOS) leading to differentiation and expansion of T_{reg} cells and inhibition of expansion of T effector (T_{eff}) cells (Han et al., 2018). In patients, large populations of T_{reg} cells have been observed in tumour tissue, lymph nodes, and PB, and have been associated with diminished T cell activity, disease recurrence, and decreased patient survival.

1.4. Immune Therapies for AML

1.4.1 Allogeneic Stem Cell Transplanation (allo-hSCT)

Cancer immunotherapies have transformed the therapeutic platform to treat r/r AML patients, in which its application is not dependent on their cytogenetic or molecular profile. Allo-hSCT is still arguably the first, most successful and curative form of immune based therapy, demonstrating the potent ability of the immune system to target the malignant clone, as evidenced by the powerful graft-versus leukaemia (GvL) phenomenon (Jenq & van den Brink, 2010). The procedure involves the transfer of MPPs (from the BM or PB) which have the capacity for self-renewal as well as cellular differentiation into various types of blood cells. The stem cells are derived from either the patient's own body (autologous), a donor with the same genetic background (syngeneic), or in most cases, from a genetically different donor (allogeneic) (Tuthill & Hatzimichael, 2010). The GvL effect is mediated by donor-derived NK and T cells which recognise minor histocompatibility antigens or tumour-associated antigens on the surface of the recipient cells.

Intensive chemotherapy regimens are known to cause BM toxicity in patients who are older, in patients who were initially heavily pre-treated, and in patients with co-morbidities leading to treatment-related mortality. These patients would benefit from allo-hSCT with a less toxic reduced intensity conditioning therapy to overcome such treatment-related toxicities. Despite the impressive curative rates in patients, allo-hSCT is still associated with relapses in a significant portion of patients. Additionally, most encounter pathogenic immune responses, with varying severity, against the non-haematopoietic tissues known as graft-versus-host-disease (GVHD), which is fatal in 15% of transplant recipients (Bleakley & Riddell, 2004) (Kolb, 2008).

1.4.2 Monoclonal Antibody Drug Conjugates

Monoclonal Antibodies (mAbs) specifically target surface antigens expressed on the leukaemia cell. While various myeloid surface antigens are being explored as potential targets for mAb therapies, CD33 (Siglec-3) is the antigen most commonly targeted to date.

The first mAb used for the treatment of AML is Gemtuzumab ozogamicin (GO or CMA-676), a humanised anti-CD33 monoclonal antibody conjugated to a DNA-damaging toxin, calicheamicin. GO was first FDA approved in 2000 based on a phase II trial demonstrating a 30% response rate with a RFS of 6.8 months in-first relapsed AML patients who previously received induction therapy (Bross et al., 2001)(Larson et al., 2005)(Burnett et al., 2012). However, a confirmatory study indicated that the addition of GO to induction therapy or GO used as a post-consolidation therapy had no significant improvement in CR, RFS or OS, but was in fact associated with a higher incidence of induction therapy mortality. In addition, GO was associated with hepatotoxicity and was therefore withdrawn from the market (Petersdorf et al., 2009)(Nabhan et al., 2004). More recently, new clinical trials with altered dosing of GO demonstrated an improvement in RFS and event-free survival in combination with induction therapy. These results were particularly profound in elderly patients considered ineligible for chemotherapy and in adult patients with favourable and intermediate cytogenetics. GO was re-approved by the FDA in September 2017 (Castaigne et al., 2014).

A newer anti-CD33 antibody conjugated to pyrrolobenzodiazepine, SGN-CD33A, demonstrated cytotoxicity in AML cell lines irrespective of multidrug-resistant status. In a Phase I r/r CD33$^+$ AML trial, almost 50% of patients demonstrated blast clearance with 27% achieving CR, of whom 73% were negative for MRD. In treatment-naïve patients, the efficacy was even greater with 54% achieving CR. Furthermore, SGN-CD33A has shown synergism with HMAs such as AZA, with a recently reported phase II study revealing >60% of patients achieving CR with an 8-week mortality of 5% in the older patients (Sutherland et al., 2010)(Fathi et al., 2015). In addition, IMGN779, another conjugated CD33 antibody has shown marked activity in pre-clinical studies. Most interestingly, its activity seems to be more selective to LSCs while sparing normal HSCs, suggesting potential for reduced myelosuppression. It is currently in a phase I trial for patients with r/r AML (NCT02674763) (Whiteman et al., 2014)(Krystal et al., 2015).

1.4.3 Bi-specific T cell Engager Antibodies

Bi-specific T cell engager (BiTE) antibodies are fusion protein constructs that consist of 2 single-chain fragment variants from 2 antibodies. One binds to the T cells via the CD3 receptor whereas the other binds to the tumour cell via a tumour-specific antigen. BiTE antibodies effectively recruit T cells and bring them in proximity to tumour cells thereby effectuating T cell mediated cytotoxic responses against tumour cells, independent of MHC I presentation or co-stimulatory molecules (Baeuerle & Reinhardt, 2009)(Nagorsen et al., 2009). Following the FDA approval of Blinatumomab, a CD19/CD3 BiTE antibody for the treatment of precursor B cell acute lymphoblastic leukaemia (B-ALL), a novel BiTE construct targeting CD33 was developed for AML, known as AMG 330. AMG 330 has demonstrated potent pre-clinical activity in CD33$^+$ AML with a Phase I clinical trial evaluating the efficacy of CD33/CD3 BiTE antibody therapy currently ongoing (NCT02520427) (Aigner et al., 2013)(Laszlo et al., 2014)(Harrington et al., 2015).

1.4.4 Immune Checkpoint Inhibitors

The most extensively studied immunosuppressive molecules are cytotoxic T lymphocyte antigen-4 (CTLA-4) and programmed cell death-1 (PD-1) which belong to the CD28 receptor family and bind to distinct members of the B7 family of ligands.

PD-1 is a surface glycoprotein cell receptor. PD-1 interaction with its ligands, namely programmed death-ligand 1 (PD-L1), also known as CD274 or B7-H1, prevents auto-immunity by inducing apoptosis of autoantigen-specific T-cells or by inhibiting T_{reg} apoptosis. PD-1 is also commonly expressed on B cells and NK cells (Yamazaki et al., 2002)(Giannopoulos, 2019). In AML, PD-1 expression was observed in $CD4^+$ effector, T_{regs}, and $CD8^+$ effector T cells both in untreated patients and in those with recurrent disease (Williams et al., 2019). The increased expression on these cells may explain the dysfunction and inhibition of the immune response during progressive AML. Moreover, PD-L1 has been detected on AML blasts. The upregulation of PD-L1 is possibly a result from pro-inflammatory cytokines such as interferon gamma (IFN-γ) produced by tumour infiltrating lymphocytes, and was associated with the negative course of the disease (Annibali et al., 2018)(Dong et al., 2002). Daver and colleagues (N. Daver et al., 2016) evaluated treatment-naïve and relapsed primary tumour samples to identify the expression of a variety of checkpoint receptors and ligands on the T cells and blasts from BM and PB and compared this to healthy donors (HD). In BM aspirates, patients with AML had significantly higher expression of PD-1, CD134 (OX40) and ICOS on T-cells compared to HD. This same group of investigators (N. Daver, Schlenk, et al., 2019) conducted a study combining the PD-1 inhibitor, nivolumab, with AZA, which produced an ORR of 34% in patients with r/r AML. Furthermore, these treated patients remained in CR for more than a year. PD-1 inhibitors are also being examined in various other clinical trials for its efficacy as maintenance therapy, post-induction or consolidation therapy for high-risk AML patients ineligible for allo-hSCT, as a combination regimen with induction chemotherapy in younger patients, and post-allo-hSCT relapsed patients (NCT02532231; NCT02464657; NCT01822509). Zeidner and colleagues (Zeidner et al., 2017) reported a 42% OR following administration of pembrolizumab after high-dose cytarabine salvage chemotherapy in patients with relapsed disease. Three of the twenty-six patients proceeded to allo-hSCT in CR or morphologic leukaemia free state (MLFS). However, anti-PD1 treatment following allo-hSCT showed modest efficacy, with some patients showing transient response and the remaining patients experiencing disease progression (Kline et al., 2018).

CTLA-4 is expressed on activated T cells, including T_{reg}, and regulates and mediates inhibitory signals to T cells. Additionally, it is also expressed on B cells and NK cells and binds to the ligands, B7.1 (CD80) and B7.2 (CD86). CTLA-4 is an important mediator of self-tolerance and tolerance to tumour antigens (Stojanovic et al., 2014)(Sage et al., 2014). Furthermore, overexpression of PD-1 and CTLA-4 on T-cells is reportedly associated with more aggressive leukaemia (Salik et al., 2020). Analysis of AML patient samples revealed 80% of tested samples at diagnosis constitutively expressed CTLA-4 on T cells (Laurent et al., 2007). Studies have shown that blockade of CTLA-4 enhances activation and amount of AML-targeting T cells. In support, another study showed that deletion or inhibition of CTLA-4 dampens the growth of murine myelogenous leukaemia through the induction of $CD8^+$ T cell immunity if the AML cells expressed the B7 molecules (LaBelle et al., 2002). A humanised anti-CTLA-4 monoclonal antibody, ipilimumab, is currently under clinical evaluation for patients with r/r AML (NCT01757639) or patients with progressive AML after allo-hSCT (NCT0822509, NCT00060372) following the FDA approval and favourable outcomes in metastatic melanoma and other solid tumour entities (Hodi et al., 2010)(Robert et al., 2011)(Calabrò et al., 2010). Davids and colleagues (Davids et al., 2016) reported that ipilimumab induced complete responses in five AML patients who mainly had leukaemia cutis or extra-medullary relapse after allo-hSCT as a single agent therapy and three of these patients remained in remission for more than a year.

More recently, the lymphocyte-activation gene-3 (LAG-3), T cell immunoglobulin (Ig) domain and mucin domain 3 (TIM-3) and the thymocyte selection-associated high mobility group box factor (TOX) have shown potential as alternative immunosuppressive molecules that can be targeted for treatment.

LAG-3 is a transmembrane protein homolog of CD4, expressed on NK cells, T_{reg} cells, γδ T cells, activated αβ T cells and B cells and binds to MHC II. $PD\text{-}1^+LAG\text{-}3^+$ expression on T cells exhibit an exhausted phenotype (Triebel et al., 1990)(Kisielow et al., 2005)(Huard et al., 1994). Interestingly, LAG-3 blockade on T cells demonstrated synergism with anti-PD-1 blocking suggesting the two signalling pathways have non-redundant and synergistic functions in dampening T cell responses (Anderson et al., 2016). In support of this, AML patients were found to exhibit higher $PD\text{-}1^+LAG\text{-}3^+$ T cells in the BM compared to HD (Williams et al., 2019). Furthermore, blockade of LAG-3 but not PD-1 in chronic lymphocytic leukaemia (CLL) patients revived T cell activation and function (Shapiro et al., 2017). A soluble form of LAG-3 (IMP321) which binds to MHC II and activates cytotoxic T cells has been evaluated in various solid tumour entities but not in AML (Teague & Kline, 2013).

TIM-3 shares a similar expression pattern as PD-1 and is expressed on T_h1 cells and T_h17 cells and binds to Galectin-9 inhibiting effector cytokine responses (Zhu et al., 2005). PD-1^+TIM-3^+ T cells were functionally deficient and strongly associated with leukaemia relapse in AML patients following allo-hSCT (Sakuishi et al., 2010)(Kong et al., 2015). Additionally, inhibition of TIM-3 in a mouse model demonstrated improved survival while combinatorial treatment of anti-TIM-3 and anti-PD-L1 were shown to induce synergistic effects.

Most recently, TOX has been identified to initiate the fate commitment, epigenetic and transcriptional programming of exhausted T cells. TOX is necessary for inducing canonical features of exhausted T cells, including the upregulation of inhibitory receptors, impaired cytolytic function and the expression of other transcription factors required for cell exhaustion (Khan et al., 2019)(Alfei et al., 2019). Epigenetic analysis revealed that exhausted T cells differ from T_{eff} and memory T cells (T_{mem}) and are therefore a distinct cell type (Sen et al., 2016). Moreover, T_{eff} and T_{mem} cells were able to form without the expression of TOX, whereas exhausted T cells could not (Khan et al., 2019). In support, recent mass cytometry studies of human $CD8^+$ T cells revealed that TOX was expressed in the vast majority of exhausted T cells from human immunodeficiency virus (HIV) or lung cancer patients (Bengsch et al., 2018). These observations are yet to be reported in other malignancies. However, these studies already provide a strong foundation for new therapeutic possibilities that modulate TOX and/or TOX-dependent epigenetic changes in exhausted T cells.

1.5 Chimeric Antigen Receptor (CAR) T cell Therapy

The effectiveness of cancer immunotherapies is based on antigen specificity of the T cells. Normally, the cytotoxic T cell response to a foreign entity is initiated through the T cell receptor (TCR) complex. This complex consists of the TCRα/β chains and the CD3γ/δ/ε/ζ subunits, which associate through hydrophobic interactions (Hedrick et al., 2005)(Malissen et al., 1984). Somatic DNA recombinations enables the generation of unique TCRα/β chains which are then responsible for the recognition of specific peptide MHC complexes (Saito & Germain, 1987). In order to elicit a response, antigen recognition triggers a signal through the TCR, specifically, the ζ subunit. The signal is transmitted through immunoreceptor tyrosine-based activation motifs (ITAMs) in the cytoplasmic tail (Letourneur & Klausner, 1992). The ITAMs are subsequently phosphorylated by protein tyrosine kinases, such as Lck, which recruit other intracellular effector molecules to interact with the TCR complex (Bu et al., 1995)(Courtney et al., 2018).

In the context of immunotherapies, the specificity for an antigen can be further enhanced by genetic modifications and redirection of the T cells towards antigens that are overexpressed on tumour cells. This approach aims to address the limitations associated with central and peripheral tolerance, enhancing the power of the immune response by generating T cells more efficient at targeting tumours without the requirement for *de novo* T cell activation in the patient (Sharpe & Mount, 2015). CAR T cells are currently the most notable and promising type of immune therapy. Its success has been demonstrated in certain types of leukemia, and is currently being explored for AML.

CARs are artificial TCRs that redirect the specificity, function, and metabolism of generic T cells following genetic modification using viral (retro-, lenti- or adenoviral) or non-viral technologies (electroporation, transposon-based, or gene-editing systems). The CAR comprises an extracellular domain consisting of the antigen binding moiety and a spacer region. There are various forms of the antigen binding moiety. However, the most commonly used is a single-chain fragment variable (scFv) derived from mouse mAb, humanised Abs or fully humanised Abs with the responsibility of recognising and binding to tumour-associated antigens (TAAs), expressed on the surface of the malignant cell. Unlike normal TCRs, the affinity and avidity is much higher between the interaction of the scFv and its target surface ligand. Furthermore, CARs recognise unprocessed antigens, as well as carbohydrate and glycolipid structures, typically expressed on the malignant cell surface irrespective of the patient's HLA type and antigen presentation through MHC. In bypassing MHC Class I and II restriction, both $CD4^+$ and $CD8^+$ CAR T cells can be recruited for redirected recognition of the target cell *(Figure 1.3)* (Schmidt-Wolf et al., 1991)(Vitale et al., 2005).

The spacer or hinge region is derived from either CD8 or IgG4 molecules that support the ligand-binding domain. The hinge is crucial for CAR expression on the cell surface as it affects the flexibility of the ScFv and hence their interaction with target cell ligand. The length of the hinge region can directly influence the quality of interaction between the T cell and target cell, depending on the position of the epitope to the target antigen. This suggests that there may be an optimal linker length between the two surfaces (Guest et al., 2005). The spacer region is connected to the transmembrane domain (TM) which, in turn, is connected with the intracellular signalling moiety. The most stable TM domain is CD28. Once the CAR engages the epitope on the target cell, a signal is transmitted to the intracellular signalling moiety. The intracellular portion consists of the concomitant co-stimulatory domain(s), which are critical for the increased secretion of cytokines, expansion and persistence of the CAR T cell, and the most important component being the CD3 ζ chain derived from the generic T cell which stimulates activation and cytolytic functions (Gill & June, 2015).

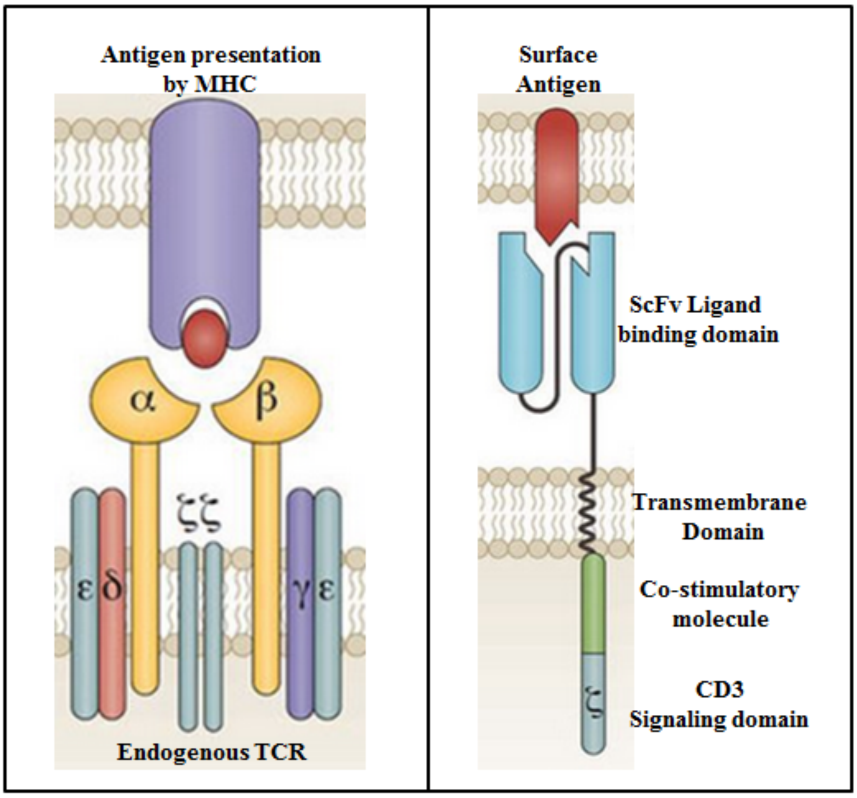

Figure 1.3. The difference between endogenous TCR and CAR T cell structure.
The endogenous TCR recognises the antigen which is processed endogenously and presented on the cell surface in the context of the specific HLA (left). The CAR recognises intact overexpressed cell surface proteins on the tumour cell and is based on the recognition machinery of a mAb, independent of HLA (right). The signalling domain of the CAR harnesses the ζ subunit of the endogenous TCR. *Illustration modified from Fujiwara H. 2014, International Journal of Hematology.*

Twenty-five years ago, the first publication (Eshhar et al., 1993) describing the genetic redirection of T cells to specific surface antigens only incorporated the CD3 ζ chain with no co-stimulatory molecule within the endodomain, and was termed the first-generation CAR (Maude et al., 2015)(Zhang et al., 2017)(Singh et al., 2016). It was only in recent years that co-stimulatory molecules were incorporated into the CAR structure, giving rise to second generation CARs (Finney et al., 1998). Second generation CARs are characterised by the dual signal for T cell activation: one triggered by the antigen recognition and another produced by the co-stimulatory molecule, the most common being CD28 or 4-1BB (CD137). The addition of the co-stimulatory molecule was shown to augment the effects of the CD3 ζ chain signalling by enhancing IL-2 synthesis to complete the activation of T cells, proliferation, persistence and avoid apoptosis *(Figure 1.4)* (Milone et al., 2009)(Singh et al., 2016)(Song et al., 2011)(Hombach et al., 2012).

Third generation CARs demonstrated enhanced responses by combining two co-stimulatory signals, most notably CD28, 4-1BB, OX40 (CD134) and CD27, with the CD3 ζ chain (Tammana et al., 2010)(Hombach et al., 2013). However, these enhanced responses may not necessarily result in better patient outcomes when compared to the second generation CARs. There are only few third generation CARs that are currently in clinical studies and therefore further studies are required to explore the potential benefits over second generation CARs as well as their safety and efficacy (Sadelain et al., 2013)(Priceman et al., 2015).

Recently, new models of CARs have emerged, such as CAR T cells redirected for universal cytokine killing (TRUCK cells). TRUCK cells produce and then release a transgenic product, such as IL-12 or IFN-γ. For instance, IL-12 activates innate immune responses against tumour cells while IFN-γ contributes to antigen-independent destruction of tumour cells through IFN-γ receptor on the tumour stroma (Yu et al., 2017)(Curran et al., 2015). Other models include dual or bi-specific CARs in order to bypass antigen loss and tumour escape. Bi-specific CARs are single transgenic receptors which recognise two distinct antigens, offering synergistic killing and enhanced function. The binding moieties for the two different antigens are in tandem and separated by a flexible hinge.

The idea is that if one target antigen is downregulated or mutated, the CAR is still functional and preserves the cytolytic capacity by targeting the second antigen (Grada et al., 2013). Studies by Wilkie and Kloss (Wilkie et al., 2012) (Kloss et al., 2013), investigated dual/bi-specific CARs in which two different CARs are co-expressed on the same T cell, each recognising a different tumour antigen and provides complementary signals. The premise is that only double-antigen positive tumours are eliminated. One CAR provides suboptimal CD3 ζ chain mediated activation while the other CAR that recognises the second antigen incorporates only the co-stimulatory molecule. T cell activation and effector functions only occur as soon as both CARs' targets are met. This provides CAR T cell specificity and prevents off-target effects (Ruella et al., 2016)(Wilkie et al., 2012)(Zah et al., 2016).

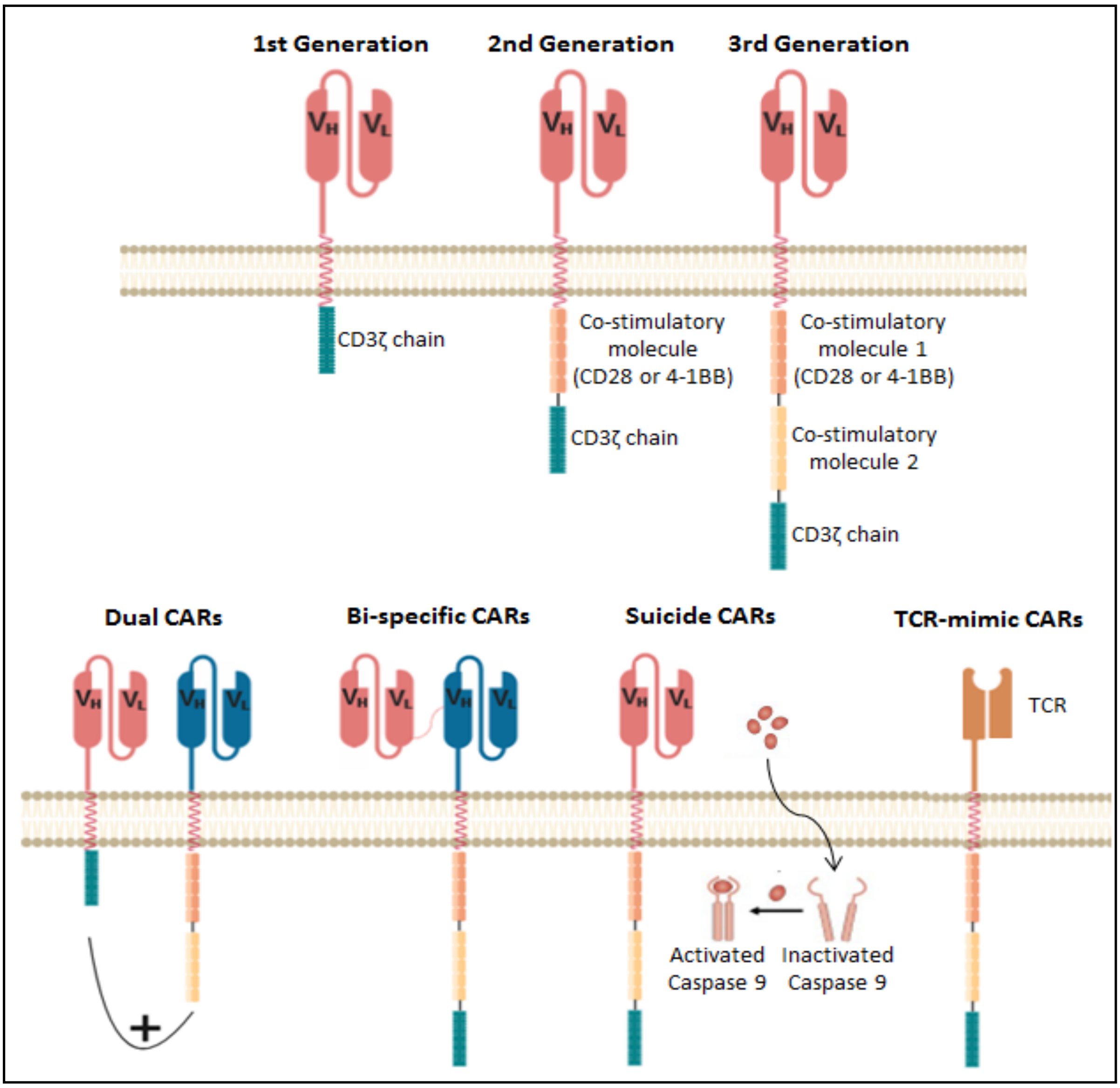
1st Generation
2nd Generation
3rd Generation
V_H
V_L
CD3ζ chain
Co-stimulatory molecule (CD28 or 4-1BB)
Co-stimulatory molecule 1 (CD28 or 4-1BB)
Co-stimulatory molecule 2
Dual CARs
Bi-specific CARs
Suicide CARs
TCR-mimic CARs
TCR
+
Activated Caspase 9
Inactivated Caspase 9

Figure 1.4. Chimeric antigen receptors currently under active investigation.
First generation CARs consist of the zeta-signalling domain of a TCR/CD3 receptor complex. In second and third generation CARs, one or co-stimulatory signalling domains are added (usually CD28, 4-1BB (CD137), OX40 (CD137), or ICOS) within the intracellular domain, respectively. More recently, new CAR designs are being tested. Dual-targeting CARs express two different antigen-specific CARs, whereas bi-specific CARs bear two linked ScFv within one CAR construct. Suicide CARs were designed as control mechanisms for better toxicity management of CAR T cells. The most notable is inducible caspase 9 (iCasp9). To address human leukocyte antigen (HLA)-presented antigens, TCR-mimic CARs directing the ScFv domain against a peptide-HLA complex are now being studied. *Illustration modified from (Hofmann et al., 2019).*

1.5.1 Anti-CD19 CAR T Cell Therapy: The Pioneer of CAR Technology

The breakthrough of CAR T cell therapy emerged in 2010 when several institutes developed a CAR targeting the CD19 antigen on B cells. Its use has engendered long-term anti-tumour efficacy and survival in pediatric and adult patients with r/r B cell malignancies, namely ALL, CLL, and B cell non-Hodgkins lymphoma (NHL). Kochenderfer and colleagues (Kochenderfer et al., 2010) at the National Cancer Institute (NCI) were the first to report on significant clinical responses in patients with advanced B cell malignancies using autologous CD19 CAR T cells. Phase I/II clinical trials revealed a 92% ORR, where 67% achieved CR. Furthermore, 4/7 patients with diffuse larger b-cell lymphoma achieved CR with CAR T cell treatment (Kochenderfer et al., 2015). The joint phase 1 clinical trial conducted at the Children's hospital of Philadelphia (CHOP) and the University of Pennsylvania (UPENN) pioneered the success of CD19 CAR T cell therapy with 90% (27/30) of heavily pre-treated paediatric and adult B-ALL patients achieving CR. This is a second generation CAR T cell product incorporating the 4-1BB co-stimulatory molecule (Imai et al., 2004). Subsequent dose-escalation studies using other second generation CD19 CAR T cells incorporating the CD28 co-stimulatory molecule performed at the NCI and the Memorial Sloan Kettering Cancer centre (MSKCC) validated the data seen at CHOP/UPENN with 70% (14/20) and 88% (14/16) of patients achieving CR/CRi (CR with incomplete count recovery), respectively (Maude et al., 2014)(D. W. Lee et al., 2015)(Davila et al., 2014) despite the differences in CAR construct design between these studies. This remarkable clinical result is credited to the high and ubiquitous expression of the CD19 antigen on the surface of the target cells which are B cells (Zhang et al., 2017)(Porter et al., 2011)(Grupp et al., 2013)(Kochenderfer et al., 2012). The expression of CD19 is also found on normal tissues, but is confined to the B cell lineage. Therefore, the predicted on-target off-tumour activity would be limited to B cell aplasia, a side effect which can be mitigated with periodic immunoglobulin-replacement therapy (June & Sadelain, 2018).

FDA approval of the first two CD19 CAR T cell products tisagenlecleucel (Kymriah, Novartis) and axicabtagene ciloleucel (Yescarta, Kite Pharma) was given in 2017. Tisagenlecleucel has been approved for r/r B-ALL in patients up to age 25, whereas both tisagenlecleucel and axicabtagene ciloleucel have been approved for patients with r/r large B cell lymphoma who have failed at least two lines of conventional therapy (Yip & Webster, 2018). The third CD19-targeted CAR T cells, lisocabtagene maraleucel (Breyanzi, Bristol Myers Squibb), was FDA approved in February 2021 for r/r large B cell lymphoma following two or more lines of therapy.

The successful proof-of-principle in utilising CAR T cells for the eradication of large tumour burdens is not accomplished without accompanied toxicities. Cytokine release syndrome (CRS) has been clinically documented as common complication following infusion of CAR T cells (Brudno & Kochenderfer, 2016)(Bonifant et al., 2016). Activated CAR T cells initiate the release of cytokines such as IFN-γ, tumour necrosis factor (TNF), granulocyte macrophage-colony stimulating factor (GM-CSF), and IL-2 in response to target antigen engagement on the tumour cell. This effect is manifested as physical symptoms in the patient such as fever, haemodynamic compromise and the production of IL-6 and other cytokines by activated macrophages (Lee et al., 2015). It is reported that the severity of CRS varies between patients, and directly correlates with the tumour burden. Clinically, CRS is currently managed by blocking IL-6 signalling with the IL-6 antagonist, tocilizumab or by suppressing cytokine production by immune cells with dexamethasone (Brudno & Kochenderfer, 2016)(Bonifant et al., 2016)(Murthy et al., 2019)(Maude et al., 2014)(Turtle et al., 2016)(Porter et al., 2011)(Sterner et al., 2019).

Furthermore, neurologic toxicities have been observed concurrently with or following CRS in a select number of patients where, in some instances, the cases have been fatal (Brudno & Kochenderfer, 2016)(D. W. Lee et al., 2015). The exact pathogenesis of neurotoxicity remains unclear. However, some studies have suggested that the elevated pro-inflammatory cytokines secreted by the CAR T cells and/or the activated macrophages contribute to increased endothelial activation thereby affecting the blood brain barrier permeability (Kochenderfer et al., 2012)(Maude et al., 2014)(Turtle et al., 2016).

1.5.2 CAR T cells for the Treatment of AML

The success of CAR T cells in B cell malignancies has encouraged the translation of this immune therapy approach to other haematological and solid organ malignancies. For AML, only few CARs have been clinically investigated to date. The vast majority of possible targetable antigens have only been investigated pre-clinically. An overview of the antigen candidates under clinical investigation are discussed below *(Figure 1.5).*

CD33

Based on the FDA approval of the above-mentioned GO drug-conjugated antibody, anti-CD33 CAR T cell therapy has been investigated extensively.

The MD Anderson Cancer Centre (MDACC) in the U.S are treating r/r AML patients with CD33 CAR T cells (NCT03126864) and will include paediatric patients if the treatment is safe and the dosage of infused cells is tolerable. The NCI and CHOP are developing a Paediatric

Bone Marrow Transplantation consortium-sponsored CD33 CAR T cell trial for children, adolescents, and young adults with r/r AML. Various clinical centres in China, mainly Beijing and Jiangsu, are assessing the safety of second-generation CD33 CAR T cells in patients with r/r AML (NCT02799680, NCT01864902, NCT02944162) (Hofmann et al., 2019)(Wang et al., 2015). To date, one report of a patient with r/r AML has been documented. The patient who was treated with anti-CD33 CAR T cells experienced pancytopenia and CRS, and had disease progression nine weeks following infusion (Wang et al., 2015). The patient's pancytopenia is unsurprising, as although the expression of CD33 is found in up to 90% of leukaemic blasts, it is also expressed on healthy myeloid progenitor and mature cells. In 2018, Kim M and colleagues (M. Y. Kim et al., 2018) demonstrated that genetic deletion of CD33 from normal haematopoietic stem and progenitor cells could allow AML specific CD33 CAR T cell anti-leukemic targeting without myelotoxicity.

Lewis Y

Lewis Y (LeY) is a carbohydrate antigen over expressed in a variety of epithelial and haematological cancers, while expressed at low levels on normal tissue. Peinert and colleagues (Peinert et al., 2010) reported the first Phase 1 clinical trial with anti-LeY CAR T cells for r/r AML patients. Four patients received an infusion of $1.3x10^9$ total T cells (CAR expression ranging from 14-38%). No severe toxicity was observed. One patient experienced transient cytogenetic remission, while the other patients showed transient blast reduction or stable disease. All patients relapsed within 23 months of CAR T cell infusion.

At the Peter MacCallum Cancer Centre in Melbourne, four adult AML patients have received a single dose of radioactively labelled second generation CAR T cells with specificity towards LeY (NCT01716364). Three patients exhibited MRD at the commencement of the study, while the fourth patient had 70% blast count in the BM at the time of CAR T cell infusion. Up to $1x10^9$ CAR T cells (transduction efficiency of 14-38%) were infused and single photon emission tomography imaging (SPECT) and quantitative polymerase chain reaction (qPCR) were used to track the CAR T cells and monitor the PB transgene levels. These analyses demonstrated localisation of the CAR T cells in the spleen and BM. Although transient responses or leukaemia reduction was observed in all patients, they all eventually relapsed (Ritchie et al., 2013).

NKG2D

More recently, other CAR T cell trials for r/r AML have emerged across the globe (Nikiforow et al., 2016)(Lonez et al., 2017). The most promising of these targets the transmembrane natural killer group 2D (NKG2D) C-type lectin-like receptor, or the NKG2D ligands (NKG2DL). While

NKG2DL has limited expression on healthy tissues on physiologic conditions, various types of cellular stress can up-regulate NKG2DL on normal tissues thereby potentially reducing specificity of NKG2D CARs for the malignant tissues (Sheppard et al., 2018). The Dana-Farber Cancer Institute reported a Phase I clinical trial where autologous NKG2D CAR T cells were infused into seven patients with AML. Interestingly, their construct is a first generation construct using the naturally-occurring NKG2D receptor as the antigen-binding domain, with endogenous DAP10 expression to provide the co-stimulation. CAR T cells were administered at varying doses without prior lymphodepletion. Unfortunately, persistence of the CAR T cell population was limited and no objective clinical responses were observed, with all patients requiring alternative therapies to manage AML progression (Baumeister et al., 2019). A subsequent trial for AML and MDS was conducted. Of the AML patients, one patient achieved a clinical response and proceeded to allo-hSCT, remaining in CR to date. An additional trial has been planned to investigate the combination of NKG2D CAR T cells in combination with AZA in allo-hSCT or intensive chemotherapy ineligible patients (NCT03612739).

CD123

CD123, a 360-amino acid containing glycoprotein, is composed of a 287-amino acid residue extracellular domain involving an Ig-like domain, two FnIII domains, a transmembrane domain of 30 amino acid residues and an intracellular domain of 53 residues. It is the transmembrane α-chain subunit of the IL-3 receptor. CD123 is the primary binding subunit for IL-3, and its high binding affinity with CD131 leads to the activation of the IL-3 receptor which promotes cell survival and proliferation (Testa et al., 2014).

The City of Hope, UPENN, Weill Cornell Medicine, MDACC, and Beijing medical centres are conducting Phase I/II CAR T cell trials targeting CD123. The initial study at the UPENN centre used a second generation CD123 CAR T cell harbouring the 4-1BB co-stimulatory molecule and demonstrated promising results where the majority of patients reached CR within a month following CAR T cell infusion. Unfortunately, this result was paired with significant on-target off-tumour toxicities, with the trial being terminated as a result. The protocol was later modified where the second UPENN study (NCT02623582) administered biodegradable RNA electroporated autologous CD123 CAR T cells every 48-72h in five adults with r/r AML. The premise of this study was to use the CD123 CAR T cells as a pre-conditioning treatment in place of chemotherapy prior to transplant. In addition, manufacturing feasibility, safety, and myelotoxicity side effects were studied. Unfortunately, CAR T cell production using RNA electroporation was suboptimal. Furthermore, all treated patients had leukaemia progression within a month of cell infusion (Cummins et al., 2017). As expected, the T cells did not persist given the short half-life of the messenger ribonucleic acid (mRNA) transduced cells. Interestingly, all patients experienced CRS necessitating tocilizumab treatment to manage the toxicity. No haematologic or neurologic side effects were observed. Given the lack of efficacy, the trial was terminated with new plans for the development of an inducible lentiviral based CD123 CAR T cell trial to be used as a bridge-to-transplant conditioning regimen (Cummins et al., 2017).

More notably, the City of Hope centre has currently infused six adults with relapsed AML following allo-hSCT with either $5x10^7$ or $1x10^8$ lentivirally transduced second generation CD123 autologous CAR T cells, containing the CD28 co-stimulatory molecule (MB-102), following lymphodepleting chemotherapy. If necessary, a second infusion was granted in select patients. One of two patients treated with the lower dose achieved a MRD level disease response following two infusions of CAR T cells. Two of four patients treated at the higher dose achieved CR following one infusion and subsequently underwent a second allo-hSCT. The other two patients treated at the higher dose only experienced a partial response. No dose limiting toxicity including myeloablation was observed in any of the patients and low-grade CRS was seen in some of the patients. A patient with blastic plasmacytoid dendritic cell neoplasm (BPDCN) was also treated at the City of Hope centre with CD123 CAR T cells. This patient also experienced CR and has not exhibited any toxicity to date (Xue & Budde, 2020). This CD123 CAR T cell, named MB-102, was granted orphan drug designation by the FDA for AML in July 2019.

Other Targetable Antigens Enrolled for Clinical Investigation

In China, cancer centres in Shenzhen and Guangdong are testing the safety of CD38, CD56, CD117, or Muc-1 CAR T cells in children and adults with r/r AML. These trials are currently ongoing and no data is available as yet *(Figure 1.5).*

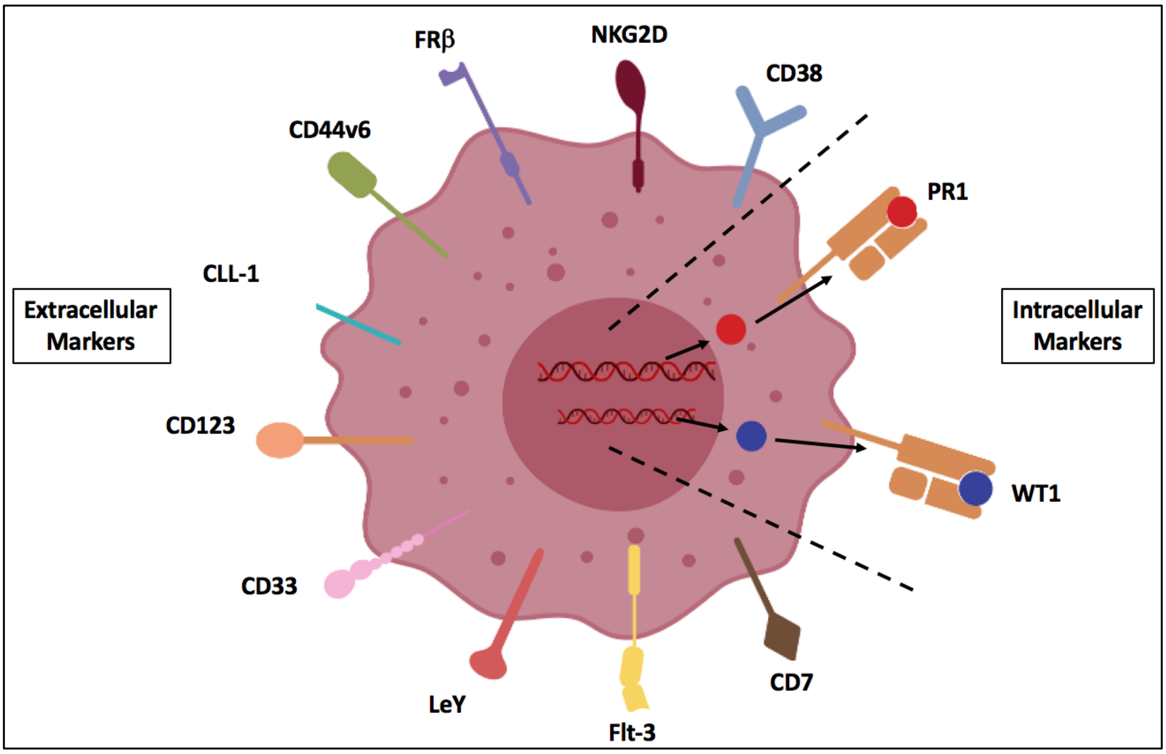

Figure 1.5. Potential targetable antigens for CAR T cell therapy in AML. Antigens are either recently identified and/or under investigation pre-clinically and clinically.

1.5.3 Bench to Bedside Challenges of CAR T cells for AML

Despite the numerous pre-clinical and clinical studies demonstrating highly efficacious cytotoxic potential of various AML antigen-targeting CAR T cells, this has not been reflected by any FDA approval. The successful utilisation of immunotherapies, in particular for targeted cellular approaches such as CAR T cell therapy, firstly requires the identification of a suitable target antigen. Ideally, the target antigen should possess attractive therapeutic features; most importantly, it should be universally and stable expressed at high levels on the malignant cell surface of all patients in order to induce clinically meaningful anti-tumour effects by the CAR T cells and be absent on the healthy hematopoietic cells in order to avoid hematotoxicity (Cheever et al., 2009).

The ideal target antigen should, therefore, be restricted to and be highly expressed on patient malignant cells, especially on malignant stem cells where they were previously refractory to other modes of treatment. This highlights inherent challenges and risks that hinder the success of CAR T cell treatment for patients with AML because these challenges are, in most part, due to the heterogeneous nature of the disease and therefore the paucity of identifying well-defined TAAs. While most patients may exhibit high expression levels of one targetable antigen, others may express that same antigen at much lower levels. Additionally, the current identified library of targetable antigens on AML blasts and LSCs, while over-expressed, are not exclusively restricted to the malignant cells and have been shown to overlap with normal haematopoiesis (Cheever et al., 2009).

As a consequence, it is possible for CAR T cells to damage tissues that express the antigen recognised by the CAR on normal cells. This phenomenon is called on-target off-tumour toxicity (Brudno & Kochenderfer, 2016). Targeting such antigens with CAR T cells raises safety concerns as the severity of off-tumour toxicities is unpredictable. In one study, CARs targeting carboxy-anhydrase-IX for patients with metastatic renal cell carcinoma resulted in liver toxicities while CEA-specific CAR T cells in colon cancer patients induced severe colitis (Lamers et al., 2006)(Parkhurst et al., 2011). In addition, high antigen load on tumour as well as healthy tissues can also elicit severe side effects such as CRS when targeted with highly reactive T cells. For example, CAR T cells targeting human epidermal growth factor receptor 2 (HER2) caused fatal CRS due to the recognition of low levels of HER2 expressed on the surface of normal lung epithelial cells (Liu et al., 2017). In consideration of these serious consequences reported in these studies and various other clinical trials, methods to reduce on-target off-tumour toxicity are currently under investigation.

AIMS & SIGNIFICANCE

Phase I clinical trials using CAR T cells that target various antigens in AML have resulted in either transient leukaemia cell clearance or complete clearance of leukaemia, however, at the expense of severe on-target off-tumour toxicities.

Based on the information provided from previously published data on CAR T cells for AML at the commencement of the project, this thesis addresses four specific aims, which attempt to enhance the feasibility and employment of CAR T cell therapy for AML. Specifically, these aims use a systematic approach in developing a third generation CAR capable of enhancing the inherent anti-tumour immunity of the T cells without propagating additional on-target off-tumour toxicities. The high relapse rates and treatment resistance in r/r AML patients is associated with significant mortality.

Furthermore, patients who are unable to receive allo-hSCT and have failed other therapeutic treatments have significant unmet clinical need. Given the attractiveness of CAR T cell technology, this project will ensure that the preparation of therapeutic immune cells will be sufficiently robust, scalable, effective, feasible, and safe for wider use in patients with CD123$^+$ malignancy.

Specific Aim #1: To determine the feasibility of employing CAR T cells for AML by targeting the CD123 antigen.

The *hypothesis* of this aim is that CD123 is over expressed on AML stem and progenitor cells and remains as the most suitable target for development of third-generation CARs.

Expression of CD123 will be analysed on BM mononuclear cells (BMMNC) from AML patients and compared to healthy BMMNC samples. Current therapies are effective at eliminating bulk leukaemia cells but inefficient at targeting the stem cells that are capable of re-populating disease once therapies are ceased. It is therefore important to ensure that the target antigen is expressed at high levels on the primitive cells of AML samples, and is absent or has low expression on HD samples.

Specific Aim #2: To optimise the humanised mRNA based anti-CD123 CAR constructs for AML using a lentiviral delivery approach as a clinical platform for delivery into individual human T cells.

The *hypothesis* of this aim is that optimisation of the conditions required for lentiviral delivery will allow for consistent and high-scale production of anti-CD123 CAR T cells.

The humanised CSL362 (CD123) mAb has previously been established and evaluated pre-clinically and clinically against AML, with promising results. In collaboration with this group, the CSL362 sequence was constructed into a ScFv. The ScFv will subsequently be cloned into 4 third-generation CD123 specific CARs signaling through (i) extended IgG4-CD28-OX40 and CD3ξ (CD123-CD28-OX40-LF), (ii) short IgG4-CD28-OX40 and CD3ξ (CD123-CD28-OX40-SF), (iii) extended IgG4-CD28-41BB and CD3ξ (CD123-CD28-41BB-LF), and (iv) short IgG4-CD28-41BB and CD3ξ (CD123-CD28-41BB-SF), using lentiviral based delivery for stable CAR expression in T cells. The process for cloning, lentivirus production, and transduction of T cells will be optimised to ensure efficient and consistent production of the CD123 CAR T cells.

Specific Aim #3: To investigate the *in vitro* functional attributes of the anti-CD123 CAR T cells.

The *hypothesis* of this aim is that CD123-specific CARs will re-direct the specificity of T cells to target AML cells and induce AML clearance while sparing healthy cells.

To address this aim, the 4 CAR constructs will be transduced into HD human T cells and subjected to multiple functional assays to assess whether the CD123 CAR T cell function is specific for CD123. Additionally, the results will reveal which of the 4 CAR constructs is most suitable for further development and evaluation *in vivo*. To achieve this, the following experiments will be conducted to evaluate CAR specificity in response to CD123^{+} targets compared to CD123^{-} targets as negative controls.

1. CD107a T cell degranulation assay
2. T cell proliferation
3. T cell cytokine production
4. T cell cytotoxicity
5. Colony formation assay
6. Phenotypic analysis of CD123 specific CAR T cells

Specific Aim #4: To investigate the short and long term *in vivo* efficacy of the anti-CD123 CAR T cells.

The *hypothesis* of this aim is that the most functionally superior CD123 specific CAR identified from the *in vitro* evaluation is capable of leukaemia cell clearance and establishing a T cell repertoire *in vivo* responsible for long term tumour surveillance and prolonged remission.

CD123^{+} leukaemia xenografts will be established in immunocompromised *Rag2*$^{-/-}$*Il2rγ*$^{-/-}$ recipients which will be treated with CD123 CAR T cells to evaluate leukaemia clearance *in vivo*. Additionally, the CD123 CAR T cells will be extensively evaluated for CD4 or CD8 T cells following *in vitro* expansion, prior to infusion in mice and following infusion into mice. Sub-phenotypic analysis will also be performed to evaluate the memory and effector cell populations and whether changes in these cell populations contribute to leukaemia clearance and propagate long term control of AML. If required, the application of combined treatment with demethylating agents will also be explored with the aim of enhancing long term survival.

Chapter 2

TARGET ANTIGEN EXPRESSION OF CD123 ON PRIMARY AML TUMOUR SAMPLES

2.1 Introduction

Based on published literature, CD123 represents an attractive target for the treatment of r/r AML patients given its preferential overexpression on the majority of CD38$^+$ leukaemic blast progenitor cells, including CD34$^+$ CD38$^-$ primitive LSCs (Jordan et al., 2000)(Testa et al., 2004). These studies reported that CD34$^+$ CD38$^-$ CD123$^+$ cells purified from primary AML samples were able to initiate and maintain the leukaemic process when introduced into immunodeficient mice, and therefore act as LSCs (Jordan et al., 2000). Testa and colleagues (Testa et al., 2004) further demonstrated that CD38$^+$ leukaemic blasts overexpressing CD123 exhibited higher cycling activity and increased resistance to apoptotic triggering elicited by growth factor deprivation. More importantly, the overexpression of CD123 on AML blasts was associated with increased cellularity at diagnosis and was associated with poor risk features (e.g. Flt-3 ITD mutations) which conferred a poor prognosis (Rollins-Raval et al., 2013).

Riccioni and colleagues (Riccioni et al., 2011), demonstrated that the enhanced and deregulated signalling conferred by IL-3R and Flt-3 contributed to the survival and proliferation of CD123^{hi} expressing leukaemic blasts in AML patients. Interestingly, high CD123 expression correlated with IL-3R β_c and GM-CSFRα expression, suggesting a concomitant overexpression of IL-3R and GM-CSFR (Riccioni et al., 2009). These findings provide convincing evidence that CD123 is an attractive therapeutic target for AML patients, mainly due to the antigen overexpression on LSCs and its association with patients with high-risk disease.

CD123, on the other hand, is reportedly expressed at low levels on some subsets of normal myeloid haematopoietic cells such as monocytes, myeloid dendritic cells and eosinophils, although others suggest otherwise (Jordan et al., 2000). For example, many studies have explored the expression of CD123 on normal CD34$^+$ cells, progenitor cells and various sub-populations isolated from various sources, including foetal liver, cord blood (CB), BM and PB. Sato and colleagues demonstrated that a portion of CD34$^+$ cells isolated from CB express CD123 and that the expression increases following the growth of these cells in the presence of cytokines. However, the primitive population of heamatopoietic progenitor cells (HPCs) expressed low or absent CD123 levels (Sato et al., 1993). Furthermore, other studies defined three subsets of CD34$^+$ cells with differing CD123 expression. Cells that were CD123^{bright} were myeloid and B-lymphoid progenitors, and CD123^{negative} cells were erythroid progenitors. CD123^{low} expressing cells contained a heterogeneous population of early and committed progenitor cells (Huang et al., 1999)(Manz et al., 2002). More recently, Testa and colleagues (Testa et al., 2014)., demonstrated similar results showing that CD123 expression during haematopoietic differentiation was sustained in the granulocytic lineage and moderately decreased in monocytic differentiation. In contrast, other studies (Jordan et al., 2000) (Al-Mawali et al., 2017) argue that CD123 is very lowly expressed on normal $CD34^{+}CD38^{-}$ BM stem cells, in particular, the regenerating stem cells. Jordan and colleagues (Jordan et al., 2000) demonstrate clearly that approximately 7% of total normal BM expresses CD123, with 1% of these cells expressing the antigen at high levels. Furthermore, CD123 expression on bulk $CD34^{+}$ cells were readily evident (12%). However, the primitive $CD34^{+}CD38^{-}$ compartment showed <1% CD123 expression.

Nevertheless, a variety of therapeutic methods to target CD123 in myeloid malignancies have been developed. Initials studies were based on using the natural ligand of IL-3, fused with a cytotoxic drug. SL-401 (Tagraxofusp) is a genetically engineered fusion toxin composed of the first 388 amino acids of the diphtheria toxin fused with a His-Met linker, and fused to human IL-3. Pre-clinical studies showed that the level of cytotoxicity was directly proportional to CD123 expression on leukaemic cells. Furthermore, cells with LSC properties were also vulnerable to SL-401(Yalcintepe et al., 2006)(Testa et al., 2005) . Recent studies have reported that SL-401 induced potent cytotoxic activity against $CD123^{+}$ AMLs and myelodysplastic syndrome blast cells. However, some activity against normal haematopoietic progenitor cells was observed (Mani et al., 2018).

The development of the humanised IL-3R mAb, CSL362 (Taclotuzumab), displayed capacity to neutralise IL-3, with potent antibody-dependent cytotoxicity against AML cells (Busfield et al., 2012). In patients, CSL362 was insufficient for the treatment of r/r AML as a monotherapy (Xie et al., 2017). Pharmacodynamic studies of the mAb revealed dose-dependent decreases of peripheral basophils and plasmacytoid dendritic cells (pDCs). No effect on the haematopoietic progenitor/stem cells was observed (Lee et al., 2012). Currently, combination treatments, such as with demethylating agents, are being explored. Furthermore, the development of the CD123-targeting antibody drug conjugate, IMGN632, demonstrated potent anti-leukaemic effects both *in vitro* and *in vivo* and was shown to be >40 fold less cytotoxic to normal myeloid progenitors than its native comparison counterpart. Importantly, the doses used that exerted anti-leukaemic effects were well below those causing cytotoxic effects to myeloid progenitors (Kovtun et al., 2018). In support of these findings, a phase I evaluation (NCT03386513) for r/r $CD123^{+}$ haematological malignancies demonstrated response in 33% of patients. Additionally, the antibody drug conjugate was well tolerated and no major myeloablative or adverse events were observed (N. G.

Daver et al., 2018). The development of a bi-specific fusion anti-CD123 and anti-CD3 mAb, on the other hand, was found to decrease $CD14^+CD123^+$ monocytes but had minimal effect on $CD34^+$ progenitors *in vitro*. These observations were mirrored in r/r AML patients (Al-Hussaini et al., 2016).

As previously mentioned, CD123 has been explored as a possible target for CAR T cell therapy. To date, all developed anti-CD123 CAR T cells, albeit second or third generation, exhibited potent anti-leukaemic activity in pre-clinical and clinical evaluation. However, the inhibitory effect on normal BM cells was variable. Tettamanti and colleagues introduced their third generation CAR into cytokine induced killer (CIK) cells and exhibited limited myeloablative effects on BM stem and progenitor cells in humanised xenograft models (Pizzitola et al., 2014)(Tettamanti et al., 2013). As previously mentioned, Mardiros and colleagues (Mardiros et al., 2013) similarly did not observe any depletive effect on normal haematopoietic progenitors by their second generation CAR. In contrast, Gill and co-workers reported a marked inhibition of normal haematopoietic cells in a model of humanised immunodeficient mice. This myeloablative effect was subsequently reflected in their phase I clinical trial (Gill et al., 2014).

The contrasting findings reported by the different pre-clinical and clinical work has caused a continued debate as to whether targeting CD123 on leukaemic cells occurs at the expense of prolonged off-target toxicity of specific normal myeloid cell subsets. There is emerging data that speculates that these off-target toxicities are, in some part, associated with CAR design and not necessarily only due to its low expression on certain haematopoietic cells (Drent et al., 2017)(Drent et al., 2019). These studies suggest that in such cases where there is low expression of the antigen on normal cells, the CARs can be, in fact, affinity tuned thereby maintaining cytotoxic capacity against tumour cells while sparing normal cells (Drent et al., 2017)(Drent et al., 2019)(Mardiros et al., 2013)(Arcangeli et al., 2017)(Bôle-Richard et al., 2020).

2.2 Rationale of the Chapter

This chapter investigates the expression levels of CD123 on key primary AML leukaemic populations, including LSCs, in order to develop CAR T cell therapy for the treatment of r/r AML. The expression of CD123 on AML leukaemic populations are also compared to that of HD samples to ensure that the target antigen exhibits a discriminatory expression pattern and, therefore, the propensity for off-tumour toxicity is significantly reduced. In addition, this chapter validates if the expression levels of this antigen on AML and HD cells are concordant with previously published literature.

2.3 Materials & Methods

Patient and HD Samples. Cryopreserved AML patient samples were obtained from the South Australian Cancer Research Biobank (SACRB), Adelaide, Australia. Using patient clinical notes, AML patient samples with a high percentage (⩾50%) of myeloblasts at diagnosis were selected for immunophenotypic analysis. For data comparison, HD mononuclear cells were obtained from aspirated BM which had undergone Lymphoprep (STEMCELL Technologies, Vancouver, BC, Canada) density gradient centrifugation (Appendix 6.4.3) and cryopreserved until use. The study was approved by the Australian institutional Human Research Ethics Committee *(Ethics approval no. R20150526 HREC/15/RAH/221)* and conducted in accordance with the Declaration of Helsinki.

Flow Cytometry. The following antibodies (Appendix 6.2.3) were purchased from BD Biosciences, San Jose, CA, USA, Biolegend, San Diego, CA, USA or Beckman Coulter, Fullerton, CA, USA, and used for phenotypic analysis on freshly thawed BMMNC (Appendix 6.4): Live dead Aqua-V500, CD13-PeCy7, CD33-V450, CD34-AF700, CD38-ECD, CD90-BV650, Lin-cocktail (CD3, CD14, CD16, CD19, CD20, CD56)-PB, CD123-PerCPCy5.5, and CD45RA-PeCy7. Cells were washed twice with ice cold FACS Buffer (general) (Appendix 6.3) and $5x10^6$ cells were aliquoted for the full stain panels, unstained, and fluorescence minus one controls (FMO). Live dead aqua fixable viability stain (LDA) was used to define viable cells. For surface staining, cells were incubated with titrated antibody *(Table 2.1)* for 30mins on ice in the dark. Cells were washed twice with ice cold FACS buffer (general) and re-suspended in 200µL FACS buffer (general). Cells were acquired with the BD LSR Fortessa™ X-20 (BD Biosciences). Data acquisition was performed using FACSDiva software (BD Biosciences) and data analysis via FlowJo v10.1 (FlowJo, LLC, Ashland, OR, USA). Instrument setup including fluorescence amplification (voltages) and compensation was optimised using compensation beads (BD Biosciences). Flow cytometer performance was checked regularly using CS&T beads (BD Biosciences). Cell populations of interest were reported as a proportion of total lymphocytes, derived from side scatter (SSC) vs. forward side scatter (FSC) gated lymphocytes, with doublet exclusion (FSC-A vs FSC-H), and dead cell discrimination (LDA^-). A minimum of $1x10^6$ events were acquired for the full panel stained tubes. Unstained and FMO controls were used to identify gating boundaries.

Table 2.1. HD and AML Immune Phenotyping Staining Panel

Antibody	**Fluorochrome**	**Titrated antibody volume/test (µL)**
Live Dead Aqua	V500	2
CD34	Alexa Fluor 700	4
CD38	ECD	5
CD123	PerCP-Cy5.5	15
CD13	PeCy7	5
CD33	V450	5

Data Representation & Statistical Analysis. Statistical analysis and graphs were prepared using GraphPad Prism v7 software (GraphPad software Inc, La Jolla, CA, USA). Unpaired Student's *t*-test (Mann-Whitney test) was used for comparing differences between groups. P-value of ≤.05 was considered significant.

2.4 Results

2.4.1 CD123 Expression in AML versus HD BM Primitive Cell Populations

In order to investigate the practicality of CD123 for CAR T cell therapy against AML, the expression of this antigen was investigated on bulk AML cell populations and LSCs on 32 primary BM diagnostic samples from patients who subsequently had r/r AML. The antigen expression on AML cells was compared with 10 BM HD samples. The AML samples had varying disease cytogenetics and were classified as either intermediate or poor risk prognosis based on the ELN classification (Döhner et al., 2010) *(Table 2.2.)*.

Table 2.2. Patient Characteristics of the Primary AML BM Samples.

Patient	Cytogenetics	Risk Group
1	Normal	Intermediate
2	Normal	Intermediate
3	Normal	Intermediate
4	Normal	Intermediate
5	Monosomy 7q	Poor
6	Normal	Intermediate
7	Normal	Intermediate
8	Trisomy 8	Intermediate
9	Normal	Intermediate
10	Normal	Intermediate
11	t(5,10); tri21	Intermediate
12	Trisomy 8, trisomy 19, 11q- and marker chromosome X 3	Poor
13	Normal	Intermediate
14	Del9q; trisomy21	Intermediate
15	Normal	Intermediate
16	Normal	Intermediate
17	Normal	Intermediate
18	Normal	Intermediate
19	Normal	Intermediate
20	Normal	Intermediate
21	11q23 rearranged, trisomy 21	Intermediate
22	Del6q	Intermediate
23	Normal	Intermediate
24	Normal	Intermediate
25	Flt3-ITD$^+$	Poor
26	Trisomy 8	Intermediate
27	Flt3-ITD$^+$	Poor
28	Flt3-ITD$^+$	Poor
29	Normal	Intermediate
30	Normal	Intermediate
31	Del5q; Monosomy 7	Poor
32	Trisomy 11	Intermediate

Multiple tumour cell subpopulations were assessed according to the gating strategy depicted in *Figure 2.1*. CD123 expression was analysed in the following AML and HD populations: viable CD13$^+$CD33$^+$, CD34$^-$, CD34$^+$, CD38$^+$ blasts, CD34$^+$CD38$^-$ LSCs/HSCs and CD34$^+$CD38$^+$ progenitor cells *(Figure 2.2-A)*.

CD34 is a primitive stem cell marker, whose positive expression is determinant of poor prognosis in AML, in particular, following allo-hSCT. Expression of CD34 is found on leukaemic blasts in a small subset of AML patients, and this is dependent on the maturation stage and lineage commitment of the leukaemic cells. Of the 32 AML samples, 44% were CD34$^+$ presenting with >20% positive cells, while the remaining 56% had CD34$^-$ blast cells. The bulk CD38$^+$ blasts exhibited a median CD123 expression of 54.4% (range 8.3%-96.9%).

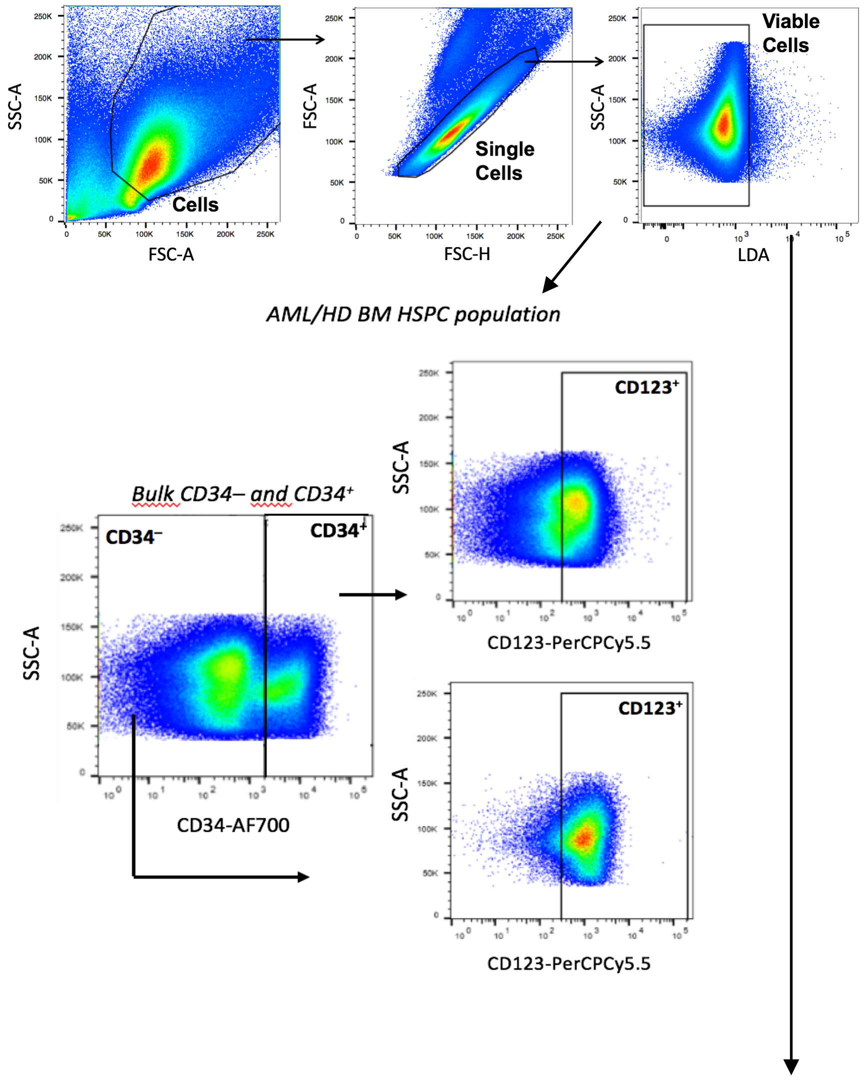

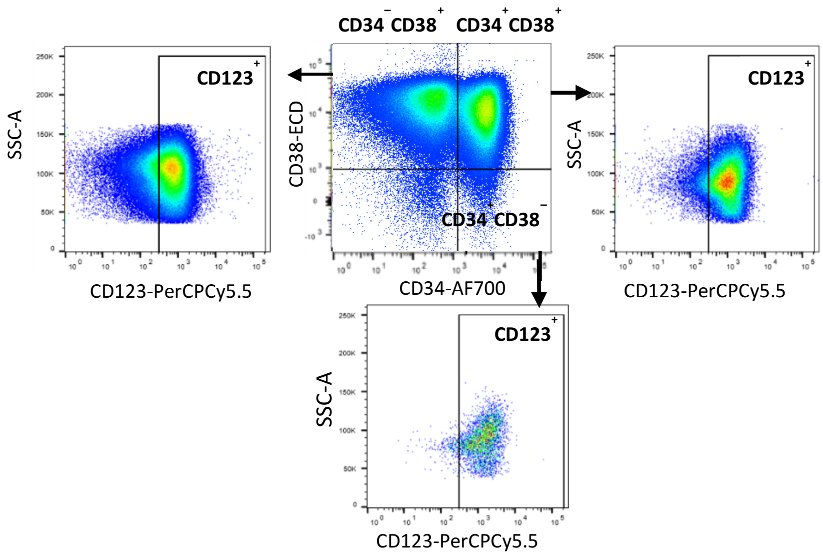

Figure 2.1. Representative flow cytometry gating strategy used to evaluate CD123 expression on AML and HD stem and progenitor cells.

Gates were first set on bulk AML or HD cells (SSC v FSC), following this; viable single cells were defined based on FSC-A v FSC-H and exclusion of dead cells by live dead aqua viability stain (LDA$^-$). Cells were then gated for bulk CD34$^+$ or CD34$^-$ and analyzed for their CD123 expression. Subsequently CD34$^+$ cells were further analyzed for their CD123 expression on primitive populations: CD38$^+$ blasts, CD34$^+$CD38$^+$, and CD34$^+$CD38$^-$.

In the CD34$^+$ population, the median CD123 expression level was 68.9% (range: 17.7%-96.1%) while the CD34$^-$ cell population exhibited median CD123 expression of 50.2% (10.4%-95.2%) *(Figure 2.2-B and D)*. In HD samples, it is expected that the majority of cells are phenotypically CD34$^-$ rather than CD34$^+$ (Lemos et al., 2018). Of the 10 samples, the median CD34$^-$ expression was 94.3% (range: 90.5%-98.5%) whilst the median CD34$^+$ expression was 2.2% (range: 0.5%-3.4%). Within the CD34$^-$ cells, the median expression of CD123 was 1.03% (range: 0.4%-4.8%) while the CD34$^+$ population showed a median CD123 expression of 2.3% (range: 0-6.3%). The results demonstrate that CD123 was expressed at significantly lower levels in the HD cohort than in the AML cohort *(Figure 2.2-B and D)*.

The CD34$^+$ population was further differentiated into CD34$^+$CD38$^-$ stem cells and CD34$^+$CD38$^+$ progenitor cells to determine if there were differences in the CD123 expression in these populations. CD34$^+$CD38$^-$ AML LSCs revealed a median CD123 expression of 68.6% (range: 11.1%-97.5%). The more mature CD34$^+$CD38$^+$ progenitor cells revealed a similar median CD123 expression of 66.9% (range: 18%-96.9%). In the HD cohort, the overall CD123 expression was significantly lower in the HSC and progenitor cell populations compared with the AML samples *(Figure 2.2-C and E)*.

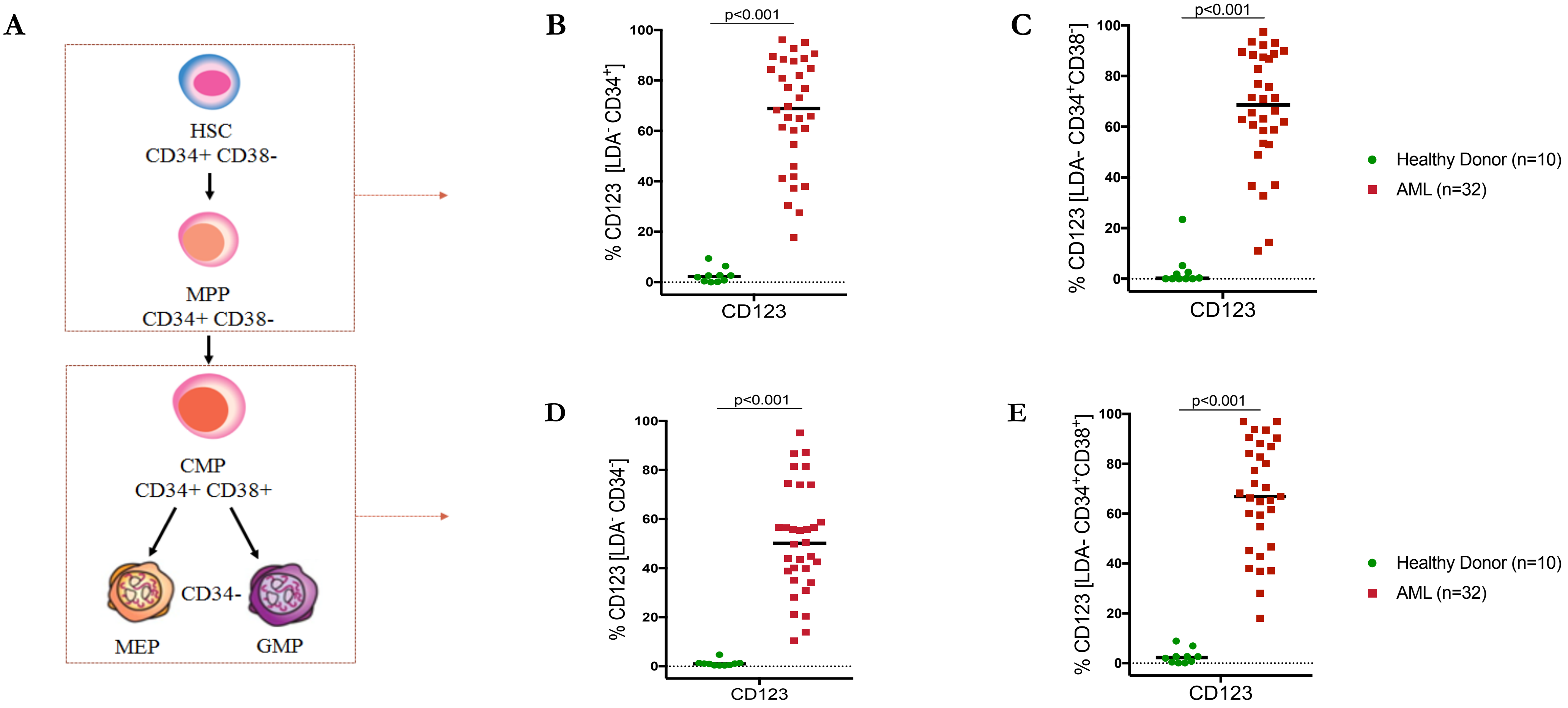

Figure 2.2. Differential expression of CD123 in AML patients compared to HD.
(A) Schematic of myeloid lineage haematopoiesis depicting the basic immune-phenotypic changes during differentiation. Primitive and differentiated cell populations from relapsed/refractory AML patient BMMNC samples (n=32) at diagnosis were analysed and compared to HD (n=10) BMMNC samples for CD123 expression on **(B)** CD34$^+$ bulk primitive cells, **(C)** CD34$^+$CD38$^-$ HSC/MPP populations, **(D)** CD34$^-$ bulk mature/differentiated cells and **(E)** CD34$^+$CD38$^+$ CMP populations by flow cytometry. Gates were set on bulk AML or HD cells (SSC v FSC), following this; viable single cells were defined based on FSC-A v FSC-H and exclusion of dead cells by live dead aqua viability stain (LDA-). Bars denote the median, with significance defined as p≤0.05.

2.4.2 CD123 Expression in Bulk AML Myeloid Cells versus HD

In addition to these data, AML and HD cells were gated for CD13$^+$CD33$^+$ cells, which represent the bulk myeloid cell population. Differential expression of CD123 was analysed in this population. From the live bulk myeloid population, AML samples exhibited a median CD123 expression of 60.4% (range: 18%-97.8%). By contrast, the median CD123 expression (0.63%, range: 0-2.96%) was minimal in the HD cohort *(Figure 2.3).*

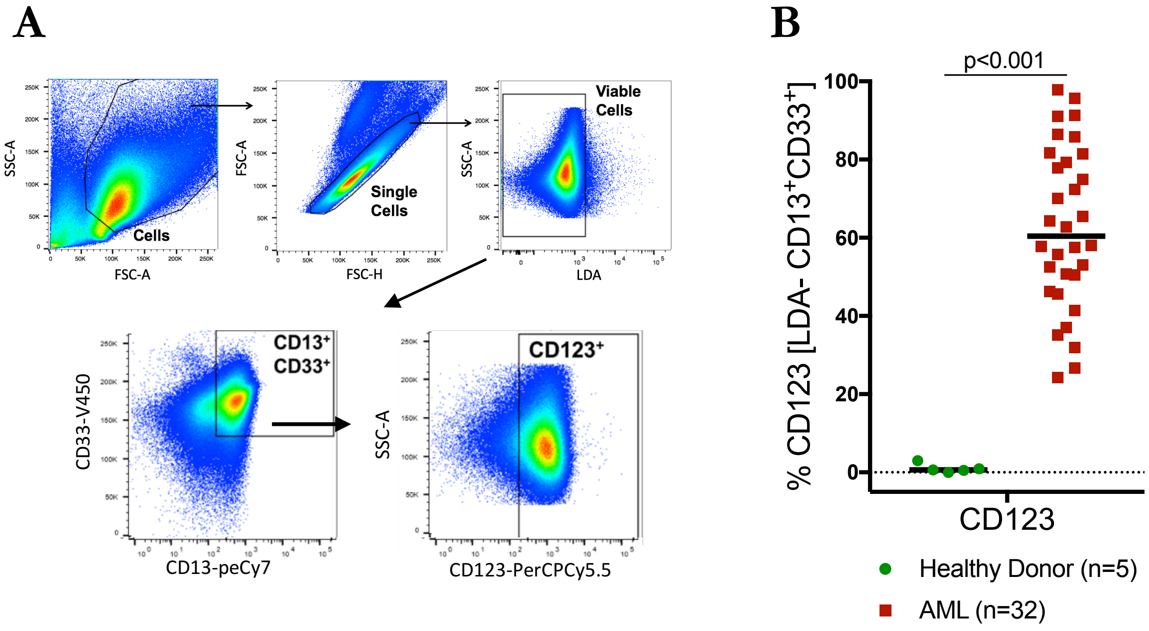

Figure 2.3. Differential expression of CD123 in AML patients compared to HD on bulk myeloid cells.

(A) Representative flow cytometry gating strategy used to evaluate CD123 expression on AML and HD CD13$^+$CD33$^+$ myeloid cells. **(B)** Bulk myeloid cells (CD13$^+$CD33$^+$) from relapsed/refractory AML patient BMMNC samples (n=32) at diagnosis were analysed and compared to HD (n=5) BMMNC samples for CD123 surface expression by flow cytometry. Gates were set on bulk AML or HD cells (SSC v FSC), following this; viable single cells were defined based on FSC-A v FSC-H and exclusion of dead cells by live dead aqua viability stain (LDA$^-$). Bars denote the median, with significance defined as $p \leq 0.05$.

2.4.3 Association of CD123 Expression with Poor Risk Cytogenetic AML Patients

Relapse of AML is thought to reflect the failure of current therapies that adequately target the rare and resistant LSCs, which are presumed to be responsible for maintenance of leukaemia, and typically enriched in the $CD34^+CD38^-$ cell population. The propensity to relapse following treatment is also higher in patients with poor risk cytogenetics (E. Estey, 2016). The mean CD123 expression was therefore examined and compared in 7 out of the 32 AML patients who had poor-risk cytogenetics. $CD34^+$ AML blasts were observed in 4/7 patients while 3/7 patients displayed a $CD34^-$ blast phenotype. On AML $CD38^+$ blasts, CD123 expression was high in 3/7 patients, ranging from 56.6%-93.5%, moderate in 3/7 patients (20.2%-38%) and low in 1 patient (9.7%) *(Table 2.3).*

Within the $CD34^+CD38^-$ AML LSCs, 5/7 patients had high CD123 expression (58.8%-86.8%), including one patient with 5q- and monosomy 7 cytogenetics while the remaining 2 patients expressed moderate CD123, 36.7% and 48.9% *(Table 2.3).*

Table 2.3. Comparison of CD123 expression on blasts and stem cells in poor risk cytogenetic AML patients.

Patient	**Genotype/Cytogenetics**	**Risk Group**	**%CD123 Expression** Blasts $CD38^+$	 Stem Cell $CD34^+CD38^-$
1	Monosomy 7q	Poor	38.0	48.9
2	Complex (tri8, tri19, 11q- and marker chr x3)	Poor	23.8	36.7
3	Normal (secondary AML; preceded by CMML)	Poor	9.7	62.0
4	Normal (Flt-3 ITD^+)	Poor	93.5	82.7
5	Normal (Flt-3 ITD^+)	Poor	56.6	86.8
6	Normal (Flt-3 ITD^+)	Poor	92.6	82.8
7	Complex (5q- and monosomy 7)	Poor	20.2	58.8
		Mean=	**47.8**	**65.5**

2.5 Conclusion & Discussion

Relapse in AML is defined as the ability of LSCs to perpetuate leukaemic cell expansion during treatment (treatment refractoriness) or following the discontinuation of treatment. Around 50% of patients in CR will eventually experience a relapse as a result of these tumour-initiating LSCs which can evade therapy and lay dormant during conventional treatments. It is therefore vital that novel treatments target not only the bulk and circulating tumour load but most importantly, these LSCs. For the past several years, many biomarker studies have aimed to uncover surface markers strictly found on LSCs. In the context of AML, it has become increasingly clear that most reported markers are not unique to LSCs but are in fact overexpressed on LSCs whilst being expressed, albeit at very low levels, on some healthy tissues.

This chapter assessed the expression profile of CD123 as a potential target antigen based on previous reports and preliminary works demonstrating clear distinctions in expression between AML and healthy tissues. Based on the results, the target was subjected to further development for CAR T cell therapy and pre-clinical assessment as a potential treatment for r/r AML.

CD123 expression was analysed in several haematopoietic subpopulations including CD34$^-$, CD34$^+$, CD38$^+$ blasts, CD34$^+$CD38$^-$ LSCs/HSCs, CD34$^+$CD38$^+$ progenitor cells and bulk myeloid CD13$^+$CD33$^+$ cells. In AML, the stem cells are contained within the population of putative primitive CD34$^+$CD38$^-$ cells. It was, therefore, important to verify that the target antigen exhibited higher over-expression in this population of cells while ensuring low to absent expression of the antigen on normal, healthy cells to avoid potential prolonged toxicities.

CD123 was expressed in 97% of AML patients, regardless of whether the main blast population was CD34$^+$ or CD34$^-$. In most of the populations analysed, the majority of AML patients had very high expression of CD123, which was consistent with previous reports (Ho et al., 2016)(Jordan et al., 2000)(Testa et al., 2004). It is well known that AML is a heterogeneous disease, and the expression profile of antigens can vary between patients. Therefore, it was unsurprising to observe a widely distributed expression profile in the AML cohort for both of these antigens. In 7/32 patients that were classified as having a poor prognosis based on their cytogenetic profile, there was also heterogeneity in the expression of CD123 in the blast cell and LSC populations. In the HD cohort, CD123 showed minimal expression in the CD34$^-$, CD34$^+$, CD38$^+$ blasts, CD34$^+$CD38$^-$ LSCs/HSCs and CD34$^+$CD38$^+$ progenitor cell populations.

CD123 was consistently expressed at low levels in the HD cohort in the majority of the populations analysed even though previous findings demonstrated that CD123 is found on the surfaces of monocytes, dendritic cells and other healthy tissues of the myeloid lineage (Gill et al., 2014)(Mardiros et al., 2013). These studies also acknowledged that targeting CD123 may result in off-tumour toxicities because of its expression on these various healthy tissues. In the CD34$^-$, CD34$^+$, CD38$^+$ blasts, CD34$^+$CD38$^+$ progenitor and CD13$^+$CD33$^+$ myeloid cell populations, the AML sample with the lowest CD123 expression did not overlap with the highest CD123 expressions found in the HD cohort. In the CD34$^+$CD38$^-$ LSC population, with the exception of one HD sample, the CD123 expression also did not overlap between the two groups. Based on the data and those previously published (Mardiros et al., 2013), it seems unlikely that myelotoxicity should occur if targeting CD123. However, this is contrary to studies published by Gill and colleagues (Gill et al., 2014), where significant myelotoxicity was encountered when targeting CD123 with anti-CD123 CAR T cells.

Some studies have argued that for myelotoxicity to occur, the minimum antigen density threshold or 'lytic threshold' needs to be reached (Arcangeli et al., 2017)(Caruso et al., 2015). Based on this hypothesis, if the maximum antigen density on the HD cell is lower than the 'lytic threshold' then it is very unlikely for off-tumour toxicities to occur. This is therefore dependent on the type of epitope and structural design of the CAR. This could, in part, explain the myelotoxicity exhibited by the anti-CD123 CAR T cells in Gill's publication. The antigen densities and lytic thresholds were not assessed or compared in this project for CD123 on AML or HD cells. Nonetheless, it is important to clarify whether myelotoxicity occurs in an individual setting as the construct design varies between research institutes.

For pre-clinical and, later, clinical development, it was necessary to ensure that: 1) the antigen was highly expressed on leukaemic cells and low on HD cells, 2) there was minimal or no overlap in expression between the AML and HD samples, and most importantly, 3) the majority of AML samples exhibited overexpression of the antigen on the putative CD34$^+$CD38$^-$ LSCs.

The data verified the overexpression of CD123 on primary AML cells, including LSCs, thereby deeming it a suitable candidate for further pre-clinical development. Conveniently, the mAb for CD123 has already been developed and assessed in pre-clinical studies by our collaborators, demonstrating its effective anti-tumour activity and minimal off-tumour toxicities (Herzog et al., 2012)(Busfield et al., 2012). The CSL362 (CD123) humanised mAb was therefore employed in the development of the scFv structure and used to develop the anti-CD123 CAR constructs used in the project.

Chapter 3

IN VITRO FUNCTIONAL CHARACTERISATION OF THE THIRD GENERATION CD123 CAR CONSTRUCTS FOR AML

3.1 Introduction

Since the introduction of CAR T cell therapy, the optimal design of the CAR is still, at present, a source of debate. Two of the three FDA approved CD19-specific CARs, tisagenlecleucel (Kymriah) and lisocabtagene maraleucel (Breyanzi), incorporate CD137 (4-1BB) as the co-stimulatory endodomain, whereas the third, axicabtagene ciloleucel (Yescarta), utilises CD28. While all three CARs have demonstrated striking clinical efficacy, the specific co-stimulatory domain used has been shown to critically determine the function, differentiation, metabolism, and persistence of these engineered T cells. In the majority of the CAR T cell pre-clinical and clinical models to date, the CD28 or 4-1BB are the best-known signalling domains incorporated into second-generation CAR structures.

In these studies, all CARs incorporating CD28 or 4-1BB CARs were shown to induce Th_1 cytokine secretion such as IL-2, TNF, IFN-γ, and GM-CSF. However, the secretion of these cytokines was brisker in CD28 CARs due to the significantly higher levels of IL-2 compared to 4-1BB CARs. While IL-2 is a critical cytokine for CAR T cell proliferation and sustains effector function, its possible effect on inducing T_{reg} cells, on the other hand, is undesirable due to its immunosuppressive effects (Loskog et al., 2006)(Savoldo et al., 2011). CARs incorporating CD28 have therefore demonstrated increased T cell proliferation, increased cytokine secretion upon target recognition, and improved anti-tumour effects *in vivo* (Kowolik et al., 2006). In contrast, CARs containing 4-1BB elicit cytokine secretion, upregulation of anti-apoptotic genes and enhanced *in vivo* persistence. As a result, CARs containing 4-1BB have so far shown the most durable results in patients (Imai et al., 2004)(Tammana et al., 2010)(Carpenito et al., 2009)(Pulè et al., 2005). Following the demonstration that CD28 and 4-1BB motifs are effective in providing co-stimulation, a range of other co-stimulatory domains have been assessed including the Ig superfamily member, the Inducible T cell co-stimulator (*ICOS*, CD278), and other members of the tumour necrosis factor receptor (TNFR) superfamily members such as OX40 (*TNFRSF4,* CD134).

CD278 is found to bind its ligand and activates the PI3K/Akt pathway within T cells in the same manner that CD28 does (Fos et al., 2008). Compared to CD28, CD278 is found to induce greater PI3K activity but is unable to recruit growth factor receptor-bound protein 2 (Grb-2) resulting in reduced IL-2 expression (Harada et al., 2003). Pre-clinically, second generation CAR T cells incorporating the ICOS co-stimulatory domain demonstrated greater PI3K activation compared to CARs using 4-1BB (Finney et al., 2004). Moreover, ICOS-based CARs demonstrated greater T_h1/T_h17 polarisation of T cells exhibiting improved anti-tumour activity and persistence compared to the CARs using CD28 or 4-1BB. Concordant to the statement reported by Harada and colleagues (Harada et al., 2003), ICOS-based CARs were also found to produce lower levels of IL-2 than CD28-based CARs (Paulos et al., 2010)(Guedan et al., 2014). Like 4-1BB, OX40 is not involved in the initial T cell activation but is found to be essential for T cell proliferation and survival and acts via the PI3K/Akt and tumour necrosis factor receptor-associated factor (TRAF) pathways. Moreover, OX40 co-stimulation has been found to antagonise the activation and development of natural and inducible T_{regs} by supressing CTLA-4, TGF-β, and forkhead box P3 (FOXP3) expression (Croft et al., 2009).

It was therefore postulated that incorporating two co-stimulatory endodomains (third generation CARs) could enhance the activity of the CAR T cells. Xenograft studies have demonstrated that third generation CAR T cells encompass the tumouricidal capacity of CD28-based CARs with the persistence generated by 4-1BB based CARs. Zhao and colleagues (Zhao et al., 2015) observed that their third generation CAR, with the CD28 domain situated proximal to the membrane and the 4-1BB domain distally, led to increased T_h1 T cell expression, increased $CD4^+$ and $CD8^+$ expansion, and improved tumour regression in B-ALL xenografts when compared to second generation CAR T cells. Furthermore, lower doses of third generation CAR T cells were required to achieve full anti-tumour capacity compared to the second generation counterparts.

In a clinical dose-escalation study, Ramos and colleagues (Ramos et al., 2018) infused a combination of second and third generation CAR T cells to patients with r/r B-NHL. In 10 of the 11 patients, up to a 40-fold greater expansion of third generation CAR T cells was observed compared to second-generation CAR T cells with a higher number of third generation CAR T cells remaining detectable up to 160 days post-infusion. Furthermore, third generation CAR T cells were found to expand significantly following infusion in patients who achieved remission following allo-hSCT. This suggested that third generation CAR T cells were capable of eradicating minimal residual disease in patients and lead to longer remissions (Ramos et al., 2018)(D. W. Lee et al., 2019). Additionally, no treatment-related mortality has so far been reported in clinical trials using third generation CAR T cells and the toxicity rates (CRS and neurotoxicity) observed are comparable with the second generation CAR T cell therapies (Schuster et al., 2019)(Enblad et al., 2018)(Neelapu et al., 2018). Despite the promising results so far, several clinical factors remain unknown. In particular, it remains unknown what the clinically optimal dose of third generation CAR T cells are that leads to improved clinical efficacy without increased toxicity risk. The combination of the co-stimulatory domains in a single CAR construct might elicit tonic CAR signalling, leading to CAR T cell exhaustion, thereby paradoxically reducing activity.

Hombach and colleagues (Hombach & Abken, 2011) elegantly demonstrated that in the absence of IL-2, second generation CAR T cells, against the carcinoembryonic antigen (CEA), encompassing different co-stimulatory motifs differentially impact cytolysis. The CARs with CD28 or OX40 motifs demonstrated superior target cell lysis compared to CARs with 4-1BB. IFN-γ secretion was comparable across the various CARs. However, T-cell response was increased in the CARs with OX40 whereas the 4-1BB motif can be a negative regulator of some T cell functions. Concordant with many published data, 4-1BB was shown to be a potent enhancer of clonal CD8$^+$ T cell expansion which led to enhanced persistence of CD8$^+$ CAR T cells. Nevertheless, (Hombach & Abken, 2011)(Hombach et al., 2012) constructed a third generation CAR with the CD28 and OX40 motifs instead of CD28 with 4-1BB since OX40 co-stimulation in a combined CAR enforces cytolysis in the absence of IL-2 leading to improved differentiation and survival of memory T cells. The third generation CAR was able to improve CD28-mediated effector functions and increase naïve and memory T cells. In contrast to the second generation CAR T cells, the third generation CAR was able to secrete substantially higher levels of IL-2 thereby sustaining T cell expansion.

3.2 Rationale of the Chapter

It can be appreciated that CAR design can influence the efficacy against target cells and therefore should be evaluated on a case-by-case manner. At the commencement of this project, third generation CAR T cells, targeting the CD123 antigen, for AML were yet to be reported. This project aimed to analyse how differences in the hinge region and the incorporation of different combinations of the two co-stimulatory motifs could affect the functionality and longevity of the CAR T cell against AML cells. Long hinge spacers have been found to provide extra flexibility and allow for better access to membrane-proximal epitope whereas CARs bearing a short hinge are more effective at binding membrane-distal epitopes (Watanabe et al., 2016). The length of the spacer is therefore crucial in providing adequate intercellular distance for immunological synaptic formation. Furthermore, the combinations of co-stimulatory signalling domains were compared to determine which combination delivered superior efficacy.

This chapter therefore aimed to directly compare the novel CARs designed for this project. Based on the literature, it was hypothesised that the CAR constructs incorporating the short hinge and the CD28-4-1BB co-stimulatory motifs would lead to stronger binding capacity, elicit superior downstream activation and efficacy against target cells, and promote longevity following leukaemia clearance.

In order to effectively evaluate the efficacy of these constructs, the delivery of such vectors into primary human T cells with high efficiency was explored and refined. The chosen method of CAR delivery into T cells was using a lentiviral-based system. Replication-deficient pseudotyped lentiviral vectors have been widely used as a basic tool in biological research. These HIV-derived lentiviral vectors are produced in a third generation system, with increased biosafety, by transfecting vectors that incorporate a self-inactivating long terminal repeat (LTR) regions together with the transgene of interest in one vector, with additional transcripts required for packaging, namely, Gag/pol, Reverse Transcriptase (Rev) and encapsulation (Env) on separate packaging plasmids (Pistello et al., 2007)(Mátrai et al., 2010). The ability of recombinant lentivirus to transduce primary human T cells still remains a challenge. Efficient gene transfer in primary T cells can therefore be laborious. While methods for lentiviral transduction of CAR T cells are now widely published, the protocols and materials used may vary between facilities. Therefore, the standard operating protocols always require optimisation. The optimised protocol should therefore result in CAR T cells produced with effective anti-leukaemic capacity as well as the ability to be traceable. Furthermore, the protocol should also allow for reproducibility and result in products of high quality.

In this chapter, the CD123 scFv sequence from the humanised CSL362 antibody was introduced into four novel third generation lentiviral-based CAR constructs and characterised *in vitro*. This chapter describes the cloning methodology, the optimised delivery of the CAR constructs into HD derived T cells via lentiviral-based transduction and finally, *in vitro* evaluation for their ability to target the human CD123$^+$ cell line, KG1a and MOLM-13, without demonstrating non-specific activity against the CD123$^-$ cell line, SUPB15. The construct that combined the highest and most effective antigen-specific effector functions against AML cells was chosen for further pre-clinical development *in vivo*.

3.3 Materials & Methods

CSL362 scFv Design. CSL362 is a humanised and affinity-matured antibody of 7G3, previously established and characterised by the project collaborators (Busfield et al., 2012). The CSL362 based scFv amino acid sequence was constructed by collaborators (Dr. Stanley Yu) to include a CD8α leader sequence followed by the V_L and V_H sequence which is connected by a $(G4S)_3$ linker sequence (sequence constructed using Benchling Life Sciences R&D, San Francisco, USA) *(Figure 3.1)*.

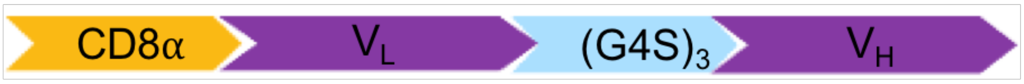

```
MALPVTALLLPLALLLHAARPDIVMTQSPDSLAVSLGERATINCESSQSLLNSGNQKNYLTWYQQKPGQPPKP
LIYWASTRESGVPDRFSGSGSGTDFTLTISSLQAEDVAVYYCQNDYSYPYTFGQGTKLEIKRTVAAPSVFIFPPS
GGGGSGGGGSGGGGSEVQLVQSGAEVKKPGESLKISCKGSGYSFTDYYMKWARQMPGKGLEWMGDIIPS
NGATFYNQKFKGQVTISADKSISTTYLQWSSLKASDTAMYYCARSHLLRASWFAYWGQGTMVTVSSASTKG
```

Figure 3.1.The anti-CD123 (CSL362) humanised scFv amino acid sequence incorporated into the third generation CAR T cell expression construct.

pPHLV-A Lentiviral Expression Vector. The plasmid DNA encoding for the pPHLV-A lentiviral vector *(Figure 3.2)* was a kind gift from Professor. John Hayball (The University of South Australia, Adelaide, Australia) and contains the LTRs of the HIV- type 1, responsible for driving transcription of the inserted gene. The vector also contains the psi (ψ) packaging signal downstream of the 5' LTR which is necessary for the encapsulation of the inserted genome into viral particles (Rivière et al., 1995).

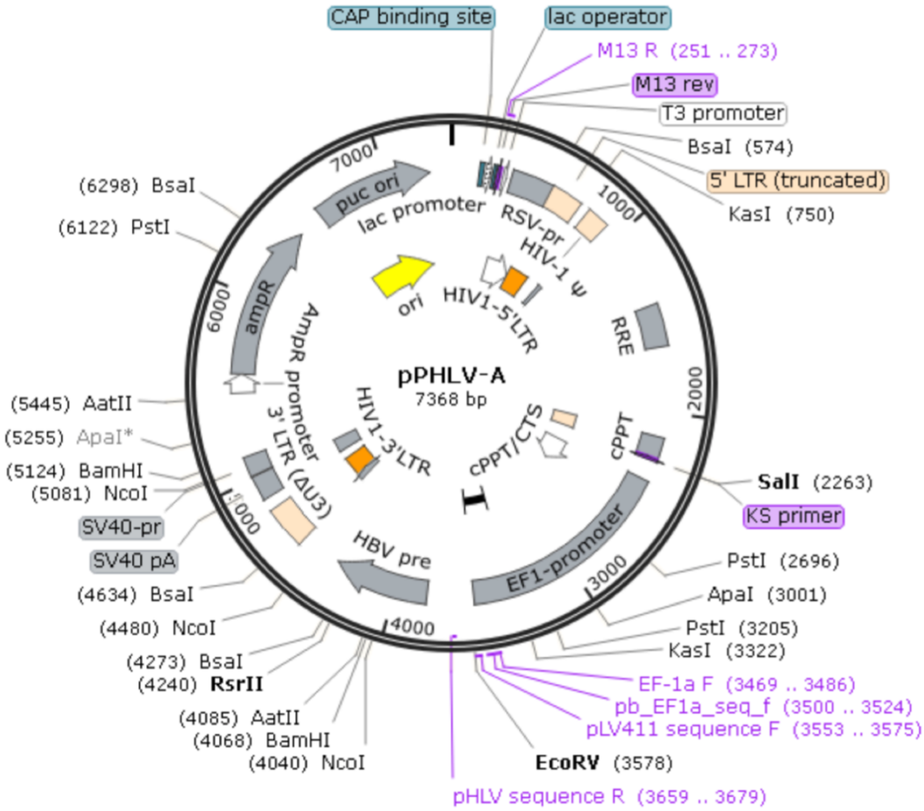
CAP binding site
lac operator
M13 R (251 .. 273)
M13 rev
T3 promoter
BsaI (574)
5' LTR (truncated)
KasI (750)
(6298) BsaI
(6122) PstI
(5445) AatII
(5255) ApaI*
(5124) BamHI
(5081) NcoI
SV40-pr
SV40 pA
(4634) BsaI
(4480) NcoI
(4273) BsaI
(4240) RsrII
(4085) AatII
(4068) BamHI
(4040) NcoI
SalI (2263)
KS primer
PstI (2696)
ApaI (3001)
PstI (3205)
KasI (3322)
EF-1a F (3469 .. 3486)
pb_EF1a_seq_f (3500 .. 3524)
pLV411 sequence F (3553 .. 3575)
EcoRV (3578)
pHLV sequence R (3659 .. 3679)
pPHLV-A
7368 bp
1000
2000
3000
4000
5000
6000
7000
puc ori
lac promoter
RSV-pr
HIV-1 ψ
ori
HIV1-5'LTR
RRE
ampR
AmpR promoter
3' LTR (ΔU3)
HIV1-3'LTR
cPPT/CTS
cPPT
EF1-promoter
HBV pre

Figure 3.2. Schematic representation of the pPHLV-A lentiviral expression vector.

CSL362-based CAR Designs.

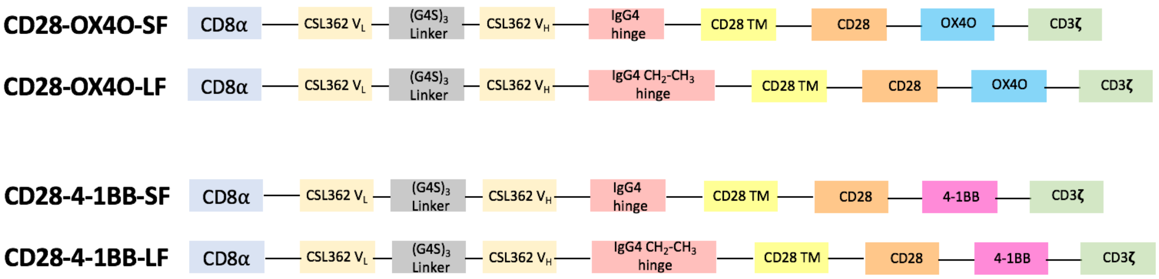
CD28-OX4O-SF
CD8α
CSL362 V_L
$(G4S)_3$ Linker
CSL362 V_H
IgG4 hinge
CD28 TM
CD28
OX4O
CD3ζ
CD28-OX4O-LF
CD8α
CSL362 V_L
$(G4S)_3$ Linker
CSL362 V_H
IgG4 CH_2-CH_3 hinge
CD28 TM
CD28
OX4O
CD3ζ
CD28-4-1BB-SF
CD8α
CSL362 V_L
$(G4S)_3$ Linker
CSL362 V_H
IgG4 hinge
CD28 TM
CD28
4-1BB
CD3ζ
CD28-4-1BB-LF
CD8α
CSL362 V_L
$(G4S)_3$ Linker
CSL362 V_H
IgG4 CH_2-CH_3 hinge
CD28 TM
CD28
4-1BB
CD3ζ

Figure 3.3. The anti-CD123 (CSL362) humanised scFv amino acid sequence incorporated into the third generation CAR T cell expression construct.

Construction of the CD123-CD28-OX40 CARs. Plasmids encoding for the short hinge CD123-CD28-OX40 (OX40-SF) and the long hinge CD123-CD28-OX40 (OX40-LF) CAR DNA sequence (Appendix 6.1) were generated by sub-cloning through an intermediate vector (pENTRY) and introduced into the pPHLV-A expression vector *(Figure 3.2-3.5).*

Restriction Digestion of plasmids, agarose gel electrophoresis, and gel extraction of CAR DNA fragments

pENTRY anti-CD123-CD28-OX40 LF and SF plasmids were previously generated and provided by collaborators (Dr. Stanley Yu, CCB, South Australia). 32µL (5µg) of DNA was digested with 4µL of digestion buffer (NEB), and 2µL each of the XbaI and AatII restriction enzymes overnight at 16°C. Meanwhile, 32µL of the pPHLV-A expression vector was digested with 4µL digestion buffer, 2µL of dH_2O and 2µL of EcoRV restriction enzyme. 5µL of the digested pENTRY plasmid was combined with 2µL loading dye and run on a 0.8% gel containing 5µL of gel red dye at a speed of 100amp for 45mins-1h. 3µL of the 1kb DNA ladder was loaded as reference. The smaller band containing the CAR fragment DNA sequences (~2200bp for LF and ~1520bp for SF) was recovered by cutting the band from the gel and placed in an eppendorf. The eppendorf was heated at 37°C to melt the gel. The plasmids were treated with the polymerase chain reaction (PCR) purification kit as per manufacturer's instructions (Invitrogen) to purify the DNA of interest from any remaining dNTPs and enzymes. The digested anti-CD123-CD28-OX40 LF and SF DNA fragments were blunted with 10µL buffer, 1µL Klenow and 0.4µL of 10mM dNTP. The mixture was incubated at 25°C for 15mins. 2.2µL of 500mM EDTA (final concentration of 10mM) was added and the mixture deactivated at 75°C for 20mins. The blunted fragments were re-treated with the PCR Purification kit. The digested pPHLV-A vector was dephosphorylated with 4µL buffer, 1µL antarctic phosphatase and incubated at 37°C for 30mins and subsequently inactivated at 80°C for 2mins. The dephosphorylated vector was similarly treated with the PCR purification kit. The isolated anti-CD123-CD28-OX40 LF and SF DNA fragments were ligated into the pPHLV-A vector (combined 7.5µL of DNA) with 0.5µL T4 DNA ligase, 2µL ligation buffer, and incubated overnight at 16°C. A no DNA template (H_2O) was included as a control.

Plasmid transformation of *Escherichia coli (E. coli)*

The ligated product was transformed into DH5-α *E. coli* competent cells. 2µL of ligated product was added to 20µL of highly efficient DH5-α cells. The mixture was left on ice for 30 mins and subsequently heated at 42°C for exactly 30secs. A no DNA template (H_2O) was included as a control. The mixture was returned to ice for 5mins before 380µL of SOC medium was added and further incubated at 37°C for 1h on a shaking platform (180rpm).

The eppendorfs were centrifuged at 4500rpm for 5mins and 320μL of supernatant was discarded. The pellet was resuspended in the residual supernatant and transferred to ampicillin treated luria broth (LB) growth plates. The cells were spread over the plates until dry and incubated at 37°C for 12-16h.

Mini-plasmid preparation of DNA

Six to twelve colonies were selected using a sterile tip and each placed in a tube with 5mL LB broth with 5μL ampicillin and incubated overnight at 37°C with shaking. One milliliter of each colony that was sub-cultured was transferred to an eppendorf and centrifuged at 13,000rpm for 2mins. The supernatant was decanted and the pellet resuspended first in 50μL of lab-made resuspension buffer followed by 50μL lysis buffer and gently mixed. 50μL of neutralisation buffer was added before centrifuging at 13,000rpm for 5mins. The pellet was resuspended in residual supernatant and the vector was run on a 0.8% agarose gel as described above. The subcultures from the clones that match the expected band size were extracted from the bacterial clones using a miniprep plasmid extraction procedure using the plasmid miniprep kit as per manufacturer's instructions (Invitrogen). The DNA concentration of each clone was quantified using nanodrop.

Validation of plasmid DNA with restriction enzyme digestion

Two microlitres of each clone was digested with 1μL buffer, 1μL EcoRV restriction enzyme and 6μL dH_2O and incubated overnight at 16°C. The digested clones were run on a 0.8% agarose gel as previously described in order to select the clones with DNA of interest in the correct orientation. The clones in the correct orientation were sent for sequencing for confirmation.

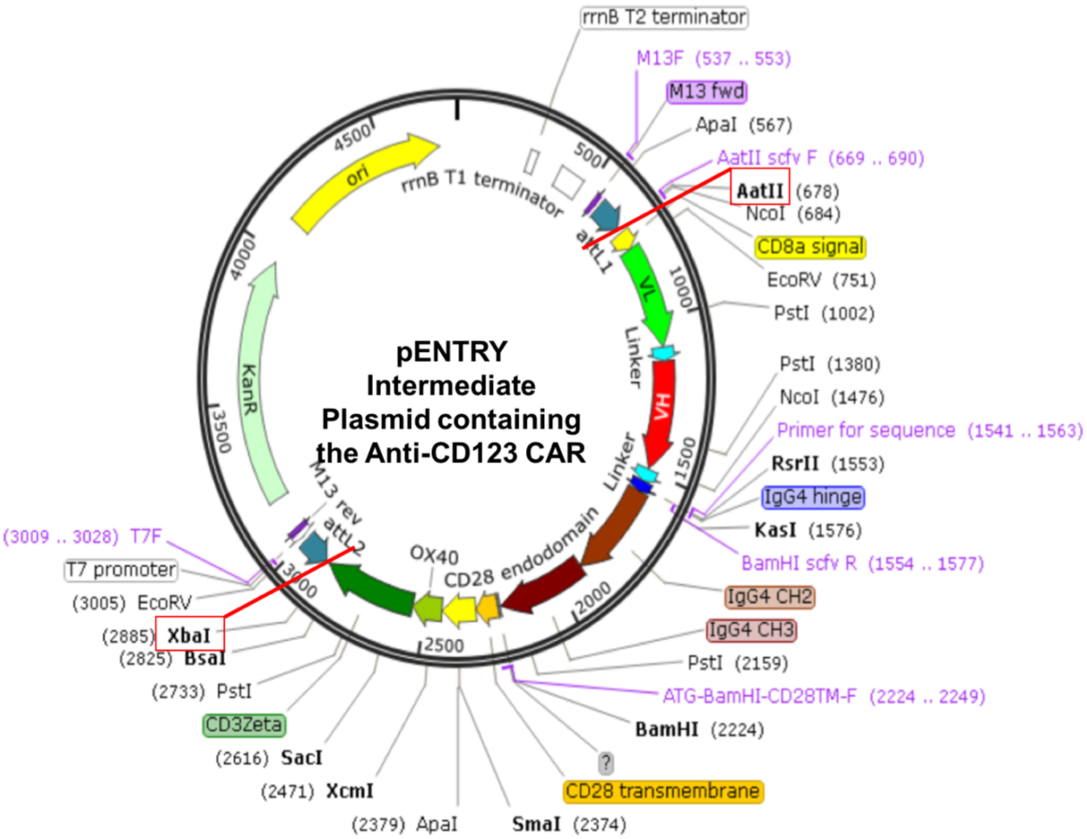
pENTRY
Intermediate
Plasmid containing
the Anti-CD123 CAR
rrnB T2 terminator
M13F (537 .. 553)
M13 fwd
ApaI (567)
AatII scfv F (669 .. 690)
AatII (678)
NcoI (684)
CD8a signal
EcoRV (751)
PstI (1002)
PstI (1380)
NcoI (1476)
Primer for sequence (1541 .. 1563)
RsrII (1553)
IgG4 hinge
KasI (1576)
BamHI scfv R (1554 .. 1577)
IgG4 CH2
IgG4 CH3
PstI (2159)
ATG-BamHI-CD28TM-F (2224 .. 2249)
BamHI (2224)
?
CD28 transmembrane
SmaI (2374)
(2379) ApaI
(2471) XcmI
(2616) SacI
CD3Zeta
(2733) PstI
(2825) BsaI
(2885) XbaI
(3005) EcoRV
T7 promoter
(3009 .. 3028) T7F
ori
rrnB T1 terminator
attL1
VL
Linker
VH
Linker
CD28 endodomain
OX40
attL2
M13 rev
KanR
500
1000
1500
2000
2500
3000
3500
4000
4500

Figure 3.4. Exemplar schematic representation of the CD28-OX40-LF CAR introduced into the intermediate pENTRY vector via the AatII and XbaI restriction sites.

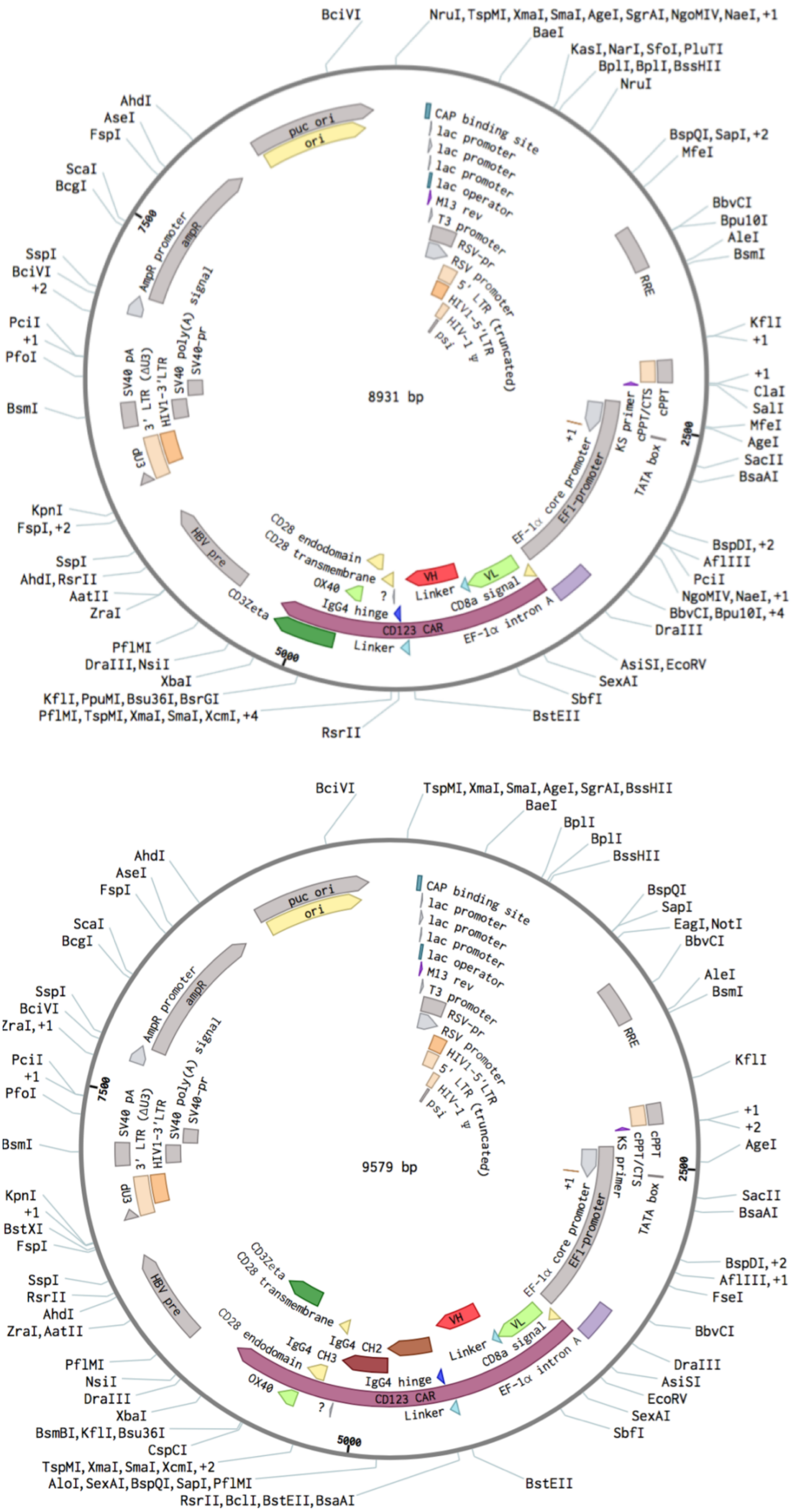
BciVI
NruI, TspMI, XmaI, SmaI, AgeI, SgrAI, NgoMIV, NaeI, +1
BaeI
KasI, NarI, SfoI, PluTI
BplI, BplI, BssHII
NruI
BspQI, SapI, +2
MfeI
BbvCI
Bpu10I
AleI
BsmI
KflI
+1
+1
ClaI
SalI
MfeI
AgeI
SacII
BsaAI
BspDI, +2
AflIII
PciI
NgoMIV, NaeI, +1
BbvCI, Bpu10I, +4
DraIII
AsiSI, EcoRV
SexAI
SbfI
BstEII
RsrII
KflI, PpuMI, Bsu36I, BsrGI
PflMI, TspMI, XmaI, SmaI, XcmI, +4
XbaI
DraIII, NsiI
PflMI
ZraI
AatII
AhdI, RsrII
SspI
FspI, +2
KpnI
BsmI
PfoI
+1
PciI
+2
BciVI
SspI
BcgI
ScaI
FspI
AseI
AhdI
puc ori
ori
CAP binding site
lac promoter
lac promoter
lac promoter
lac operator
M13 rev
T3 promoter
RSV-pr
RSV promoter
5' LTR (truncated)
HIV1-5'LTR
HIV-1 Ψ
psi
RRE
cPPT
cPPT/CTS
KS primer
TATA box
+1
EF-1α core promoter
EF1-promoter
EF-1α intron A
CD8a signal
VL
Linker
VH
CD123 CAR
Linker
IgG4 hinge
?
OX40
CD28 transmembrane
CD28 endodomain
CD3Zeta
HBV pre
dU3
3' LTR (ΔU3)
HIV1-3'LTR
SV40 pA
SV40 poly(A) signal
SV40-pr
AmpR promoter
ampR
8931 bp
7500
5000
2500
BciVI
TspMI, XmaI, SmaI, AgeI, SgrAI, BssHII
BaeI
BplI
BplI
BssHII
BspQI
SapI
EagI, NotI
BbvCI
AleI
BsmI
KflI
+1
+2
AgeI
SacII
BsaAI
BspDI, +2
AflIII, +1
FseI
BbvCI
DraIII
AsiSI
EcoRV
SexAI
SbfI
BstEII
RsrII, BclI, BstEII, BsaAI
AloI, SexAI, BspQI, SapI, PflMI
TspMI, XmaI, SmaI, XcmI, +2
CspCI
BsmBI, KflI, Bsu36I
XbaI
DraIII
NsiI
PflMI
ZraI, AatII
AhdI
RsrII
SspI
FspI
BstXI
+1
KpnI
BsmI
PfoI
+1
PciI
ZraI, +1
BciVI
SspI
BcgI
ScaI
FspI
AseI
AhdI
puc ori
ori
CAP binding site
lac promoter
lac promoter
lac promoter
lac operator
M13 rev
T3 promoter
RSV-pr
RSV promoter
HIV1-5'LTR
5' LTR (truncated)
HIV-1 Ψ
psi
RRE
cPPT
cPPT/CTS
KS primer
TATA box
+1
EF-1α core promoter
EF1-promoter
EF-1α intron A
CD8a signal
VL
Linker
VH
IgG4 CH2
IgG4 hinge
CD123 CAR
Linker
IgG4 CH3
?
OX40
CD28 endodomain
CD28 transmembrane
CD3Zeta
HBV pre
dU3
3' LTR (ΔU3)
HIV1-3'LTR
SV40 pA
SV40 poly(A) signal
SV40-pr
AmpR promoter
ampR
9579 bp
7500
5000
2500

Figure 3.5. Schematic Representation of the anti-CD123 (CSL362) CD28-OX40 SF (top) or LF (bottom) CARs cloned into the pPHLV-A expression vector via the EcoRV restriction site.

Construction of the CD123-CD28-4-1BB CARs. In order to generate the pPHLV-A plasmids encoding for the short hinge (SF) and long hinge (LF) CD123-CD28-4-1BB CAR DNA sequences (Appendix 6.1) *(Figure 3.6),* the co-stimulatory signalling domain from the pENTRY anti-CD123-CD28-OX40 LF and SF plasmids were first replaced with the CD28-4-1BB co-stimulatory signalling domain. The DNA fragments of the CD28-4-1BB signalling motifs were generated and provided by collaborators (Dr. Stanley Yu, CCB, South Australia).

Thirty-two microlitres of DNA were digested with 4μL of digestion buffer (NEB), and 2μL each of the BamHI and SacI (NEB) restriction enzymes overnight at 16ºC. The digested pENTRY plasmid was run on a 0.8% gel containing 5μL of gel red dye for 45mins-1h. The larger band was recovered by cutting the band from the gel and placed in an eppendorf. The eppendorf was heated at 37ºC to melt the gel. A combined 7.5μL of the digested pENTRY intermediate vector and CD28-4-1BB DNA fragment was ligated with 0.5μL T4 DNA ligase, 2μL buffer, and incubated overnight at 16ºC. A no DNA template (H_2O) was included as a control. The ligated product was transformed into DH5-α E.Coli competent cells as described above and plated on kanamycin treated LB growth plates. Six to- twelve colonies were selected and cultured in 5mL LB broth with 5μL kanamycin. The selected clones were checked for the expected band size, correct orientation, extracted for DNA using the miniprep procedure, and sent for sequencing as described above. The successfully cloned pENTRY anti-CD123-CD28-4-1BB SF and LF intermediate plasmids were then digested and introduced into the pPHLV-A expression vector as described above. The final constructs were pPHLV-A encoding the CD123-CD28-4-1BB SF CAR (4-1BB-SF) and the CD123-CD28-4-1BB LF CAR (4-1BB-LF).

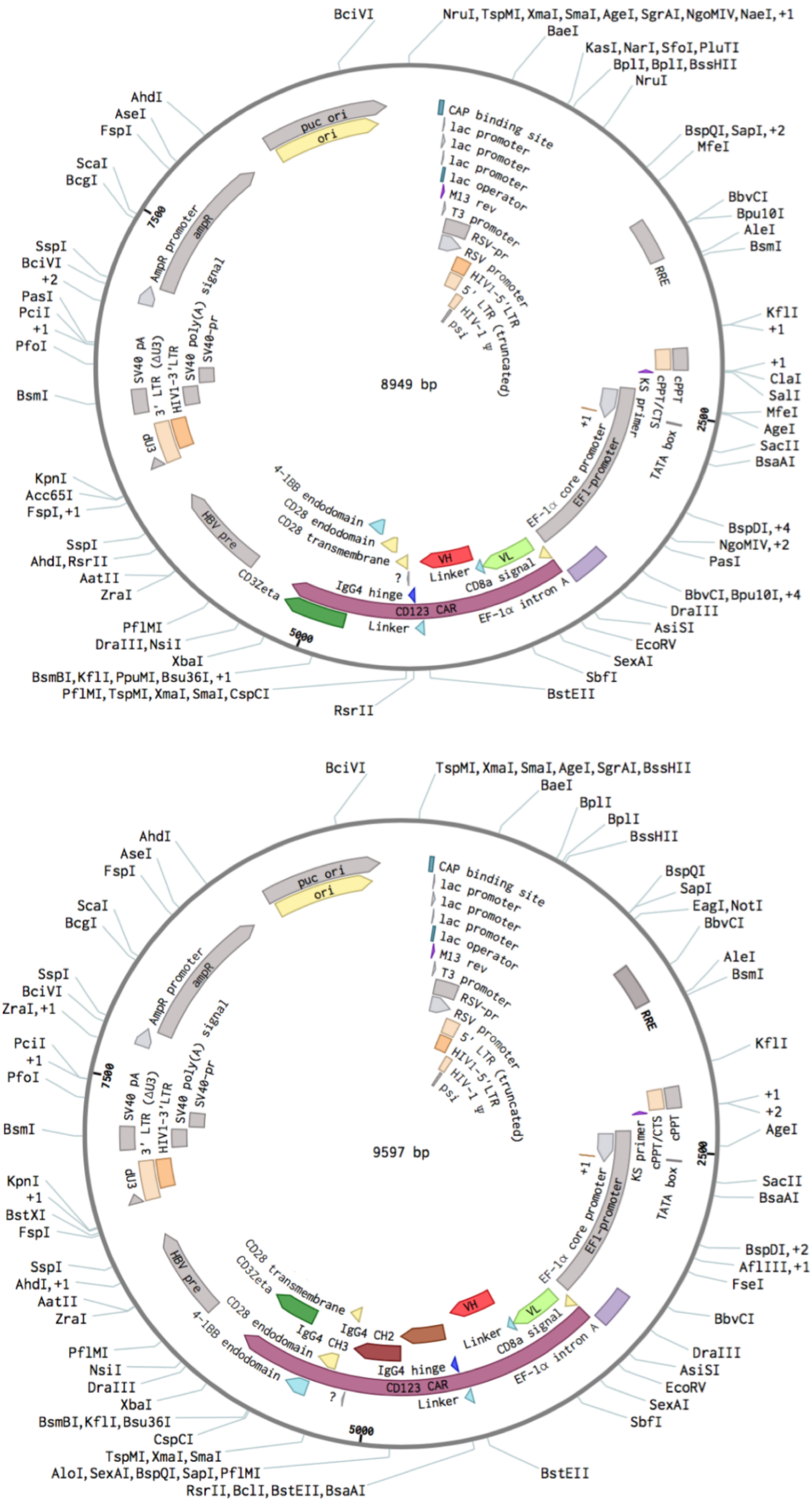
BciVI
NruI,TspMI,XmaI,SmaI,AgeI,SgrAI,NgoMIV,NaeI,+1
BaeI
KasI,NarI,SfoI,PluTI
BplI,BplI,BssHII
NruI
BspQI,SapI,+2
MfeI
BbvCI
Bpu10I
AleI
BsmI
KflI
+1
+1
ClaI
SalI
MfeI
AgeI
SacII
BsaAI
BspDI,+4
NgoMIV,+2
PasI
BbvCI,Bpu10I,+4
DraIII
AsiSI
EcoRV
SexAI
SbfI
BstEII
RsrII
PflMI,TspMI,XmaI,SmaI,CspCI
BsmBI,KflI,PpuMI,Bsu36I,+1
XbaI
DraIII,NsiI
PflMI
ZraI
AatII
AhdI,RsrII
SspI
FspI,+1
Acc65I
KpnI
BsmI
PfoI
+1
PciI
PasI
+2
BciVI
SspI
BcgI
ScaI
FspI
AseI
AhdI
puc ori
ori
CAP binding site
lac promoter
lac promoter
lac promoter
lac operator
M13 rev
T3 promoter
RSV-pr
RSV promoter
HIV1-5'LTR
5' LTR (truncated)
HIV-1 Ψ
psi
RRE
cPPT
cPPT/CTS
KS primer
TATA box
2500
+1
EF-1α core promoter
EF1-promoter
8949 bp
AmpR promoter
ampR
7500
signal
SV40 poly(A) signal
SV40-pr
SV40 pA
3' LTR (ΔU3)
HIV1-3'LTR
dU3
HBV pre
4-1BB endodomain
CD28 endodomain
CD28 transmembrane
?
CD3Zeta
IgG4 hinge
VH
Linker
VL
CD8a signal
EF-1α intron A
CD123 CAR
Linker
5000
BciVI
TspMI,XmaI,SmaI,AgeI,SgrAI,BssHII
BaeI
BplI
BplI
BssHII
BspQI
SapI
EagI,NotI
BbvCI
AleI
BsmI
KflI
+1
+2
AgeI
SacII
BsaAI
BspDI,+2
AflIII,+1
FseI
BbvCI
DraIII
AsiSI
EcoRV
SexAI
SbfI
BstEII
RsrII,BclI,BstEII,BsaAI
AloI,SexAI,BspQI,SapI,PflMI
TspMI,XmaI,SmaI
CspCI
BsmBI,KflI,Bsu36I
XbaI
DraIII
NsiI
PflMI
ZraI
AatII
AhdI,+1
SspI
FspI
BstXI
+1
KpnI
BsmI
PfoI
+1
PciI
ZraI,+1
BciVI
SspI
BcgI
ScaI
FspI
AseI
AhdI
puc ori
ori
CAP binding site
lac promoter
lac promoter
lac promoter
lac operator
M13 rev
T3 promoter
RSV-pr
RSV promoter
5' LTR (truncated)
HIV1-5'LTR
HIV-1 Ψ
psi
RRE
cPPT
cPPT/CTS
KS primer
TATA box
2500
+1
EF-1α core promoter
EF1-promoter
9597 bp
AmpR promoter
ampR
signal
SV40 poly(A) signal
SV40-pr
7500
SV40 pA
3' LTR (ΔU3)
HIV1-3'LTR
dU3
HBV pre
CD28 transmembrane
CD3Zeta
CD28 endodomain
4-1BB endodomain
IgG4 CH3
IgG4 CH2
?
IgG4 hinge
CD123 CAR
VH
Linker
VL
CD8a signal
EF-1α intron A
Linker
5000

Figure 3.6. Schematic representation of the anti-CD123 (CSL362) CD28-4-1BB SF (top) or LF (bottom) CARs cloned into the pPHLV-A expression vector via the EcoRV restriction site.

Finalised Protocol:

HEK-293T Transfection. T75 flasks were coated with Poly-D-lysine at a final concentration of 10μg/cm^3 for 4-6h at room temperature (RT) under a biosafety cabinet hood (BSH). The poly-D-lysine solution was aspirated and the flask was gently washed twice with 10mL of 1xPBS. 3.5x10^6 HEK-293T cells were seeded in 15mL of transfection media and incubated overnight at 37°C, 5% CO_2. The media was aspirated the next day and replaced with 15mL pre-warmed transfection media. Meanwhile, the transfection mixture was prepared. For each flask, 5.15μg of each vector DNA (pRSV-Rev, pMD2.G, pMDL/pPRRE, anti-CD123) was mixed in a 5mL polypropylene tube with 41.22μL (2μL/μg DNA) of P3000 reagent, 30.93μL Lipofectamine 3000 reagent and 1.5mL of Opti-MEM serum free medium. The solution was gently mixed by pipetting up and down and incubated in the BSH at RT for 25mins. The solution was added drop-wise to the flask and spread over the cells by gently rocking the flask from side to side. The flasks were incubated for 16h at 37°C, 5%CO_2. The media was replaced with 15mL pre-warmed HEK-293T culture media and incubated for a further 24h to generate virus. Viral supernatant from transfected HEK-293T cells was collected, centrifuged at 1400rpm, 5mins at 4°C and 0.45μM sterile filtered. For a second viral harvest, 15mL of fresh pre-warmed HEK-293T growth medium was added to the plates and the process repeated 24h later.

Concentration of Lentivirus (Ultracentrifugation). 15mL or 30mL of un-concentrated virus was placed in a sterile thinwall, polypropylene tube under sterile conditions. The amount of virus placed in each tube was dependent on the centrifuge and rotor available. The virus was placed in the pre-cooled rotor buckets and centrifuged at 20,000rpm for 90mins at 4°C. The viral supernatant was very gently decanted and 50μL (for every 15ml of unconcentrated virus that was centrifuged) of ice-cold sterile 1xPBS was added. The viral pellet was carefully resuspended using a pipette, avoiding the generation of bubbles. The tube was left to stand on ice in the BSH for 45mins. The virus was pooled and 50μL of virus was aliquoted to each eppendorf. 25μL of crude virus was aliquoted to an Eppendorf for viral titer. The concentrated viral aliquots were stored at -80°C until use.

Lentiviral Titre & Calculation. Titration of lentivirus was carried out by transduction of Jurkat T cells. 25μL of concentrated virus was thawed on ice and 1-5-fold dilutions of the virus was prepared in Jurkat T cell culture media (Appendix 6.3) in a final volume of 250μL. 1x10^5 Jurkat T cells was resuspended in each dilution and plated in a 24-well plate. 6μg/mL polybrene was added to each well to facilitate transduction and plates were spun at 800 *x g* for 1h at 32°C. The plate was incubated for 24h at 37°C, 5% CO_2. The plate was centrifuged at 400 *x g* for 10mins, RT to allow cells to adhere to the bottom of the plate. The supernatant was gently removed and 750µL of fresh pre-warmed Jurkat T cell culture media was added to the cells. The plate was further incubated for 3 days.

Cells from each well were harvested into separate FACs tubes and washed thrice with ice cold 1xPBS. 1µg of Biotinylated Protein-L was added for every $1x10^6$ Jurkat T cells and incubated on ice, in the dark for 45mins. Following incubation, the cells were washed twice with ice cold 1xPBS. Cells were stained with 1:50 Streptavidin-PE antibody and 5µL of 7-AAD live/dead antibody and incubated for 30mins on ice in the dark. An unstained control and Protein-L (PE) FMO (FMO was defined, here, as the exclusion of the primary antibody) was included. Cells were washed twice with ice cold FACs buffer (general) and re-suspended in 200ul FACs buffer (general). Cells were acquired with the BD LSR Fortessa™ X-20 (BD Biosciences). Instrument setup and performance, data acquisition, and data analysis were performed as previously described *(Chapter 2).* Cell populations of interest were reported as a proportion of total lymphocytes, derived from SSC vs. FSC gated lymphocytes, with doublet exclusion (FSC-A vs FSC-H), and dead cell discrimination (7-AAD^-). A minimum of $1x10^5$ events was acquired for the full panel stained tubes. Unstained and FMO controls were used to identify gating boundaries.

For a simple and universal method to detect the surface expression of CARs on transduced lymphocytes, Protein-L staining was employed. Protein-L is an Ig-binding protein that binds to the variable light chains of Ig. It can therefore bind to scFv and antigen binding fragments (Fab) without interfering with the antigen binding site.

For titre calculation, the dilution with 10-20% Protein-L PE^+ cells were selected. The titre was calculated as follows:

Titre (TU/ml) = (N x P)/(V x D), where:

N= Cell Concentration in each well at the time of transduction

P= % of Protein-L PE^+ cells

V= Volume of virus supernatant used for infection (e.g. 25µL was added = 0.025mL)

D= Dilution fold

Primary HD T Cell Isolation, Activation, Transduction, and Expansion

Isolation and Activation

HD PBMCs were thawed (Appendix 6.4.2) and incubated at 37°C for at least 4h to promote cell recovery. T cells were isolated using the 'human pan T cell isolation kit' according manufacturer's instructions (Miltenyi Biotec). Isolated T cells were washed twice with ice cold FACS Buffer (general) and $2x10^5$ cells were aliquoted for the full stain panels and the unstained and FMO to check for purity of the population. For surface staining, cells were incubated with titrated antibody *(Table 3.1)* for 30mins on ice in the dark. Cells were washed twice with ice cold FACS buffer (general) and re-suspended in 200µL FACS buffer (general).

Table 3.1. Healthy Donor T Cell Isolation Purity Check Staining Panel

Antibody	**Fluorochrome**	**Titrated antibody volume/test (µL)**
Live Dead Aqua	V500	2
CD3	PerCP Cy5.5	3
CD8	APC	10

Cells were acquired with the BD II CANTO (BD Biosciences). Instrument setup and performance, data acquisition, and data analysis were performed as previously described. Cell populations of interest were reported as a proportion of total lymphocytes, derived from SSC vs. FSC gated lymphocytes, with doublet exclusion (FSC-A vs FSC-H), and dead cell discrimination (7-AAD^-). A minimum of $5x10^4$ events was acquired for the full panel stained tubes. Unstained and FMO controls were used to identify gating boundaries.

For the remainder of the cells, 10ng/µL (50IU/mL) human rIL-2 and 2µL of human CD3/CD28 T cell activation dynabeads were added for every $1x10^5$ cells. $1x10^5$ cells were plated into each well of a 96-well U-bottom plate in a final volume of 100µL T cell culture media (Appendix 6.3). The plate was incubated at 37°C for 48h until transduction.

Transduction (Initial Method)

250μL of Lenti-X concentrated virus was thawed on ice and a 1-fold dilution of the virus was prepared in T cell culture media to a final volume of 2.5mL. 2.5x10^7 T cells was added to the 2.5mL of virus supernatant with 6μg/mL polybrene. 2.5x10^6 T cells (in 250μL) was plated into each well of a 12-well plate. The plate was centrifuged at 400 *x g* for 10mins and incubated at 37°C, 5%CO_2 for 24h. The plate was centrifuged at 400 *x g* for 10mins, RT to allow cells to adhere to the bottom of the plate. The supernatant was gently removed and 1mL of fresh pre-warmed T cell culture media was added to the cells. The plate was further incubated for 3 days.

T cell Transduction (Finalised Method). Twenty-four hours prior to transduction, 24-well non-treated tissue culture plates were coated with 500μL RetroNectin (recombinant human fibronectin fragment) at a concentration of 32μg/mL, parafilmed and incubated overnight at 4°C. The RetroNectin was removed and the plate was blocked with 500μL of sterile 2% BSA-PBS at RT for 30mins. During the incubation, lentivirus aliquots were thawed on ice to transduce T cells at a multiplicity of infection (MOI) 5 per well based on the titre calculations. For example, if per well, 5μL of virus supernatant is required to transduce the cells at MOI 5, the appropriate amount of total virus required was thawed. The appropriate amount of T cell culture medium was added to the lentivirus so that the final volume per well was 250μL. The plates were washed once with sterile 1xPBS and 250μL of supernatant was added to each well. The plate was centrifuged at 3500rpm for 90mins, 37°C with acceleration of 3 and no-brake for de-acceleration. The virus supernatant was aspirated and 6x10^5 T cells in 500μL fresh pre-warmed culture media supplemented with 10ng/μL human rIL-2 was added to each well. The plate was centrifuged at 1200rpm for 15mins, 37°C to facilitate adherence and contact of T cells to the virus coated plate. The plate was incubated overnight at 37°C for 24h. The supernatant was gently removed and 1mL of fresh pre-warmed culture media supplemented with 10ng/μL human rIL-2 was added to the cells. The plate was further incubated for 5 days with a media replacement every 2 days.

For the detection or isolation of Protein-L^+ CAR T cells, cells were prepared and stained as previously described in *'lentiviral titre and calculation'*.

T cell Expansion. HD T cells were expanded for 10-14 days following transduction with R-10 media with 20% FCS and 1% pen/strep with additional human 10ng/μL rIL-2. Media was replaced every 2-3 days until end of expansion period.

In Vitro T-cell phenotypic Subset Analysis. T cells were harvested prior to lentiviral transduction as well as post *in vitro* culture expansion, and phenotypically analysed. Cells were washed twice with 1x PBS supplemented with 2mM EDTA, 2% FCS, and 5% Sodium Azide, resuspended in 100μL and stained with 2μL of 1:20 Live dead aqua viability dye-V500, 3μL CD3-PerCPCy5.5, 5μL CD8-APC, 5μL CD27-APC-ef780, 5μL CD45RO-PeCy7 (BD Biosciences) for 30mins on ice, in the dark. Cells were washed twice and resuspended in a final volume of 200μL prior to flow cytometric analysis. Unstained and FMO controls were used to identify gating boundaries.

Human Samples. In Australia, primary AML and HD BMMNC samples were obtained from SACRB, Adelaide. In Germany, primary AML and HD PB were obtained from the University Medical Center, Freiburg. Written informed consent was obtained from each donor. The study was approved by the Australian Institutional Human Research Ethics Committee (*Ethics approval no's*: R20150526, HREC/15/RAH/221, and 509/16) and conducted in accordance with the Declaration of Helsinki.

CD107a Degranulation Assay. $CD4^+$ and $CD8^+$ CD107a degranulation assay was performed as previously described (Hughes et al., 2017)(Betts & Koup, 2004). CAR T cells were rested in culture in the absence of CD3/CD28 dynabeads and recombinant hIL-2, 16 hours prior to co-culture experiments. $5x10^5$ anti-CD123 CAR T cells were co-cultured with $5x10^5$, $2.5x10^5$, $1x10^5$ or $5x10^4$ KG1a ($CD123^+$) or SUPB15 ($CD123^-$) target cells for 6h at 37°C, 5%CO_2 with 5μL FITC-CD107a (BD Biosciences) and 5μL of a 1:10 dilution of the protein transport inhibitor monensin (BD GolgiStop). Each effector to target (E:T) ratio was set up in triplicate with a total volume of 200μL per well in a 96 well U-bottom plate. Cells were subsequently harvested, transferred to separate FACS tubes per replicate and centrifuged with 2mL ice-cold FACS buffer at 1400rpm for 10mins, twice. Cells were re-suspended in residual buffer and each tube was stained with 3μL CD3-PerCPCy5.5, 5μL CD8-APC, and 2μL of a 1:20 LDA viability stain (eBiosciences, BD Biosciences, Life technologies) for 30mins at 4°C, in the dark. Cells were washed twice with 2mL ice-cold FACS buffer and centrifuged at 1400rpm for 10mins. Cells were re-suspended in 150μL FACS buffer and kept in the dark at 4°C until analysis. 1μg/mL Staphylococcus aureus, Enterotoxin Type B (SEB) (Merck Millipore) was used a positive control for degranulation instead of target cells. Negative controls received RF10 culture medium (RPMI containing 20% FCS, and 1% penicillin/streptomycin) instead of target cells. Cells were acquired with the BD FACS CANTO II (BD Biosciences). Data acquisition was performed using FACSDiva software (BD Biosciences) and data analysis via FlowJo v10.1 (FlowJo, LLC, Ashland, OR, USA). Instrument setup including fluorescence amplification (voltages) and compensation was optimised using compensation beads (BD Biosciences). Flow cytometer performance was checked regularly using CS&T beads (BD Biosciences). Cell populations of interest were reported as a proportion of total lymphocytes, derived from SSC vs. FSC gated lymphocytes, with doublet exclusion (FSC-A vs FSC-H), and dead cell discrimination (LDA^-). A minimum of $5x10^5$ events were acquired for the full panel stained tubes. Unstained and FMO controls were used to identify gating boundaries.

CellTrace Violet Proliferation Assay. A total of $6x10^6$ Anti-CD123 CAR T cells were harvested from culture, washed twice with 10mL of 1x PBS, centrifuged at 1400rpm for 10mins and re-suspended in $1x10^6$ cells/mL with 1x PBS. One microlitre of CellTrace Violet dye (Invitrogen, Thermo Fischer Scientific) was added per mL of cell suspension for a final concentration of 5μM and stained for 30mins at 37°C, 5%CO_2 in the dark. The reaction was quenched with 5x the staining volume of RF10 medium (as above). Cells were centrifuged and washed thrice more with 25mL of 1x PBS. Cells were re-suspended in 3mL of fresh RF10 medium and 500μL of anti-CD123 CAR T cells were incubated at a 1:1 ratio ($1x10^6$: $1x10^6$) with 500μL of SUPB15 or KG1a target cells, previously irradiated at 100Gy, in a 48-well plate for 96h. Negative controls received 500μL RF10 medium instead of target cells. Cells were harvested washed twice with ice-cold FACS buffer and re-suspended in buffer. Cell were subsequently stained with 3μL CD3-PerCpCy5.5, 5μL CD8-BV711, and 2μL live dead far red (Far Red) fixable dead cell stain (eBiosciences, BD Biosciences, Life Technologies) and incubated for 30mins at 4°C in the dark. Cells were washed twice with 2mL ice-cold FACS buffer and centrifuged at 1400rpm for 10mins. Cells were re-suspended in 150μL FACS buffer and kept in the dark at 4°C until analysis. Cells were acquired with the BD FACS CANTO II (BD Biosciences). Data acquisition was performed using FACSDiva software (BD Biosciences) and data analysis via FlowJo v10.1 (FlowJo, LLC, Ashland, OR, USA). Instrument setup including fluorescence amplification (voltages) and compensation was optimised using compensation beads (BD Biosciences). Flow cytometer performance was checked regularly using CS&T beads (BD Biosciences). Cell populations of interest were reported as a proportion of total lymphocytes, derived from SSC vs. FSC gated lymphocytes, with doublet exclusion (FSC-A vs FSC-H), and dead cell discrimination (Far Red^{-}). A minimum of 1x10^{6} events were acquired for the full panel stained tubes. Unstained, stained CAR T cells only (prior to commencement of co-culture, t=0 hours) and FMO controls were used to identify gating boundaries.

Anti-CD123 CAR T Cell Phenotypic Exhaustion Analysis. Anti-CD123 CAR T cells were harvested at pre- and post- co-culture with target cells *(Table 3.2)* and serially analysed for surface expression of TIM-3, CTLA-4, LAG-3 and PD-1 markers of exhaustion. A total of 2x10^{5} cells were transferred into a FACS staining tube, anti-CD3/CD28 dynabeads were removed using a magnet, and cells were washed twice with 2mL ice-cold FACS buffer and centrifuged at 1400rpm for 10mins. Cells were subsequently stained with 2µL of 1:20 dilution of LDA (Life Technologies), 5µL CTLA-4-BV786, 5µL of CD8-BV711, 5µL TIM-3-BV650, 3µL CD3-PerCPCy5.5, 8µL PD-1-PE, 5µL LAG-3-AlexaFluor 647 (BD Biosciences) for 30mins at 4°C in the dark. Unstained and FMO controls used 1x10^{5} cells. Cells were washed twice with 2mL ice-cold FACS buffer and centrifuged at 1400rpm for 10mins and re-suspended in 150µL FACS buffer and kept at 4°C in the dark until analysis. Cells were acquired with the BD LSR FORTESSA (BD Biosciences). Data acquisition, instrument setup and flow cytometer performance was performed as described above. Cell populations of interest were reported as a proportion of total lymphocytes, derived from SSC vs. FSC gated lymphocytes, with doublet exclusion (FSC-A vs FSC-H), and dead cell discrimination (LDA^{-}). A minimum of 1x10^{5} events were acquired for the full panel stained tubes. Unstained and FMO controls were used to identify gating boundaries.

Table 3.2. Serial Time Points for Immunophenotypic Exhaustion Analysis of CAR T cells.

Time Point	Point of Cell Culture
Day 17	T cells expanded in culture for 10 days following sort purification
Day 21	T cells after short term *in vitro* experiment

16h Cytotoxicity Assay. A total of $3x10^6$ KG1a or SUPB15 target cells were harvested from culture, washed twice with 10mL of 1x PBS, centrifuged at 1400rpm for 10mins, and re-suspended in $1x10^6$ cells/mL with 1x PBS. 1μL of CellTrace Violet dye (Invitrogen, Thermo Fischer Scientific) was added per mL of cell suspension for a final concentration of 5μM and stained for 30mins at 37°C, 5%CO_2 in the dark. The reaction was quenched with 5x the staining volume of RF10 medium (as above). Cells were centrifuged and washed thrice more with 25mL of 1x PBS. Cells were re-suspended in 4.5mL of fresh RF10 medium and 150μL of target cells ($1x10^5$) were incubated with 150μL of anti-CD123 CAR T cells at a cell concentration of $1x10^6$, $5x10^5$, $2x10^5$, $1x10^5$, $5x10^4$, $2.5x10^4$, or 0. Each E:T ratio was plated in triplicate in a 48-well plate. For the triplicates containing no CAR T cells, 150μL RF10 medium was added instead. For the remaining target cells, 150μL ($1x10^5$) was plated into each well and topped up with 150μL RF10 media to be used as positive and negative controls, herein referred to as max. and min., respectively. The plate was centrifuged at 1400rpm for 10mins, RT to promote contact between effector and target cells. The plate was incubated at 37°C, 5%CO_2 for 16h.

Following incubation, each well was transferred into a separate FACS staining tube and cells were washed twice with 2mL ice-cold FACS buffer and centrifuged at 1400rpm for 10mins. Each tube was subsequently stained with 5μL 7-AAD (BD Biosciences) for 20mins at 4°C in the dark. Cells were washed twice with 2mL ice-cold FACS buffer and centrifuged at 1400rpm for 10mins and resuspended in 300μL FACS buffer. For the max. wells, 25μL of 10% Triton X-100 (Merck Millipore) was added to the cells. Cells were acquired with the BD FACS CANTO II (BD Biosciences).

Data acquisition, instrument setup and flow cytometer performance was performed as described above. Prior to the acquisition of each tube, 15μL of Countbright beads (Life Technologies) were added and the tube was vortexed briefly. Cell populations of interest were reported as a proportion of total lymphocytes, derived from SSC vs. FSC gated lymphocytes, with doublet exclusion (FSC-A vs FSC-H). Residual live target cells were defined as CellTrace Violet$^+$ 7-AAD$^-$. Strictly, 10,000 bead events were acquired per tube. Unstained target cells and FMO controls were used to identify gating boundaries. The absolute cell count of live and dead cells was calculated as per manufacturer's instructions (Countbright beads-Life Technologies). The percent cytolysis for each tube was determined by the following formula:

$$\textbf{\% Cytolysis} = \textbf{Absolute cell count}_{(\text{CellTrace}^{+}\ \text{7-ADD}^{-})} / \textbf{Absolute cell count}_{(\text{Total amount of target cells})}\ \textbf{X 100}$$

The percentage of specific lysis was then determined by the formula:

$$\textbf{\% Specific lysis} = (\textbf{\%cytolysis}_{\text{sample}} - \textbf{\%cytolysis}_{\text{average target Min. control}}) / (\textbf{\%cytolysis}_{\text{average target Max. controls}} - \textbf{\%cytolysis}_{\text{average target Min. control}})\ \textbf{X 100}$$

Cytokine Secretion Assay. A total of 5×10^4 KG1a or SUPB15 target cells were incubated with 5×10^5 anti-CD123 CAR T cells in 300µL RF10 culture media (E:T ratio of 10:1) per replicate in a 48-well plate. For control wells, 300µL RF10 culture media was plated for each replicate or 5×10^5 anti-CD123 CAR T cells were plated in 300µL RF10 culture media. The plate was cultured for 24h at 37°C, 5%CO_2. Following incubation, the cells were harvested along with the supernatant and transferred to 2mL eppendorfs. The eppendorfs were centrifuged 2750rpm for 3mins. The 300µL of supernatant was divided into single use aliquots (50µL) and stored at -80°C until use. The supernatant was thawed at RT, diluted 1:5 with RF10 culture media, cytokines were measured by a 30-plex cytokine array, with an overnight incubation and analysed according to the manufacturer's instructions (Merck Millipore).

Data Representation & Statistical Analysis. Statistical analysis was performed using GraphPad Prism v7 or v8 software (GraphPad Software Inc, La Jolla, CA). Two-way Unpaired Student's *t*-test (Mann-Whitney test) or 1-way ANOVA was used for comparing differences between groups. Data are given as mean ± standard error of the mean (SEM). A *P*-value of $\leq .05$ was considered significant.

3.4 Results

3.4.1 Generation of the anti-CD123 CAR lentiviral expression constructs

To enable high level expression of transgene and downstream evaluation of the four anti-CD123 CAR products (previously designed and produced by Dr. Stanley Yu), the constructs were cloned into lentiviral expression vectors. Each of the four CAR DNA fragments were amplified by PCR and sub-cloned into the intermediate expression vector pENTRY, digested from the pENTRY intermediate vector with AatII and XbaI restriction enzymes and then blunted using Klenow *(Figure 3.7).* The pPHLV-A lentiviral expression vector was digested at the EcoRV restriction site, dephosphorylated, and PCR purified prior to ligation with one of each of the four CD123 CAR products.

The four ligated products were transformed into DH5-α E.Coli competent cells and several colonies were picked from each, miniprepped, and subjected to a colony PCR. The selected colonies were checked for the scFv DNA insert release by digestion with EcoRV *(Figure 3.8).* Correct orientation of the clones successfully containing the DNA insert were confirmed by sequencing.

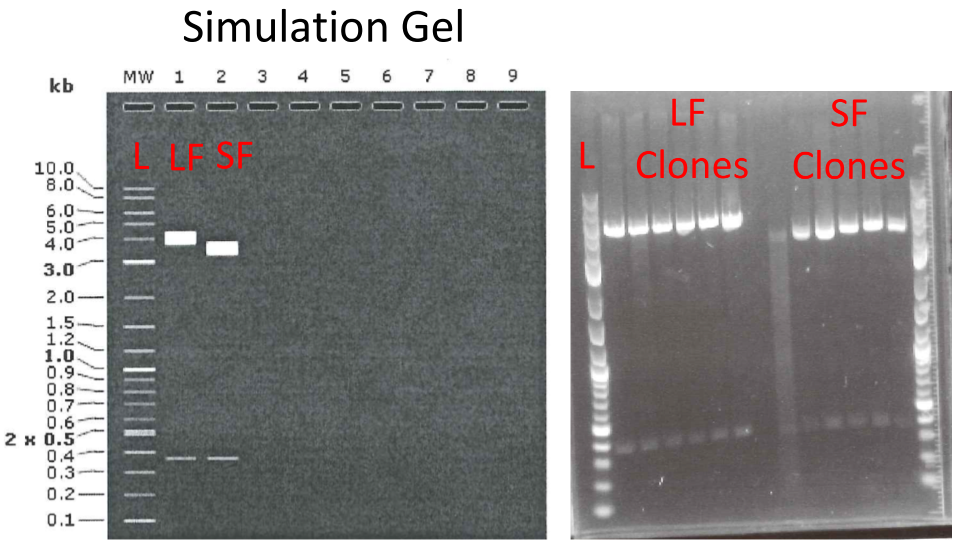
Simulation Gel
kb
MW
1
2
3
4
5
6
7
8
9
L
LF
SF
10.0
8.0
6.0
5.0
4.0
3.0
2.0
1.5
1.2
1.0
0.9
0.8
0.7
0.6
2 x 0.5
0.4
0.3
0.2
0.1
L
LF
Clones
SF
Clones

Figure 3.7. Sub-cloning of the CD123–CD28-41BB CAR construct into the pENTRY lentiviral expression vector.

'L' corresponds to the DNA ladder. Left panel depicts a simulation agarose gel containing successful insertion of either the CD123-CD28-4-1BB LF or SF CAR constructs in the pENTRY expression vector. Right panel represents a colony PCR of the selected transformed colonies. LF colonies indicate the colonies incorporating the CD123-CD28-4-1BB LF CARs while the SF colonies indicate the colonies incorporating the CD123-CD28-4-1BB SF CARs.

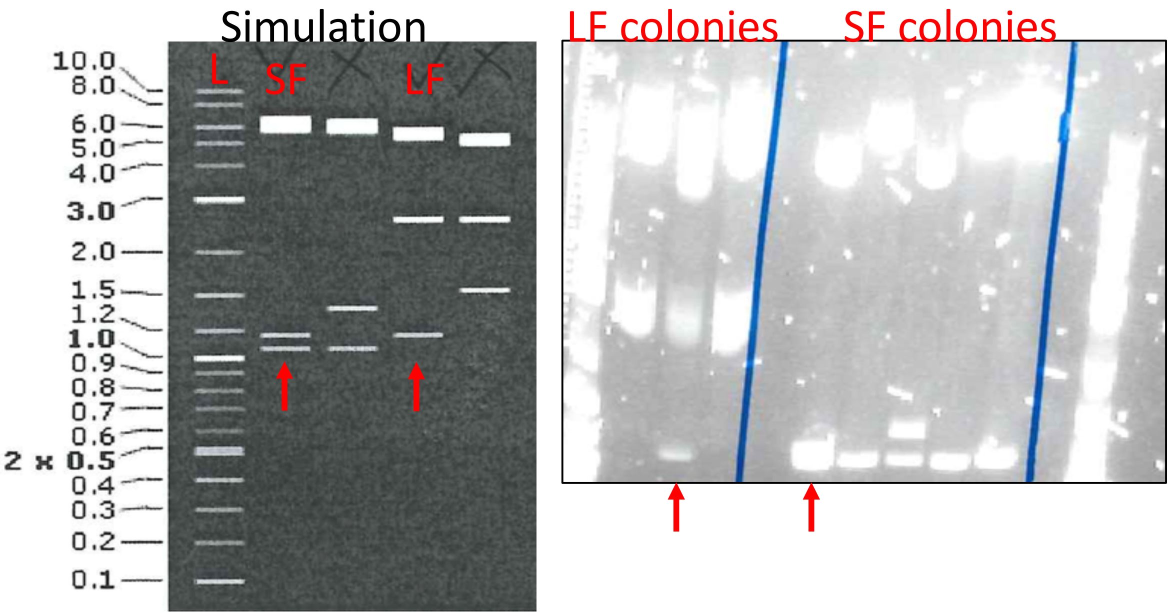
Simulation
L
SF
LF
10.0
8.0
6.0
5.0
4.0
3.0
2.0
1.5
1.2
1.0
0.9
0.8
0.7
0.6
2 x 0.5
0.4
0.3
0.2
0.1
LF colonies
SF colonies

Figure 3.8. Cloning of the CD123-CD28-OX40 scFv construct into the pPHLV-A lentiviral expression vector.

'L' corresponds to the DNA ladder. Left panel depicts a simulation agarose gel containing successful insertion of either the CD123-CD28-OX40 SF or LF CAR constructs in the pPHLV-A expression vector. The red arrows depict the SF or LF constructs in the correct orientation. Right panel represents a colony PCR of the selected transformed colonies. LF colonies indicate the colonies incorporating the CD123-CD28-OX40 LF CARs while the SF colonies indicate the colonies incorporating the CD123-CD28-OX40 SF CARs. Of the colonies that were checked, the red arrows indicate the LF and SF clone that incorporate the CAR DNA insert cloned into the pPHLV-A lentiviral vector with the correct orientation.

3.4.2 High-yield production of CAR lentivirus

To date, lentiviral vectors are the most commonly employed method for the production of CAR T cells both pre-clinically and clinically. In order to develop an efficient platform for lentiviral production, several stages of the transduction process required optimising. Introducing a gene of interest within an expression vector into primary cells is notoriously difficult. For this reason, four factors were evaluated that could potentially affect transfection efficiency and virus output: (1) the ratio of the four-plasmid lentivirus production system, (2) using freshly harvested virus versus frozen virus, (3) time of harvesting the viral particles, and (4) viral supernatant concentration method. All factors to optimise lentivirus production were performed using the CD123-CD28-OX40-SF CAR as this plasmid construct was the first to be successfully cloned.

To generate a high yield of lentivirus for effective primary T cell transduction, the ratio of plasmids in a four-plasmid lentivirus production system is crucial. To optimise this variable, four different combinations of pCAR:VSVg:gag/pol:rev plasmids were examined for their ability to transfect HEK-293T cells. The various ratio combinations were selected based on what has been previously described (Merten et al., 2011)(Tiscornia et al., 2006). As displayed in *Figure 3.9A*, the ratios containing the same or twice the amount of CAR plasmid to the three packaging plasmids (1:1:1:1 and 2:1:1:1) resulted in the highest transfection efficiency compared to the other plasmid ratio combinations. No difference was found between the 1:1:1:1 and 2:1:1:1 ratios. Based on these observations, the 1:1:1:1 plasmids ratio was selected for further optimisation.

Lipofectamine 3000 is reported to be less toxic to HEK-293T cells while maintaining a high transfection efficiency compared to Lipofectamine 2000. In generic transfection protocols, a media change 14-16h following transfection is recommended to preserve cell viability and cell recovery due to the toxicity of the lipofectamine reagent. The transfection efficiency of HEK-293T cells was therefore examined for cells that were subjected to a media change 14-16h following transfection versus cells that did not undergo a media change. Forty-eight hours following transfection, no difference was observed in the percentage efficiency between the two groups *(Figure 3.9B)*.

To determine the optimal timepoint for harvesting viral supernatant that yields the highest lentivirus production, the virus titre was examined at 48h, 72h, and pooled 48h and 72h supernatant. Virus supernatant harvested at 48h had a slightly higher titre than virus harvested at 72h although this increase was not significant. The highest lentivirus production was observed when 48h and 72h collections were combined. In this case, the first harvest was made at 48h and stored at 4°C overnight, with the addition of fresh culture medium to the cells and a second collection following another 24h before being pooled *(Figure 3.9C)*.

To investigate whether freshly harvested virus yields a higher transduction efficiency than cryopreserved virus, Jurkat T cells were transduced with freshly or cryopreserved pooled virus from 48h and 72h harvest in the presence of polybrene. Protein-L staining was employed to determine Jurkat T cells that successfully incorporated the CD123-CD28-OX40-SF CAR 96h following transduction. Transduction with fresh virus yielded a higher efficiency compared to transduction with cryopreserved virus (92%±3.7% vs. 52%±4.2%) *(Figure 3.9D)*.

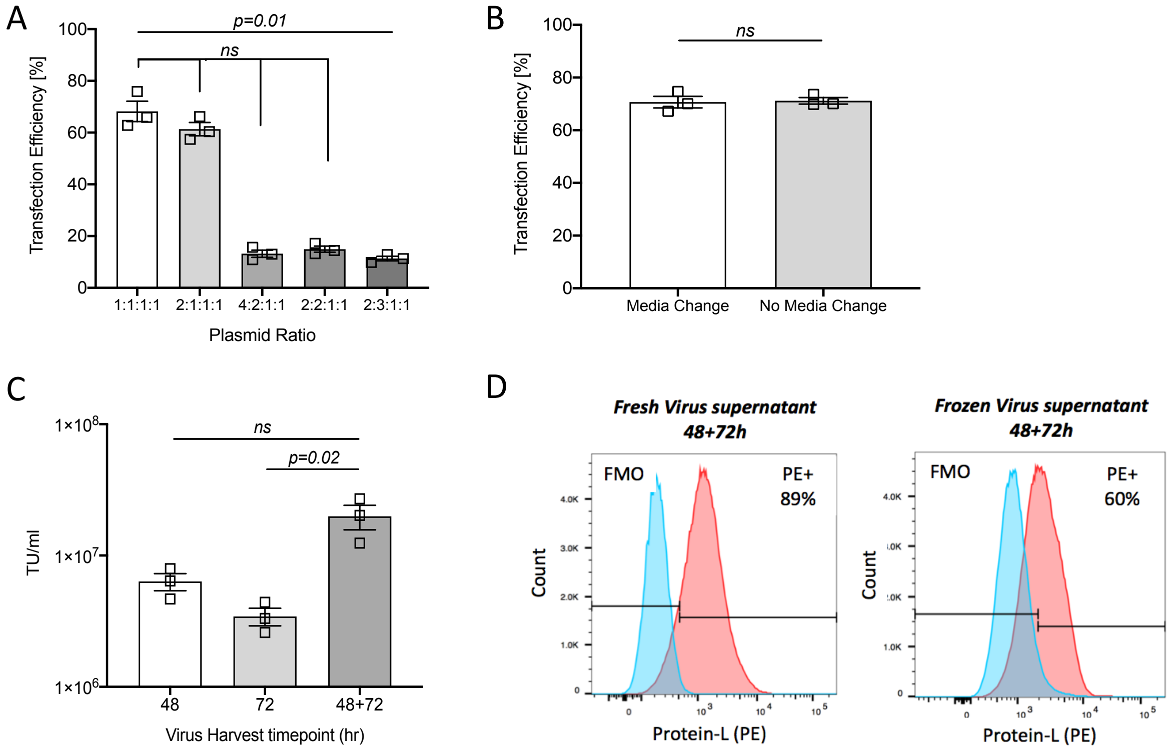

Figure 3.9. Establishment of optimal conditions for efficient and high yield lentivirus production using the CD123-CD28-OX40-SF CAR plasmid.
(A) Transfection efficiency of HEK-293T cells using different plasmid ratios (transgene-pCAR:VSV-G:gag/pol:rev). **(B)** The effect of media change 14-16h post transfection on transfection efficiency of HEK-293T cells. **(C)** The effect of viral supernatant harvesting times on viral titre (TU/mL). Single harvests were performed 48h or 72h post transfections or pooled harvests from 48h and 72h. Viral titre experiments and calculations were performed based on the transfection efficiency of HEK-293T cells. **(D)** The effect of fresh or cryopreserved viral supernatant from a pooled harvest at 48h and 72h on Jurkat T cell transduction. Jurkat T cells that were successfully transduced with lentivirus were quantified by surface staining of Protein-L (PE) 96h following transduction. All graphed data are represented as mean ± SEM, and pooled from 3 independent experiments (n=3). P-values were calculated using non-parametric 1-way ANOVA (a, c) or Student's *t*-test (Mann-Whitney) (b).

To determine whether the same transduction efficiencies could be observed with primary T cells, $CD3^+$ T cells from PBMCs were isolated from HDs and transduced with freshly harvested or cryopreserved virus in the presence of polybrene. Primary T cells that successfully incorporated the CD123-CD28-OX40-SF CAR 96h following transduction was determined by Protein-L. While transduction efficiencies in Jurkat T cells were high, transduction efficiencies of T cells were no more than 5% regardless of fresh or cryopreserved virus *(Figure 3.10)*.

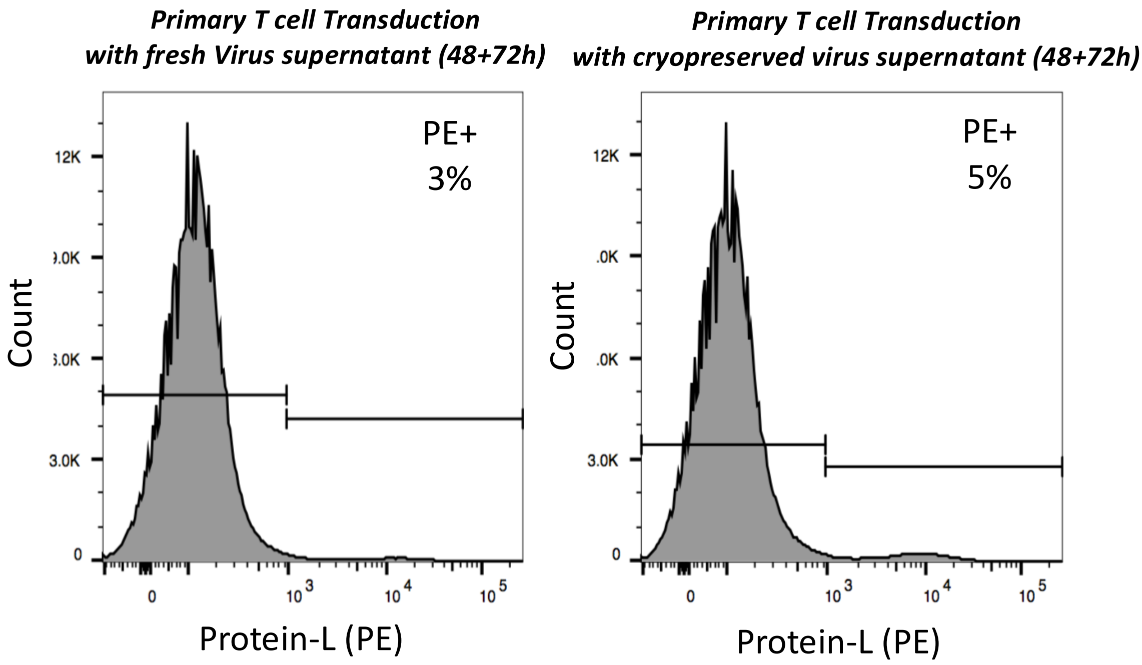

Figure 3.10. Transduction efficiency of primary T cells with fresh or cryopreserved virus supernatant from the CD123-CD28-OX40-SF CAR plasmid.
The effect of fresh or cryopreserved viral supernatant from a pooled harvest at 48h and 72h on primary isolated T cell transduction. T cells that were successfully transduced with lentivirus were quantified by surface staining of Protein-L (PE) 96h following transduction.

Despite the extensive optimisation thus far, the transduction efficiency observed with Jurkat T cells did not translate to primary isolated T cells. To obtain a higher transduction efficiency with primary T cells, the harvested lentiviral supernatant was concentrated. Several publications document that it is commonplace to concentrate lentivirus for gene transfer into primary cells. This allows for stable and sufficient viral titres at a specific MOI. Furthermore, several concentration methods also help remove contaminating impurities for sensitive applications such as this. The standard procedure for concentration of virus involves ultracentrifugation at 20,000rpm for 90mins. The standard procedure was compared to a commercially available reagent, Lenti-X concentrator (Takara Bio), that is reported to be fast, user-friendly, efficient, and able to concentrate virus 10-100-fold.

Both methods of concentration of lentivirus resulted in a 1-1.5 log fold increase in virus titre compared to unconcentrated virus. Furthermore, ultracentrifugation of lentivirus led to a slight but not statistically significant increase in viral titre over the Lenti-X reagent *(Figure 3.11A)*. To determine whether concentration of virus allows for successful CAR expression in Jurkat T cells, the cells were transduced at a MOI 1 (equivalent transducing units with concentrated virus to T cells) with lentivirus concentrated using ultracentrifugation. Jurkat T cells demonstrated high CAR expression, based on Protein-L staining, 72h following transduction *(Figure 3.11B)*.

To evaluate whether the transduction efficiencies observed with Jurkat T cells using the concentrated virus could be translated to primary T cells, $CD3^+$ T cells from PBMCs were isolated from HDs and transduced with cryopreserved concentrated virus at a MOI 1 in the presence of polybrene. Primary T cells that successfully incorporated the CD123-CD28-OX40-SF CAR 96h was determined with Protein-L. With the concentration of virus, transduction efficiencies in primary T cells increased to 20-30% as compared to using unconcentrated virus *(Figure 3.11C)*. The increased transduction efficiency observed could also be attributed to the removal of impurities in the virus supernatant following concentration.

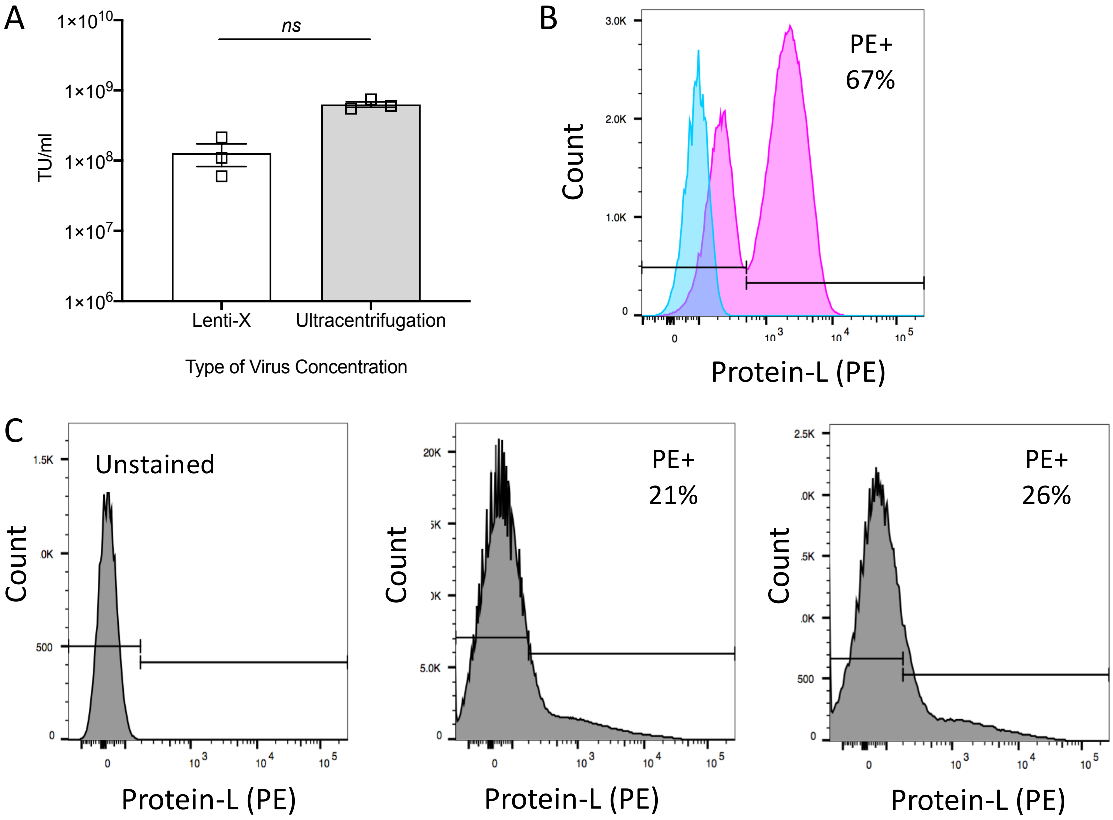

Figure 3.11. Confirmation of optimal virus concentration methodology to generate primary T cells incorporating the CD123-CD28-OX40-SF CAR plasmid with good efficiency.
(A) Virus titre measured and compared with supernatant concentrated using Lenti-X concentrator reagent or ultracentrifugation. **(B)** Representative histogram of Jurkat T cells transduced with cryopreserved virus following concentration with ultracentrifugation. Transduction efficiency was measured by staining for surface expression of Protein-L (PE) by flow cytometry. The blue denotes Protein-L FMO control while the Pink denotes stained Jurkat cells. **(C)** Representative histogram of primary isolated T cells transduced with cryopreserved virus following concentration with ultracentrifugation. Transduction efficiency was measured by staining for surface expression of Protein-L (PE) by flow cytometry. Left panel depicts the unstained cells and the middle and right panel depict T cells transduction in 2 independent HDs. All graphed data are represented as mean ± SEM, and pooled from 3 independent experiments (n=3). P-values were calculated using non-parametric Student's *t*-test (Mann-Whitney) (a).

3.4.3 Achieving high transduction of primary T cells

Having established the optimal conditions for production of high yield lentivirus, the optimal transduction and culture conditions of primary T cells was the next consideration. Various publications have reported the importance of inducing cell-cycle entry into the G_{1b} phase via stimulation of the T cell receptor. This suggests that the strength of TCR signalling is of importance to increase the transduction efficiency of naïve T cells (Korin & Zack, 1998)(Maurice et al., 2002). To determine the optimal time for activation of T cells that results in the highest transduction efficiency, T cell were activated with anti-CD3/CD28 beads for 24, 48, or 72h prior to transduction. Transduction efficiencies were observed to be highest when the primary T cells were activated for 48h prior to exposure with lentivirus. This increased efficiency was statistically significant compared to T cells activated for 72h but not 24h (*Figure 3.12A).*

While the optimisation so far has allowed for increased transduction efficiency, the primary T cells succumbed to the transduction process and were not able to recover for rapid expansion in culture. All transductions have thus far been facilitated by polybrene. While polybrene is the general facilitator for gene transduction of various types of cells, it is reported to be cytotoxic to hard-to-transduce cells such as primary cells. Conversely, the recombinant human fribronectin fragment, RetroNectin, has been documented to increase transduction efficiency of primary cells while maintaining viability of the cells. While only a trending increase was observed in the transgene expression of CD123 CAR T cells between cells transduced with retronectin over polybrene, cell viability decreased when cell transduction was facilitated by polybrene. Conversely, cell transduction facilitated by retronectin resulted in close to 100% cell recovery 48h following exposure to virus *(Figure 3.12B-C).*

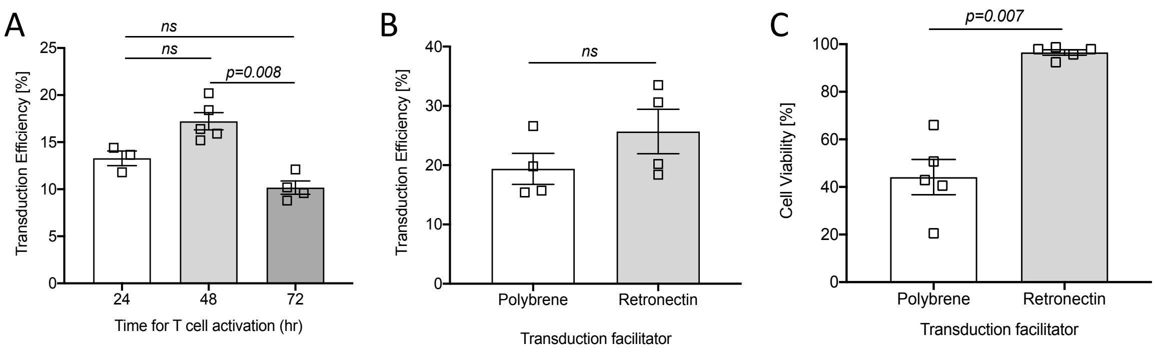

Figure 3.12. Optimal conditions for primary T cell transductions using the CD123-CD28-OX40-SF CAR plasmid.

(A) Effect of primary T cell activation time prior to transduction (24h, 48h, or 72h) on transduction efficiencies/transgene expression *(n=3, n=5, n=4, respectively)*. **(B)** Effect of different transduction facilitators, polybrene *(n=4)* or retronectin *(n=4)*, on transduction efficiencies/transgene expression. **(C)** Effect of different transduction facilitators, polybrene *(n=5)* or retronectin *(n=5)*, on cell viability and recovery 48h following transduction. Data was pooled from independent experiments and graphed data are represented as mean ± SEM.

In order to achieve a high and consistent level of gene expression in primary T cells, the number of viral particles introduced during the transduction should be kept uniform. The concentration of lentivirus allows the calculation of total viral particles from each batch of virus produced thereby enabling a fixed amount of lentivirus to be exposed to the T cells. The majority of published protocols report an MOI 1-5. Therefore, T cells were transduced at MOI 1, 2, and 5. Transduction efficiencies increased with increased MOI, with the highest efficiency observed with MOI 5. The T cells were able to withstand the transduction process and recovered for expansion *(Figure 3.13)*.

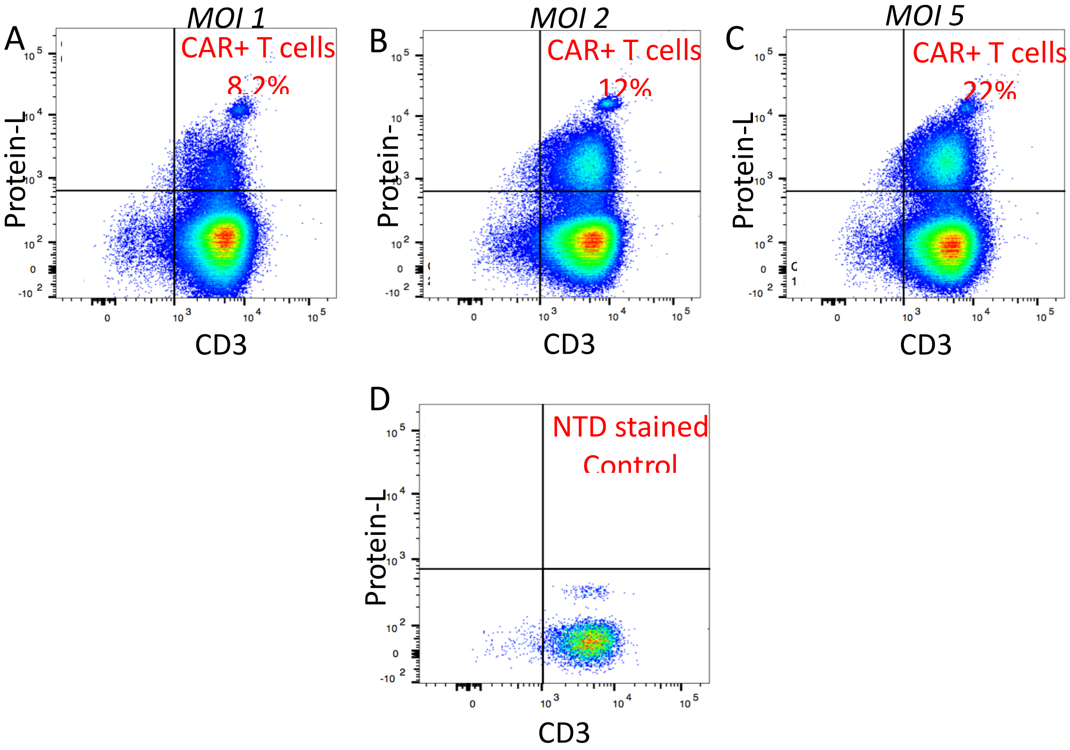

Figure 3.13. Determining the optimal viral multiplicity of infection (MOI) for consistent delivery of CAR transgene into primary T cells.
Primary T cells transduced at an **(A)** MOI 1, **(B)** MOI 2, and **(C)** MOI 5 with lentivirus generated from the CD123-CD28-OX40-SF CAR plasmid. **(D) Non-transduced (NTD) T cells stained with Protein-L as a control.**

3.4.4 Successful generation and expansion of primary anti-CD123 CAR T cells

With the optimised protocol, primary T cells were transduced with each of the four CAR lentiviral plasmids. Enriched CD3$^+$ T cells derived from HD PBMCs or BMMNCs were activated with anti-CD3/CD28 beads for 48h at a ratio of 2:1 and transduced with the lentiviral vector at a MOI 5 to express each of the four anti-CD123 CARs. T cells were cultured for 5 days following transduction and sort purified using Protein-L staining (sort purity: >95% consistenly) for CAR expressing T cells prior to expansion *in vitro* for a further 10 days in the presence of human recombinant interleukin-2 (rIL-2) *(Figure 3.14A)*. The sort purification allows analysis of function and efficacy strictly from the CAR T cells without the possibility of NTD cells contributing or dampening the anti-leukemia effect.

This protocol enabled the average production of at least 1x10^8 CAR T cells at the end of expansion which represented an average 150-fold increase from the initial cell concentration. Furthermore, the optimised protocol allowed consistent transduction efficiencies, ranging from 15-35% in primary isolated polyclonal T cells prior to sort purification with all CAR lentiviral plasmids (*Figure 3.14B*). The polyclonal T cells used for transduction often maintained a majority CD4^{+} phenotype over CD8^{+} phenotype under expansion with rIL-2 and were usually effector-, central- memory, or terminally differentiated effector cells at the end of expansion (*Figure 3.14C*).

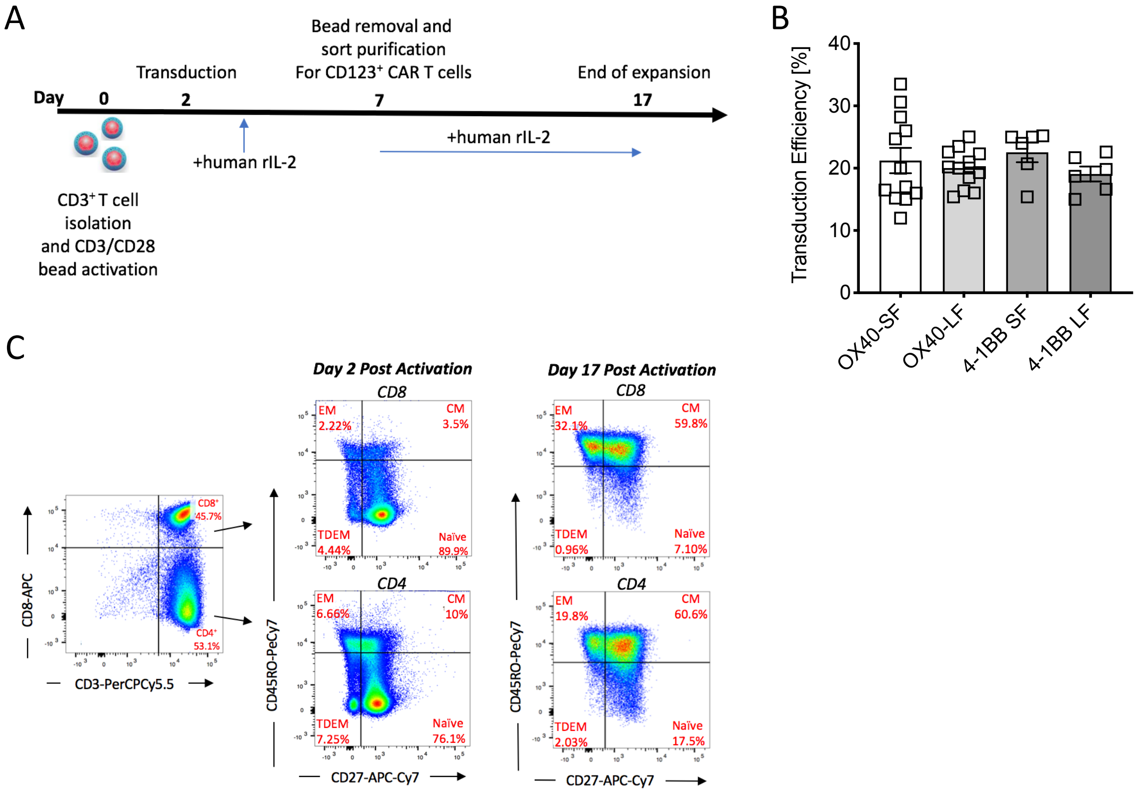

Figure 3.14. Generation and production of CD123 CAR T cells.
(A) Schematic diagram of the timeline and protocol for the production of CD123 CAR T cells. **(B)** Transduction efficiencies of primary T cells with the finalised protocol. T cells incorporating each of the CAR plasmids yielded average efficiencies of 20-25%: OX40-SF *(n=12),* OX40-LF *(n=12),* 4-1BB-SF *(n=6),* 4-1BB-LF *(n=6).* All graphed data are represented as mean ± SEM. **(C)** Representative flow cytometry dot plots demonstrating the phenotype of HD T cells prior to activation with CD3/CD28 dynabeads and CD123 CAR lentiviral transduction. The majority of T cells from healthy donors were CD4^{+} phenotype (left panel). The majority of CD8^{+} (middle top panel) and CD4^{+} (middle lower panel) T cells possess a naive phenotype prior to activation. However, a small portion of cells are phenotypically central memory (CM), effector memory (EM) or terminally differentiated effector memory (TDEM). Following 17 days of expansion, and post CD123 CAR lentiviral transduction, the majority of CD8^{+} (right top panel) and CD4+ T cells (right bottom panel) possess a CM or EM phenotype.

3.4.5 Third generation CD123 CAR T cells activate multiple effector functions in the presence of CD123$^+$ target cells *in vitro*

In order to examine the effector function of the 4 third generation CAR T cells, the four different CD123 CAR T cell constructs were therefore co-incubated with the human AML cell line, KG1a (>80% CD123$^+$ surface expression) or the SUPB15 ALL cell line (CD123$^-$) and measured for their ability to degranulate and proliferate.

Leukaemia cells are recognised and killed by cytotoxic lymphocytes such as T cells, mainly through the immune secretion of lytic granules that kill the target cells. This process therefore involves the fusion of the granule membrane with the cytoplasmic membrane of the immune effector cell, resulting in surface exposure of lysosomal-associated proteins on the cell membrane, for example, by CD107a (LAMP-1). The membrane expression of CD107a therefore acts as a surrogate marker of immune cell activation and cytotoxic degranulation. The expression level of CD107a on the surface of HD derived CD123 CD4$^+$ and CD8$^+$ CAR T cells was assessed as an indicator of anti-tumour activity.

CD3$^+$ CAR T cells were starved of recombinant hIL-2 and CD3/CD28 dynabeads were removed 16h prior to co-culture to exclude the possibility of exogenous growth cytokines affecting CAR T cell function. Following a 6h co-culture of CD3$^+$ CAR T cells with KG1a or SUPB15, the CAR T cells were analysed by flow cytometry for upregulation of CD107a expression on CD8$^+$ and CD4$^+$ T cell populations in response to the cell lines. For the OX40 CAR constructs, both T cell sub-populations were able to degranulate in the presence of the target cells with increased degranulation correlating with increasing E:T ratios. The OX40 CAR constructs demonstrated a higher rate of degranulation. At an E:T ratio of 10:1, OX40-LF and OX40-SF CD8$^+$ CAR T cells demonstrated an average CD107a expression of 45.17% and 43.6%, respectively *(Figure 3.15)*. In contrast, the 4-1BB-LF and 4-1BB-SF CD8$^+$ CAR T cells demonstrated a reduced average expression of CD107a of only 22.8% and 25.54%, respectively *(Figure 3.16)*. CD4$^+$ CAR T cell degranulation was variable between the groups. Of all the constructs, the OX40-LF construct demonstrated the highest expression of CD107a on CD4$^+$ CAR T cells (65.01%) whereas the OX40-SF and 4-1BB SF constructs displayed 38.9% and 42.6% CD107a expression, respectively. Surprisingly, the 4-1BB LF CD4$^+$ CAR T cells displayed decreased CD107a expression (21.2%) *(Figure 3.15-3.16)*. While the OX40 constructs as well as the 4-1BB-SF constructs demonstrated minimal degranulation when cultured with SUPB15 cells, the 4-1BB-LF CAR T cells demonstrated non-specific degranulation at all E:T ratios *(Figure 3.16)*.

CD123-CD28-OX40-LF

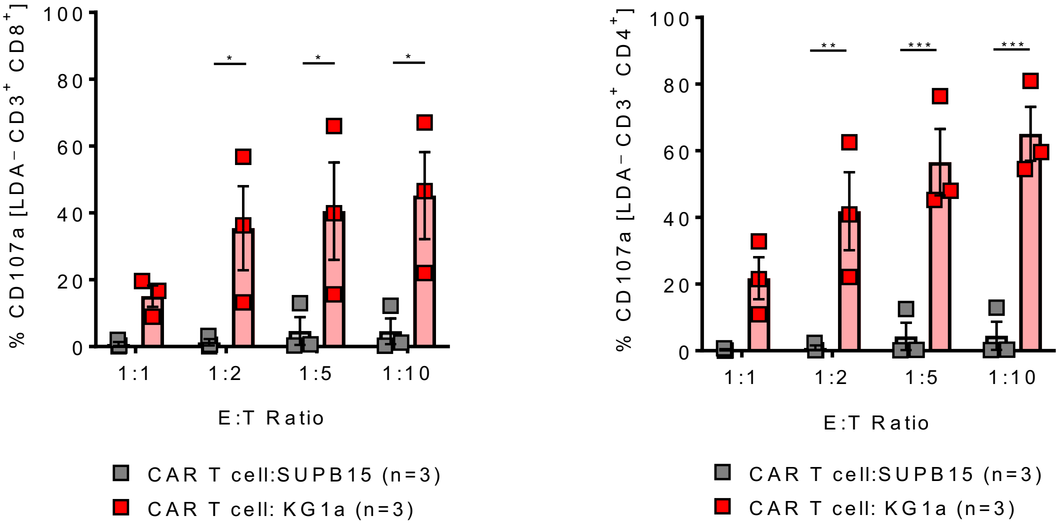

CD123-CD28-OX40-SF

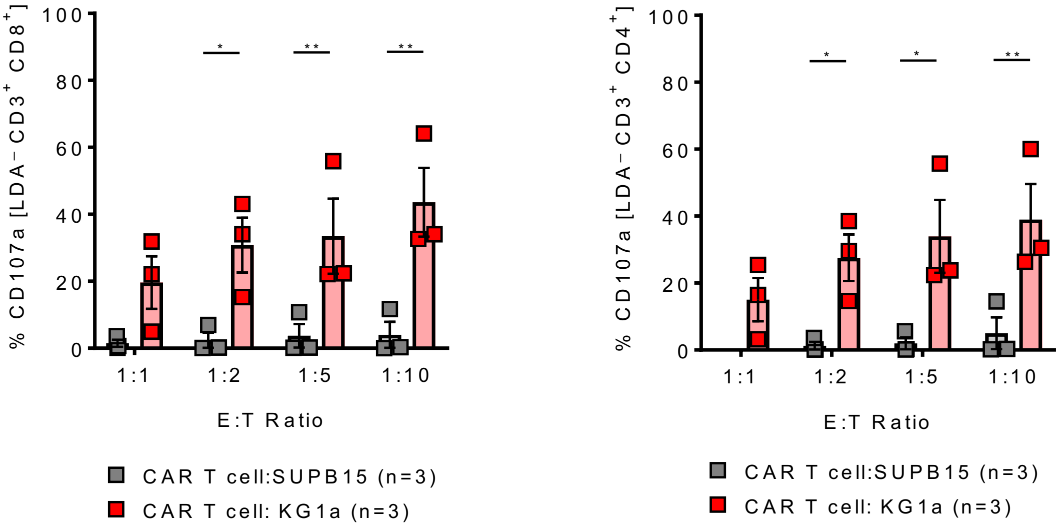

Figure 3.15. Degranulation of CD123 CAR T cells incorporating CD28-OX40 co-stimulatory motifs in the presence of CD123$^+$ AML cells.
CD123-CD28-OX40 short hinge fragment (SF) and long hinge fragment (LF) CAR construct effector T cell degranulation. CD123-OX40-LF CD8$^+$ CAR T cells (top left panel), CD123-OX40-LF CD4$^+$ CAR T cells (top right panel), CD123-OX40-SF CD8$^+$ CAR T cells (bottom left panel) and CD123-OX40-SF CD4$^+$ CAR T cells (bottom right panel) were analysed for percentage CD107a surface expression following co-culture with KG1a (CD123$^+$) or SUPB15 (CD123$^-$) cells at increasing E:T ratios. Experiment was carried out in media without growth factors (IL-2 and CD3/CD28 Dynabeads). Data were pooled from 3 independent experiments plated in duplicates. Data is presented as mean (of each duplicate) ± SEM. *<0.05, **<0.01, ***<0.001.

CD123-CD28-4-1BB LF

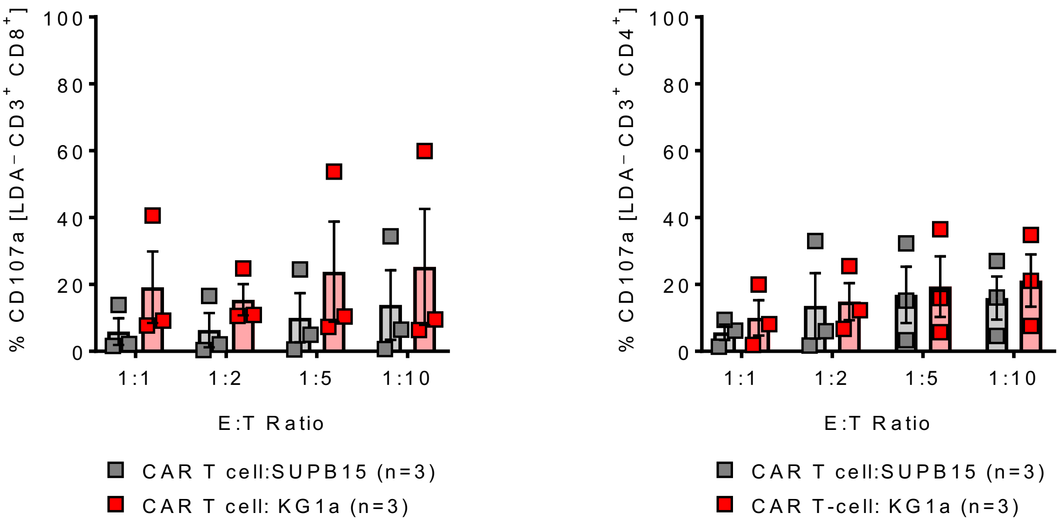

CD123-CD28-4-1BB SF

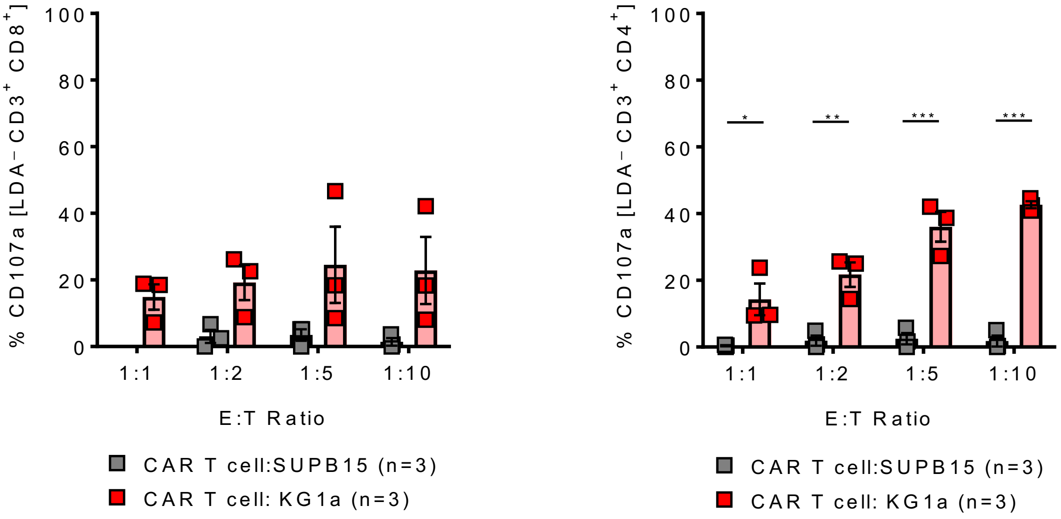

Figure 3.16. Degranulation of CD123 CAR T cells incoporating CD28-4-1BB co-stimulatory motifs in the presence of CD123$^+$ AML cells.

CD123-CD28-4-1BB short hinge fragment (SF) and long hinge fragment (LF) CAR construct effector T cell degranulation. CD123-4-1BB-LF CD8$^+$ CAR T cells (top left panel), CD123-4-1BB-LF CD4$^+$ CAR T cells (top right panel), CD123-4-1BB-SF CD8$^+$ CAR T cells (bottom left panel), and CD123-4-1BB-SF CD4$^+$ CAR T cells (bottom right panel) were analysed for percentage CD107a surface expression following co-culture with KG1a (CD123$^+$) or SUPB15 (CD123$^-$) cells at increasing E:T ratios. Experiment was carried out in media without growth factors (IL-2 and CD3/CD28 Dynabeads). Data were pooled from 3 independent experiments plated in duplicates. Data is presented as mean (of each duplicate) ± SEM. *<0.05, **<0.01, ***<0.001.

The ability of the CAR T cells to proliferate upon exposure to the target antigen is another important functional feature when selecting the best performing CAR construct for further investigation and pre-clinical development. HD derived CAR T cells incorporating each CAR construct was subjected to KG1a cells, SUPB15 cells or media only in the absence of recombinant hIL-2 and CD3/CD28 dynabeads for 96h and measured for the amount of cell division. For the CAR T cells containing the CD123-CD28-OX40-LF construct, $CD8^+$ T cells exhibited five cell divisions while the $CD4^+$ T cells exhibited four cell divisions. The CAR T cells containing the CD123-OX40-SF construct demonstrated similar proliferative capacity with both $CD8^+$ and $CD4^+$ T cells displaying four cell divisions *(Figure 3.17)*.

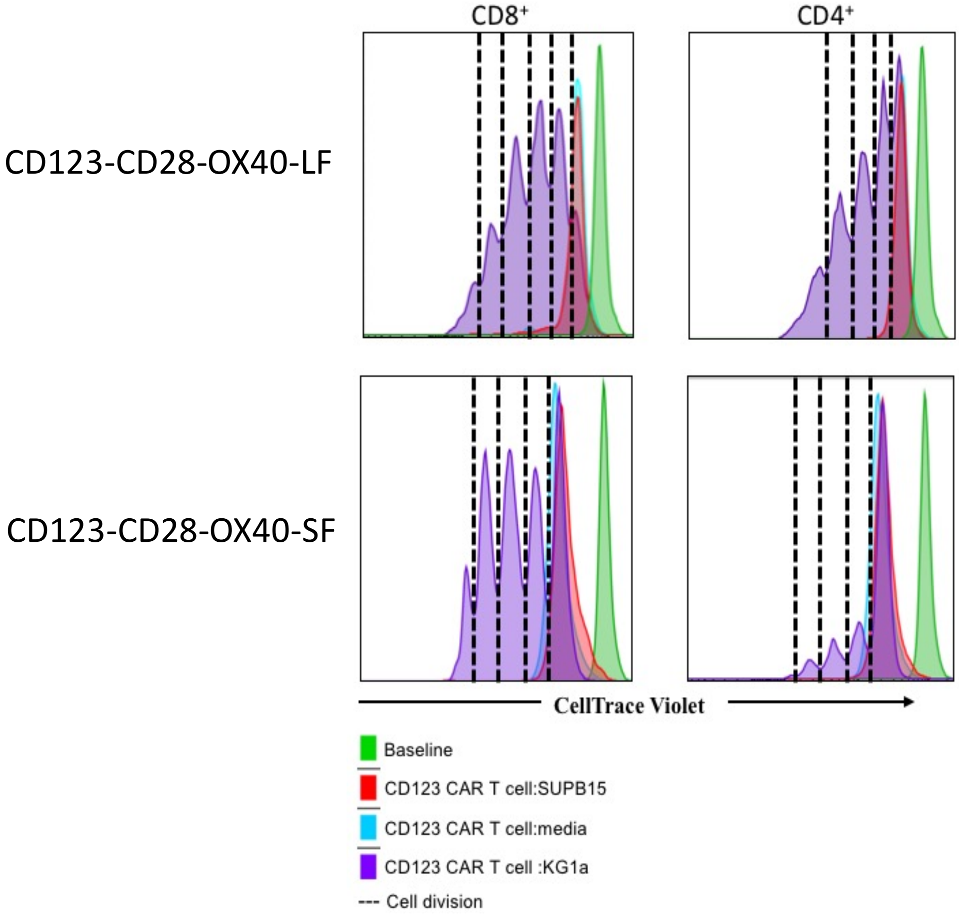

Figure 3.17. The proliferative capacity of CD123 CAR T cells incorporating CD28-OX40 co-stimulatory motifs in the presence of $CD123^+$ AML cells.
Representative histogram depicting the proliferation of $CD8^+$ (left panels) and $CD4^+$ (right panels) CD123-OX40 LF and SF CAR T cells as examined by CellTrace Violet dye dilution following 96h of co-culture with media (untreated), KG1a or SUPB15 cells at an E:T ratio of 1:1. Experiment was carried out in media without growth factors (IL-2 and CD3/CD28 Dynabeads). Each dotted line represents one cell division. Baseline represents CellTrace Violet dye stained CAR T cells at t=0h prior to co-culture. The experiment was performed in triplicate with similar results to the one represented in the figure.

In contrast proliferation was not observed by the CAR T cells expressing the CD123-CD28-OX40 constructs when they were co-cultured with the CD123$^-$ cell line, SUPB15 or in media alone *(Figure 3.17)*. The CAR T cells that incorporated the CD28-4-1BB LF and SF constructs exhibited similar CD8$^+$ proliferation to that of the CD28-OX40 constructs. However, the ability of the CD4$^+$ T cells, with the CD28-4-1BB constructs, to proliferate in the presence of KG1a cells was significantly hampered. In particular the CAR T cells incorporating the CD28-4-1BB-LF construct displayed only one cell division during the course of the co-culture *(Figure 3.18)*. However, no CD4$^+$ or CD8$^+$ CAR T cell proliferation was observed when co-cultured with SUPB15 cells or media only *(Figured 3.18)*.

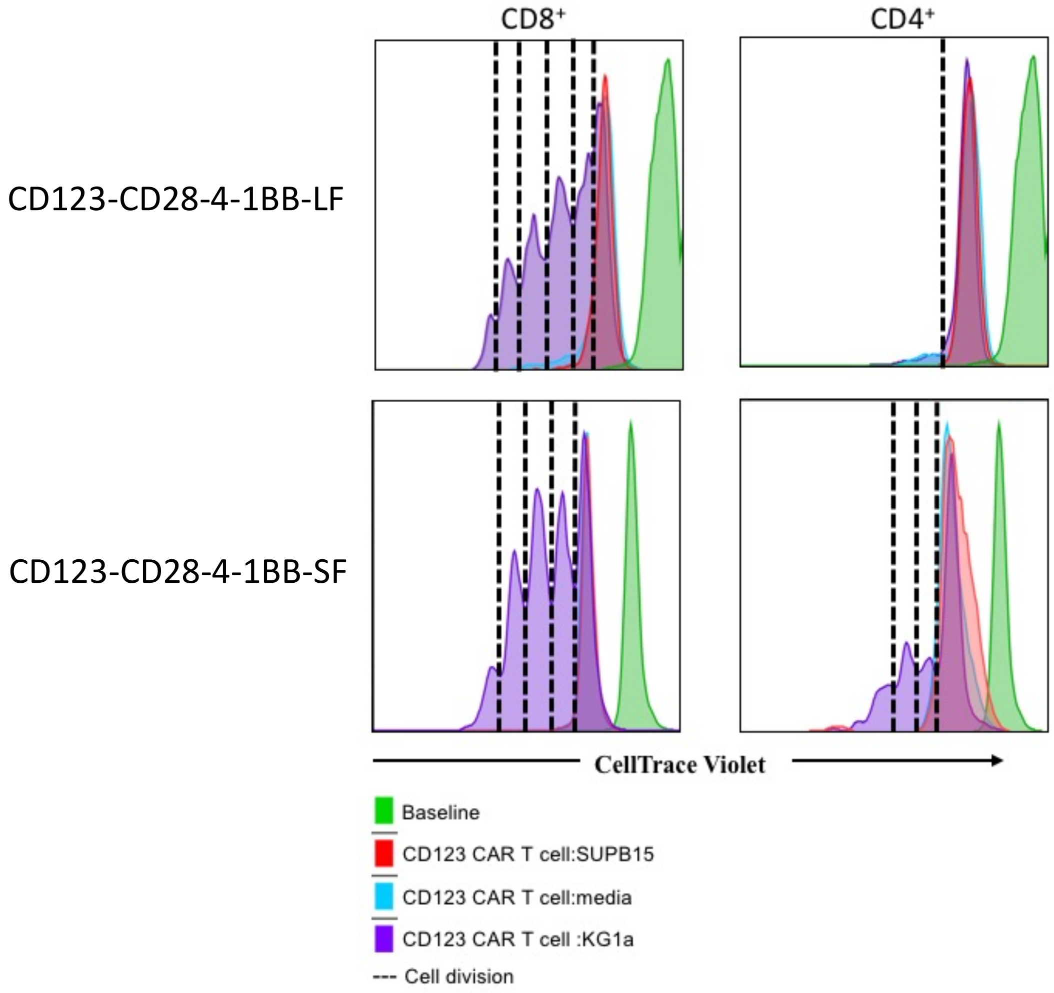

Figure 3.18. The proliferative capacity of CD123 CAR T cells incorporating CD28-4-1BB co-stimulatory motifs in the presence of CD123$^+$ AML cells.
Representative histogram depicting the proliferation of CD8$^+$ (left panels) and CD4$^+$ (right panels) CD123-4-1BB LF and SF CAR T cells as examined by CellTrace Violet dye dilution following 96h of co-culture with media (untreated), KG1a or SUPB15 cells at an E:T ratio of 1:1. Experiment was carried out in media without growth factors (IL-2 and CD3/CD28 Dynabeads). Each dotted line represents one cell division. Baseline represents CellTrace Violet dye stained CAR T cells at t=0h prior to co-culture. The experiment was performed in triplicate with similar results to the one represented in the figure.

3.4.6 Immune activation/exhaustion phenotypes of the third generation CD123 CAR T cells

Exposure of CAR T cells to target leukaemic cells have often been associated with increased senescence and an exhausted phenotype leading to terminal differentiation and/or depletion of the CAR T cells. Upregulation of key immune checkpoint markers has shown to significantly inhibit T cell function therefore leading to impaired function and efficacy in targeting leukaemia cells. In order to delineate the CAR constructs that are more prone to exhaustion, the CAR T cells were expanded for 10 days *in vitro* following sort purification with high dose recombinant human IL-2 (150U/mL). The CD123 CAR T cells incorporating the various CAR constructs were profiled for surface expression of the immune exhaustion markers: LAG-3, TIM-3, CTLA-4, and PD-1 by flow cytometry prior to and following 72h co-culture with CD123$^+$ KG1a AML cells in the absence of exogenous hIL-2.

Prior to co-culture the CAR T cells encompassing the CD123-CD28-OX40-LF and CD123-CD28-4-1BB-LF exhibited a high expression of TIM-3 in both CD4$^+$ and CD8$^+$ T cells subsets and moderate levels of PD-1 whilst CD123-CD28-4-1BB-SF expressed moderate levels of TIM-3 in both T cell subsets and low to absent levels of PD-1. In contrast, the CD123-CD28-OX40-SF revealed very low to absent levels of all immune exhaustion markers in the CD4$^+$ and CD8$^+$ T cells with the exception of CD8$^+$ T cells exhibiting 40% expression of TIM-3 *(Figure 3.19A).* No major differences between the CAR constructs was observed for CTLA-4 and PD-1.

Following the 72h co-culture with CD123$^+$ KG1a target AML cells, the CAR T cells encompassing the CD123-CD28-OX40-SF and CD123-CD28-4-1BB-SF CARs exhibited expression levels below 10% for all immune exhaustion markers. Interestingly, the expression of CTLA-4 was elevated in the CAR T cells incorporating the CD123-CD28-OX40-LF and CD123-C28-4-1BB-LF CAR constructs post co-culture with targets cells in comparison to the expression levels prior to co-culture *(Figure 3.19B).* Furthermore, expression of LAG-3 remained stable and did not increase significantly following co-culture. In contrast, expression of PD-1 and TIM-3 decreased in both CD4$^+$ and CD8$^+$ CAR T cells of the LF constructs. Collectively, a higher immune exhaustion profile was observed in the CAR T cells incorporating the LF constructs as compared to the SF constructs *(Figure 3.19B).* This suggests that the LF constructs may be prone to exhaustion more rapidly and may therefore affect the anti-tumour efficacy as well as the persistence of the CAR T cells *in vivo* or in patients.

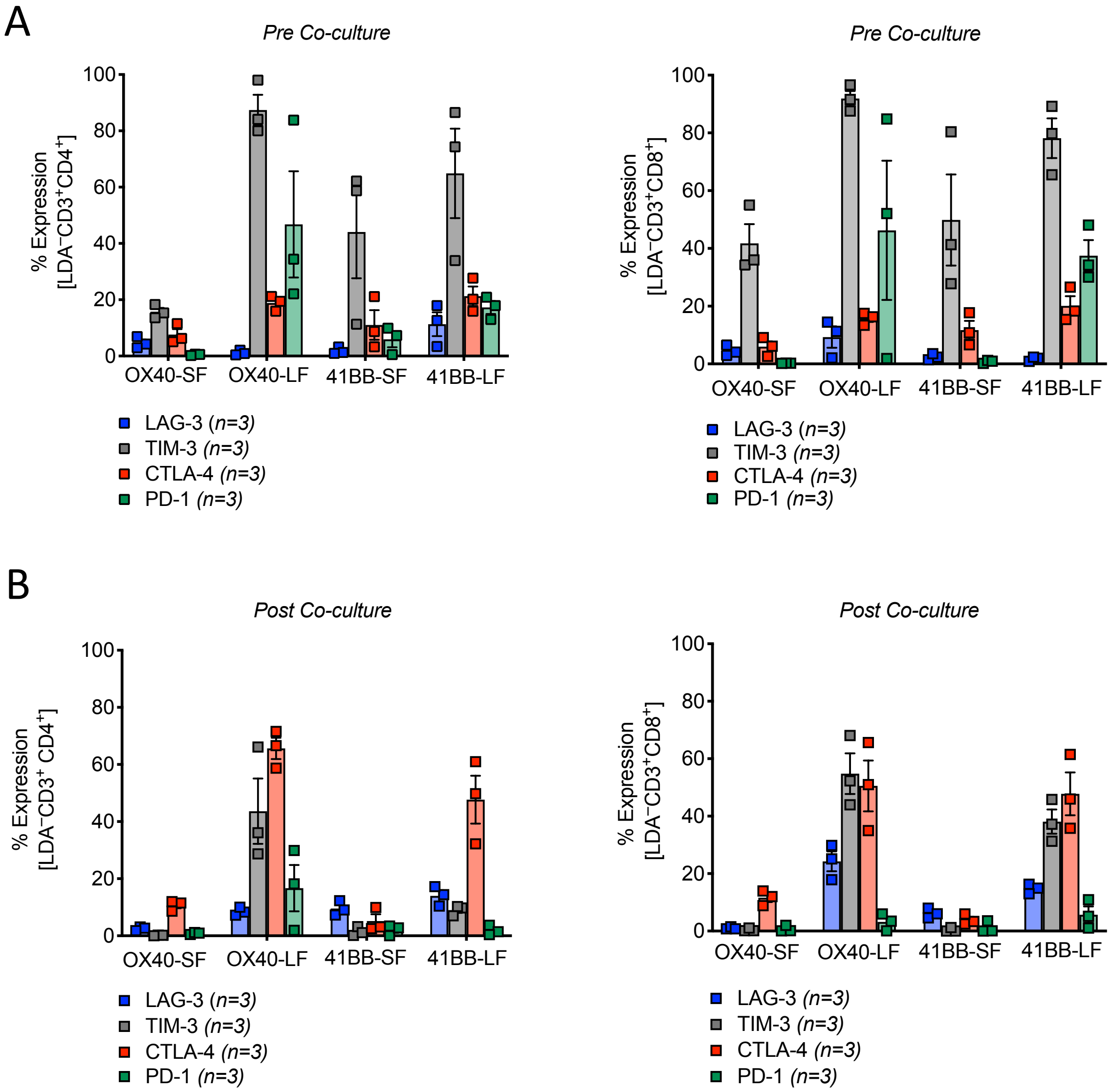

Figure 3.19. The expression of immune exhaustion markers of the third generation CD123 CAR T cells in the absence or presence of CD123$^+$ AML cells.

Scatter plots depicting the expression of exhaustion markers: LAG-3, TIM-3, CTLA-4, and PD-1 on CD4 T cells (left panels) and CD8 T cells (right panels) **(A)** 17 days following activation and prior to 72h co-incubation with target AML cells or **(B)** 72h (day 21) following incubation with target AML cells at an E:T ratio of 1:1**.** The data is pooled from 3 independent transductions and are presented as mean ± SEM.

3.4.7 Third generation CD123 CAR T cells demonstrate killing capacity against CD123$^+$ leukaemia cells *in vitro*, which is mediated by the secretion of anti-tumour related cytokines

To confirm the specificity of the CD123 CAR T cells, the genetically modified T cells were examined for their ability to lyse the CD123$^+$ KG1a AML cell line and were compared to the SUPB15 cell line which lacks CD123 expression. The CAR T cells were co-cultured with CellTrace Violet labelled KG1a or SUPB15 cells for 16h and assessed for percentage cell specific lysis using flow cytometry with absolute cell counting beads.

All CD123 CAR constructs demonstrated efficient lysis of KG1a cells with increased cytotoxic capacity correlated with increased E:T ratio. At an E:T ratio of 10:1 all constructs demonstrated at least 60% lysis. Moreover, the CD123-CD28-OX40 LF and SF constructs as well as the CD123-CD28-4-1BB SF demonstrated minimal non-specific targeting (less than 20% at all E:T ratios; $p<0.001$) of the control CD123$^-$ cell line, SUPB15 *(Figure 3.20A-B, D)*. In contrast, the CD123-CD28-4-1BB LF demonstrated significant non-specific killing of the SUPB15 with a specific lysis of 50% at the E:T ratio of 10:1. This suggested that this CAR is not discriminant in its killing abilities *(Figure 3.20C)*. This observation was concordant with the CD107a degranulation where non-specific degranulation was observed from both CD4$^+$ and CD8$^+$ CAR T cells. Based on the aforementioned results, it was concluded that the CD123-CD28-4-1BB LF CAR would not be suitable for further *in vitro* and *in vivo* intervention and was left out of experiments subsequently.

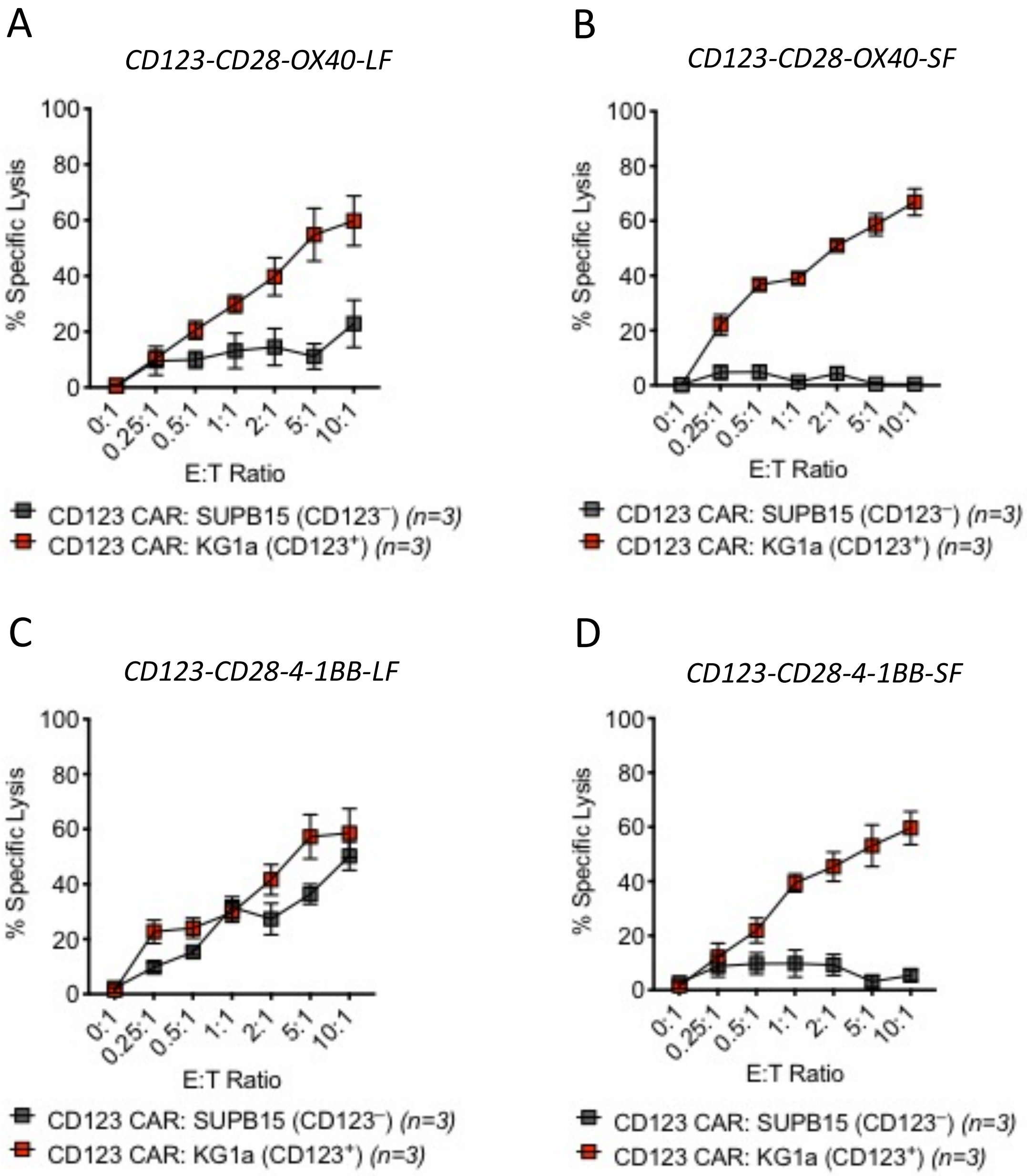

Figure 3.20. The effect of the third generation CD123 CAR T cells to lyse the CD123$^+$ KG1a AML cell line.

(A) Specific cytotoxicity of CD123-CD28-OX40-LF **(B)** CD123-CD28-OX40-SF **(C)** CD123-CD28-4-1BB-LF **(D)** CD123-CD28-4-1BB-SF CAR T cells against CD123$^+$ KG1a cells or CD123$^-$ SUPB15 cells (CellTrace violet labelled) by flow cytometric analysis following a 16h co-incubation. The experiment was performed with 3 pair-matched HD derived CAR T cells plated in triplicate for all constructs. The data are represented as mean values ± SEM.

To examine whether cytotoxicity observed was correlated with the release of cytokines required for an anti-tumour effect, the CD123-CD28-OX40-SF, LF, and CD123-CD28-4-1BB-SF CARs were measured for secretion of multiple effector and homeostatic cytokines and chemokines. The CARs were cultured in media, with SUPB15 control cells or with KG1a cells in the absence of additional exogenous recombinant hIL-2 for 24h. The supernatant from the co-culture was collected for each condition and measured using a 32-plex cytokine and chemokine kit to determine the cytokines where changes were observed.

Of the 32 cytokines and chemokines measured, 9 were shown to be secreted by the T cells with differences between the groups; IFNγ, GM-CSF, CXCL10, TN, IL-2, IL-5, IL-13, macrophage inflammatory protein 1 α or chemokine ligand 3 (MIP-1α or CCL3), and macrophage inflammatory protein 1β or chemokine ligand 4 (MIP-1β or CCL4).

CAR T cell products incorporating the CD123-CD28-OX40-SF CAR demonstrated robust ability to secrete several pro-inflammatory cytokines with an observed significant increase of IFNγ, TNF, IL-2, IL-5, IL-13, CXCL10, MIP-1β when cultured with KG1a cells compared to the SUPB15 or media only controls. Increased concentrations of GM-CSF and MIP-1α were also observed however these data were not significant. For the CD123-CD28-OX40-LF CAR, significant increases ($p<0.02$) in the secretion levels were observed only for IFNγ, TNF, CXCL10, and GM-CSF when cultured with KG1a cells compared to co-culture with SUPB15 or media only. By contrast, a significant increase was only observed for IL-13 when CD123-CD28-4-1BB-SF CAR T cells were cultured with KG1a cells compared to the control conditions. No significant difference was observed for the other cytokines analysed *(Figure 3.21-Figure 3.23).*

Collectively, the superior effector functions exhibited by the CD123-CD28-OX40-SF CAR illustrated its ability to orchestrate potent immune responses in the presence of CD123^{+} leukaemic cells. Therefore, this CAR was selected as the most suitable CAR construct for further evaluation with primary AML cells and *in vivo* investigation (Chapter 4).

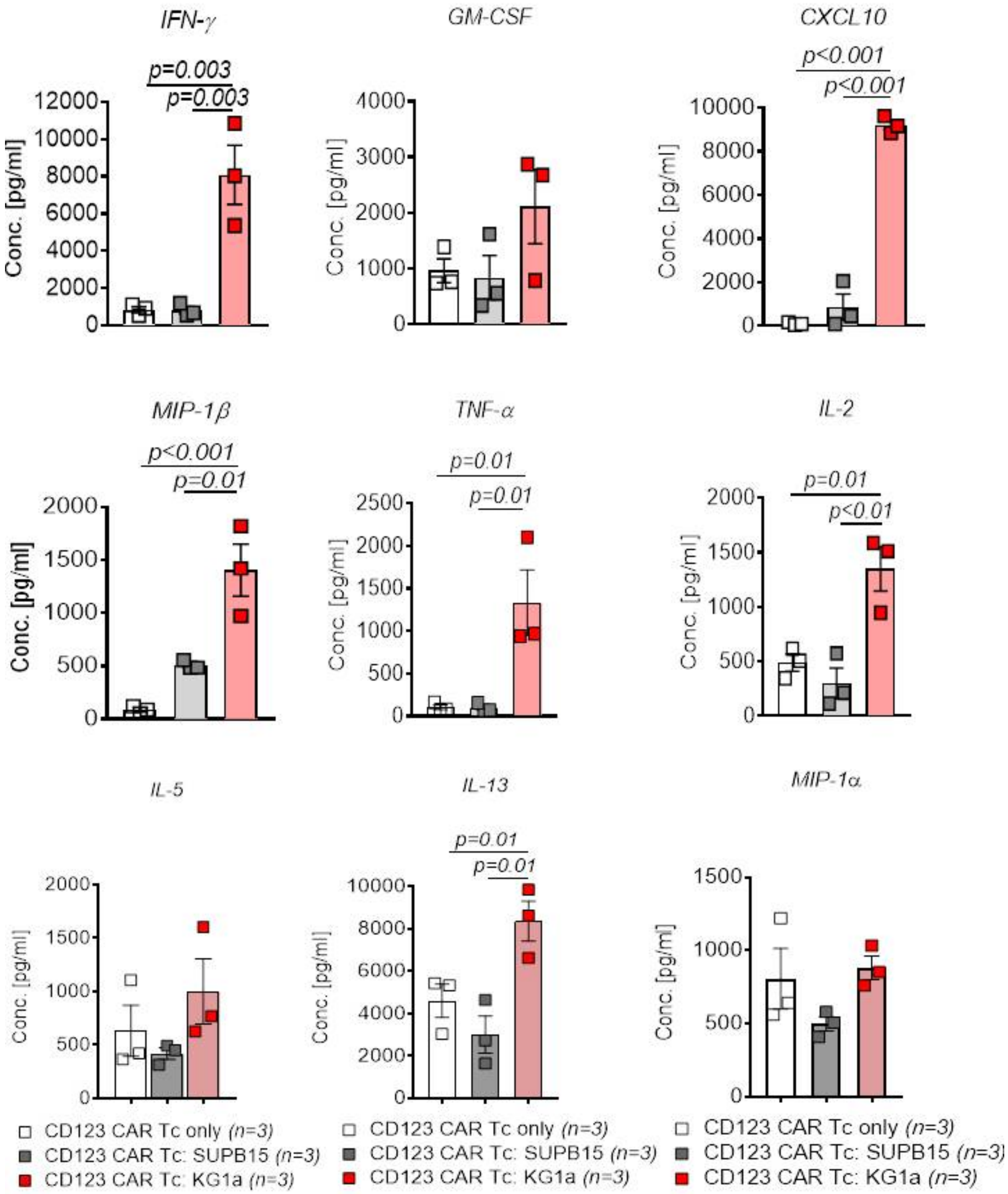

Figure 3.21. *In vitro* cytokine production by CD123-CD28-OX40-SF CAR T cells following 24h co-culture with CD123$^+$ AML cells.

CD123-CD28-OX40-SF CAR T cells were co-cultured with media only (untreated), SUPB15 or KG1a cells at an E:T ratio of 10:1 for 24h. The supernatant was analysed and quantified for the release of various cytokines and chemokines. The cytokines/chemokines with differences between the treatment groups are depicted. All graphed data is presented as mean ± SEM. *P*-values were calculated using 1-way ANOVA.

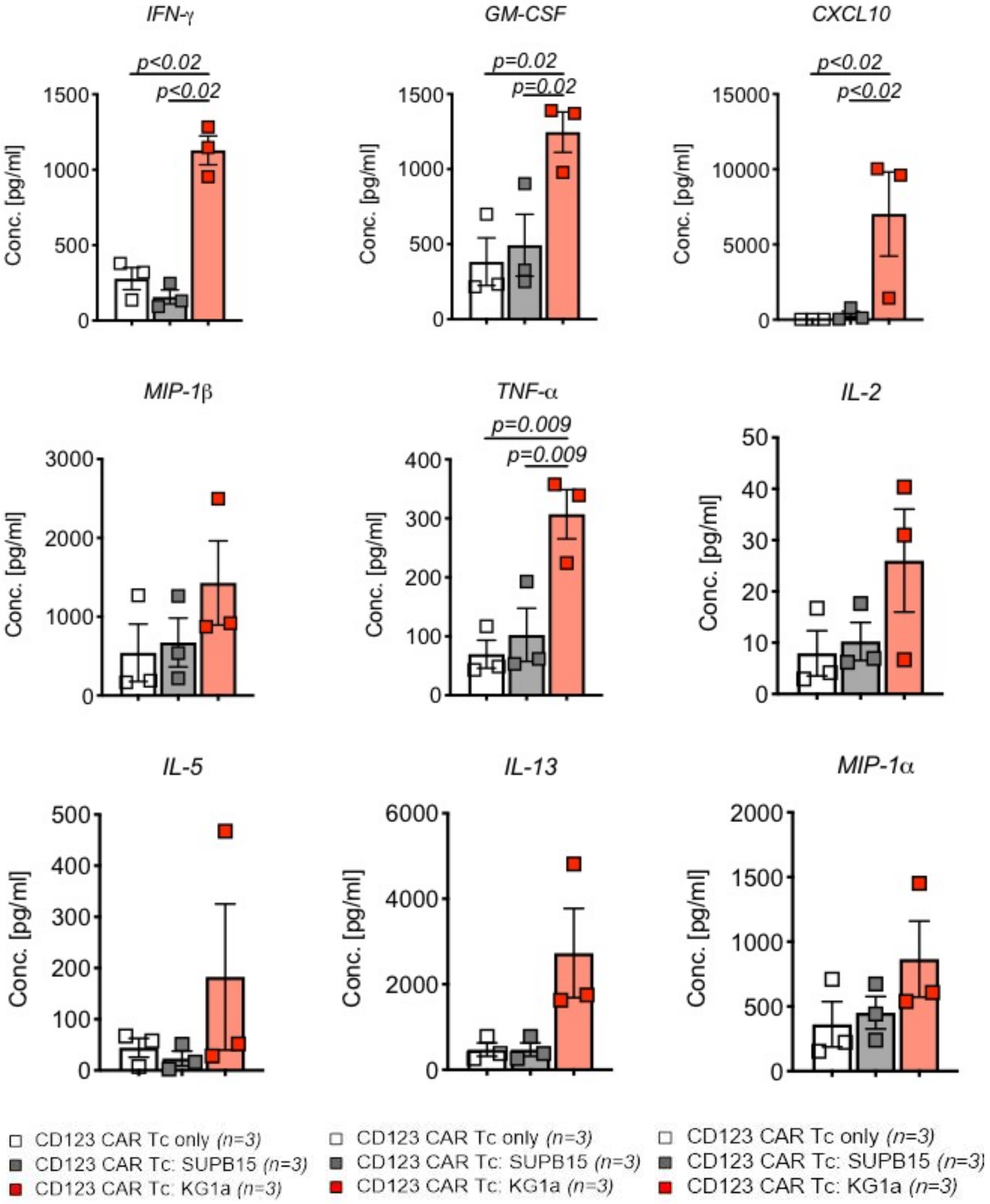

Figure 3.22. *In vitro* cytokine production by CD123-CD28-OX40-LF CAR T cells following 24h co-culture with CD123$^+$ AML cells.

CD123-CD28-OX40-LF CAR T cells were co-cultured with media only (untreated), SUPB15 or KG1a cells at an E:T ratio of 10:1 for 24h. The supernatant was analysed and quantified for the release of various cytokines and chemokines. The cytokines/chemokines with differences between the treatment groups are depicted. All graphed data is presented as mean ± SEM. *P*-values were calculated using 1-way ANOVA.

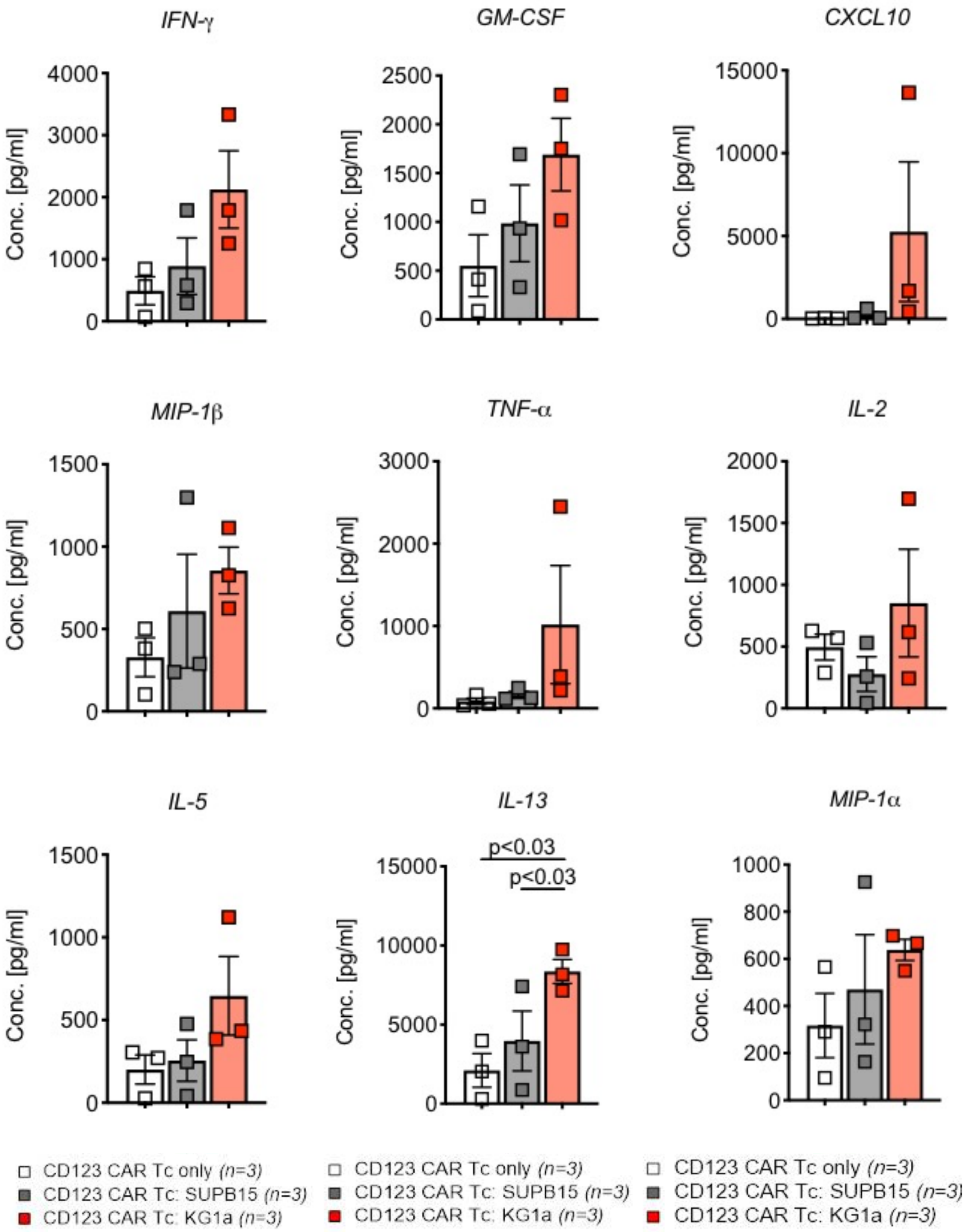

Figure 3.23. *In vitro* cytokine production by CD123-CD28-4-1BB-SF CAR T cells following 24h co-culture with CD123⁺ AML cells.
CD123-CD28-4-1BB-SF CAR T cells were co-cultured with media only (untreated), SUPB15 or KG1a cells at an E:T ratio of 10:1 for 24h. The supernatant was analysed and quantified for the release of various cytokines and chemokines. The cytokines/chemokines with differences between the treatment groups are depicted. All graphed data is presented as mean ± SEM. *P*-values were calculated using 1-way ANOVA.

3.4.8 Third generation CD123-CD28-OX40-SF CAR T cells eradicate primary AML patient derived BMMCs and are capable of preventing colony formation of leukaemic progenitor cells *in vitro*

To evaluate the tumoricidal ability of the CD123-CD28-OX40-SF CAR T cells on primary AML cells, the CAR T cells were co-cultured with CellTrace Violet labelled BM derived AML cells or BM derived HD cells for 16h and assessed for percentage cell specific lysis using flow cytometry with absolute cell counting beads. The CD123-CD28-OX40-SF CAR T cells demonstrated robust lysis of all primary AML patient samples tested with a maximum of 65% killing at a E:T ratio of 10:1 for AML Patients 1 and 2 whereas the CAR T cells were able to eliminate almost 80% of AML cells from patient 3 in 16h *(Figure 3.24)*. In contrast, significantly lower or no cytotoxicity was observed when the CD123 CAR T cells were co-cultured with BM derived HD cells.

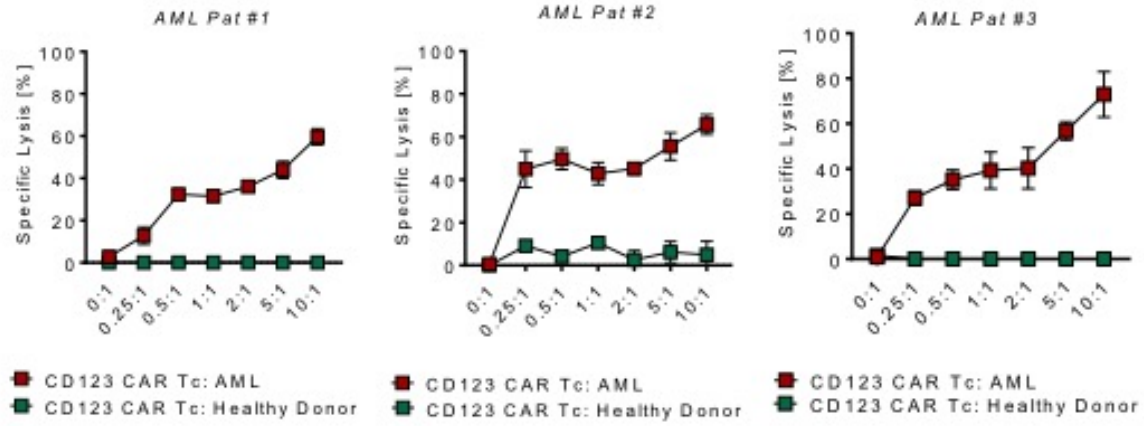

Figure 3.24. CD123-CD28-OX40-SF CAR T cells specifically target and lyse primary AML BMMNCs.
Specific cytotoxicity of CD123 CAR T cells against 3 patient primary AML BMMNC cells, with varying CD123$^+$ expression, or HD BMMNC cells (CellTrace violet labelled) by flow cytometric analysis following a 16h co-incubation. Each timepoint was plated in triplicate for each patient or HD with a fixed number of target cells/well for all E:T ratios. Counting beads were used to quantify the absolute number of residual live target cells at the end of the co-culture. Residual live target cells were CellTrace violet$^+$ 7-AAD$^-$. All graphed data are represented as mean values ± SEM.

To further validate the specificity of the CD123-CD28-OX40-SF CAR T cells against AML, the CAR T cells were evaluated for their ability to inhibit growth of primary clonogenic CD34$^+$ and CD34$^-$ enriched BM derived AML cells. The AML BMMC cells were first incubated with non-transduced (NTD) T cells, with the CD123-CD28-OX40 SF CAR T cells, or with media only for 6 hours at an E:T ratio of 10:1.

The cell suspension was plated and enumerated after 14 days. The results demonstrated significant inhibition of the AML cells to form leukaemic colonies when cultured with the CD123-CD28-OX40 CAR T cells compared to AML BMMC cultured alone or with NTD T cells *(Figure 3.25A-B).* Collectively, these data demonstrate the capacity of the novel third generation CAR T cells, directed against CD123, to specifically eliminate primary AML cells consequently preventing their proliferation and leukaemic clonogenic capacity.

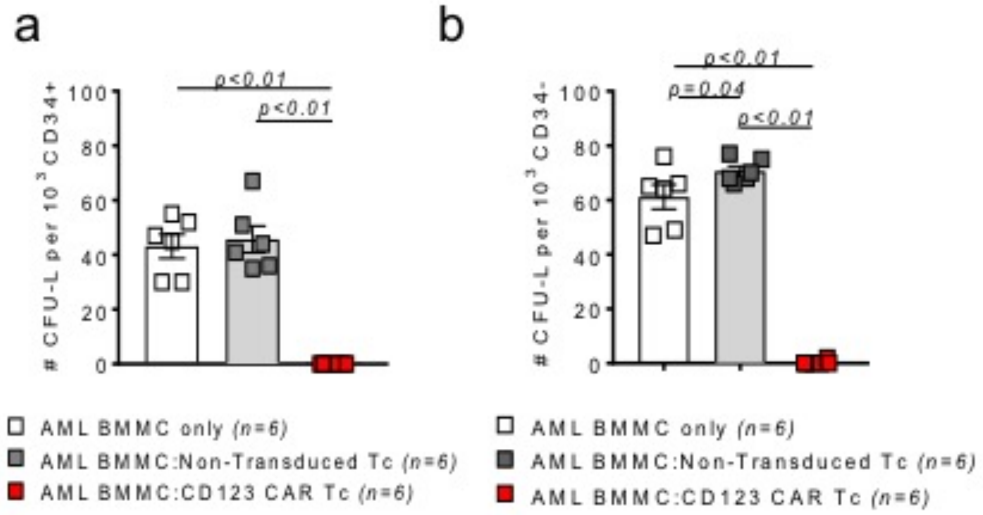

Figure 3.25. Effect of CD123-CD28-OX40-SF CAR T cells on leukaemic progenitor cell colony formation.

(A) CD34$^+$ or **(B)** CD34$^-$ AML BM cells were immunomagnetically selected and co-cultured in media only (untreated), with CD123 CAR T cells or NTD T cells for 6h at an E:T ratio of 10:1. The cells were subsequently plated in semisolid methylcellulose progenitor media, cultured for 14 days, and scored using an inverted microscope for the presence of leukaemia colony-forming units (CFU-L). The experiment was performed using 3 primary AML patient samples, each plated in duplicate. Colony numbers are represented per 1000 plated cells. All graphed data are represented as mean values ± SEM. *P*-values were calculated with 1-way ANOVA.

3.5 Conclusion & Discussion

The transfer of CARs into primary T cells to target TAAs such as CD123 has emerged as a promising and effective method of cancer immunotherapy. However, the introduction of exogenous genes into primary cells via viral methods is technically challenging and time consuming. While there are a variety of methods available that have been employed in the production of CAR T cells, the lentiviral vector production system is still, to date, the most effective and clinically safe.

Therefore, this thesis project employed a gene transfer platform which included lentiviral production of virus and *ex vivo* transduction and expansion of genetically modified primary T cells. A third generation vector system which consists of four-plasmids was used to generate virus as this is considered the safest viral system currently used in various clinical settings (Dull et al., 1998)(Montini et al., 2009). The disadvantage of using such a system is the labourious production of viral particles. Due to this, several conditions during virus production were evaluated and optimised in order to establish a protocol that resulted in high levels of lentivirus and efficient *ex vivo* transgene delivery into T cells.

Of the various steps in the protocol that were evaluated and optimised, a lentiviral packaging plasmid ratio of 1:1:1:1 (transgene:VSV-G:gag/pol:rev), using lipofectamine 3000 as a suitable transfection agent, and a double harvest of virus at 48 and 72h post-transfection resulted in the highest viral particle numbers obtained. However, the viral supernatants generated did not translate into sufficient and consistent transduction efficiencies in T cells. As a result, the viral supernatant was concentrated. The concentration of virus using ultracentrifugation allowed the transduction of T cells with a fixed MOI while reducing contaminating material in the supernatant. The transduction efficacy improved significantly when T cells were infected at MOI 5 with viral particles in the presence of RetroNectin. Sort purification of T cells successfully incorporating the CAR transgene were able to expand 100-250 fold *ex vivo* under IL-2 stimulation over 10 days to generate sufficient numbers of CAR T cells for *in vitro* functional profiling and adoptive transfer *in vivo.*

In order to delineate the CAR construct which demonstrated the best potential for *in vivo* evaluation and clinical translation, the antigen specificity of each of the four CARs was functionally evaluated in this chapter. Dynamic profiling of antitumor activity of the CAR T cells was assessed using different *in vitro* assays, including degranulation assay, proliferation assay, and short and long term cytotoxic capacity in response to CD123$^+$ targets.

In this body of work, polyclonal T cells from primary HD PBMCs were used to generate the CAR T cells. In some prior studies, only CD8$^+$ CAR T cells were generated and used to target the tumour cells as they were observed to be the main population of T cells found to efficiently lyse antigen-expressing targets by their production of IFN-γ. However, it was recently demonstrated that a combination of CD4$^+$ and CD8$^+$ T cells were essential to promote long term and effective anti-tumour responses (Turtle et al., 2016) (Sommermeyer et al., 2016). Sommermeyer and colleagues (Sommermeyer et al., 2016) observed that while CD8$^+$ CAR T cells were the cells mainly responsible for lysing target cells, CD4$^+$ CAR T cells were necessary for the production of cytokines such as IL-2, TNF, and IFN-γ which stimulated their proliferation and promoted a potent response *in vivo*.

For these reasons, it was hypothesised that the transfer of polyclonal CAR T cells would, instead, generate potent cytototxic T lymphocytes and that the presence of CD4$^+$ T cells would ensure enhanced efficacy *in vivo*. T cells from HD PBMCs generally consisted of more CD4$^+$ to CD8$^+$ T cells (2:1). Regardless of the CAR, the transduction, and expansion procedure in the presence of IL-2 maintained this cell phenotype ratio in the majority of cases. However, in some instances a 1:1 ratio was achieved. The phenotypic composition of the CAR T cell product is also associated with efficacy *in vitro* and *in vivo,* with evidence to suggest that naïve or CM T cells lead to better engraftment and proliferation capacity *in vivo* compared to EM or terminally differentiated effector cells (Gattinoni et al., 2011)(Sommermeyer et al., 2016). In all cases, the phenotype of the polyclonal CAR T cells generated here were either a CM or EM phenotype at the time of *in vitro* or *in vivo* evaluation (Chapter 4).

Polyclonal T cells expressing the CD123-CD28-OX40 CARs were found to degranulate and proliferate more efficiently against CD123$^+$ expressing leukaemia cell lines. This effect was not only exerted by CD8$^+$ T cells, but equally, CD4$^+$ T cells demonstrating its role in supporting cell lysis of the target cells. Conversely, T cells expressing these CARs were not able to elicit a response in the presence of a CD123$^-$ expressing leukaemia cell line demonstrating cell antigen specificity.

To a lesser extent, $CD8^+$ and $CD4^+$ T cells incorporating the CD123-CD28-4-1BB-SF CAR exhibited the similar effect. While the $CD4^+$ CAR T cells showed increased degranulation capacity with increased E:T ratio, this was not observed with the $CD8^+$ CAR T cells. This suggests the possibility that the target antigen binding affinity may not be strong enough to activate the intracellular downstream signaling machinery compared to the cells with the CD28-OX40 intracellular signaling. More interestingly, the $CD8^+$ and $CD4^+$ T cells incorporating the CD123-CD28-4-1BB-LF CAR showed no degranulation capacity, especially the $CD4^+$ T cells. In line with these results, the $CD4^+$ T cells also showed no ability to proliferate in the presence of target cells while the capacity of the $CD8^+$ CAR T cells to proliferate remained intact. This observation, to an extent, supports those reported by Sommermeyer (Sommermeyer et al., 2016) where $CD4^+$ T cell support is essential for efficient $CD8^+$ T cell lytic function.

An additional assessment of efficient CAR function *in vitro* and an indicator for long term efficacy is the ability of the CAR T cells to control markers associated with cell exhaustion in the absence and presence of antigen stimulation. The most comonly reported surface immune markers associated with cell exhaustion are PD-1, LAG-3, TIM-3, and CTLA-4. PD-1 expression is a marker that is physiologically induced in response to TCR engagement and activation as well as to common gamma-chain cytokines such as IL-2, IL-15, and IL-7 (Vibhakar et al., 1997)(Kinter et al., 2008).

Considering the CAR T cells were pre-activated with CD3/CD28 activating beads and expanded in the presence of IL-2 prior to downstream functional assessment, the high expression of this marker might be the result of background signaling. Like PD-1, LAG-3 is another marker similarly induced following T cell engagement and activation. Therefore, it was suggested that these two markers work in synergy and may reflect the activation status of the CAR-expressing T cells (Workman et al., 2002). Therefore, the expression of these two markers may not exclusively be associated with exhaustion of T cells, contrary to other published studies (Wherry et al., 2007)(Topalian et al., 2015)(Śledzińska et al., 2015).

Recently, the role of TIM-3 in the context of cancers has been studied extensively. High expression of TIM-3 on effector T cells is indicative of T cell exhaustion and downregulates anti-tumour immunity by inhibiting cell proliferation and the secretion of TNF, and IFN-γ. When bound to its ligand, galectin-9 (Gal-9), $TIM-3^+$ T effector cells undergo apoptosis

(Kashio et al., 2003)(Zhu et al., 2005). CTLA-4 expression similarly occurs following T cell activation and dampens the T cell response (Stamper et al., 2001)(Collins et al., 2002)(Rowshanravan et al., 2018). While CTLA-4 is predominantly found in intracellular vesicles of activated conventional T cells, T_{reg} $CD4^+$ cells have been documented to constitutively express CTLA-4 at high levels on the cell surface (Linsley et al., 1996)(Rowshanravan et al., 2018).

In vitro assesment of these markers demonstrated that $CD4^+$ and $CD8^+$ T cells incorporating the CD123-CD28-OX40 SF and CD123-CD28-4-1BB-SF CARs were the most functional at the time of *in vitro* evaluation. During the period of cell expansion and in the absence of target antigen stimulation, T cells harbouring the CD123-CD28-OX40-LF and CD123-CD28-4-1BB-LF CARs expressed high expression levels of TIM-3 and PD-1 compared to the T cells with the SF CARs. Following target antigen exposure, the T cells expressing the LF CARs demonstrated a decrease in PD-1 expression, however TIM-3 expression remained high. Similarly, a high expression level of CTLA-4 was also observed following target antigen exposure. In contrast, surface expression levels of these markers were very low to absent in T cells expressing the SF CARs. While expression of TIM-3 and CTLA-4 may initially be a result of T cell activation and stimulation, the potential for accelerated exhaustion and therefore decreased anti-tumour responses is highly probable *in vivo*.

Furthermore, upregulation of TIM-3 on CAR T cells following *in vitro* co-culture with AML cells has also been previously described in other works and was shown to have a significant negative impact on the anti-leukaemia responses (Kenderian et al., 2017). All tested CAR constructs, with the exception of CD123-CD28-4-1BB-LF, demonstrated the ability to mediate effector activity against cell lines, evincing antigen specific cytotoxicity which was accompanied by the production of various anti-tumour related inflammatory cytokines.

The collective assessment of all functional attributes revealed that, in general, the LF CARs were not as efficient as the SF CARs. The inefficacy of the LF CARs could be, in most part, be attributed to the spacer domain. The hinge or spacer regions provide stability for efficient CAR expression and activity. Moreover, it provides flexibility for target antigen binding (Guest et al., 2005). Several studies have demonstrated that extended or longer spacers provide extra flexibility to access epitopes that are membrane-proximal while short hinges are found to be more effective for membrane-distal epitopes (James et al., 2008)(Hudecek et al., 2013). The hinge length is reported to be crucial for adequate intracellular distance for immunological synapse formation and downstream signaling (Srivastava & Riddell, 2015). As a proof of concept, Hudaceck and colleagues demonstrated that an extended IgG4 CH_2CH_3 spacer region used in their constructed demonstrated reduced persistence of the CAR T cells through interaction with Fc receptors *in vivo* (Hudecek et al., 2015)

Based on the combined attributes, the CD123-CD28-OX40-SF displayed the most consistent profile of effector functions against $CD123^+$ targets. The feasibility of pursuing this construct was cemented following its ability to lyse or prevent the colony formation of primary AML cells.

In summary, the CAR gene expression was observed in both $CD4^+$ and $CD8^+$ T cells maintaining a consistent fraction of EM or CM T cells. The four constructs were subjected to *in vitro* validation with the CD123-CD28-OX40-SF construct collectively demonstrating a consistent, and efficient anti-tumour profile. To correlate the *in vitro* function to efficacy *in vivo,* a well established AML mouse model was used. Chapter 4 will describe the establishment of AML by transplantation of MOLM-13 Flt3-ITD cells to test efficacy of the CD123-CD28-OX40-SF CAR T cells *in vivo.*

Chapter 4

COMBINING AZACITIDINE AND CD123 CAR T CELLS FOR THE TREATMENT OF AML *IN VIVO*

4.1 Introduction

Efforts to expand adoptive immunotherapeutic strategies such as CAR T cells for AML has been limited in comparison to CAR T cell therapy for B cell haematological malignancies. The novel third generation CD123 CAR T cells developed in this project demonstrated strong capacity for *in vitro* elimination of target AML cells. While the CAR T cells further demonstrated strong capacity for tumour regression in the MOLM-13$^{FLT3-ITD}$ xenograft models, it was not able to completely eliminate the AML cells. In the clinical setting, this would mean that patients have suboptimal responses to the CAR T cells and/or potentially relapse. The AML microenvironment, as discussed in the introduction of the thesis, is known to be highly immunosuppressive and uses a variety of mechanisms to escape the host immune surveillance which may hamper the efficacy of CAR T cell therapy in AML.

To improve the long-term efficacy of the CAR T cells, combination therapy with demethlyating agents was explored. DNA methyltransferase (DNMT) inhibitors, such as AZA, better referred to as HMAs, are cytidine nucleoside analogues that result in transient and variable DNA hypomethylation. These HMAs have a relatively short plasma half-life as they are unstable following absorption owing to spontaneous hydrolysis and deamination by cytidine deaminase (Chabner & Oliverio, 1975). Upon cellular intake via nucleoside transporters, they are phosphorylated by intracellular kinases. The majority of the phosphorylated metabolite (5-aza-CTP) of AZA is incorporated in RNA while a minority is converted to 5-aza-dCTP by the ribonucleotide reductase and is incorporated into the DNA during replication *(Figure 4.1)*. The resultant effect promotes progressive reduction of DNA methylation, with subsequent upregulation of the expression of key epigenetically silenced genes (tumour suppressor genes), inducing senescence, and apoptosis (Goodyear et al., 2010).

The use of HMAs to treat patients with haematological malignancies was first documented in the AZA-001 study and led to AZA becoming the FDA approved standard of care in patients with high-risk MDS who are ineligible for allo-hSCT and for low-blast count elderly AML patients. The study demonstrated improved overall survival and delayed AML transformation in patients compared to those treated with intensive chemotherapy (Fenaux et al., 2009). HMAs have since demonstrated clinical importance in the management of patients with AML who are ineligible for intensive chemotherapy or are chemo-refractory. Clinical trials have shown that AZA improves survival outcomes in older adults with AML in high-risk subgroups with adverse cytogenetics or myelodysplasia-related changes (Dombret et al., 2015)(Fenaux et al., 2010)(Döhner et al., 2018) and, more recently, was shown to possess significant clinical activity in patients with r/r disease (Craddock et al., 2013)(Ram et al., 2019).

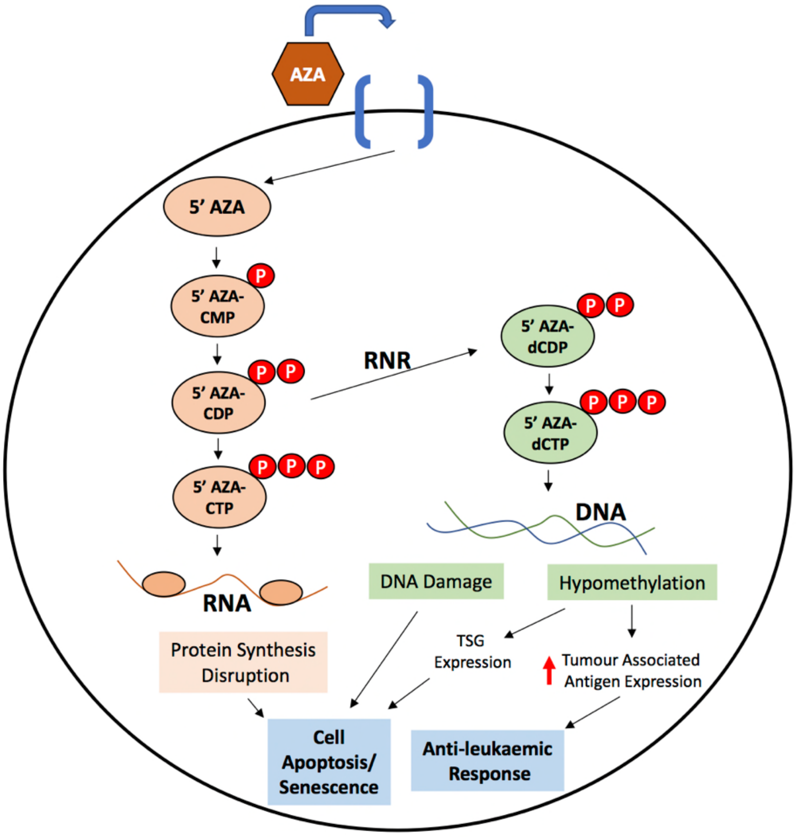
AZA
5' AZA
5' AZA-CMP
P
5' AZA-CDP
P P
5' AZA-CTP
P P P
RNR
5' AZA-dCDP
5' AZA-dCTP
DNA
RNA
DNA Damage
Hypomethylation
TSG Expression
Tumour Associated Antigen Expression
Protein Synthesis Disruption
Cell Apoptosis/ Senescence
Anti-leukaemic Response

Figure 4.1. Molecular and cellular mechanisms of Azacitidine.
Following cellular uptake via nucleoside transporters, AZA undergoes successive phosphorylation by intracellular kinases. The majority of bi-phosphorylated metabolite of AZA (5' AZA-CDP) is further phosphorylated to 5' AZA-CTP and is incorporated in RNA. The incorporation into RNA leads to protein synthesis disruption consequently leading to cell apoptosis and senescence. A minority of the bi-phosphorylated AZA is converted to 5' AZA-dCTP by the ribonucleotide reductase and is incorporated in DNA during replication. The DNA binds DNMT1 and leads to degradation, promoting a progressive DNA hypomethylation after several rounds of replication. The consequence of these series of events leads to upregulation of the expression of key repressed tumour suppressor genes, inducing senescence and apoptosis as well as increased expression of tumour associated antigens that aids in anti-tumour immune responses. *Image adapted from (Duchmann & Itzykson, 2019).*

More recently, AZA was shown to upregulate the expression of leukaemia-associated antigens (LAA) and induce T cell responses against AML cells (Goodyear et al., 2010). However, AZA as a monotherapy is ineffective in eradicating LSCs in AML as demonstrated by the low rates of CR despite continuing therapy (Craddock et al., 2013). However, co-administration of AZA with other inhibitors augments effective killing of leukaemic cells. Most recently, AZA combined with the Bcl2 inhibitor, venetoclax, was found to be a highly effective therapy for a proportion of AML patients (Jin et al., 2020)(Jilg et al., 2019). Furthermore, HMAs are currently under investigation as a combinatorial therapy with other inhibitors, for example, with IDH inhibitors for patients with *IDH1* and *IDH2* mutations (DiNardo et al., 2019) as well as with immune checkpoint inhibitors, CTLA-4 and PD-1 (N. Daver, Garcia-Manero, et al., 2019)(Garcia-Manero et al., 2016).

4.2 Rationale of the Chapter

Based on these results, I hypothesised that combining the DNMT inhibitor, AZA, with the third generation CD123 CAR T cells would be an attractive cellular therapy as both have demonstrated activity against AML, and may be potentially synergistic or additive. Furthermore, the combination of the two components may be a universal therapy for AML patients regardless of cytogenetic profile as most, if not all, patients are found to express the CD123 antigen on leukaemic stem and progenitor cells.

This chapter describes the ability of the novel third generation CD123-CD28-OX40-SF CAR T cell product combined with AZA to induce long-term control of AML in a MOLM-13$^{FLT3-ITD}$ xenograft model. Furthermore, this chapter elucidates the mechanism by which AZA treatment led to increased function and longevity of a unique subset of CD4 T cells which contributed to long-term immune surveillance.

4.3 Manuscript Authorship Consent Form

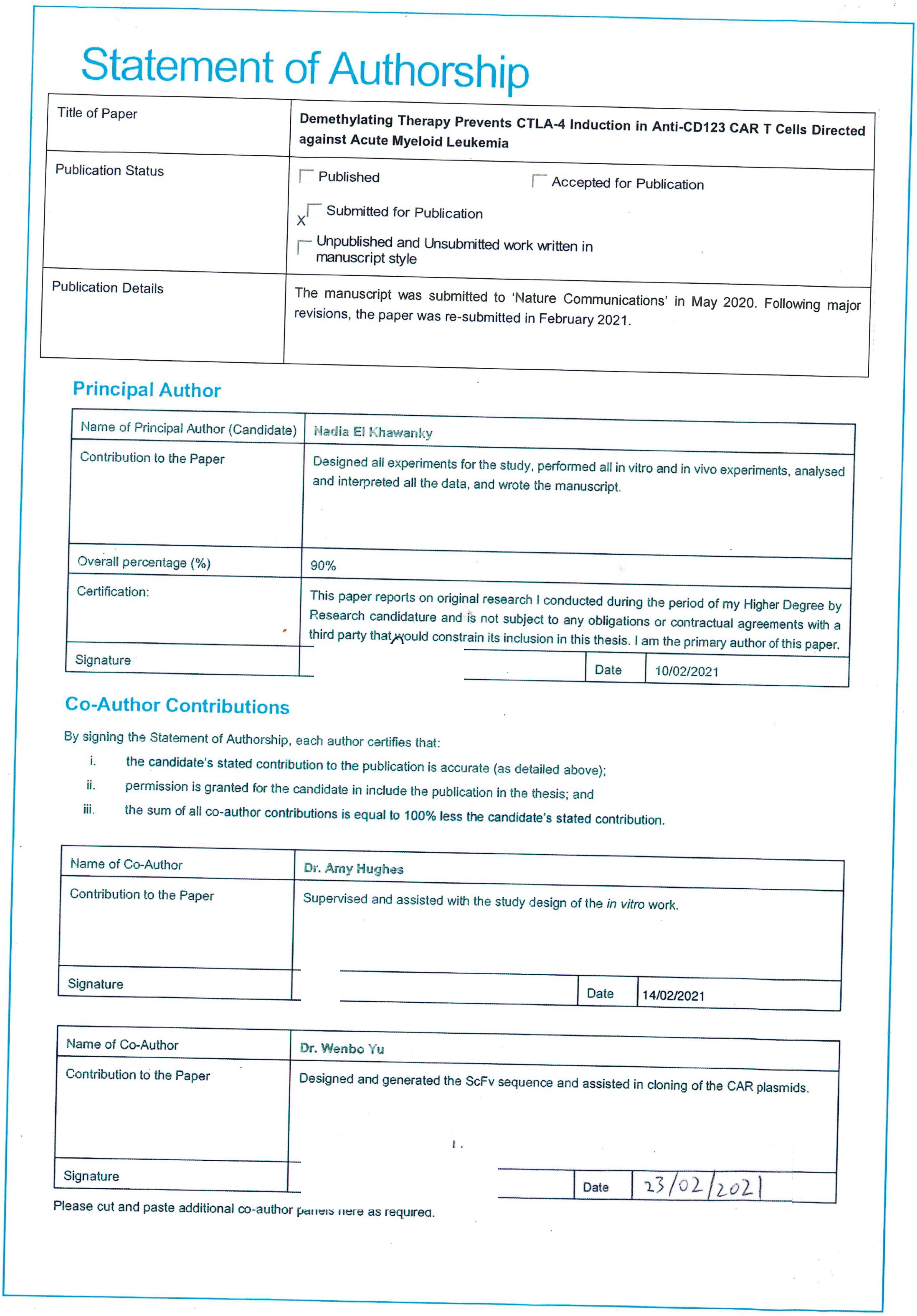

Statement of Authorship

Title of Paper	**Demethylating Therapy Prevents CTLA-4 Induction in Anti-CD123 CAR T Cells Directed against Acute Myeloid Leukemia**
Publication Status	☐ Published ☐ Accepted for Publication ☒ Submitted for Publication ☐ Unpublished and Unsubmitted work written in manuscript style
Publication Details	The manuscript was submitted to 'Nature Communications' in May 2020. Following major revisions, the paper was re-submitted in February 2021.

Principal Author

Name of Principal Author (Candidate)	**Nadia El Khawanky**		
Contribution to the Paper	Designed all experiments for the study, performed all in vitro and in vivo experiments, analysed and interpreted all the data, and wrote the manuscript.		
Overall percentage (%)	90%		
Certification:	This paper reports on original research I conducted during the period of my Higher Degree by Research candidature and is not subject to any obligations or contractual agreements with a third party that would constrain its inclusion in this thesis. I am the primary author of this paper.		
Signature		Date	10/02/2021

Co-Author Contributions

By signing the Statement of Authorship, each author certifies that:

i. the candidate's stated contribution to the publication is accurate (as detailed above);
ii. permission is granted for the candidate in include the publication in the thesis; and
iii. the sum of all co-author contributions is equal to 100% less the candidate's stated contribution.

Name of Co-Author	**Dr. Amy Hughes**		
Contribution to the Paper	Supervised and assisted with the study design of the *in vitro* work.		
Signature		Date	14/02/2021

Name of Co-Author	**Dr. Wenbo Yu**		
Contribution to the Paper	Designed and generated the ScFv sequence and assisted in cloning of the CAR plasmids.		
Signature		Date	23/02/2021

Please cut and paste additional co-author panels here as required.

Name of Co-Author	**Dr. Renier Myburgh**		
Contribution to the Paper	Assisted with all humanised mouse experiments, including transplantation of human CD34$^+$ cells, engraftment checks, and downstream *ex vivo* analysis.		
Signature		Date	19.2.21

Name of Co-Author	**Dr. Sanaz Taromi**		
Contribution to the Paper	Assisted in the establishment of an AML mouse model.		
Signature		Date	14.02.21

Name of Co-Author	**Dr. Konrad Aumann**		
Contribution to the Paper	Certified pathologist that assisted in histological analysis of mouse tissue samples.		
Signature		Date	24.2.21

Name of Co-Author	**Jade Clarson**		
Contribution to the Paper	Assisted in the processing of human samples and technical aid of *in vitro* experiments.		
Signature		Date	24/02/21

Name of Co-Author	**Janaki Manoja Vinnakota**		
Contribution to the Paper	Technical aid in performing revision experiments for the manuscript.		
Signature		Date	14/2/21

Name of Co-Author	**Dr. Khalid Shoumariyeh**		
Contribution to the Paper	Acquisition of, and assisting in the processing of human patient samples.		
Signature		Date	15/2/21

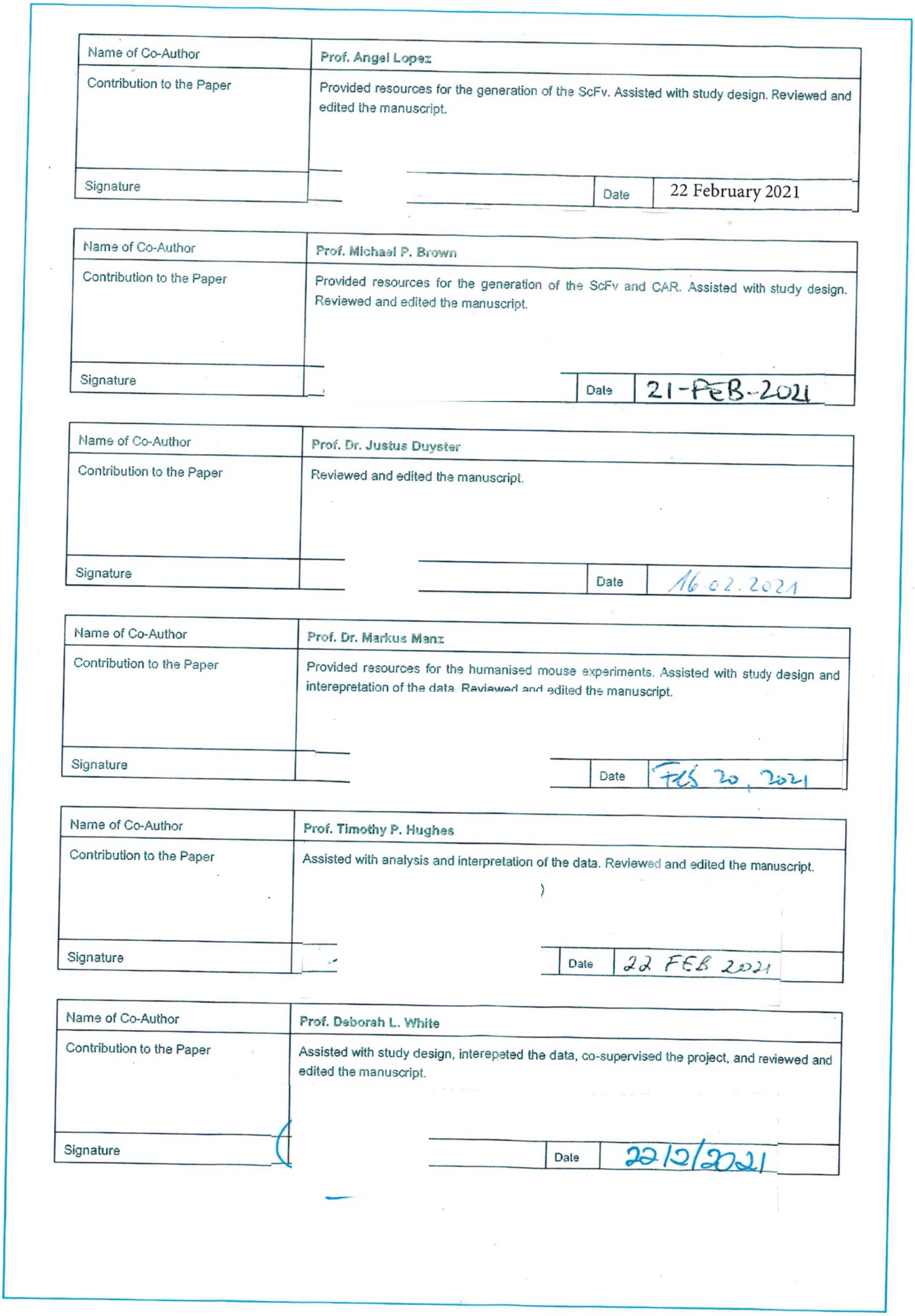

Name of Co-Author	**Prof. Angel Lopez**		
Contribution to the Paper	Provided resources for the generation of the ScFv. Assisted with study design. Reviewed and edited the manuscript.		
Signature		Date	22 February 2021

Name of Co-Author	**Prof. Michael P. Brown**		
Contribution to the Paper	Provided resources for the generation of the ScFv and CAR. Assisted with study design. Reviewed and edited the manuscript.		
Signature		Date	21-FEB-2021

Name of Co-Author	**Prof. Dr. Justus Duyster**		
Contribution to the Paper	Reviewed and edited the manuscript.		
Signature		Date	16.02.2021

Name of Co-Author	**Prof. Dr. Markus Manz**		
Contribution to the Paper	Provided resources for the humanised mouse experiments. Assisted with study design and interepretation of the data. Reviewed and edited the manuscript.		
Signature		Date	Feb 20, 2021

Name of Co-Author	**Prof. Timothy P. Hughes**		
Contribution to the Paper	Assisted with analysis and interpretation of the data. Reviewed and edited the manuscript.		
Signature		Date	22 FEB 2021

Name of Co-Author	**Prof. Deborah L. White**		
Contribution to the Paper	Assisted with study design, interepeted the data, co-supervised the project, and reviewed and edited the manuscript.		
Signature		Date	22/2/2021

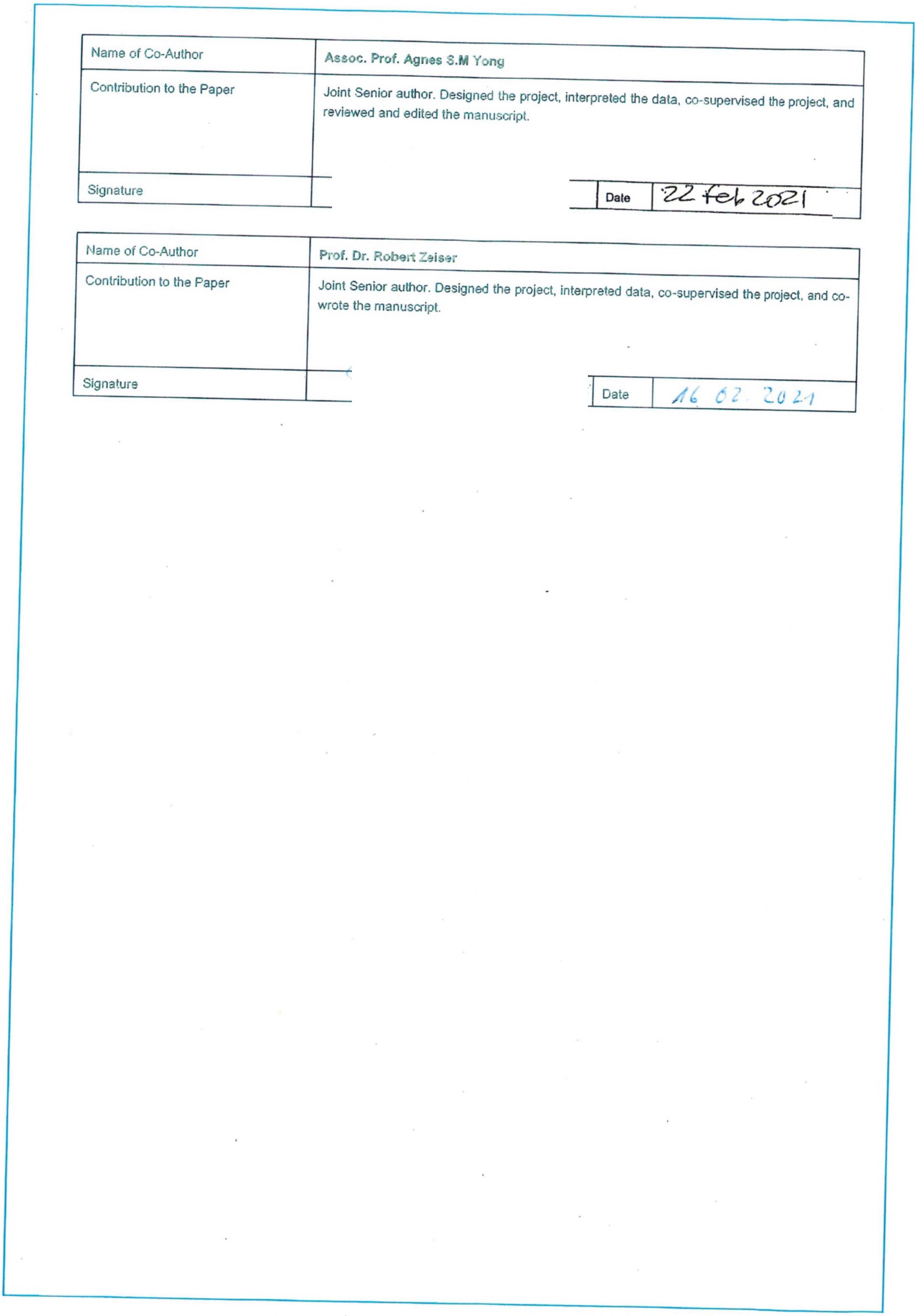

Name of Co-Author	**Assoc. Prof. Agnes S.M Yong**		
Contribution to the Paper	Joint Senior author. Designed the project, interpreted the data, co-supervised the project, and reviewed and edited the manuscript.		
Signature		Date	22 feb 2021

Name of Co-Author	**Prof. Dr. Robert Zeiser**		
Contribution to the Paper	Joint Senior author. Designed the project, interpreted data, co-supervised the project, and co-wrote the manuscript.		
Signature		Date	16.02.2021

Demethylating therapy prevents CTLA-4 induction in anti-CD123 CAR T cells directed against acute myeloid leukemia

Nadia El Khawanky[1-4], Amy Hughes[2], Wenbo Yu[5], Renier Myburgh[6], Sanaz Taromi[3,7], Konrad Aumann[8], Jade Clarson[1,9], Janaki Manoja Vinnakota[3], Khalid Shoumariyeh[3], Angel Lopez[2,5], Michael P. Brown[5,10], Justus Duyster[3], Markus Manz[6], Timothy P. Hughes[1,2,9], Deborah L. White[1,2,11], Agnes S.M Yong[1,2,12,13*], Robert Zeiser[3,14*]

[1] Precision Medicine Theme, South Australian Health and Medical Research Institute (SAHMRI), Adelaide, Australia

[2] School of Medicine, Faculty of Health and Medical Sciences, University of Adelaide, Australia

[3]Department of Medicine I, Medical Center - University of Freiburg, Faculty of Medicine, University of Freiburg, Freiburg, Germany

[4] Faculty of Biology, University of Freiburg, Freiburg, Germany

[5]Centre for Cancer Biology, SA Pathology and University of South Australia, Adelaide, Australia

[6]Department of Medical Oncology and Hematology, University Hospital Zurich and University of Zurich, Comprehensive Cancer Center Zurich (CCCZ), Zurich, Switzerland

[7]Faculty of Medical and Life Sciences, University Furtwangen, Villingen-Schwenningen, Germany

[8]Department of Pathology, Institute for Clinical Pathology, University Medical Center Freiburg, Freiburg, Germany

[9]Department of Haematology, Royal Adelaide Hospital, Adelaide, Australia

[10]Cancer Clinical Trials Unit, Department of Medical Oncology, Royal Adelaide Hospital, Adelaide, Australia

[11]School of Biological Sciences, Faculty of Science, University of Adelaide, Australia

[12]Department of Haematology, Royal Perth Hospital, Perth, Western Australia, Australia

[13] School of Medicine, The University of Western Australia, Perth, Western Australia, Australia

[14] Signaling Research Centres BIOSS and CIBSS- Centre for Integrative Biological Signalling Studies, University of Freiburg, Freiburg, Germany

*A.S.M.Y and R.Z contributed equally

***Corresponding Author(s):**

Robert Zeiser, MD

Department of Hematology, Oncology and Stem cell transplantation, University Medical Center Freiburg, 79106 Freiburg, Germany

Tel: +49-761-270-34580, Fax: +49-761-270-71570

robert.zeiser@uniklinik-freiburg.de

Agnes Yong, MD, PhD

Department of Haematology, Royal Perth Hospital, Perth, Western Australia, Australia.

Tel: +61-08-9224-3085

agnes.yong@health.wa.gov.au

Running Title: Induction of cytotoxic CTLA-4^{negative} CAR T cells by Azacitidine

Key points:

- Azacitidine treatment enhanced CAR T cell activity *in vivo* and increased CTLA-4^{negative} anti-CD123 CAR T cell numbers.
- CTLA-4^{negative} anti-CD123 CAR T cells exhibited superior cytotoxicity against AML cells and higher TNF production compared to CTLA-4^{positive} anti-CD123 CAR T cells.
-Anti-CD123 CAR T cells demonstrated high phosphorylation of key intracellular markers Lck and Zap70 in the presence of Azacitidine pre-treated AML cells.

Abstract

Successful treatment of acute myeloid leukemia (AML) with chimeric antigen receptor (CAR) T cells is hampered by toxicity on normal hematopoietic progenitor cells and low CAR T cell persistence. We developed third-generation anti-CD123 CAR T cells with a humanized CSL362-based scFv and a CD28-OX40-CD3ζ intracellular signaling domain. This CAR demonstrated anti-AML activity without affecting the healthy hematopoietic system, or causing epithelial tissue damage in a xenograft model. CD123 expression on leukemia cells increased upon 5'-Azacitidine (AZA) treatment. AZA treatment of leukemia-bearing mice caused increased CTLA-4^{negative} anti-CD123 CAR T cell numbers following infusion. Functionally, the CTLA-4^{negative} anti-CD123 CAR T cells exhibited superior cytotoxicity against AML cells, accompanied by higher TNF production and enhanced downstream phosphorylation of key T cell activation molecules. Our findings indicate that AZA increases the immunogenicity of AML cells, allowing enhanced recognition and elimination of malignant cells by highly efficient CTLA-4^{negative} anti-CD123 CAR T cells.

Introduction

Despite recent advances in the field of allogeneic hematopoietic cell transplantation (allo-HCT)[1] and the introduction of disease specific inhibitors (e.g. FLT3 inhibition)[2], the prognosis of AML remains unfavorable in the majority of patients. While standard induction chemotherapy and allo-HCT can induce complete remissions, most patients eventually relapse and succumb to the disease[3]. Post-relapse treatment combinations with tyrosine kinase inhibitors (TKIs) and donor lymphocyte infusions (DLI) have led to long-term remission in a fraction of patients with FLT3-ITD AML[1, 4]. In recent years, a plethora of immunotherapy-based treatment approaches have been developed. One of the most successful approaches uses T cells that express chimeric antigen receptors (CARs) where T cell specificity is re-directed towards cell surface antigens overexpressed on the cancer cell. The CAR T cell products (Kymriah™ and Yescarta™) targeting the CD19 antigen on B cells were approved by the American Food and Drug Administration for several B-lymphoid malignancies based on the high and durable clinical responses[5, 6, 7].

Conversely, the use of CAR T cells against AML is more difficult due to undesired effects on normal myeloid progenitor cells that share most targetable antigens with AML cells. Of the antigens currently explored, CD123, the transmembrane α chain of the interleukin-3 receptor remains the most promising target because of its ubiquitous expression on AML blasts[8, 9]. Several pre-clinical and clinical studies[10] have reported potent anti-leukemic activity of anti-CD123 CAR T cells against AML. However, myelotoxicity or reduced CAR T cell efficacy has been reported due to the immunosuppressive environment induced by AML cells hinder its broader applicability[10, 11, 12].

Here, we used a third-generation anti-CD123 CAR product with the scFv derived from the humanized and Fc optimized CSL362 monoclonal antibody (mAb)[13]. The anti-CD123 CAR T cells demonstrated anti-leukemic activity with no severe toxicity to the healthy hematopoietic system *in vivo*. To increase potency, combination therapy with the demethylating agent, 5'Azacitidine (AZA) was explored. Hypomethylating agents (HMAs) such as AZA are cytidine nucleoside analogues that induce transient and variable DNA hypomethylation. The resultant effect promotes reactivation of key epigenetically silenced genes thereby inducing senescence and apoptosis[14, 15]. More importantly, AZA has previously been shown to upregulate the expression of leukemia-associated antigens and increase T cell responses against AML and other cancers[15]. However, AZA treatment alone is ineffective at eradicating leukemia stem cells in AML[16]. Most recently, AZA combined with the Bcl2 inhibitor, venetoclax, has proven to be an effective therapy for a proportion of AML patients[17, 18]. Additionally, HMAs in combination with other agents, such as isocitrate dehydrogenase (IDH) or immune checkpoint inhibitors, are also under investigation[19, 20, 21]. Therefore, we proposed that combining AZA with anti-CD123 CAR T cells represents an attractive cellular therapy as both have demonstrated activity against AML and may present as a highly efficacious universal therapy for AML patients.

Here, we demonstrated that our third-generation anti-CD123 CAR T cells lead to long-term control of AML in a xenograft model when combined with AZA. We showed that AML-bearing mice, pre-treated with AZA, resulted in reduced numbers of cytotoxic T lymphocyte antigen-4 (CTLA-4) expressing CAR T cells *in vivo*. CLTA-4 is a regulator of T cell activation and function, in which T cells with a low expression of this molecule showed increased longevity and activity [22]. AML-bearing mice infused with CTLA-4^{negative} anti-CD123 CAR T cells exhibited superior cytotoxicity against AML cells, with higher TNF production. TNF was also previously shown to be required for T cell subset mediated cytotoxicity against tumor cells [23]. Furthermore, CTLA-4^{negative} anti-CD123 CAR T cells demonstrated proliferative capacity and longer survival compared to AML-bearing mice infused with CTLA-4^{positive} anti-CD123 CAR T cells.

Additionally, CD4^{+} anti-CD123 CAR T cells, exposed to AZA pre-treated MOLM-13 AML cells, exhibited higher intracellular retention of CTLA-4 compared to naive MOLM-13 cells. This observation was accompanied by higher phosphorylation levels of the T cell signaling and activation molecules, Lck and Zap70. Mechanistically, we postulate that AZA pre-treatment of AML cells enhances the downstream signaling events of the CAR T cells by prolonging phosphorylation of molecules associated with T cell activation and function thereby preventing the induction of CTLA-4 on the surface of the CAR T cells. Our findings pave the way for a novel CAR T cell and AZA combination therapy for AML.

Materials and Methods

Human Samples

Primary AML and healthy donor (HD) bone marrow (BM) samples were obtained from the South Australian Cancer Research Biobank (SACRB). Primary AML and HD peripheral blood (PB) was obtained from the University Medical Center, Freiburg, Germany. Written informed consent was obtained from each donor. HD cord blood (CB) samples were obtained from umbilical cords of healthy full-term newborns and processed by the biobank of the department of Medical Oncology and Hematology, Switzerland, University Hospital Zürich. The studies were approved by the Australian Institutional Human Research Ethics Committee, the Institutional Ethics Review Board of the Medical Center, University of Freiburg, Germany, and the Cantonal Ethics Board Zürich, Switzerland (Ethics approval no's: R20150526, HREC/15/RAH/221 and 509/16, and 2009-0062 respectively) and conducted in accordance with the Declaration of Helsinki.

Peripheral Blood Mononuclear Cell (PBMC) Preparation

PBMCs were isolated by density gradient centrifugation using Lymphoprep or Pancoll (STEMCELL Technologies, Vancouver, BC, Canada; Pan Biotech, Germany). Briefly, blood samples were diluted 1:3 with 1x PBS, layered onto Lymphoprep/Pancoll and centrifuged (30min, 440xg) without brake. PBMCs were isolated and cryopreserved in 90% heat-inactivated fetal calf serum (FCS, Sigma Aldrich, Germany) and 10% dimethyl sulfoxide (DMSO, Sigma Aldrich, Germany). Cells were stored overnight at -80^{o}C and subsequently transferred into liquid nitrogen. All analyses were conducted on cryopreserved material. Following thawing of sample material, cells were manually counted using trypan blue (Sigma-Aldrich, Germany) staining.

Mice

Rag2$^{-/-}$*Il2rγ*$^{-/-}$ immunocompromised mice were bred in-house at the University clinic (University of Freiburg) animal facility. Male and female mice were used between 8-10 weeks of age. Animal protocols were approved by the animal ethics committee Regierungspräsidium Freiburg, Freiburg, Germany (No: G18-019) or the Cantonal Veterinary Office Zürich (194/2018).

MOLM-13 AML$^{FLT3\ ITD}$ Xenograft Model

For this model, *Rag2*$^{-/-}$*Il2rγ*$^{-/-}$ recipients were transplanted with 1x10^{5} MOLM-13^{Luc+}cells intravenously following sub-lethal irradiation with 3.5Gy one day prior. Mice were subsequently left for 7 days for leukemia to develop. Successful engraftment was confirmed on day 7 using *in vivo* bioluminescence imaging (BLI) before mice were distributed randomly into each treatment group. *In vivo* BLI was performed as previously described[24]. On day 7, mice were intravenously injected with 100µl PBS, 5x10^6 non-transduced (NTD) T cells in 100µl PBS, or 5x10^6 anti-CD123 CAR T cells in 100µl PBS. BLI was performed at weekly intervals to track leukemia progression or regression. Twenty-eight days following T cell injection, mice were either sacrificed for PB and BM analyses by flow cytometry for the detection of residual AML cells (hCD45$^+$CD3$^-$CD123$^+$) and T cells (hCD45$^+$CD4$^+$/CD8$^+$), or mice were left until day 60 for survival analysis (see schematic in Fig 1a).

MOLM-13 AML$^{FLT3\ ITD}$ Xenograft Model with AZA Treatment

For this model, *Rag2*$^{-/-}$*Il2rγ*$^{-/-}$ recipients were transplanted as above. Following confirmation of engraftment on day 7, mice were randomized and split into six groups: (1) PBS, (2) NTD T cells, (3) anti-CD123 CAR T cells only, (4) AZA only, (5) AZA with NTD T cells, and (6) AZA with anti-CD123 CAR T cells. Mice in the PBS control group were treated intravenously with 100µl PBS; mice in the anti-CD123 CAR T cells or NTD T cells only group were intravenously injected with 5x10^6 anti-CD123 CAR T cells or NTD T cells, respectively. The AZA only, AZA with NTD T cells, and AZA with anti-CD123 CAR T cell treatment groups were first given one dose of 2.5mg/kg AZA (Sigma-Aldrich, Germany) in sterile PBS intraperitoneally every 3 days for a total of 4 doses. Twenty-four hours following the final dose of AZA, the dual treatment group was intravenously injected with 5x10^6 NTD T cells or anti-CD123 CAR T cells in 100µl PBS. A cohort of the mice from each group were sacrificed 28 days following anti-CD123 CAR T cell injection for flow cytometry analysis. The remaining cohort of mice from each group was left until day 60 for survival analysis (see schematic in Fig 3a).

Humanized Hematopoietic Progenitor Cell (HSPC) Xenograft Model

Humanized cytokine knock-in mice (CSF1h/hIL-3/CSF2h/hhSIRPAtgTPOh/hRag2$^{-/-}$Il-2rg$^{-/-}$) with human genes encoding cytokines important for myelopoiesis (macrophage colony-stimulating factor, interleukin-3, granulocyte-macrophage colony-stimulating factor and thrombopoietin) were generated as previously described[25]. Mice were bred and maintained at the University Hospital Zürich animal facility according to the Swiss Federal Veterinary Office guidelines and the Cantonal Veterinary Office Zürich (194/2018). Newborn mice were sub-lethally irradiated with 1.5Gy and injected intra-hepatically with 2x10^5 CD34$^+$ isolated human CB hematopoietic progenitor cells[26]. The post-transplant lifespan of these mice depends on the level of engraftment and generally do not exceed 16 weeks. $5x10^6$ anti-CD123 CAR T cells or NTD T cells were intravenously transferred 6-7 weeks following transplantation and confirmed $hCD45^+$ myeloid engraftment. Mice were sacrificed 14 days following T cell transfer due to high engraftment-associated anemia. BM and PB were FACS-analyzed for changes in multi-lineage engraftment.

Flow Cytometry

Anti-human antibodies purchased from BioLegend, eBioscience, BD Biosciences, or Becton Dickinson were used for flow cytometry and are listed in **Suppl. Table 3**. For cell surface staining, cells were isolated and washed twice with ice-cold 1x PBS prior to staining with the relevant antibodies for 30 minutes on ice, in the dark. For cells isolated from the BM or PB of mice, Fc receptor blockade (1:25) (Miltenyi Biotec, Germany) was performed for 15-20 minutes on ice prior to staining. Cells were washed twice with ice-cold 1x PBS after staining and re-suspended in 250µl 1x PBS supplemented with 2% FCS prior to analysis. For intracellular cytokine staining, cells were treated with 1µl/ml of Brefeldin A (GolgiPlug) (BD Biosciences, Germany) in cRPMI-1640 medium for 4 hours prior to staining using the BD Cytofix/Cytoperm kit (BD Biosciences, Germany) according to manufacturer's instructions. In all analyses, the population of interest was gated based on forward vs. side scatter followed by singlet gating and dead cell exclusion ($7\text{-}AAD^-$ or live dead aqua (LDA^-)). Instrument setup including fluorescence amplification (voltages) and identification of gating boundaries was optimized using unstained and FMO controls. Compensation was optimized using compensation beads (BD Biosciences). Flow analyses were performed on the FACSCanto II or LSRFortessa (BD Biosciences) and the data was analyzed using the FlowJo software v10.4 (Treestar, Ashland, OR).

T cell Mediated Cytotoxicity Assay

CellTrace violet (Invitrogen, Thermo Fisher Scientific, Germany) labelled KG1a, MOLM-13, SUPB15 cells, or primary AML cells (target cells) were used for the T cell mediated cytotoxicity assay. In brief, anti-CD123 CAR T cells (effector cells) were incubated with target cells at the indicated ratios for 16 hours in cRPMI-1640 medium (supplemented with 20% FCS, 2mM glutamine, 100U/ml penicillin/streptomycin). Percentage specific lysis of the target cells was determined using flow cytometry. Cells were harvested following the incubation period, stained with 7-AAD (BD Biosciences, Germany) and 10µl CountBright™ absolute counting beads (Invitrogen, Thermo Fisher Scientific, Germany) were added to each sample in a fixed volume just prior to flow acquisition. A uniform number of bead events were acquired for each sample on the flow cytometer. Residual live target cells were CellTrace^{TM} violet^{+} 7-AAD-. Unstained and fluorescence minus one (FMO) controls were used to identify gating boundaries.

AZA Treatment of MOLM-13 AML cells and Primary cells

MOLM-13, primary AML, or HD cells were maintained in cRPMI-1640 medium and 1µM AZA (Sigma-Aldrich, Germany). For primary AML or HD cells, the culture medium was additionally supplemented with 5ng/mL recombinant human stem cell factor (hSCF) (Peprotech, Germany). The media was replaced every 3-4 days to maintain the cells.

Colony Formation Assay

CD34^{+} and CD34^{-} cells were isolated from bone marrow mononuclear cells (BMMNCs) of HD and primary AML samples using the CD34 Ultrapure Microbead kit (Miltenyi Biotec). In the experiments where AZA was used, HD cells were first cultured with 1µm AZA in cRPMI-1640 media supplemented with 5ng/ml hSCF for 24 hours. 5×10^{3} CD34^{+} or CD34^{-} cells were then incubated with media alone, or with NTD T cells or anti-CD123 CAR T cells at an effector:target (E:T) ratio of 10:1 in cRPMI-1640 medium for 6 hours. Following incubation, the cell suspension was added to a semi-solid methylcellulose based medium (Methocult opti H3404, Stem Cell Technologies, Vancouver, BC, Canada) and plated into 3cm tissue culture dishes. Colonies were enumerated using established criteria according to the manufacturer’s instructions and scored using an inverted microscope (Zeiss SteREO Discovery; 4X) after 14 days.

Statistical analyses

Statistical analyses and significance were determined using GraphPad Prism v7 or v8 software (GraphPad Software Inc. LA Jolla, CA). All data were subjected to normality tests. Based on the results of the normality tests, unpaired Student’s *t*-test, unpaired Student’s *t*-test (Mann-Whitney test), one-way ANOVA, or Log-rank (Mantel-Cox) was used, where appropriate, for comparing differences between groups. Log-rank test was used to calculate significance between survival curves. All graphed data, except for survival curves, are presented as mean ± standard error of the mean (SEM). In all cases, a *p*-value of ≤ 0.05 was considered significant.

Results

Third-generation anti-CD123 CAR T cells exhibit anti-AML activity *in vitro*

In order to develop anti-CD123 CAR T cell therapy for AML, we first confirmed the expression of CD123 and its suitability as a target antigen on primary human AML BM specimens in comparison to HD BM **(Suppl. Figure 1, Suppl. Figure 2a).** Concordant with previous reports[27, 28], CD123 was highly expressed in most AML specimens while in the HD specimens, the overall CD123 expression was low **(Suppl. Figure 2b-d)**. While some AML samples had CD123^{low} expression, this was still higher than that of the HD cells.

We therefore designed a third-generation anti-CD123 CAR construct incorporating the humanized CSL362-based[13] scFv fused to a CD28-OX40-CD3ζ intracellular signaling domain **(Suppl. Figure 3a)**. This construct demonstrated consistent capacity for lentiviral transduction into polyclonal T cells with expansion and differentiation into effector- or central- memory T cells from naïve T cells **(Suppl. Figure 3b-d)**. Furthermore, extended exposure of the CAR T cells to recombinant human IL-2 during expansion did not induce high expressions of surface markers associated with activation and/or exhaustion including LAG-3, TIM-3, CTLA-4 and PD-1. This demonstrated that the CAR T cells were functionally active prior to interaction with leukemia cells **(Suppl. Figure 3e).**

The anti-CD123 CAR T cells demonstrated ability *in vitro* to express the lysosomal-associated membrane protein 1 (LAMP-1 or CD107a), a surrogate marker of degranulation on T lymphocytes, proliferate, lyse target cells, and produce effector and homeostatic cytokines and chemokines against the human CD123^{+} cell line KG1a compared to the CD123^{-} cell line, SUPB15 **(Suppl. Figure 4).** Furthermore, cytotoxic activity of the CAR T cells against the MOLM-13 cells reached 90% at the 10:1 effector to target (E:T) ratio, while there was less than 10% cytotoxicity caused by the NTD T cells at any E:T ratio (**Suppl. Figure 5a**). More importantly, the high cytotoxic activity of the anti-CD123 CAR T cells were observed against primary AML cells from 3 different patients with less than 10% cytotoxicity caused by the NTD T cells (**Suppl. Figure 5b**). To test for cytolytic activity against colony forming unit (CFU) capacity of BM derived AML cells, we studied CFU in CD34^{+} and CD34^{-} AML cell populations. We observed that CFU was suppressed only by anti-CD123 CAR T cells while NTD T cells had no activity **(Suppl. Figure 5c, d).** These findings show the capacity of the novel third-generation anti-CD123 CAR T cells to induce robust anti-leukemic effects *in vitro*.

Anti-CD123 CAR T cells exhibit *in vivo* activity against AML cells

We used a previously established xenogeneic MOLM-13 AML model[4] to test the anti-AML *in vivo* activity of the anti-CD123 CAR T cells. This model allowed us to measure AML cell expansion using bioluminescence imaging (BLI) (**Figure 1a**). With this xenograft model, the mice that received the anti-CD123 CAR T cells exhibited a modest improvement in survival compared to the groups treated with PBS or NTD T cells (**Figure 1b**). The AML-derived BLI signal showed the typical distribution pattern of the leukemic cells with major infiltration in the BM and peripheral organs. Additionally, we observed that the AML-derived BLI signal was lower when the AML-bearing mice received the anti-CD123 CAR T cells compared to mice that were PBS or NTD T cell treated (**Figure 1c, d**). Additionally, flow cytometric analysis of the absolute cell count of residual human $CD45^+$ (hCD45), and hCD45 $CD123^+$ leukemia cells on day 35 following tumor inoculation was lower in mice that received the anti-CD123 CAR T cells compared to mice treated with PBS or NTD T cells (**Figure 1e-g**). Despite the anti-leukemic activity of the anti-CD123 CAR T cells, complete eradication of disease was not observed, indicating the need for a combinatorial therapeutic approach.

AZA increases CD123 expression on AML cells and enhances the anti-leukemic activity of CD123 CAR T cells *in vivo*

Since the anti-CD123 CAR T cell treated mice did not eliminate the AML cells entirely, we sought a combination partner that would increase *in vivo* efficacy by upregulating the expression of CD123 on AML cells. Based on our knowledge of currently approved therapeutic agents for the treatment of high-risk myelodysplastic syndrome (MDS) and AML, we investigated the impact of the DNA methyltransferase inhibitor, AZA, on CD123 expression[16, 29].

We observed a sustained increase in CD123 expression on the AML cell lines HL-60 and ML-2 and transient increases on MOLM-13 cells over an 8-day exposure to AZA (**Figure 2a-d**). Cell viability did not decrease upon AZA exposure for ML-2 and MOLM-13 cells but was significantly decreased for HL-60 cells (**Figure 2e**). CD123 expression was induced in some primary PB AML cells within 24h of AZA administration. The overall peak increase in CD123 expression was observed on day 4 of exposure to AZA and decreased by day 8 in both bulk $CD34^+$ and $CD34^+CD38^+$ blast populations (**Figure 2f-h**). Based on these observations, administration of CAR T cells within a 24-hour time frame of AZA is likely to be most efficient.

To test for increased *in vivo* efficacy, AZA was given until 24h before infusion of anti-CD123 CAR T cells to treat MOLM-13^{luc+} AML-bearing mice (**Figure 3a**). We intentionally did not treat the mice with CAR Tc and AZA simultaneously because AZA, when in direct contact with T cells, has been shown in several studies to induce Tregs[30], which could suppress the immune response against the leukemia cells. We observed that the AML-derived BLI signal was lowest in the AZA / anti-CD123 CAR T cell combination group as compared to all other groups (**Figure 3b, c**). Consistent with *in vivo* elimination of AML as seen in the BLI analysis, we also observed that the AML-bearing mice that received AZA with anti-CD123 CAR T cells exhibited superior survival compared to AZA alone, CAR T cells alone, or AZA with NTD Tc (**Figure 3d**). The number of residual hCD45$^+$ and hCD45$^+$ MOLM-13 leukemia cells, found in the BM of mice that received AZA along with anti-CD123 CAR T cells, was significantly lower compared to the other treatment groups (**Figure 4a-c**).

The AZA / anti-CD123 CAR T cell treatment combination does not cause inflammatory organ damage or hematopoietic insufficiency

One major concern of anti-CD123 CAR T cells is organ damage by activation of the endogenous T cell receptor and activity against the healthy hematopoietic cells that express CD123. We therefore analyzed different GVHD target organs [31, 32] as well as the ability of normal hematopoietic cells to form CFUs. We found no inflammatory organ damage in the colon, small intestine, and liver of the mice that received anti-CD123 CAR T cells or the AZA / anti-CD123 CAR T cell combination **(Suppl. Figure 6a-d**). We did however, observe leukemia cell infiltration in the liver of some mice treated with PBS or NTD T cells but not those treated with anti-CD123 CAR T cells or the combination treated mice **(Suppl. Figure 6e)**. This supports the concept that the anti-CD123 CAR T cells are mainly activated via their CAR while activation via their endogenous TCR plays only a limited role.

The expression of CD123 on several populations of normal hematopoietic cells, including circulating B cells, myeloid progenitors, dendritic cells, and megakaryocytes raises concerns regarding potential on-target, off-tumor effects. To analyze the potential hematopoietic toxicity of the anti-CD123 CAR T cells, we next exposed healthy hematopoietic BM cells to the CAR T cells and studied their ability to form CFU-GM, CFU-GEMM, and BFU-E colonies. We observed that the ability to form CFU-GM, CFU-GEMM, and BFU-E colonies was still intact when BMMNC were exposed to the CAR T cells compared to medium only or NTD T cells (**Figure 5a-c**).

To investigate the effect of the anti-CD123 CAR T cells on hematopoietic insufficiency *in vivo*, humanized cytokine knock-in Rag2$^{-/-}$Il-2rg$^{-/-}$ mice[26] were engrafted with HD CD34$^+$ CB cells and treated with either anti-CD123 CAR or NTD T cells. Changes to the peripheral B-lymphoid, monocyte, myeloid, and plasmacytoid dendritic cells (pDC) graft were evaluated over 7 days. Mice were terminated at day 14 and changes to the above-mentioned populations and the primitive hematopoietic populations were analyzed in the spleen and BM. While trending decreases were observed in the peripheral B-lymphoid and monocyte grafts, this was not significantly different when compared to mice treated with NTD T cells. Additionally, no differences were observed between the groups for myeloid and pDC grafts in the PB **(Figure 5d)**. Similarly, no differences in B-lymphoid, myeloid, monocyte, and pDC specific grafts were observed between the mice treated with anti-CD123 CAR T cells and NTD T cells in the spleen and BM. In addition, the anti-CD123 CAR T cells had no effect on CD123$^+$ primitive cell populations **(Figure 5e-f).**

Since AZA was found to increase the expression of CD123 on AML cells, it was important to evaluate whether the same pattern would be observed in healthy cells. We observed that the expression of CD123 on CD34$^+$ and CD34$^-$ HD BMMC was not significantly increased in the presence of AZA (**Figure 6a-c**). In the clinic, AZA is reported to cause pancytopenia[33]. Concordant with published data[33] we observed that AZA treatment significantly decreased the ability of the HD BMMC to form CFU-GM, CFU-GEMM, and BFU-E colonies compared to BMMC in medium only (**Figure 6d-f**). However, the AZA / anti-CD123 CAR T cell combination did not further reduce CFU-GM colony formation compared to the AZA only treatment (**Figure 6d**). These findings indicate that the AZA / anti-CD123 CAR T cell combination is unlikely to cause inflammatory organ damage or profound hematopoietic insufficiency at a higher rate than AZA alone.

AZA treatment induces a CTLA-4^{negative} CAR T cell fraction *in vivo*

To better characterize the mechanism by which AZA improves the *in vivo* efficacy of anti-CD123 CAR T cells, we next analyzed CAR T cells isolated from monotherapy treated mice or from the AZA / anti-CD123 CAR T cell treated mice. We observed that there was no difference in the number of residual CD4$^+$ and CD8$^+$ T cells in the BM and PB of mice **(Suppl. Fig. 7a, b; Suppl. Fig. 8a, b)** or the number of residual CD4$^+$ and CD8$^+$ CAR T cells that were PD-1^{negative} TIM-3^{negative} between the treatment groups **(Suppl. Fig. 7c, d; Suppl. Fig. 8 c, d)**. Interestingly, we found that CAR T cells isolated from AML-bearing mice that received prior AZA treatment exhibited a significantly higher residual number of CTLA-4^{negative} CD4$^+$ ant-CD123 CAR T cells in the BM 28 days following anti-CD123 CAR T cell infusion, but not the PB (**Figure 7a, b; Suppl. Fig. 8e**). Additionally, we observed a similar trend for CD8$^+$ CAR T cells. However, these data were not significant **(Suppl. Fig. 7e; Suppl. Fig. 8f)**. Within the CD4$^+$ and CD8$^+$ T cell compartments, there were no consistent differences in the phenotypic distribution of $T_{scm\text{-}like}$, T_{cm}, T_{em}, and T_{eff} cells between the two treatment groups in both BM and PB **(Suppl. Fig. 9)**.

CTLA-4^{negative} anti-CD123 CAR T cells allow for robust anti-leukemic efficacy *in vivo*

To functionally validate whether CTLA-4^{negative} anti-CD123 CAR T cells are responsible for sustained anti-leukemia effects and subsequent improved survival in AML-bearing mice, CTLA-4^{negative} or CTLA-4^{positive} CAR T cells were transferred into leukemia bearing mice. In this model, the anti-CD123 CAR T cells were first exposed to MOLM-13 cells for 7 days, *in vitro,* to generate CTLA-4^{negative} and CTLA-4^{positive} populations. These populations were sort purified and injected into MOLM-13 engrafted mice on day 7 **(Figure 7c).** Prior to the transfer of cells in the mice, we observed a 60:40 ratio of CD4:CD8 T cells in both CTLA-4^{positive} and CTLA-4^{negative} populations. Interestingly, in the BM and PB 28 days post CAR T cell infusion, the residual T cells were predominantly CD4^{+} T cells **(Figure 7d)**. Tregs were also analyzed in both CD4^{+} CTLA-4^{positive} and CTLA-4^{negative} anti-CD123 CAR T cells post-sorting. We found no Tregs in the sorted CD4^{+} CTLA-4^{negative} anti-CD123 CAR T cells and a moderate population in the CTLA-4^{positive} cells **(Figure 7e).**

We found that the mice treated with CTLA-4^{negative} anti-CD123 CAR T cells demonstrated effective leukemia control whereas the mice treated with CTLA-4^{positive} anti-CD123 CAR T cells had exponential tumor progression **(Figure 7f)**. This observation was in agreement with an improved survival of mice injected with CTLA-4^{negative} anti-CD123 CAR T cells compared to mice injected with CTLA-4^{positive} CAR T cells **(Figure 7g)**. Flow cytometry-based analysis of the BM and PB 28 days following CAR T cell infusion also showed a significantly higher number of residual leukemia cells in mice injected with CTLA-4^{positive} anti-CD123 CAR T cells compared to the CTLA-4^{negative} group **(Figure 7h)**. The number of residual CD4^{+} T cells was significantly higher in the mice treated with CTLA-4^{negative} anti-CD123 CAR T cells compared to the mice treated with CTLA-4^{positive} anti-CD123 CAR T cells **(Figure 7i)**. Mice treated with CTLA-4^{positive} anti-CD123 CAR T cells remained positive for CTLA-4 in the BM and PB, whereas mice that had received CTLA-4^{negative} anti-CD123 CAR T cells had a high fraction of cells in both BM and PB that remained negative for CTLA-4 28 days following T cell injection **(Figure 7j)**. We also observed that mice treated with CTLA-4^{negative} anti-CD123 CAR T cells exhibited a higher expression of TNF compared to the mice that were treated with CTLA-4^{positive} anti-CD123 CAR T cells **(Figure 7k).** No residual CD8^{+} T cells were observed in either of the treatment groups. Additionally, no difference in the percentage of CTLA-4^{negative} or the expression of TNF in CD8^{+} T cells was seen **(Suppl. Fig. 10)**.

CTLA-4^{negative} anti-CD123 CAR T cells exhibit recall immunity

An important feature of successful CAR T cell therapy is their capability to recall an immune response against the malignancy in the event of relapse. To determine efficacy of CTLA-4^{negative} anti-CD123 CAR T cells derived from AZA treated leukemia bearing mice, we evaluated their immune recall capacity. CTLA-4^{negative} and CTLA-4^{positive} anti-CD123 CAR T cells were isolated 28 days following inoculation into primary recipients **(Figure 8a)**. Cells were maintained in low dose IL-2 and re-inoculated into secondary MOLM-13 leukemia-bearing mice. CTLA-4^{positive} anti-CD123 CAR T cell treated secondary recipients failed to recall an anti-leukemia immune response and did not survive longer than PBS treated mice **(Figure 8b)**. Conversely, secondary recipients treated with CTLA-4^{negative} anti-CD123 CAR T cells demonstrated a significantly longer survival compared to mice treated with PBS or CTLA-4^{positive} anti-CD123 CAR T cells **(Figure 8b)**. *In vitro,* we subjected the sorted CAR T cells to MOLM-13 leukemia cells for 24 hours and tested their cytolytic ability. We demonstrated that CTLA-4^{negative} anti-CD123 CAR T cells exerted high leukemia cell lysis, while CTLA-4^{positive} anti-CD123 CAR T cells exerted less than 10% killing of the MOLM-13 cells. The NTD T cells showed no killing capacity **(Figure 8c)**. The ability of the sorted CTLA-4^{negative} anti-CD123 CAR T cells to effectively kill leukemia cells was also seen using three independent patient-derived AML samples. No killing of the AML PBMCs was observed with the CTLA-4^{positive} anti-CD123 CAR T cells **(Figure 8d)**. We observed that the production of TNF was significantly higher in the CTLA-4^{negative} anti-CD123 CAR T cells compared to the CTLA-4^{positive} anti-CD123 CAR T cells. **(Figure 8e, f)**. Additionally, proliferation of CTLA-4^{negative} anti-CD123 CAR T cells in the presence of MOLM-13 cells was higher compared to CTLA-4^{positive} anti-CD123 CAR T cells or NTD T cells **(Figure 8g).**

AZA primed leukemia cells support intracellular retention of CTLA-4 in CD4^{+} anti-CD123 CAR T cells and enhances proximal signaling

CTLA-4 is a surface receptor that mediates T cell responses. Prolonged extracellular expression is reported to inhibit T cell function by reducing intracellular downstream protein tyrosine phosphorylation of key signaling effectors such as zeta-associate protein of 70kDa (Zap70) and p56 (Lck)[34]. We therefore sought to evaluate the extracellular and intracellular expression levels of CTLA-4 when CD4^{+} anti-CD123 CAR T cells were exposed to untreated or AZA pre-treated MOLM-13 cells. The CTLA-4 expression was compared to NTD T cells to discount possible expression as a result of TCR signaling. CD4^{+} anti-CD123 CAR T cells exposed to untreated MOLM-13 cells expressed significantly higher levels of surface CTLA-4 compared to CAR T cells exposed to AZA pre-treated MOLM-13 cells **(Figure 9a).** Furthermore, surface expression of CTLA-4 in the CAR T cells exposed to AZA pre-treated MOLM-13 cells was similar to that of resting CAR T cells cultured in media only. The opposite was observed with significantly higher intracellular levels of CTLA-4 when CD4$^+$ anti-CD123 CAR T cells were cultured with AZA pre-treated MOLM-13 cells compared to untreated MOLM-13 cells **(Figure 9b, c).**

To understand whether the high expression of surface CTLA-4 was associated with an arrest in phosphorylation of Lck and Zap70, CD4$^+$ and CD8$^+$ anti-CD123 CAR T cells were co-cultured for 96 hours in media, untreated MOLM-13 or AZA pre-treated MOLM-13 cells. CD4$^+$ anti-CD123 CAR T cells demonstrated higher phosphorylation levels of Lck and Zap70 when cultured with AZA pre-treated MOLM-13 cells or naive MOLM-13 cells **(Figure 9d-g)**. This was similarly observed with CD8$^+$ anti-CD123 CAR T cells for Lck but not Zap70 **(Suppl. Figure 11).**

These data indicate that mainly CTLA-4$^{\text{negative}}$ CD4$^+$ anti-CD123 CAR T cells are responsible for prolonged leukemia control and survival. Improved leukemia control is likely due to the ability of this population of CAR T cells to continuously produce TNF and maintain phosphorylation of key intracellular molecules imperative for T cell activation and function.

Discussion

The development of CAR T cells has caused a significant paradigm shift in the use of immunotherapeutic strategies for various malignancies. While its success has demonstrated improved survival outcomes for patients with certain B-lymphoid malignancies[5, 6], no comparable success has been achieved with CAR T cells directed against myeloid malignancies. The efficacy of CAR T cell therapy is reduced by loss of target antigen which is associated with lack of persistence, due to absence of activation. Both, antigen loss[35] and failure of persistence of the CAR T cell population[36] have been described. The clinical translation of CAR T cell therapy for AML has been further hindered by the development of an immunosuppressive microenvironment as well as on-target off-tumor toxicities. In this study, we used AZA to increase target antigen expression and test if this was associated with increased CAR T cell efficacy.

To achieve this, we used novel third-generation anti-CD123 CAR T cells with a humanized CSL362-based[13] scFv and a CD28-OX40-CD3ζ signaling domain that exhibits anti-leukemic efficacy *in vitro* and *in vivo*. While the CAR T cells demonstrated anti-leukemic activity, disease eradication in the mice was incomplete. Therefore, we developed a novel approach to augment expression of the target antigen, CD123, by pre-treating AML cells or leukemia-bearing mice with AZA. It is well documented that hypomethylating agents play a role in the prolonged survival of patients with myelodysplastic syndromes and relapsed/refractory AML by increasing the immunogenicity of tumor cells thereby enhancing T cell mediated responses[37]. We found that the pre-treatment of leukemia-bearing mice with AZA followed by infusion of anti-CD123 CAR T cells led to improved AML rejection *in vivo,* which was associated with an improved survival of the mice.

We hypothesized that increased expression of CD123 on the AML cells would promote the expansion of functionally superior CAR T cells *in vivo*. Consistent with this concept, we found that pre-treatment of AML cells with AZA resulted in higher absolute numbers of $CD4^+$ CTLA-$4^{negative}$ CAR T cells compared to the CAR T cell only treated group. Functionally, these CTLA-$4^{negative}$ CAR T cells were more potent compared to CTLA-$4^{positive}$ CAR T cells *in vitro* with respect to their cytotoxicity against leukemia cells. Additionally, we also observed increased AML control *in vivo* which was associated with increased TNF production. TNF was shown to play a major role in leukemia control after allo-HCT[38]. Moreover, CTLA-$4^{negative}$ CAR T cells were able to demonstrate continuous immune response in secondary AML-bearing mice while CTLA-$4^{positive}$ CAR T cells did not. This finding is consistent with reports showing that the negative regulator of T cell activation, CTLA-4[39], is mainly expressed on less effective T cells[22, 40, 41]. So far, no report had shown that the fraction of CTLA-$4^{negative}$ anti-CD123 CAR T cells can be increased indirectly by AZA pre-treatment of the AML-bearing mice. In previous studies, AZA has been found to reduce the effects of DLI by promoting inhibitory T_{reg} cells while diminishing $CD8^+$ effector T cell numbers[30]. Because of these previous observations we avoided a direct contact of AZA to the transferred CAR T cells but only used an AZA pre-treatment regimen inducing CD123 on leukemia cells.

Enhanced expression of PD-L1, PD-L2, PD-1, and CTLA4 in myelodysplastic syndromes upon treatment with hypomethylating agents has been reported[42]. Conversely, hypomethylating agents were also shown to induce an interferon response in cancer via dsRNA derived from endogenous retroviruses[15, 43]. This indicates that hypomethylating agents can cause both, upregulation of inhibitory molecules and pro-inflammatory effects. The combination of AZA and SL-401 (tagraxofusp), the anti-CD123 directed cytotoxin which consists of recombinant interleukin-3 fused to a truncated diphtheria toxin, is currently being tested in an ongoing clinical trial (ClinicalTrials.gov Identifier: NCT03113643) for patients with MDS or AML. Also consistent with our results, the combination of tagraxofusp and AZA was effective in patient-derived xenografts[44].

Further analysis revealed that exposure of leukemia cells to AZA not only increased antigen recognition by the anti-CD123 CAR T cells, but that immediate downstream consequences of antigen recognition strengthened CD3ξ ITAM phosphorylation.

Previous studies have demonstrated that phosphorylation of CD3ξ occurs at a much greater intensity in CD28 co-stimulatory containing CARs due to the proline-rich region with which Lck associates[45, 46]. In the presence of low antigen levels, inefficient Lck-mediated ITAM phosphorylation and Zap-70 activation can limit CAR T cell anti-leukemic responses[47], while recent data show that non-canonical binding of Lck to CD3ε promotes TCR signaling and CAR function[48]. We observed that pretreatment of leukemia cells with AZA was connected to increased Lck and Zap70 phosphorylation in CD4$^+$ CAR T cells upon contact with the pretreated leukemia cells.

There are conflicting reports showing that targeting of CD123 causes myelosuppression of healthy cells, which may be due to the different CAR constructs in use. We observed that the anti-CD123 CAR construct we used did not affect the viability and frequency of CFU-GM, CFU-GEMM, and BFU-E colonies *in vitro* nor *in vivo*. These findings were in line with those of others[10, 44, 49]. A recent study demonstrated in humanized mouse models that a third generation construct comparable to our construct namely CD28/4-1BB CAR T cells targeting CD123 exert no major cytotoxicity against various subsets of normal cells with low CD123 expression, indicating a low on-target/off-tumor toxicity effect[49]. Another study on a patient with a blastic plasmacytoid dendritic cell neoplasm enrolled in a clinical trial of anti-CD123 CAR T-cell therapy (ChiCTR1900022058) showed activity of the CAR T cells without significant hematotoxicity[50].

In contrast, other studies have shown myelosuppression by CD123-directed CAR T cells[27, 51]. The variances observed across the studies could be due to the different structural designs of the CAR. Nevertheless, recent studies have shown that attractive tumor target antigens that are also shared on healthy tissues can be ‘affinity-tuned’ in order to avoid significant hematotoxicity[52]. We further confirmed that the increase in CD123 expression on AML cells was not observed in healthy hematopoietic cells under AZA induction. Additionally, the combination therapy did not significantly affect the ability of healthy CD34$^+$ cells to form CFU-GM colonies which demonstrates that the addition of AZA into the treatment regimen would not bring any additional toxicities.

Besides myelosuppression, there is concern that the transfer of allogeneic CAR T cells may induce inflammatory organ damage or GVHD. Our pre-clinical studies found no evidence of TCR engagement from allogeneic transferred CAR T cells alone or combined with AZA as we did not observe any major tissue damage in GVHD target organs. In line with these findings, Ghosh A et al.[53] similarly reported that CAR T cells harboring the CD28 co-stimulatory motif demonstrated significantly decreased occurrence of GVHD compared to CAR T cells with the 4-1BB costimulatory motif. The combination of AZA and immunotherapy for AML is attractive and has already been tested e.g. with immune checkpoint inhibition[21] and DLIs with AZA for AML relapse after allo-HCT[33, 54, 55]. In contrast to the potential of polyclonal DLI to recognize major or minor MHC mismatches on leukemia cells, CAR T cells rely on the recognition of a defined target antigen which makes this approach more specific. Our study is the first report on a combination of AZA and CAR T cells for AML.

In summary, our studies show that AZA treatment increases expression of the CAR target, CD123, leading to improved leukemia control *in vivo*. Mechanistically, the treatment induced higher numbers of CTLA-4$^{\text{negative}}$ anti-CD123 CAR T cells which exhibited superior cytotoxicity compared to CTLA-4$^{\text{positive}}$ anti-CD123 CAR T cells against AML target cells *in vitro* and *in vivo.* More importantly, these CTLA-4$^{\text{negative}}$ CD123 CAR T cells exhibited prolonged phosphorylation of key intracellular markers important for cell activation and function thereby demonstrating capacity for immune memory in secondary non-AZA-treated AML-bearing mice. Since the combination of AZA with anti-CD123 CAR T cells did not cause epithelial tissue damage or significant hematopoietic insufficiency, our findings pave the way for a clinical trial combining AZA and anti-CD123 CAR T cells for AML treatment.

Acknowledgments: The authors thank M. Kappenstein and N. von Bubnoff for providing us with the MOLM-13-GFP-ffLuc cells, R. Grose from the South Australian Health and Medical Research Institute (SAHMRI), Adelaide, Australia for cell sorting as well as K. Geiger, D. Herchenbach, and J. Bodinek from the lighthouse core facility, Freiburg, Germany for cell sorting.

Author Contributions: N.E.K helped with study design, performed all the experiments, analyzed and interpreted the data, and co-wrote the manuscript. A.H helped with study design and supervision of the *in vitro* experiments. M.P.B, A.L and W.Y contributed to the lenti-vector concept and design, and W.Y helped to develop the CAR. R.M, S.T, J.C, and M.J.V assisted with the experiments, K.S provided AML patient samples, K.A, A.L, M.P.B, J.D, M.M, and T.P.H helped with analysis or interpretation of the data, D.L.W helped with study design, interpreted the data, and co-supervised the project, A.S.M.Y designed the project, interpreted the data, and co-supervised the project, R.Z designed the project, interpreted the data, co-supervised the project, and co-wrote the manuscript. All authors reviewed and edited the manuscript.

Funding: This study was supported by the DFG under Germany’s Excellence Strategy – EXC 2189 Project ID: 390939984, TRR167 to RZ, SFB1160 TP B09 to R.Z., the European Union: Proposal n° 681012 GvHDCure (ERC consolidator grant to R.Z.), the Deutsche Krebshilfe (grant number 70113473), the Jose-Carreras Leukemia foundation (grant number DJCLS 01R/2019) (R.Z.), Beat Cancer Hospital Research package funded by Cancer Council South Australia and the Department of Health Services Charitable Gifts Board, Adelaide, South Australia (M.P.B, T.P.H, A.S.M.Y, and A.L).

Conflict of Interest: None.

Figure 1

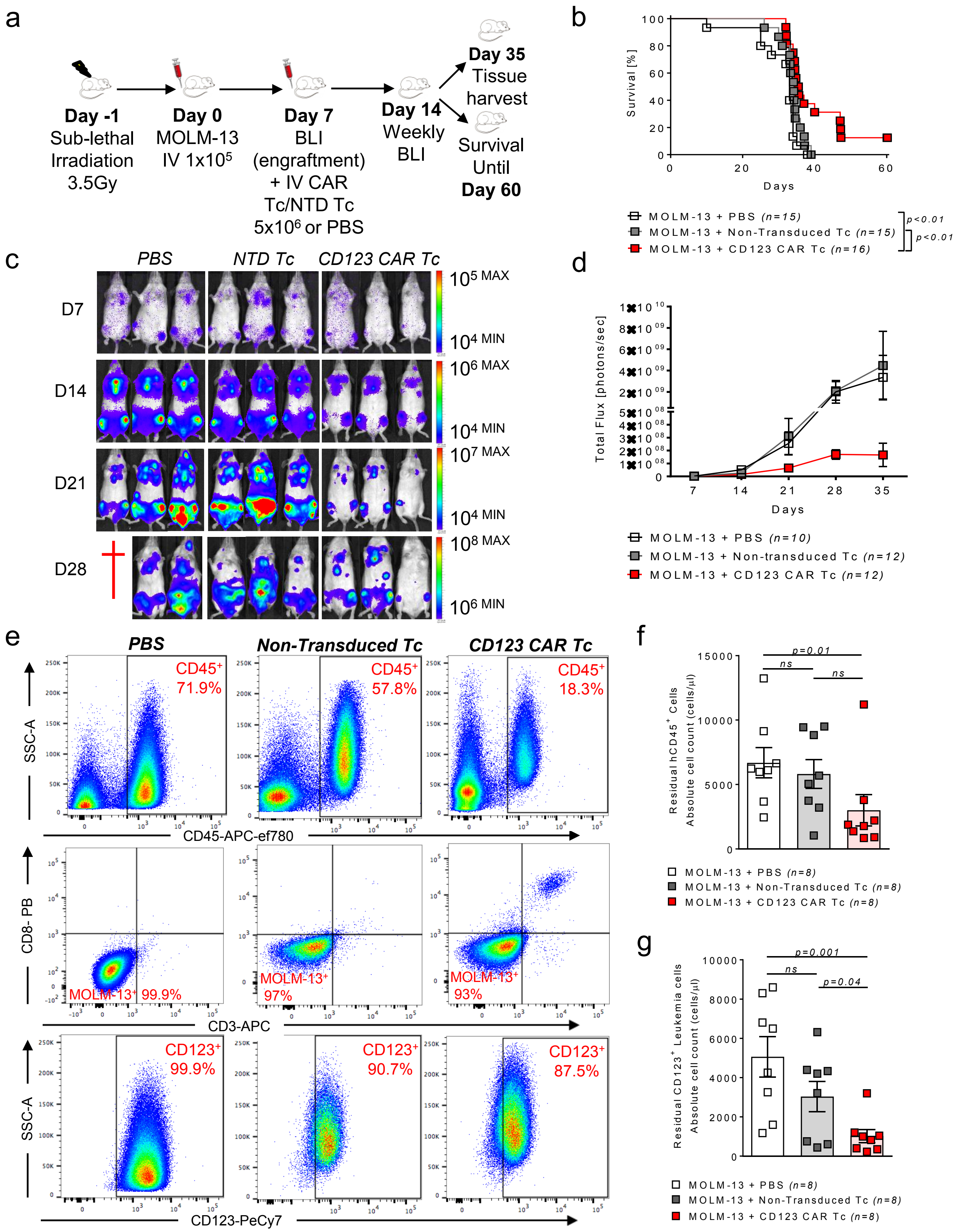
a
Day -1
Sub-lethal Irradiation 3.5Gy
Day 0
MOLM-13 IV 1x10^5
Day 7
BLI (engraftment) + IV CAR Tc/NTD Tc 5x10^6 or PBS
Day 14
Weekly BLI
Day 35
Tissue harvest
Survival Until Day 60
b
Survival [%]
Days
MOLM-13 + PBS (n=15)
MOLM-13 + Non-Transduced Tc (n=15)
MOLM-13 + CD123 CAR Tc (n=16)
p<0.01
p<0.01
c
PBS
NTD Tc
CD123 CAR Tc
D7
D14
D21
D28
10^5 MAX
10^4 MIN
10^6 MAX
10^4 MIN
10^7 MAX
10^4 MIN
10^8 MAX
10^6 MIN
d
Total Flux [photons/sec]
Days
MOLM-13 + PBS (n=10)
MOLM-13 + Non-transduced Tc (n=12)
MOLM-13 + CD123 CAR Tc (n=12)
e
PBS
Non-Transduced Tc
CD123 CAR Tc
SSC-A
CD45-APC-ef780
CD45+ 71.9%
CD45+ 57.8%
CD45+ 18.3%
CD8- PB
CD3-APC
MOLM-13+ 99.9%
MOLM-13+ 97%
MOLM-13+ 93%
CD123-PeCy7
CD123+ 99.9%
CD123+ 90.7%
CD123+ 87.5%
f
Residual hCD45+ Cells Absolute cell count (cells/µl)
p=0.01
ns
ns
MOLM-13 + PBS (n=8)
MOLM-13 + Non-Transduced Tc (n=8)
MOLM-13 + CD123 CAR Tc (n=8)
g
Residual CD123+ Leukemia cells Absolute cell count (cells/µl)
p=0.001
ns
p=0.04
MOLM-13 + PBS (n=8)
MOLM-13 + Non-Transduced Tc (n=8)
MOLM-13 + CD123 CAR Tc (n=8)

Figure 1: CD123 CAR T cells demonstrate anti-leukemic effects in MOLM-13 AML xenograft mice.

(a) Schematic diagram of the MOLM-13 AML xenograft model. Rag2$^{-/-}$Il2rγ$^{-/-}$ mice were sub-lethally irradiated (3.5Gy) on day -1 and then injected via tail vein with 1x10^{5} green fluorescent protein/luciferase^{+} MOLM-13 cells on day 0. Bioluminescent imaging (BLI) was performed on day 7 to confirm and quantify engraftment and mice were randomized into treatment groups. Saline (PBS), 5x10^{6} NTD T cells or 5x10^{6} anti-CD123 CAR T cells were injected on day 7, and mice were followed with weekly BLI until day 35. Quantification of BLI radiance was used as a surrogate measurement of AML burden. Mice were either sacrificed on day 35 (28 days following T cell infusion) for flow cytometric analysis or left until day 60 for survival analysis.

(b) Kaplan-Meier analysis for percentage survival for each treatment group. Data were pooled from 3 independent experiments. *P*-value was calculated using the 2-sided Mantel-Cox (Log-rank) test. Attrition of mice was due to paralysis in both hind legs, growth of subcutaneous tumors >2cm, or BLI-detectable AML progression in the head.

(c) Representative serial BLI depicting leukemia burden of MOLM-13 engrafted mice treated with PBS, NTD T cells or anti-CD123 CAR T cells. Data are represented colorimetrically with the scale bars indication upper (max) and lower (min) BLI thresholds at each analysis time point.

(d) Quantification of the BLI signal at the indicated time points for each treatment group. Data was pooled from 2 independent experiments, and represented as mean ± SEM for each treatment group. On day 35, at least 5 mice per group were still alive and included in the analysis.

(e) Representative flow cytometry gating strategy of the analysed bone marrow of mice treated with PBS, NTD Tc or anti-CD123 CAR Tc for total human CD45, residual MOLM-13 leukemia cells and their CD123 expression as well as residual CD4/CD8 T cells.

Flow cytometric analysis depicting absolute counts (cells/μl) of live residual **(f)** human CD45^{+} and **(g)** hD45^{+} CD3^{-}CD123^{+} leukemia cells in the BM of PBS, NTD T cell or anti-CD123 CAR T cell treated mice. Data were pooled from 2 independent experiments and represented as mean absolute cell counts ± SEM for each treatment group. *P*-values were calculated using 1-way ANOVA.

Figure 2

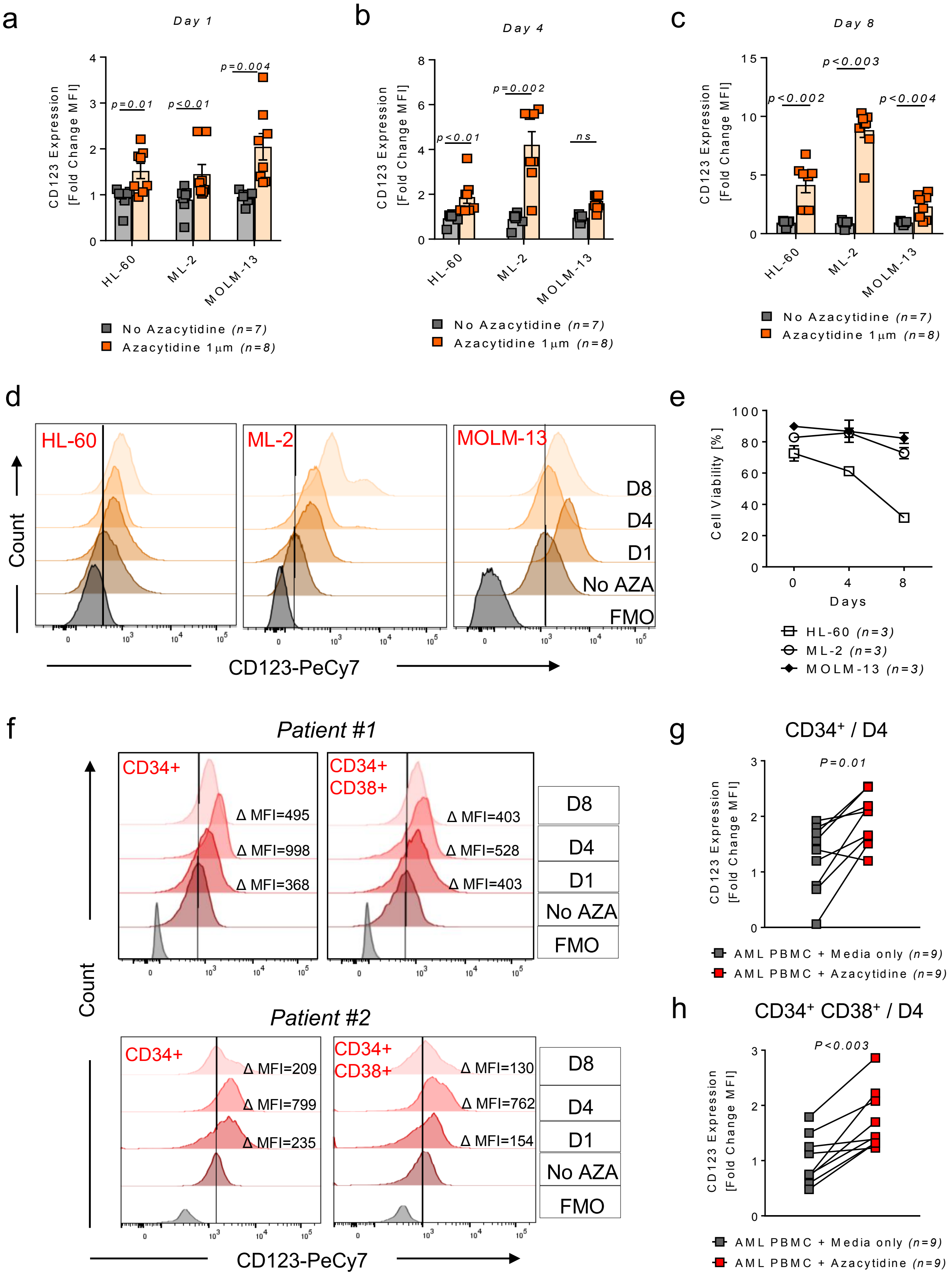
a
Day 1
CD123 Expression [Fold Change MFI]
p=0.01
p<0.01
p=0.004
0
1
2
3
4
HL-60
ML-2
MOLM-13
No Azacytidine (n=7)
Azacytidine 1µm (n=8)
b
Day 4
CD123 Expression [Fold Change MFI]
p<0.01
p=0.002
ns
0
2
4
6
8
HL-60
ML-2
MOLM-13
No Azacytidine (n=7)
Azacytidine 1µm (n=8)
c
Day 8
CD123 Expression [Fold Change MFI]
p<0.002
p<0.003
p<0.004
0
5
10
15
HL-60
ML-2
MOLM-13
No Azacytidine (n=7)
Azacytidine 1µm (n=8)
d
Count
HL-60
ML-2
MOLM-13
D8
D4
D1
No AZA
FMO
0
10³
10⁴
10⁵
CD123-PeCy7
e
Cell Viability [%]
0
20
40
60
80
100
0
4
8
Days
HL-60 (n=3)
ML-2 (n=3)
MOLM-13 (n=3)
f
Patient #1
CD34+
Δ MFI=495
Δ MFI=998
Δ MFI=368
CD34+ CD38+
Δ MFI=403
Δ MFI=528
Δ MFI=403
D8
D4
D1
No AZA
FMO
Count
Patient #2
CD34+
Δ MFI=209
Δ MFI=799
Δ MFI=235
CD34+ CD38+
Δ MFI=130
Δ MFI=762
Δ MFI=154
D8
D4
D1
No AZA
FMO
0
10³
10⁴
10⁵
CD123-PeCy7
g
CD34⁺ / D4
P=0.01
CD123 Expression [Fold Change MFI]
0
1
2
3
AML PBMC + Media only (n=9)
AML PBMC + Azacytidine (n=9)
h
CD34⁺ CD38⁺ / D4
P<0.003
CD123 Expression [Fold Change MFI]
0
1
2
3
AML PBMC + Media only (n=9)
AML PBMC + Azacytidine (n=9)

Figure 2: AZA treatment leads to enhanced CD123 expression on AML cells.

Scatter plot showing the expression of CD123 represented as a fold change of mean fluorescence intensity (MFI) with respect to mean MFI of untreated controls on **(a)** day 1, **(b)** day 4, and **(c)** day 8 following culture with 1µM AZA. *P*-values were calculated using unpaired student's *t*-test (Mann-Whitney).

(d) Representative flow cytometric analysis of CD123 on AML cell lines (with varying basal CD123 expression levels) following culture in the absence or presence of 1µM AZA for 1, 4, and 8 days. Histograms depict staining with anti-human CD123 Ab (PeCy7) compared to the fluorescence minus one (FMO) control.

(e) Percentage cell viability (using trypan blue) of AML cell lines at baseline (day 0) and upon exposure to 1µM AZA after 4 days and 8 days.

(f) Representative flow cytometric analysis of CD123 on 2 primary patient AML $CD34^+$ and $CD34^+CD38^+$ blast cells following culture in the absence or presence of 1µM AZA for 1, 4, and 8 days. Histograms depict staining with anti-human CD123 Ab (PeCy7) compared to the FMO control. Inset numbers state the absolute difference in MFI between treated and non-treated cells.

Scatter plot showing the expression of CD123 on primary AML **(g)** $CD34^+$ and **(h)** $CD34^+$ $CD38^+$ cells represented as a fold change of MFI with respect to MFI of untreated controls on day 4 following culture with 1µM AZA. *P*-values were calculated using unpaired Student's *t*-test (Mann-Whitney). All graphed data in this figure were represented as mean values ± SEM.

Figure 3

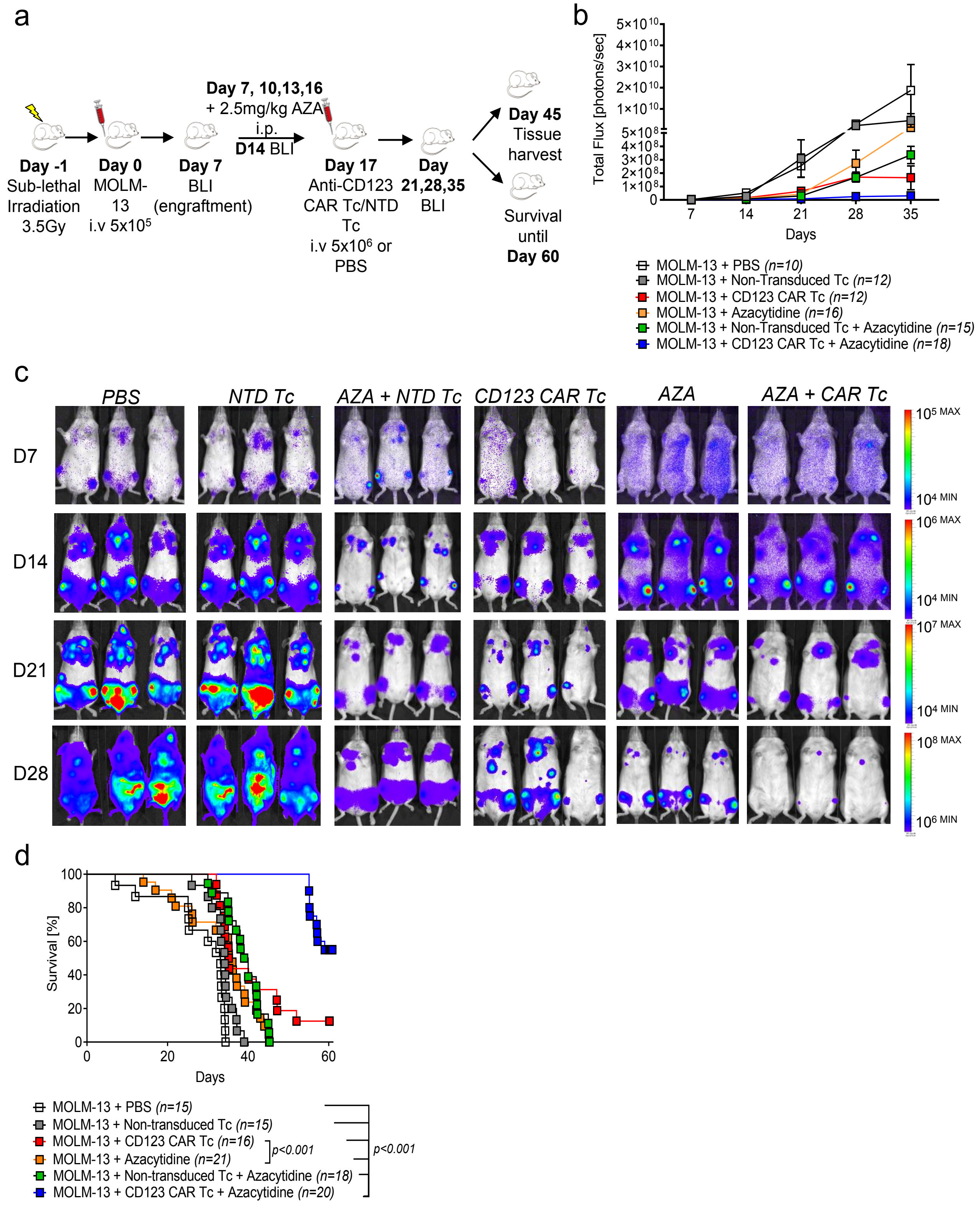
a
Day -1
Sub-lethal Irradiation 3.5Gy
Day 0
MOLM-13 i.v 5x10^5
Day 7
BLI (engraftment)
Day 7, 10,13,16
+ 2.5mg/kg AZA i.p.
D14 BLI
Day 17
Anti-CD123 CAR Tc/NTD Tc i.v 5x10^6 or PBS
Day 21,28,35
BLI
Day 45
Tissue harvest
Survival until
Day 60
b
Total Flux [photons/sec]
5×10^10
4×10^10
3×10^10
2×10^10
1×10^10
5×10^8
4×10^8
3×10^8
2×10^8
1×10^8
0
7
14
21
28
35
Days
MOLM-13 + PBS (n=10)
MOLM-13 + Non-Transduced Tc (n=12)
MOLM-13 + CD123 CAR Tc (n=12)
MOLM-13 + Azacytidine (n=16)
MOLM-13 + Non-Transduced Tc + Azacytidine (n=15)
MOLM-13 + CD123 CAR Tc + Azacytidine (n=18)
c
PBS
NTD Tc
AZA + NTD Tc
CD123 CAR Tc
AZA
AZA + CAR Tc
D7
D14
D21
D28
10^5 MAX
10^4 MIN
10^6 MAX
10^4 MIN
10^7 MAX
10^4 MIN
10^8 MAX
10^6 MIN
d
Survival [%]
100
80
60
40
20
0
0
20
40
60
Days
MOLM-13 + PBS (n=15)
MOLM-13 + Non-transduced Tc (n=15)
MOLM-13 + CD123 CAR Tc (n=16)
MOLM-13 + Azacytidine (n=21)
p<0.001
MOLM-13 + Non-transduced Tc + Azacytidine (n=18)
MOLM-13 + CD123 CAR Tc + Azacytidine (n=20)
p<0.001

Figure 3: AZA treatment supports the increased anti-leukemic effect of anti-CD123 CAR T cells in MOLM-13 xenograft mice.

(a) Schematic diagram of the MOLM-13 AML xenograft model. Engraftment was performed as described in Figure 2. On day 7, mice were injected with AZA at a concentration of 2.5mg/kg every 3 days intraperitoneally for the groups receiving AZA monotherapy or dual treatment. Mice receiving anti-CD123 CAR T cells only were injected with $5x10^6$ anti-CD123 CAR T cells intravenously and control mice received PBS. On day 17, AZA only mice received PBS while mice in the dual treatment group were intravenously injected with $5x10^6$ anti-CD123 CAR T cells. Mice were subjected to weekly BLI analysis from day 14 until day 35. Quantification of BLI signal was used as a surrogate measurement of AML burden. A cohort of mice in the PBS or CAR T cell only group were sacrificed at D35 and the AZA treated or dual treated group were sacrificed on D45 (both 28 days following AZA treatment or T cell infusion) for flow cytometric analysis. The remaining mice were left until day 60 for survival analysis.
(b) Quantification of the BLI signal for each treatment group over time. Data were pooled from 2 independent experiments. On day 35, at least 5 mice per group were still alive and included in the analysis.
(c) Representative serial BLI depicting leukemia burden in MOLM-13 engrafted mice treated with PBS, NTD Tc, anti-CD123 CAR T cells, AZA only, AZA with NTD Tc, and AZA with CD123 CAR Tc. Data is represented colorimetrically with the scale bars indicating upper (max) and lower (min) BLI thresholds at each analysis time point.
(**d**) Kaplan-Meier analysis of percentage survival for each treatment group. Data were pooled from 3 independent experiments. Attrition of mice was due to paralysis in hind legs, growth of subcutaneous tumors >2cm, or due to BLI-detectable AML progression in the head. All graphed data are represented as mean ± SEM. *P*-values were calculated using 2-sided Mantel-Cox test (log-rank) **(d).**

Figure 4

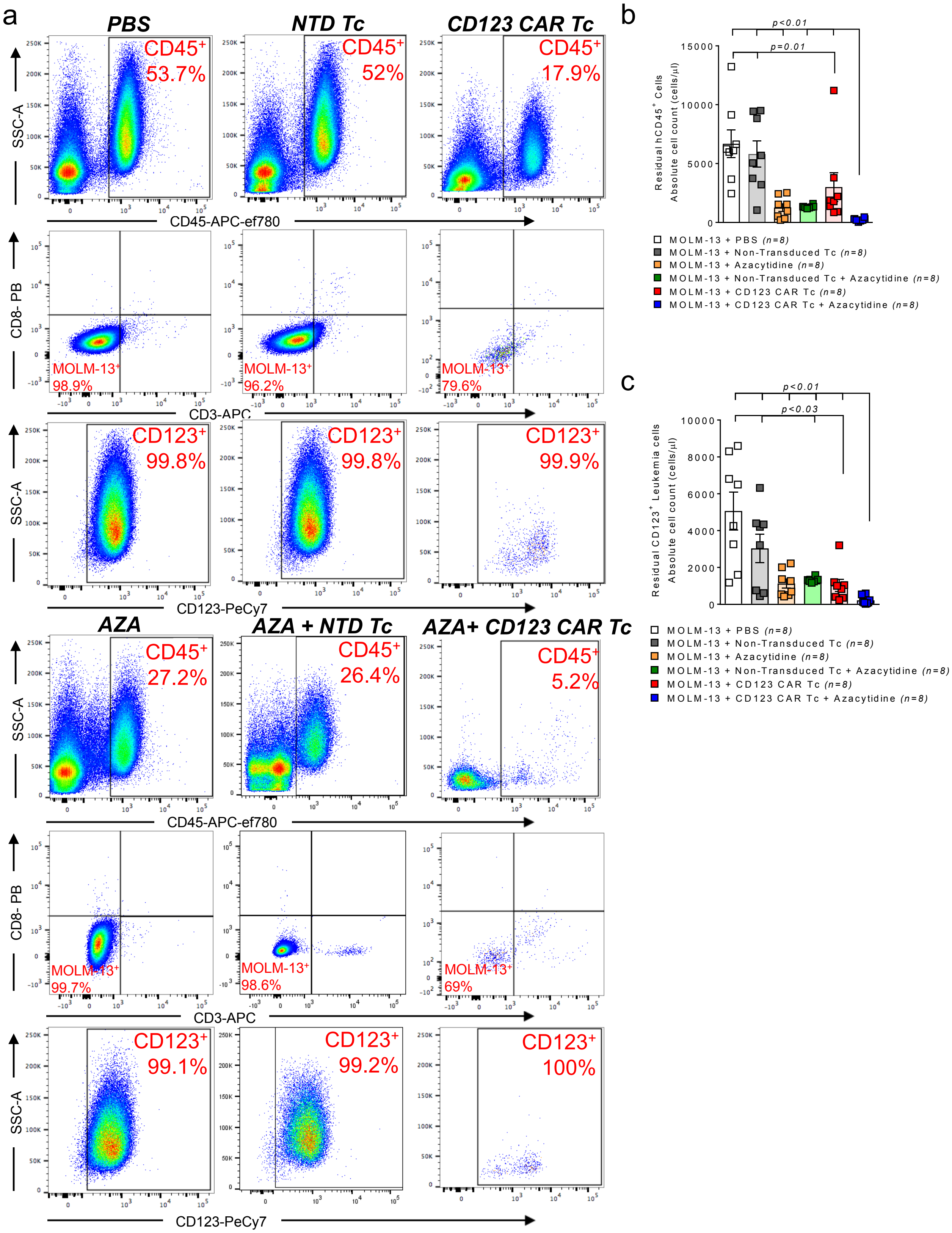
a
PBS
NTD Tc
CD123 CAR Tc
SSC-A
CD45⁺ 53.7%
CD45⁺ 52%
CD45⁺ 17.9%
CD45-APC-ef780
CD8- PB
MOLM-13⁺ 98.9%
MOLM-13⁺ 96.2%
MOLM-13⁺ 79.6%
CD3-APC
CD123⁺ 99.8%
CD123⁺ 99.8%
CD123⁺ 99.9%
CD123-PeCy7
AZA
AZA + NTD Tc
AZA+ CD123 CAR Tc
CD45⁺ 27.2%
CD45⁺ 26.4%
CD45⁺ 5.2%
CD45-APC-ef780
MOLM-13⁺ 99.7%
MOLM-13⁺ 98.6%
MOLM-13⁺ 69%
CD3-APC
CD123⁺ 99.1%
CD123⁺ 99.2%
CD123⁺ 100%
CD123-PeCy7
b
p<0.01
p=0.01
Residual hCD45⁺ Cells
Absolute cell count (cells/µl)
15000
10000
5000
0
☐ MOLM-13 + PBS (n=8)
■ MOLM-13 + Non-Transduced Tc (n=8)
■ MOLM-13 + Azacytidine (n=8)
■ MOLM-13 + Non-Transduced Tc + Azacytidine (n=8)
■ MOLM-13 + CD123 CAR Tc (n=8)
■ MOLM-13 + CD123 CAR Tc + Azacytidine (n=8)
c
p<0.01
p<0.03
Residual CD123⁺ Leukemia cells
Absolute cell count (cells/µl)
10000
8000
6000
4000
2000
0
☐ MOLM-13 + PBS (n=8)
■ MOLM-13 + Non-Transduced Tc (n=8)
■ MOLM-13 + Azacytidine (n=8)
■ MOLM-13 + Non-Transduced Tc + Azacytidine (n=8)
■ MOLM-13 + CD123 CAR Tc (n=8)
■ MOLM-13 + CD123 CAR Tc + Azacytidine (n=8)

Figure 4: AZA-pretreatment enhances anti-CD123 CAR T cell mediated AML elimination.

(a) Representative gating strategy used for flow cytometry based analysis of the bone marrow of mice treated with PBS, NTD Tc, anti-CD123 CAR Tc, AZA only, AZA with NTD Tc or AZA with anti-CD123 CAR Tc. Shown are total human CD45 cells, residual MOLM-13 leukemia cells and their CD123 expression as well as residual CD4/CD8 T cells.

Flow cytometric analysis depicting absolute counts (cells/μl) of residual **(b)** hCD45$^+$ and **(c)** CD123$^+$ leukemia cells in the BM of the various treatment groups. Data were pooled from 2 independent experiments. All graphed data are represented as mean ± SEM. *P*-values were calculated using 1-way ANOVA **(b, c)**.

Figure 5

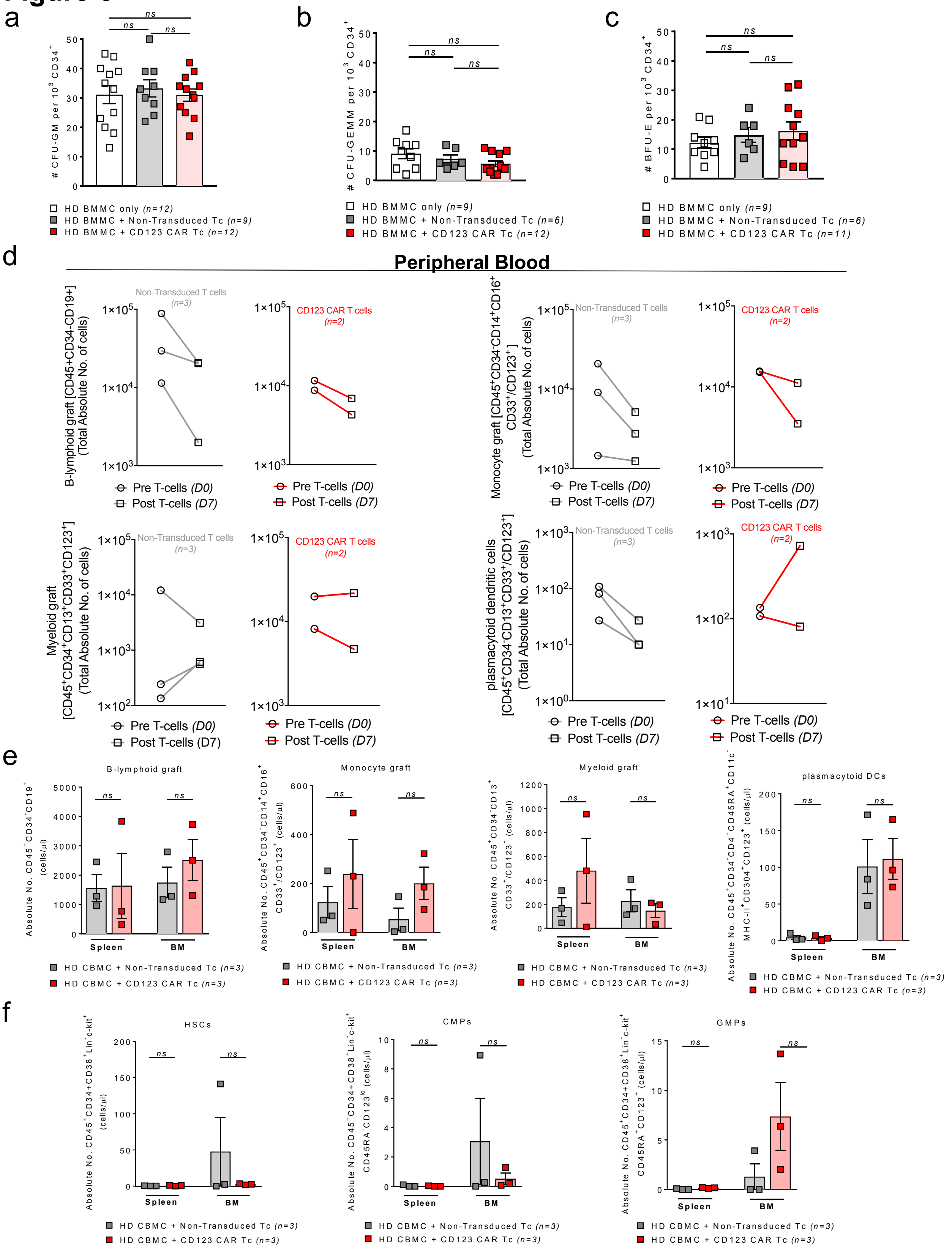
a
# CFU-GM per 10^3 CD34+
ns
ns
ns
☐ HD BMMC only (n=12)
▨ HD BMMC + Non-Transduced Tc (n=9)
🟥 HD BMMC + CD123 CAR Tc (n=12)
b
# CFU-GEMM per 10^3 CD34+
☐ HD BMMC only (n=9)
▨ HD BMMC + Non-Transduced Tc (n=6)
🟥 HD BMMC + CD123 CAR Tc (n=12)
c
# BFU-E per 10^3 CD34+
☐ HD BMMC only (n=9)
▨ HD BMMC + Non-Transduced Tc (n=6)
🟥 HD BMMC + CD123 CAR Tc (n=11)
d
Peripheral Blood
Non-Transduced T cells (n=3)
CD123 CAR T cells (n=2)
B-lymphoid graft [CD45+CD34-CD19+] (Total Absolute No. of cells)
Monocyte graft [CD45+CD34-CD14+CD16+ CD33+/CD123+] (Total Absolute No. of cells)
Myeloid graft [CD45+CD34+CD13+CD33+CD123+] (Total Absolute No. of cells)
plasmacytoid dendritic cells [CD45+CD34-CD13+CD33+/CD123+] (Total Absolute No. of cells)
Pre T-cells (D0)
Post T-cells (D7)
e
B-lymphoid graft
Monocyte graft
Myeloid graft
plasmacytoid DCs
Absolute No. CD45+CD34-CD19+ (cells/μl)
Absolute No. CD45+CD34-CD14+CD16+ CD33+/CD123+ (cells/μl)
Absolute No. CD45+CD34-CD13+ CD33+/CD123+ (cells/μl)
Absolute No. CD45+CD34-CD4+CD45RA+CD11c- MHC-II+CD304+CD123+ (cells/μl)
Spleen
BM
ns
▨ HD CBMC + Non-Transduced Tc (n=3)
🟥 HD CBMC + CD123 CAR Tc (n=3)
f
HSCs
CMPs
GMPs
Absolute No. CD45+CD34+CD38+Lin-c-kit+ (cells/μl)
Absolute No. CD45+CD34+CD38+Lin-c-kit+ CD45RA-CD123lo (cells/μl)
Absolute No. CD45+CD34+CD38+Lin-c-kit+ CD45RA+CD123+ (cells/μl)
Spleen
BM
ns
▨ HD CBMC + Non-Transduced Tc (n=3)
🟥 HD CBMC + CD123 CAR Tc (n=3)

Figure 5: The effect of anti-CD123 CAR T cells on normal hematopoietic progenitor cell development.

(a) CFU-GM, **(b)** CFU-GEMM, and **(c)** BFU-E colonies were scored using an inverted microscope following a 14-day culture in methocult supplemented with hSCF, IL-3, EPO, G-CSF, and GM-CSF. $CD34^+$ HD BMMC were first co-cultured in media only (untreated), with NTD T cells, or anti-CD123 CAR T cells at an E:T ratio of 1:1 for 6 hours before the cell suspension was transferred and plated in methocult. Colony numbers are represented per 1000 plated cells. Data was pooled from 3 different primary HD samples, each plated in at least duplicates.

(d) Flow cytometry based analysis depicting the total absolute cell numbers of B-lymphoid ($CD45^+CD34^-CD19^+$), Monocyte ($CD45^+CD34^-CD14^+CD16^+CD33^+/CD123^+$), Myeloid ($CD45^+CD34^-CD13^+CD33^+/CD123^+$), and plasmacytoid dendritic cell (pDC) ($CD45^+CD34^-CD4^+CD45RA^+CD11c^-MHC\text{-}II^+CD304^+CD123^+$) graft in the PB of HD $CD34^+$ cord blood (CBMC) engrafted mice pre- (day 0) and post-infusion (day 7) with $5x10^6$ anti-CD123 CAR or NTD T cells.

(e) Flow cytometry based analysis depicting the absolute cell numbers (cells/µl) of B-lymphoid, monocyte, myeloid, and pDCs in the spleen and BM of HD $CD34^+$ CBMC engrafted mice 14 days following infusion with $5x10^6$ anti-CD123 CAR or NTD T cells.

(f) Flow cytometry based analysis depicting the absolute cell numbers (cells/µl) of hematopoietic stem cells (HSCs), common myeloid progenitors (CMPs), and granulocytic macrophage progenitors (GMPs) in the BM of HD $CD34^+$ CBMC engrafted mice 14 days following infusion with $5x10^6$ anti-CD123 CAR or NTD T cells. All graphed data are represented as mean ± SEM. *P*-values were calculated using 1-way ANOVA **(a-c)** or unpaired Student's *t*-test (Mann-Whitney) **(d-f)**.

Figure 6

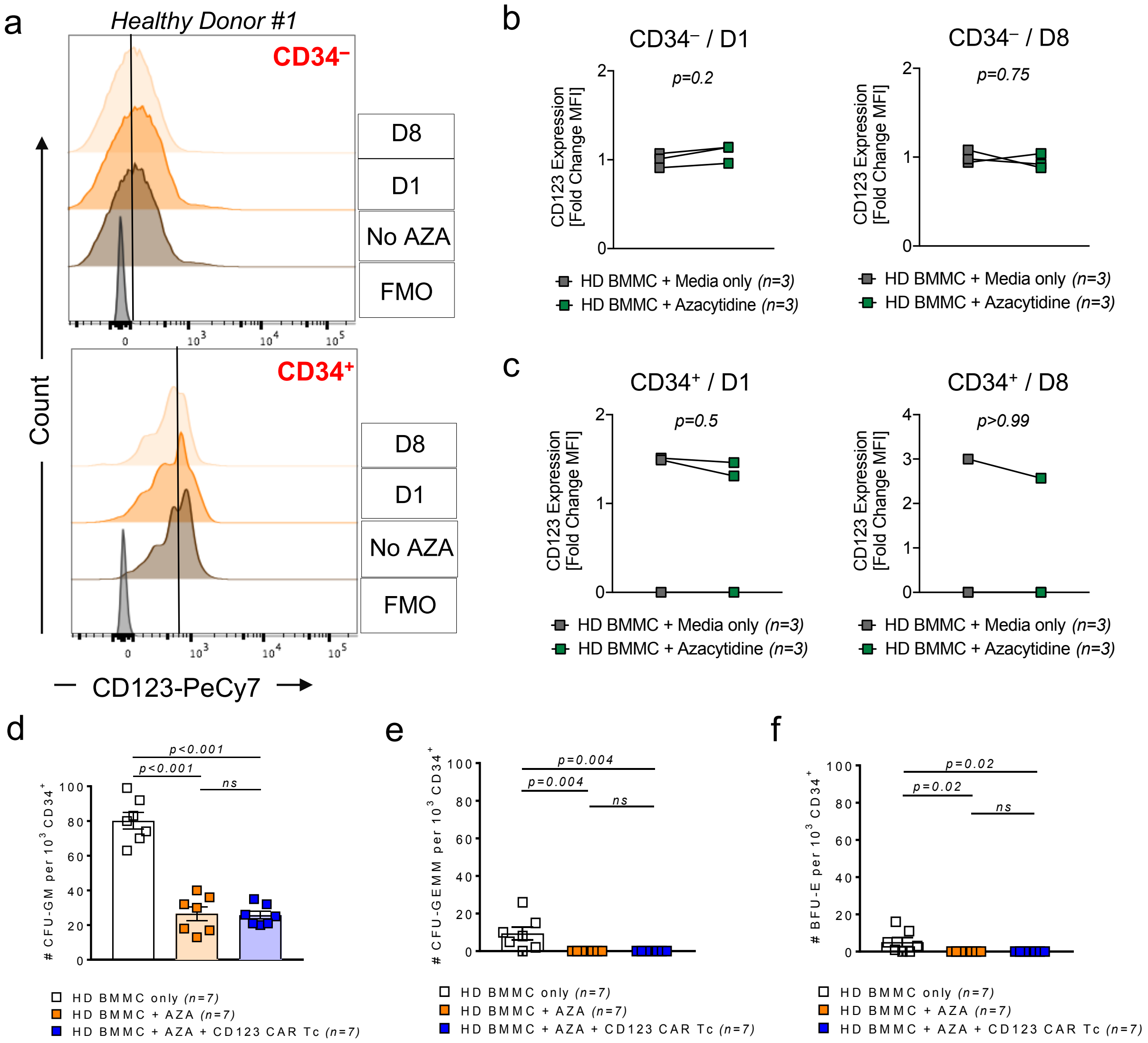
a
Healthy Donor #1
CD34⁻
D8
D1
No AZA
FMO
0
10³
10⁴
10⁵
CD34⁺
D8
D1
No AZA
FMO
Count
CD123-PeCy7
b
CD34⁻ / D1
p=0.2
CD123 Expression [Fold Change MFI]
HD BMMC + Media only (n=3)
HD BMMC + Azacytidine (n=3)
CD34⁻ / D8
p=0.75
c
CD34⁺ / D1
p=0.5
CD34⁺ / D8
p>0.99
d
# CFU-GM per 10³ CD34⁺
p<0.001
p<0.001
ns
HD BMMC only (n=7)
HD BMMC + AZA (n=7)
HD BMMC + AZA + CD123 CAR Tc (n=7)
e
# CFU-GEMM per 10³ CD34⁺
p=0.004
p=0.004
ns
f
# BFU-E per 10³ CD34⁺
p=0.02
p=0.02
ns

Figure 6: Impact of AZA pretreatment followed by anti-CD123 CAR T cell exposure on hematopoietic progenitor cell development.

(a) Representative flow cytometry based analysis of CD123 expression on $CD34^+$ and $CD34^-$ cells from a HD following culture in the absence or presence of 1µM AZA for 1 or 8 days. Histograms depict staining with anti-human CD123 Ab (PeCy7) compared to the FMO control. Scatter plots showing the expression of CD123 on primary HD **(b)** $CD34^-$ and **(c)** $CD34^+$ cells represented as a fold change of MFI with respect to MFI of untreated controls on day 1 and 8 following culture with 1µM AZA.

(d) CFU-GM, **(e)** CFU-GEMM, and **(f)** BFU-E colonies were scored using an inverted microscope following a 14-day co-culture in methocult supplemented with hSCF, IL-3, EPO, G-CSF, and GM-SCF. $CD34^+$ HD BMMC was first co-cultured in the presence or absence of 1µM AZA for 24 hours. The following day the cells were washed. Untreated cells were cultured in media only and treated cells were cultured in media only or with anti-CD123 CAR T cells at an E:T ratio of 1:1 for 6 hours. The cell suspension was subsequently transferred and plated in methocult. Colony numbers are represented per 1000 plated cells. Data were pooled from 3 primary HD samples, each plated in at least duplicates. All graphed data are represented as mean ± SEM. *P*-values were calculated using unpaired Student's *t*-test (Mann-Whitney) **(b, c)** and 1-way ANOVA **(d-f).**

Figure 7

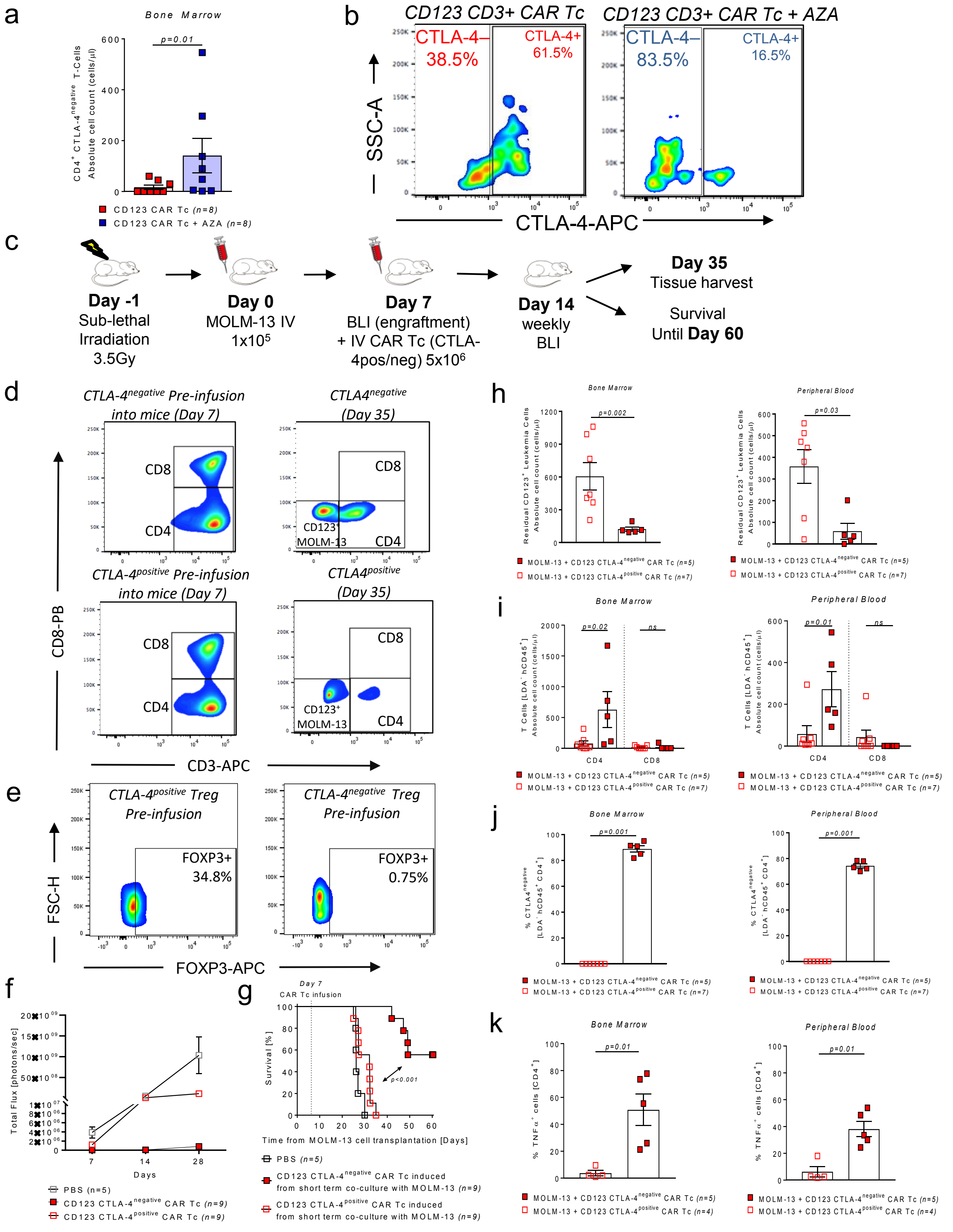
a
Bone Marrow
p=0.01
CD4+ CTLA-4negative T-Cells Absolute cell count (cells/µl)
600
400
200
0
CD123 CAR Tc (n=8)
CD123 CAR Tc + AZA (n=8)
b
CD123 CD3+ CAR Tc
CD123 CD3+ CAR Tc + AZA
CTLA-4–
38.5%
CTLA-4+
61.5%
CTLA-4–
83.5%
CTLA-4+
16.5%
SSC-A
CTLA-4-APC
c
Day -1
Sub-lethal Irradiation 3.5Gy
Day 0
MOLM-13 IV 1x10^5
Day 7
BLI (engraftment) + IV CAR Tc (CTLA-4pos/neg) 5x10^6
Day 14
weekly BLI
Day 35
Tissue harvest
Survival
Until Day 60
d
CTLA-4negative Pre-infusion into mice (Day 7)
CTLA4negative (Day 35)
CTLA-4positive Pre-infusion into mice (Day 7)
CTLA4positive (Day 35)
CD8
CD4
CD123+ MOLM-13
CD8-PB
CD3-APC
e
CTLA-4positive Treg Pre-infusion
FOXP3+
34.8%
CTLA-4negative Treg Pre-infusion
FOXP3+
0.75%
FSC-H
FOXP3-APC
f
Total Flux [photons/sec]
Days
7
14
28
PBS (n=5)
CD123 CTLA-4negative CAR Tc (n=9)
CD123 CTLA-4positive CAR Tc (n=9)
g
Day 7
CAR Tc infusion
Survival [%]
p<0.001
Time from MOLM-13 cell transplantation [Days]
PBS (n=5)
CD123 CTLA-4negative CAR Tc induced from short term co-culture with MOLM-13 (n=9)
CD123 CTLA-4positive CAR Tc induced from short term co-culture with MOLM-13 (n=9)
h
Bone Marrow
p=0.002
Peripheral Blood
p=0.03
Residual CD123+ Leukemia Cells Absolute cell count (cells/µl)
MOLM-13 + CD123 CTLA-4negative CAR Tc (n=5)
MOLM-13 + CD123 CTLA-4positive CAR Tc (n=7)
i
Bone Marrow
p=0.02
ns
Peripheral Blood
p=0.01
ns
T Cells [LDA- hCD45+] Absolute cell count (cells/µl)
CD4
CD8
MOLM-13 + CD123 CTLA-4negative CAR Tc (n=5)
MOLM-13 + CD123 CTLA-4positive CAR Tc (n=7)
j
Bone Marrow
p=0.001
Peripheral Blood
p=0.001
% CTLA4negative [LDA- hCD45+ CD4+]
MOLM-13 + CD123 CTLA-4negative CAR Tc (n=5)
MOLM-13 + CD123 CTLA-4positive CAR Tc (n=7)
k
Bone Marrow
p=0.01
Peripheral Blood
p=0.01
% TNFα+ cells [CD4+]
MOLM-13 + CD123 CTLA-4negative CAR Tc (n=5)
MOLM-13 + CD123 CTLA-4positive CAR Tc (n=4)

Figure 7: AZA pre-treatment induces a population of cytotoxic CTLA-4^{negative} anti-CD123 CAR T cells in MOLM-13 xenograft mice.

(a) Scatter plot demonstrating the residual CD4$^+$ CTLA-4^{negative} anti-CD123 CAR T cells isolated from the BM of MOLM-13 AML xenograft mice that were treated with anti-CD123 CAR T cells only, or with AZA and anti-CD123 CAR T cells. Data was pooled from 2 independent experiments.

(b) Representative flow cytometry gating used to evaluate CTLA-4 expression on pan (CD3$^+$) T cells from mice treated with anti-CD123 CAR T cells only (left panel), or AZA with anti-CD123 CAR T cells (right panel).

(c) Schematic diagram depicting sub-lethal irradiation (3.5Gy) of Rag2$^{-/-}$Il2rγ$^{-/-}$ mice on day -1 and subsequently injected via tail vein with 1x10^5 green fluorescent protein/luciferase$^+$ MOLM-13 cells on day 0. BLI was performed on day 7 to confirm and quantify engraftment and mice were randomized into treatment groups. Mice received either 5x10^6 CTLA-4^{negative} or CTLA-4^{positive} anti-CD123 CAR T cells intravenously on day 7, and mice were followed with BLI until day 28. Quantification of BLI signal was used as a surrogate measurement of AML burden. A cohort of mice from each treatment group was sacrificed on day 35 (28 days following CAR T cell infusion) for flow cytometry based analysis. The remaining mice were left until day 60 for survival analysis.

(d) Flow cytometry plots demonstrating the CD4$^+$ and CD8$^+$ phenotypic distribution of the CTLA-4^{negative} or CTLA-4^{positive} anti-CD123 CAR T cells pre-infusion into the mice versus on day 35 following infusion into the mice.

(e) Representative flow cytometry plots depicting Tregs (CD4$^+$CD25^{hi}CD127^{lo}FOXP3$^+$) in the sorted CTLA-4^{negative} or CTLA-4^{positive} anti-CD123 CAR T cells, before infusion into the mice.

(f) Summary BLI signals for each treatment group over time.

(g) Kaplan-Meier analysis of percentage survival for each treatment group. Attrition of mice was due to paralysis in hind legs or growth of subcutaneous tumors >2cm. Scatter plot depicting the absolute cell count of residual CD123$^+$ leukemia cells from live hCD45$^+$ cells in the **(h)** BM and PB of mice treated with CTLA-4^{negative} or CTLA-4^{positive} anti-CD123 CAR T cells. **(i)** Scatter plot depicting the absolute cell count of residual CD4$^+$ and CD8$^+$ T cells from live hCD45$^+$ cells in the BM and PB of mice treated with CTLA-4^{negative} or CTLA-4^{positive} anti-CD123 CAR T cells.

(j) Scatter plot depicting the percentage of CTLA-4^{negative} and the **(k)** percentage of TNF expression on CD4$^+$ T cells in the BM and PB of mice treated with CTLA-4^{negative} or CTLA-4^{positive} anti-CD123 CAR T cells. All graphed data, apart from survival analysis are represented as mean ± SEM. *P*-values were calculated using Mantel-Cox test (log-rank) **(g)** or unpaired Student's *t*-test (Mann-Whitney) **(f, h-k)**.

Figure 8

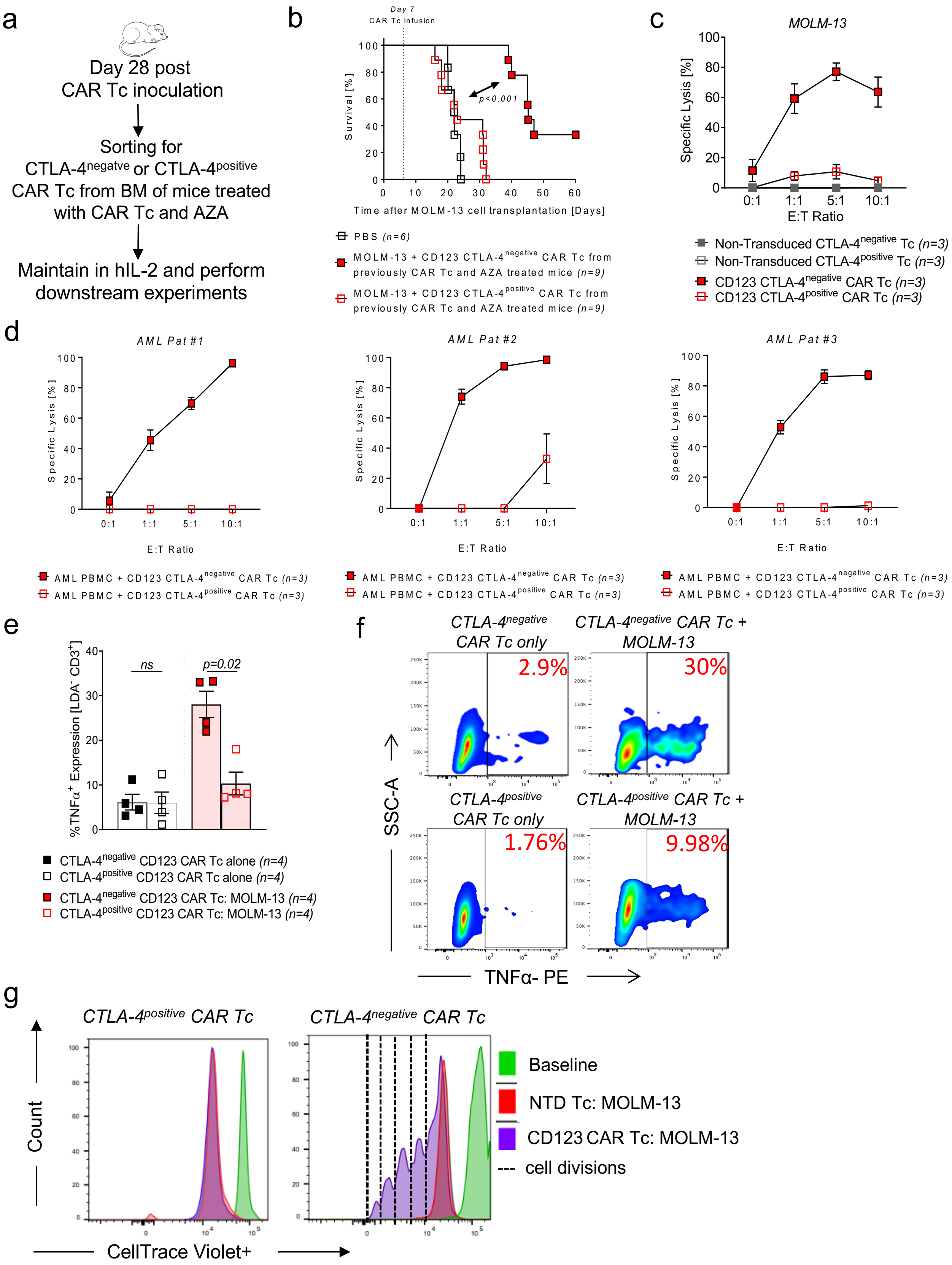
a
Day 28 post CAR Tc inoculation
Sorting for CTLA-4negatve or CTLA-4positive CAR Tc from BM of mice treated with CAR Tc and AZA
Maintain in hIL-2 and perform downstream experiments
b
Day 7 CAR Tc Infusion
Survival [%]
p<0.001
Time after MOLM-13 cell transplantation [Days]
PBS (n=6)
MOLM-13 + CD123 CTLA-4negative CAR Tc from previously CAR Tc and AZA treated mice (n=9)
MOLM-13 + CD123 CTLA-4positive CAR Tc from previously CAR Tc and AZA treated mice (n=9)
c
MOLM-13
Specific Lysis [%]
E:T Ratio
0:1
1:1
5:1
10:1
Non-Transduced CTLA-4negative Tc (n=3)
Non-Transduced CTLA-4positive Tc (n=3)
CD123 CTLA-4negative CAR Tc (n=3)
CD123 CTLA-4positive CAR Tc (n=3)
d
AML Pat #1
AML Pat #2
AML Pat #3
Specific Lysis [%]
E:T Ratio
AML PBMC + CD123 CTLA-4negative CAR Tc (n=3)
AML PBMC + CD123 CTLA-4positive CAR Tc (n=3)
e
%TNFα+ Expression [LDA- CD3+]
ns
p=0.02
CTLA-4negative CD123 CAR Tc alone (n=4)
CTLA-4positive CD123 CAR Tc alone (n=4)
CTLA-4negative CD123 CAR Tc: MOLM-13 (n=4)
CTLA-4positive CD123 CAR Tc: MOLM-13 (n=4)
f
CTLA-4negative CAR Tc only
CTLA-4negative CAR Tc + MOLM-13
CTLA-4positive CAR Tc only
CTLA-4positive CAR Tc + MOLM-13
2.9%
30%
1.76%
9.98%
SSC-A
TNFα- PE
g
CTLA-4positive CAR Tc
CTLA-4negative CAR Tc
Count
CellTrace Violet+
Baseline
NTD Tc: MOLM-13
CD123 CAR Tc: MOLM-13
--- cell divisions

Figure 8: Recall immunity and long term leukemia control.

(a) Schematic diagram depicting the isolation of residual anti-CD123 CAR T cells from the BM or mice 28 days post inoculation. Cells were flow sorted for CTLA-4^{negative} or CTLA-4^{positive} cells and maintained in low dose recombinant hIL-2 for 72h prior to usage in in vitro or in vivo experiments.

(b) Kaplan-Meier analysis of percentage survival for each treatment group. Secondary recipient mice were engrafted with 5x10^5 MOLM-13 Luc$^+$ cells on day 0. On Day 7, mice were randomly distributed and received either 100μl PBS, 2.5x10^6 CTLA-4^{positive} or CTLA-4^{negative} anti-CD123 CAR T cells isolated from primary engrafted mice. Attrition of mice was due to paralysis in hind legs or growth of subcutaneous tumors >2cm.

(c) Specific cytotoxicity of MOLM-13 following co-culture with NTD or anti-CD123 CTLA-4^{negative} or CTLA-4^{positive} T cells. The assay was performed in triplicate with a fixed number of target cells/well for all E:T ratios. In both cases, counting beads were used to quantify the absolute number of residual live target cells at the end of the co-culture. Residual live target cells were CellTrace violet$^+$ 7-AAD$^-$.

(d) Specific cytotoxicity of anti-CD123 CTLA-4^{positive} and CTLA-4^{negative} CAR T cells against 3 primary patient AML peripheral blood PBMCs with varying CD123$^+$ expression following a 16h co-incubation. The assay was performed in triplicate with a fixed number of target cells/well for all E:T ratios. In both cases, counting beads were used to quantify the absolute number of residual live target cells. Residual live target cells were CellTrace violet$^+$ 7-AAD$^-$.

(e) Scatter plot showing the percentage quantification of TNF from live CTLA-4^{negative} or CTLA-4^{positive} CD3$^+$ anti-CD123 CAR T cells following a 24h co-culture with media only or MOLM-13 cells.

(f) Representative flow cytometry plot from each condition from (e) is shown.

(g) Representative histograms depicting the proliferation of CTLA-4^{positive} (left panel) and CTLA-4^{negative} (right panel) CD123 CAR T cells or NTD T cells as examined by CellTrace violet dye dilution. Cells were co-cultured for 96 hours with MOLM-13 cells at an E:T ratio of 1:1. Each dotted line represents one cell division. All graphed data are represented as mean ± SEM. *P*-values were calculated using **(b)** Mantel-Cox test (log-rank) or unpaired Student's *t*-test (Mann-Whitney) **(e).**

Figure 9

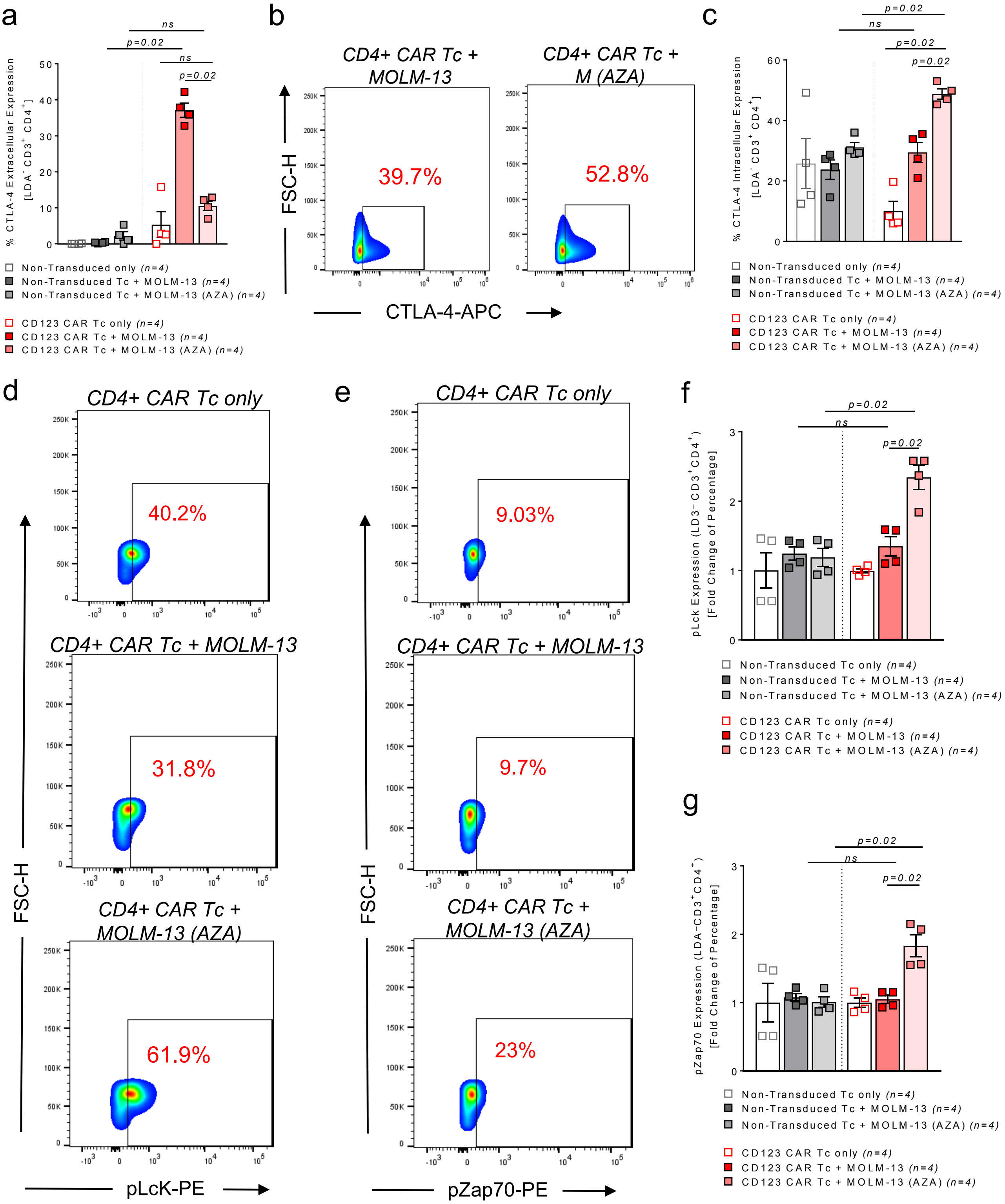
a
ns
p=0.02
ns
p=0.02
% CTLA-4 Extracellular Expression [LDA$^-$ CD3$^+$ CD4$^+$]
50
40
30
20
10
0
☐ Non-Transduced only (n=4)
■ Non-Transduced Tc + MOLM-13 (n=4)
▨ Non-Transduced Tc + MOLM-13 (AZA) (n=4)
☐ CD123 CAR Tc only (n=4)
■ CD123 CAR Tc + MOLM-13 (n=4)
▨ CD123 CAR Tc + MOLM-13 (AZA) (n=4)
b
CD4+ CAR Tc + MOLM-13
CD4+ CAR Tc + M (AZA)
39.7%
52.8%
FSC-H
CTLA-4-APC
c
p=0.02
ns
p=0.02
p=0.02
% CTLA-4 Intracellular Expression [LDA$^-$ CD3$^+$ CD4$^+$]
60
40
20
0
☐ Non-Transduced only (n=4)
■ Non-Transduced Tc + MOLM-13 (n=4)
▨ Non-Transduced Tc + MOLM-13 (AZA) (n=4)
☐ CD123 CAR Tc only (n=4)
■ CD123 CAR Tc + MOLM-13 (n=4)
▨ CD123 CAR Tc + MOLM-13 (AZA) (n=4)
d
CD4+ CAR Tc only
40.2%
CD4+ CAR Tc + MOLM-13
31.8%
CD4+ CAR Tc + MOLM-13 (AZA)
61.9%
FSC-H
pLcK-PE
e
CD4+ CAR Tc only
9.03%
CD4+ CAR Tc + MOLM-13
9.7%
CD4+ CAR Tc + MOLM-13 (AZA)
23%
FSC-H
pZap70-PE
f
p=0.02
ns
p=0.02
pLck Expression (LD3$^-$ CD3$^+$CD4$^+$) [Fold Change of Percentage]
3
2
1
0
☐ Non-Transduced Tc only (n=4)
■ Non-Transduced Tc + MOLM-13 (n=4)
▨ Non-Transduced Tc + MOLM-13 (AZA) (n=4)
☐ CD123 CAR Tc only (n=4)
■ CD123 CAR Tc + MOLM-13 (n=4)
▨ CD123 CAR Tc + MOLM-13 (AZA) (n=4)
g
p=0.02
ns
p=0.02
pZap70 Expression (LDA$^-$CD3$^+$CD4$^+$) [Fold Change of Percentage]
3
2
1
0
☐ Non-Transduced Tc only (n=4)
■ Non-Transduced Tc + MOLM-13 (n=4)
▨ Non-Transduced Tc + MOLM-13 (AZA) (n=4)
☐ CD123 CAR Tc only (n=4)
■ CD123 CAR Tc + MOLM-13 (n=4)
▨ CD123 CAR Tc + MOLM-13 (AZA) (n=4)

Figure 9: AZA pre-treatment of the leukemia cells promotes intracellular retention of CTLA-4 while enhancing Lck and ZAP70 signaling in the anti-CD123 CAR T cells.

(a) Scatter plot showing the extracellular expression levels of CTLA-4 in $CD4^+$ anti-CD123 CAR or NTD T cells following a 96h co-culture in the presence of media only, naive MOLM-13 cells, or MOLM-13 cells pre-treated with 1μM AZA. Data was pooled from 4 independent experiments.

(b) Representative flow cytometry plot depicting intracellular levels of CTLA-4 in $CD4^+$ anti-CD123 CAR or NTD T cells.

(c) Scatter plot showing the intracellular expression levels of CTLA-4 in $CD4^+$ anti-CD123 CAR or NTD T cells following a 96h co-culture in the presence of media only, naive MOLM-13 cells, or MOLM-13 cells pre-treated with 1μM AZA. Since raw intracellular expression levels could include surface levels of CTLA-4, extracellular and intracellular staining from the same sample were set up side by side and analyzed. The scatter plot depicts the difference between intracellular levels with extracellular levels to give the 'true' intracellular expression of CTLA-4 in the cells. Data was pooled from 4 independent experiments.

(d) Representative flow cytometry plot depicting the phosphorylated level of LcK (pLck) in $CD4^+$ anti-CD123 CAR T cells that have been exposed for 96h to media only, untreated MOLM-13 cells, or MOLM-13 cells pre-treated with 1μM AZA.

(e) Representative flow cytometry plot depicting the phosphorylated level of Zap70 (pZap70) in $CD4^+$ anti-CD123 CAR T cells that have been exposed for 96h to media only, untreated MOLM-13 cells, or MOLM-13 cells pre-treated with 1μM AZA.

(f) Scatter plot depicting the fold change in percentage expression of pLcK in $CD4^+$ anti-CD123 CAR T cells. Data were pooled from 4 independent experiments.

(g) Scatter plot depicting the fold change in percentage expression of pZap70 in $CD4^+$ anti-CD123 CAR T cells. Data were pooled from 4 independent experiments. All graphed data are represented as mean ± SEM. *P*-values were unpaired Student's *t*-test (Mann-Whitney).

Supplementary Materials and Methods

Fig. S1: Phenotypic analysis of CD123 expression on primary healthy donor bone marrow cells

Fig. S2: CD123 is overexpressed on primary AML while low to absent on healthy donor cells

Fig. S3: Third-generation anti-CD123 CAR T cell construct and the phenotypic evaluation of the CAR T cells prior to functional analysis

Fig. S4: *In vitro* effector functions of anti-CD123 CAR T cells against AML cell lines

Fig. S5: Third-generation anti-CD123 CAR T cells recognize and eliminate $CD123^+$ AML cells *in vitro*.

Fig. S6: Treatment of AML with azacitidine and CD123 CAR T cells does not cause epithelial tissue damage

Fig. S7: Analysis of residual T cells and their expression for exhaustion markers in the bone marrow of MOLM-13 AML xenograft mice

Fig. S8: Analysis of residual T cells and their expression for exhaustion markers in the peripheral blood of MOLM-13 AML xenograft mice

Fig. S9: Analysis of residual $CD4^+$ and $CD8^+$ T cell subsets in the bone marrow and peripheral blood of MOLM-13 AML xenograft mice

Fig. S10: Analysis of CTLA-$4^{negative}$ and TNF expression on residual $CD8^+$ T cells in the bone marrow and peripheral blood of MOLM-13 AML xenograft mice treated with CTLA-$4^{negative}$ or CTLA-$4^{positive}$ anti-CD123 CAR T cells

Fig. S11: Assessment of the phosphorylation of intracellular Lck and Zap70 in CD8+ anti-CD123 CAR T cells in the presence of MOLM-13 AML cells.

Table S1: AML Patient Characteristics (SAHMRI, Adelaide, Australia)
Table S2: AML Patient Characteristics (University Medical Clinic, Freiburg, Germany)
Table S3: Antibodies for flow cytometry

Supplementary Figure 1

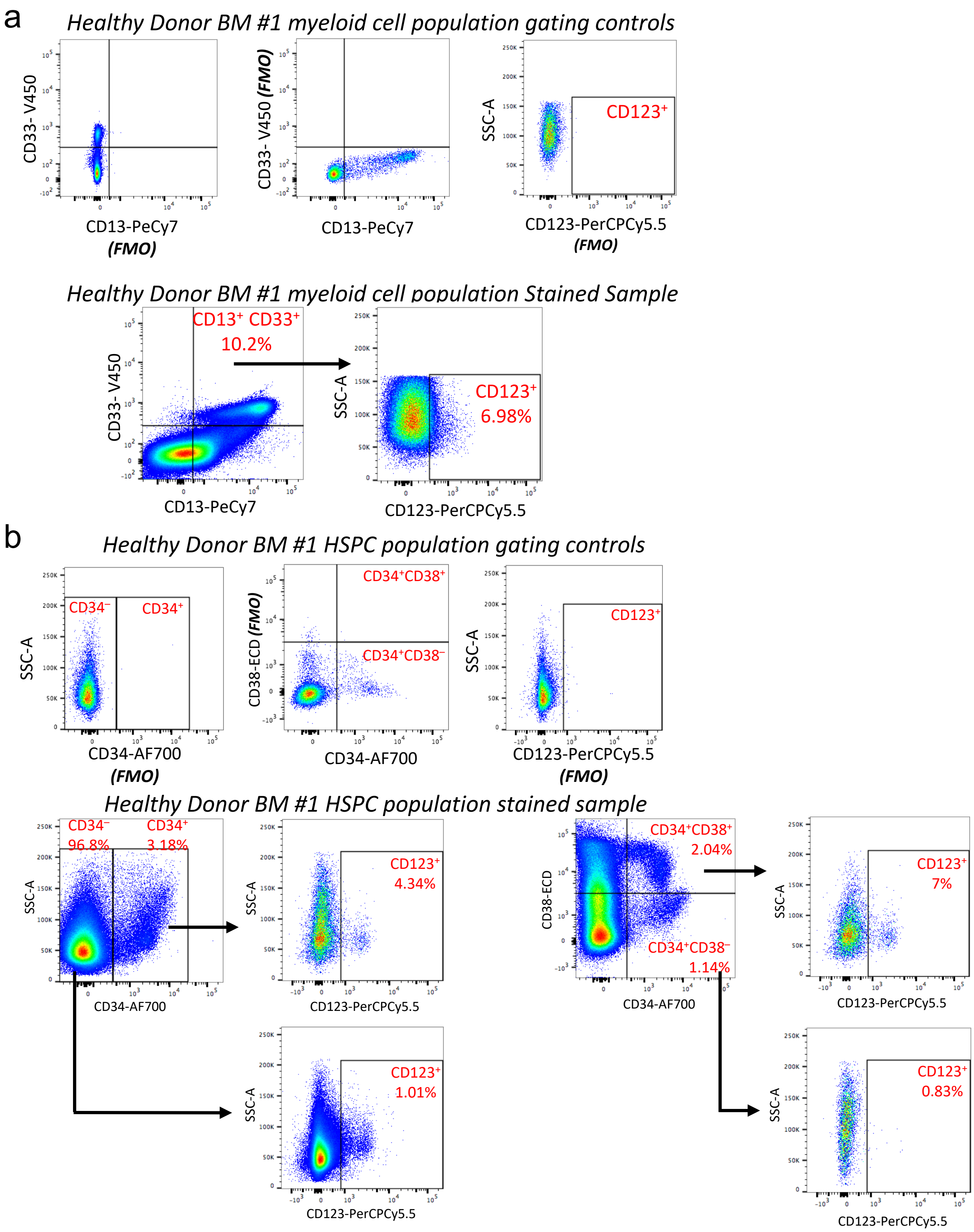

Supplementary Figure 1: Phenotypic analysis of CD123 expression on primary healthy donor bone marrow cells

(a) Representative flow cytometry gating strategy, including fluorescence minus one (FMO) controls, used to evaluate CD123 expression on bulk HD myeloid cells.

(b) Representative flow cytometry gating strategy, including fluorescence minus one (FMO) controls, used to evaluate CD123 expression on HD stem and progenitor cell populations.

Supplementary Figure 2

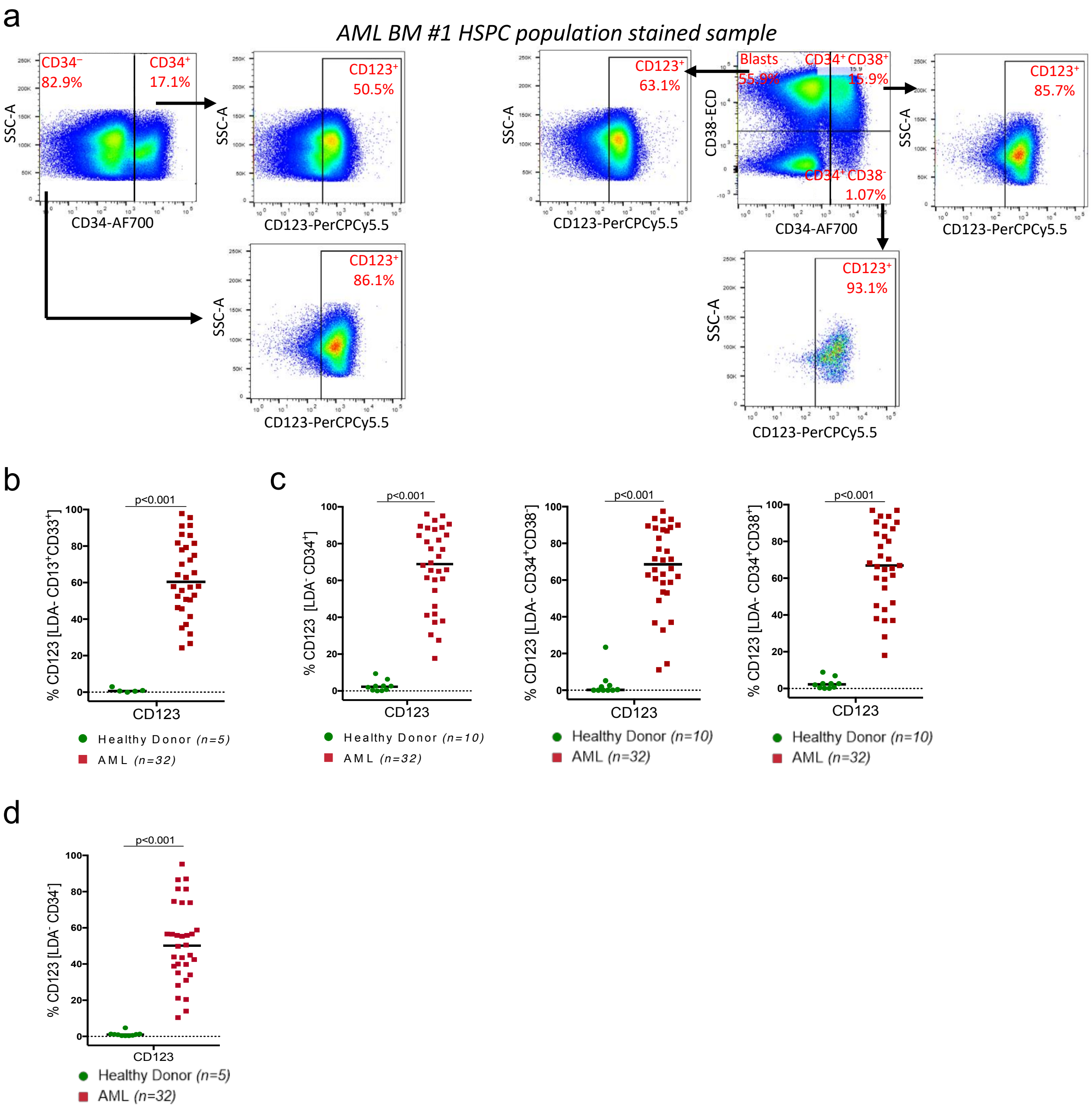

Supplementary Figure 2: CD123 is overexpressed on primary AML while low to absent on healthy donor cells.

(a) Representative flow cytometry gating strategy used to evaluate CD123 expression on AML stem and progenitor cells. Primitive and differentiated cell populations from relapsed/refractory AML patient BMMNC samples at diagnosis were analyzed and compared to HD BMMNC samples for CD123 expression on **(b)** $CD13^{+}CD33^{+}$ bulk myeloid cells, **(c)** $CD34^{+}$ bulk primitive cells (left panel), $CD34^{+}CD38^{-}$ progenitor cells (middle panel), $CD34^{+}CD38^{+}$ HSC/MPP populations (right panel), and **(d)** $CD34^{-}$ bulk mature/differentiated cells by flow cytometry. Gates were set on bulk AML or HD cells (SSC v FSC), following this; viable single cells were defined based on FSC-A v FSC-H and exclusion of dead cells by live dead aqua viability stain (LDA^{-}). Data are represented as individual values with bars representing the median value of each group. *P*-values were calculated using unpaired Student's *t*-test (Mann-Whitney).

Supplementary Figure 3

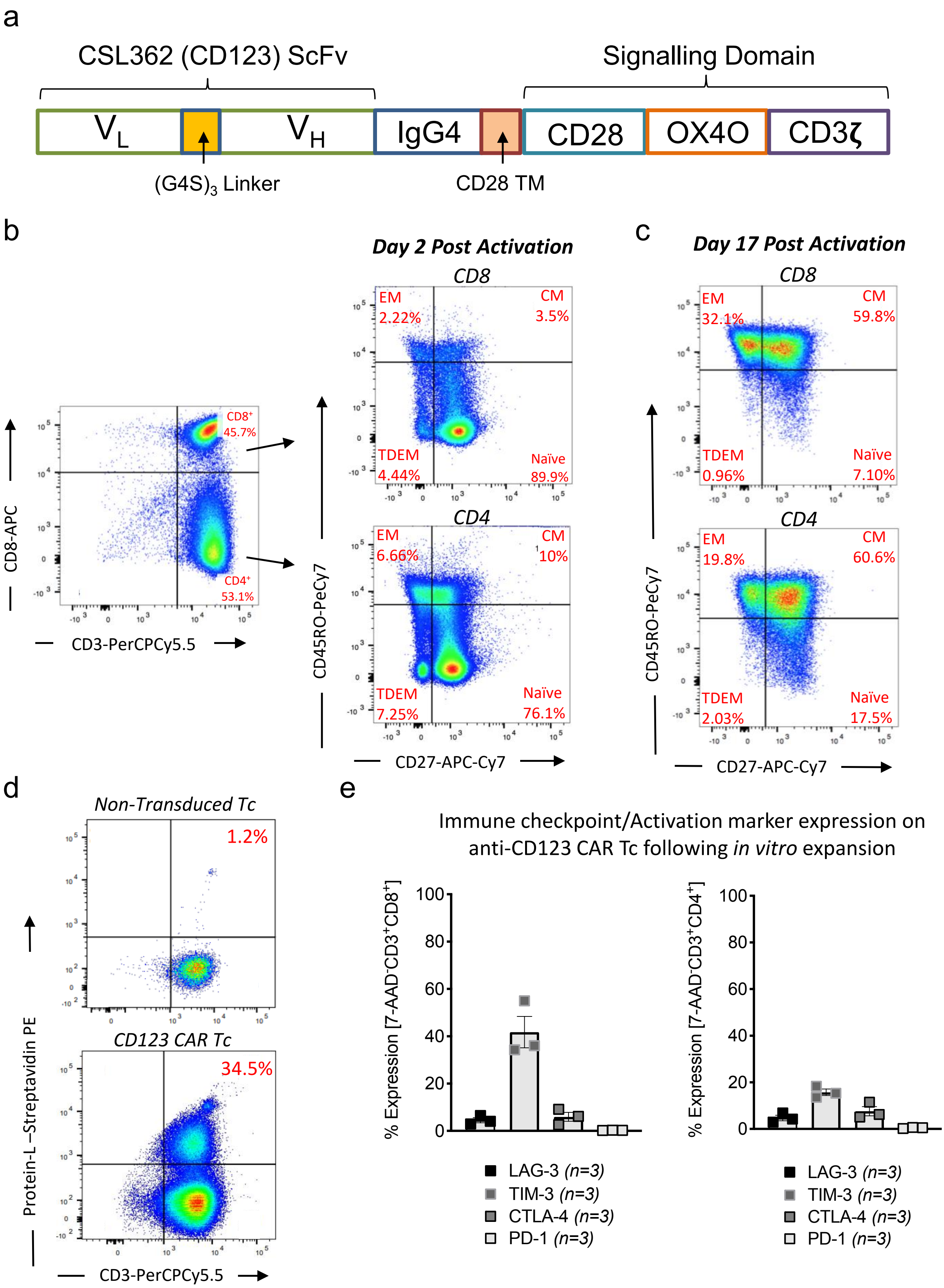

Supplementary Figure 3: Third-generation anti-CD123 CAR T cell construct and the phenotypic evaluation of the CAR T cells prior to functional analysis.

(a) Schematic of the third-generation CAR construct. The single chain variable fragment (scFv) was derived from the fully humanized CD123 (CSL362) neutralizing antibody connected with a $(G4S)_3$ linker. The scFv was fused to an IgG4 hinge spacer, CD28 transmembrane domain, and intracellular signaling module. The intracellular signaling module consists of two co-stimulatory molecules: CD28 and OX4O which are attached to the CD3ζ chain.

(b) Representative flow cytometry dot plots demonstrating the phenotype of healthy donor derived T cells prior to activation with CD3/CD28 dynabeads and CD123 CAR lentiviral transduction. The majority of T cells from healthy donors were $CD4^+$ phenotype (left panel). The majority of $CD8^+$ (right top panel) and $CD4^+$ (right lower panel) T cells possess a naive phenotype prior to activation. However, a small portion of cells are phenotypically central memory (CM), effector memory (EM) or terminally differentiated effector memory (TDEM).

(c) Representative flow cytometry dot plots demonstrating the change in phenotype of healthy donor derived T cells following 17 days of activation and expansion, and post CD123 CAR lentivirus transduction. By day 17 the majority of $CD8^+$ (top panel) and $CD4^+$ T cells (bottom panel) possess a CM or EM phenotype.

(d) Representative flow cytometry dot plot showing the expression of $CD3^+$ T cells transduced with Protein-L on day 5 post transduction. Cells that are double positive for CD3 and Protein-L successfully harbor the CD123 CAR. Non-transduced (NTD) T cells are included for comparison. Cells were then enriched for $CD3^+$ Protein-L^+ by flow sorting prior to functional testing.

(e) Scatter plots depicting the expression of exhaustion markers: LAG-3, TIM-3, CTLA-4, and PD-1 on CD8 T cells (left panel) and CD4 T cells (right panel) 17 days following activation and pre-exposure to $CD123^+$ target cells. The data is pooled from 3 independent transductions and are presented as mean ± SEM.

Supplementary Figure 4

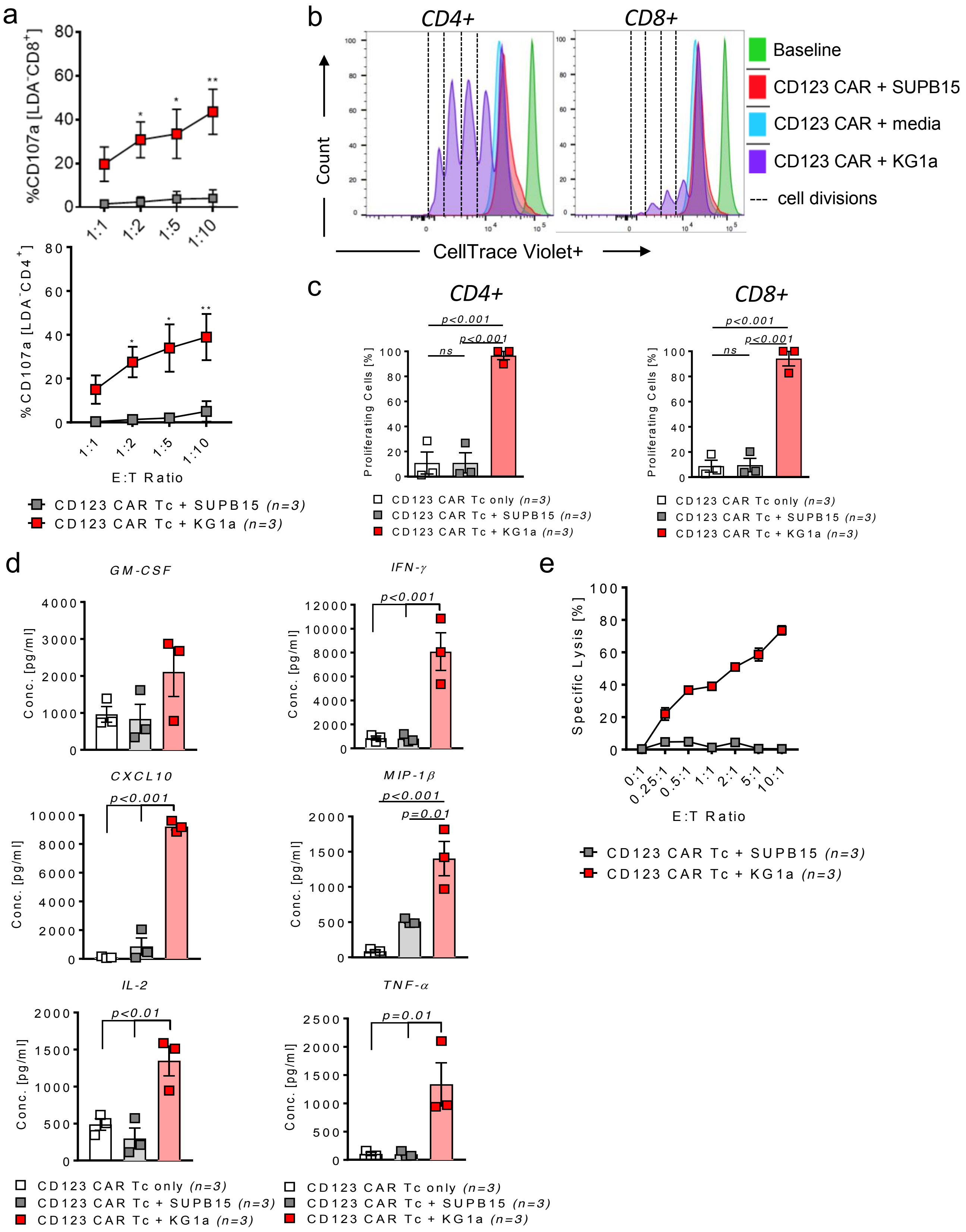

Supplementary Figure 4: *In vitro* effector functions of anti-CD123 CAR T cells against AML cell lines.

CD123 CD8$^+$ (top panel) and CD4$^+$ (bottom panel) CAR T cells were co-cultured for 4 hours with KG1a (CD123$^+$) or SUPB15 (CD123$^-$) cells at different E:T ratios and analyzed for surface CD107a expression. Data is pooled from 3 independent experiments, each plated in duplicate. **(b)** Representative histograms depicting the proliferation of CD8$^+$ (left panel) and CD4$^+$ (right panel) anti-CD123 CAR T cells examined by CellTrace^{TM} violet dye dilution following 96 hours of co-culture with media (untreated), KG1a or SUPB15 cells at an E:T ratio of 1:1. Each dotted line represents one cell division. **(c)** Scatter plot graphs denoting the total proliferating CD8$^+$ and CD4$^+$ CAR T cells following the 96-hour co-culture with media, KG1a or SUPB15 cells. **(d)** Atni-CD123 CAR T cells were co-cultured with media only (untreated), KG1a or SUPB15 cells at an E:T ratio of 10:1 for 24h. The supernatant was analyzed and quantified for the release of various cytokines. The cytokines/chemokines with major differences between each treatment group are depicted. **(e)** Specific cytotoxicity of anti-CD123 CAR T cells against KG1a or SUPB15 cells (CellTrace^{TM} violet labelled) by flow cytometric analysis following a 16h co-incubation. Assay was performed in triplicate with a fixed number of target cells/well for all E:T ratios. Counting beads were used to quantify the absolute number of residual live target cells at the end of the co-culture. Residual live target cells were CellTrace violet$^+$ 7-AAD$^-$. All graphed data is presented as mean ± SEM. *P*-values were calculated using 1-way ANOVA.

Supplementary Figure 5

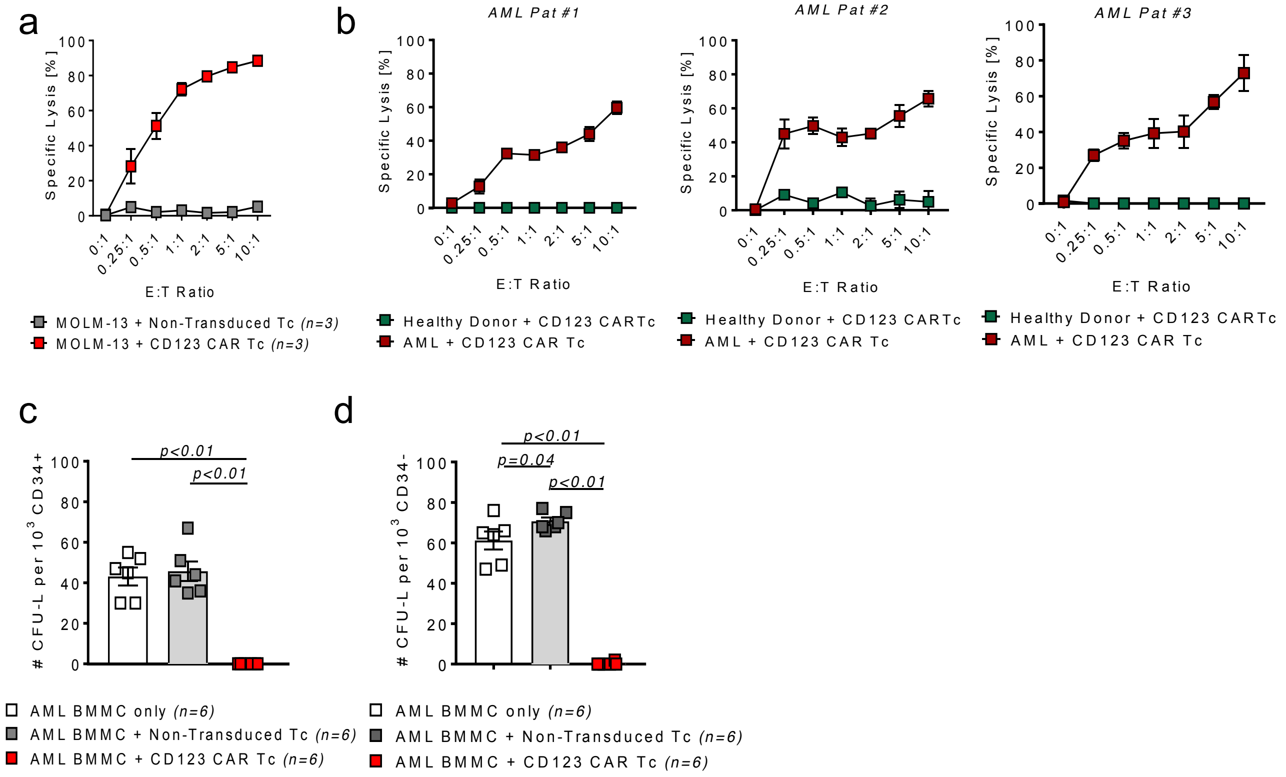

Supplementary Figure 5: Third-generation anti-CD123 CAR T cells recognize and eliminate CD123$^+$ AML cells *in vitro*.

(a) Specific cytotoxicity of anti-CD123 CAR T cells or NTD T cells against CD123$^+$ MOLM-13 cells (CellTrace violet labelled) by flow cytometric analysis following a 16h co-incubation. **(b)** Specific cytotoxicity of anti-CD123 CAR T cells against 3 patient primary AML bone marrow cells with varying CD123$^+$ expression or healthy donor (HD) bone marrow cells (CellTrace violet labelled) by flow cytometry based analysis following a 16h co-incubation. In both cases, the assays were performed in triplicate with a fixed number of target cells/well for all E:T ratios. Counting beads were used to quantify the absolute number of residual live target cells at the end of the co-culture. Residual live target cells were CellTrace violet$^+$ 7-AAD$^-$. **(c)** CD34$^+$ or **(d)** CD34$^-$ cells were immunomagnetically selected and co-cultured in media only (untreated), with anti-CD123 CAR T cells or NTD T cells for 6 hours at an E:T ratio of 10:1. The cells were subsequently plated in semisolid methylcellulose progenitor media, cultured for 14 days, and scored using an inverted microscope for the presence of leukemia colony-forming units (CFU-L). The experiment was performed using 3 primary AML patient samples, each plated in duplicate. Colony numbers are represented per 1000 plated cells. All graphed data are represented as mean values ± SEM. *P*-values were calculated with 1-way ANOVA.

Supplementary Figure 6

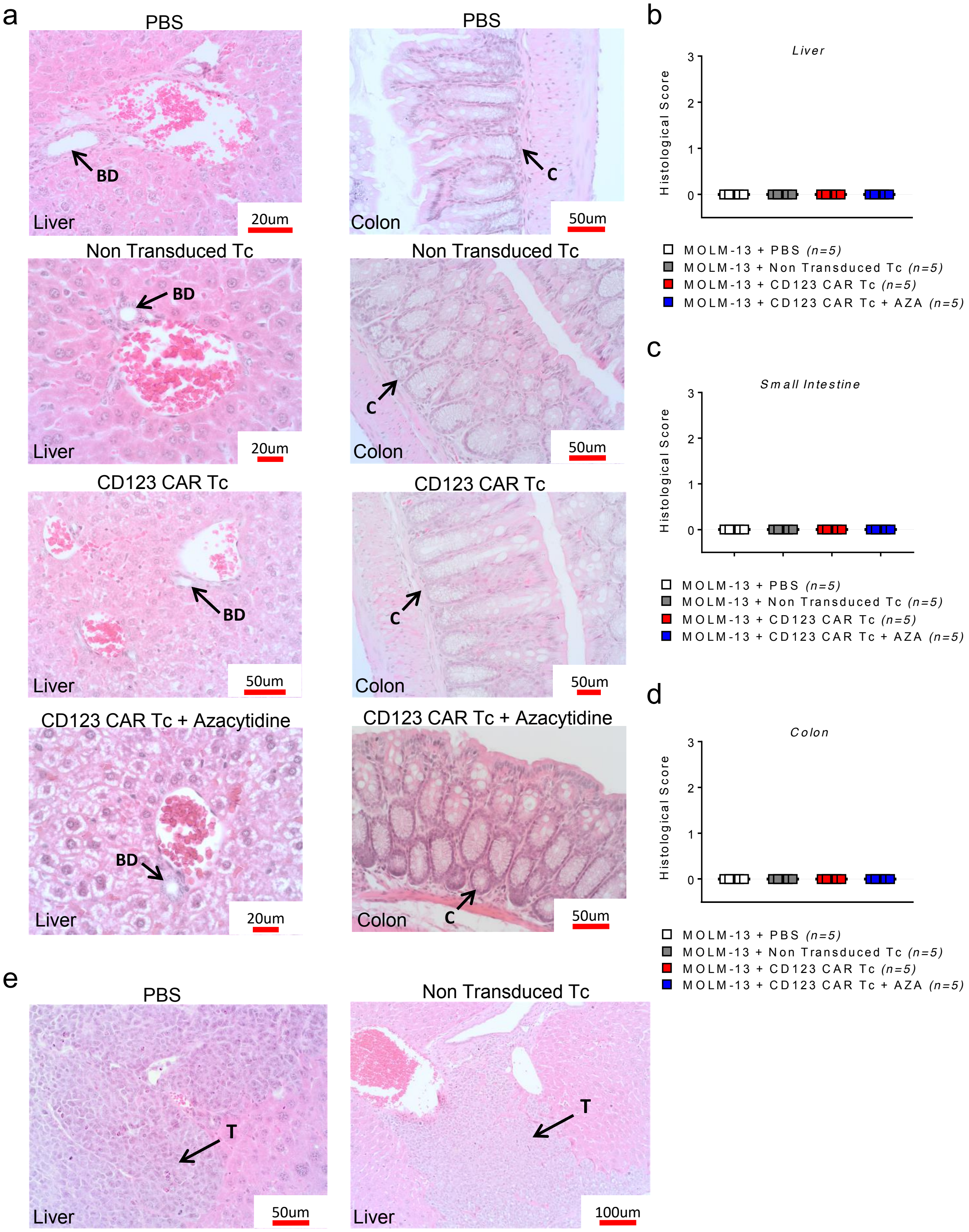
a
PBS
BD
Liver
20um
PBS
C
Colon
50um
Non Transduced Tc
BD
Liver
20um
Non Transduced Tc
C
Colon
50um
CD123 CAR Tc
BD
Liver
50um
CD123 CAR Tc
C
Colon
50um
CD123 CAR Tc + Azacytidine
BD
Liver
20um
CD123 CAR Tc + Azacytidine
C
Colon
50um
b
Liver
Histological Score
0
1
2
3
☐ MOLM-13 + PBS (n=5)
▨ MOLM-13 + Non Transduced Tc (n=5)
🟥 MOLM-13 + CD123 CAR Tc (n=5)
🟦 MOLM-13 + CD123 CAR Tc + AZA (n=5)
c
Small Intestine
Histological Score
0
1
2
3
☐ MOLM-13 + PBS (n=5)
▨ MOLM-13 + Non Transduced Tc (n=5)
🟥 MOLM-13 + CD123 CAR Tc (n=5)
🟦 MOLM-13 + CD123 CAR Tc + AZA (n=5)
d
Colon
Histological Score
0
1
2
3
☐ MOLM-13 + PBS (n=5)
▨ MOLM-13 + Non Transduced Tc (n=5)
🟥 MOLM-13 + CD123 CAR Tc (n=5)
🟦 MOLM-13 + CD123 CAR Tc + AZA (n=5)
e
PBS
T
Liver
50um
Non Transduced Tc
T
Liver
100um

Supplementary Figure 6: Treatment of AML with azacitidine and anti-CD123 CAR T cells does not cause epithelial tissue damage.

(a) Representative hematoxylin and eosin (H&E) staining of liver and colon tissues of MOLM-13 engrafted Rag2$^{-/-}$Il2rγ$^{-/-}$ mice treated with PBS, 5x10^{6} NTD T cells, 5x10^{6} CD123 anti-CAR T cells, or AZA with 5x10^{6} anti-CD123 CAR T cells to detect the presence of epithelial tissue damage. Images were taken at magnifications: 100x, 200x, 400x (represented on the scale bar as 20µm, 50µm, 100µm).

(b-d) Liver, small intestine, and colon tissues of PBS, NTD T cells, anti-CD123 CAR T cells or AZA with anti-CD123 CAR T cells were scored for degree of tissue damage and quantified. Data were pooled from 2 independent experiments.

(e) Representative H&E staining of liver tissue from MOLM-13 engrafted Rag2$^{-/-}$Il2rγ$^{-/-}$ mice treated with PBS or NTD T cells. Images show tumor cell infiltration in the liver tissues. Images were taken at a magnifications 200x and 400x (represented on the scale bar as 50µm and 100µm). Abbreviations: *BD*: Biliary duct- without intraepithelial lymphocytic infiltration and without bile duct destruction. *C*: crypt- no apoptosis within the epithelium of the crypt base and without crypt destruction. *T*: tumor- infiltration of tumor cells with undifferentiated phenotype.

Supplementary Figure 7

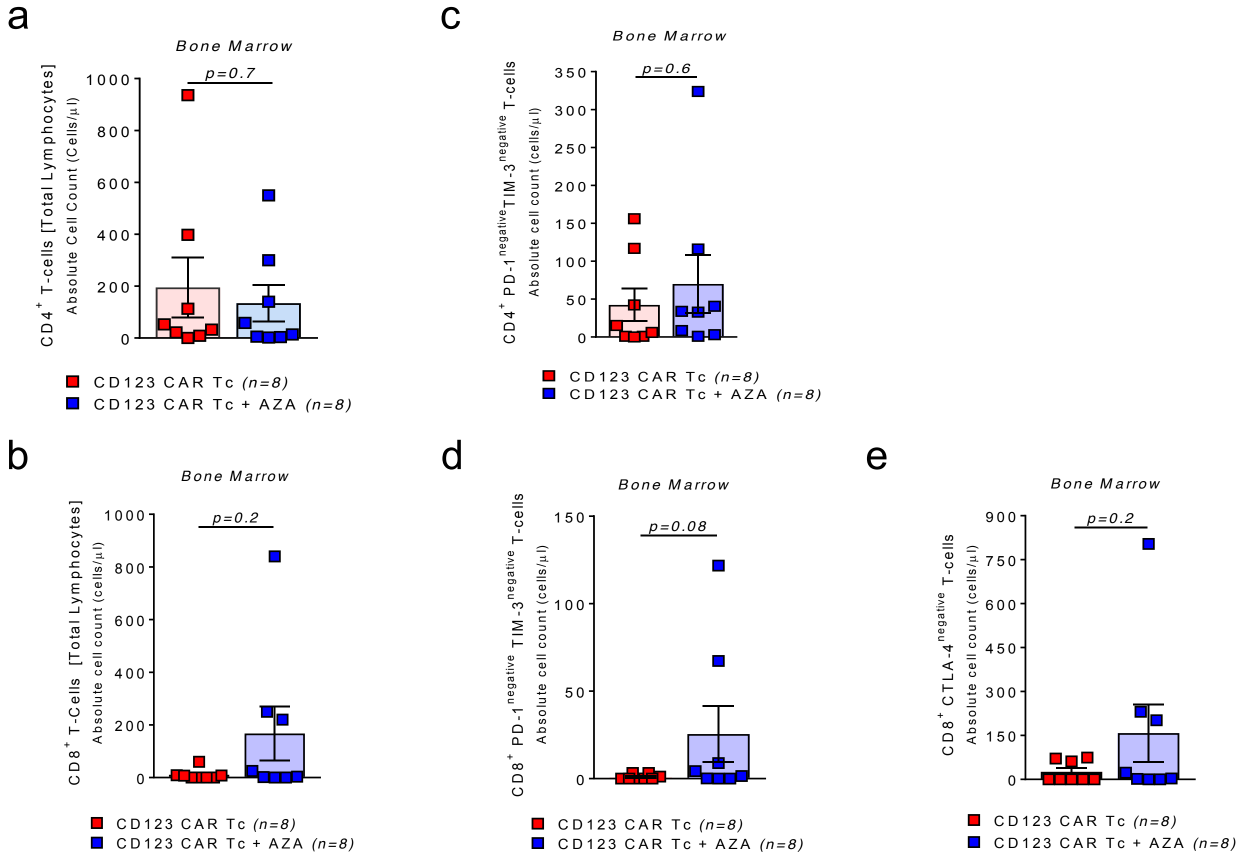

Supplementary Figure 7: Analysis of residual T cells and their expression for exhaustion markers in the bone marrow of MOLM-13 AML xenograft mice.

(a) Scatter plot graph depicting the residual CD4$^+$ T cells in the mice treated with anti-CD123 CAR T cells only versus the mice treated with AZA and anti-CD123 CAR T cells. **(b)** Scatter plot graph depicting the residual CD8$^+$ T cells in the mice treated with anti-CD123 CAR T cells only versus the mice treated with AZA and anti-CD123 CAR T cells. Scatter plot graphs depicting the expression of residual CD4$^+$ T cells from mice treated with anti-CD123 CAR T cell only versus AZA and anti-CD123 CAR T cells that were **(c)** PD-1^{negative} TIM-3^{negative}. Scatter plot graphs depicting the expression of residual CD8$^+$ T cells from mice treated with CD123 CAR T cell only versus AZA and anti-CD123 CAR T cells that were **(d)** PD-1^{negative} TIM-3^{negative} and **(e)** CTLA-4^{negative}. All data were pooled from 2 independent experiments and presented as mean absolute cell count ± SEM. *P*-values were calculated using unpaired Student's *t*-test (Mann-Whitney).

Supplementary Figure 8

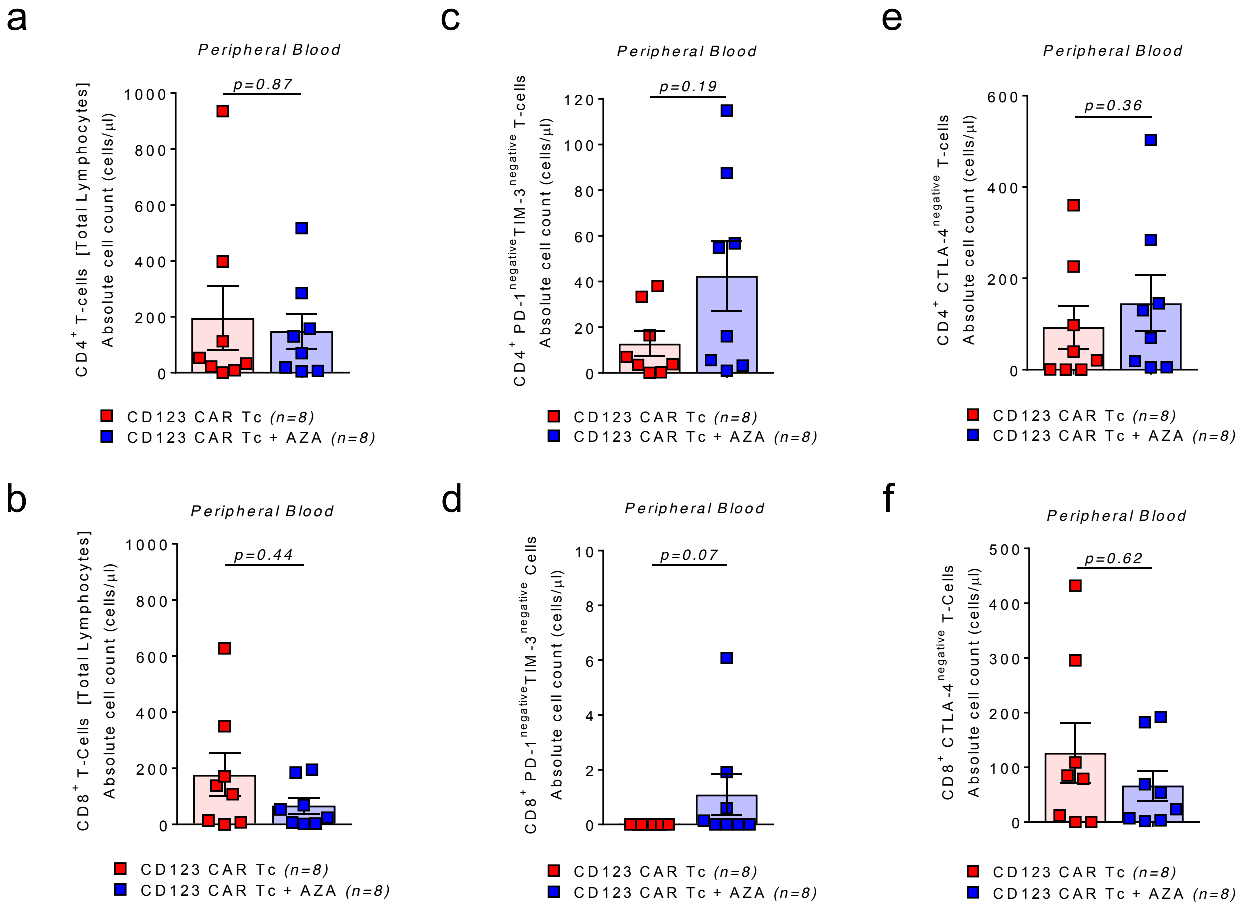

Supplementary Figure 8: Analysis of residual T cells and their expression for exhaustion markers in the peripheral blood of MOLM-13 AML xenograft mice.

(a) Scatter plot graph depicting the residual CD4$^+$ T cells in the mice treated with anti-CD123 CAR T cells only versus the mice treated with AZA and anti-CD123 CAR T cells. **(b)** Scatter plot graph depicting the residual CD8$^+$ T cells in the mice treated with anti-CD123 CAR T cells only versus the mice treated with AZA and anti-CD123 CAR T cells. Scatter plot graphs depicting the expression of residual CD4$^+$ T cells from mice treated with anti-CD123 CAR T cell only versus AZA and anti-CD123 CAR T cells that were **(c)** PD-1^{negative} TIM-3^{negative}. Scatter plot graphs depicting the expression of residual CD8$^+$ T cells from mice treated with anti-CD123 CAR T cell only versus AZA and anti-CD123 CAR T cells that were **(d)** PD-1^{negative} TIM-3^{negative}. Scatter plot graphs depicting the expression of residual CD4$^+$ T cells from mice treated with anti-CD123 CAR T cell only versus AZA and anti-CD123 CAR T cells that were **(e)** CTLA-4^{negative}. Scatter plot graphs depicting the expression of residual CD8$^+$ T cells from mice treated with anti-CD123 CAR T cell only versus AZA and anti-CD123 CAR T cells that were **(f)** CTLA-4^{negative}. All data were pooled from 2 independent experiments and presented as mean absolute cell count ± SEM. *P*-values were calculated using unpaired Student's *t*-test (Mann-Whitney).

Supplementary Figure 9

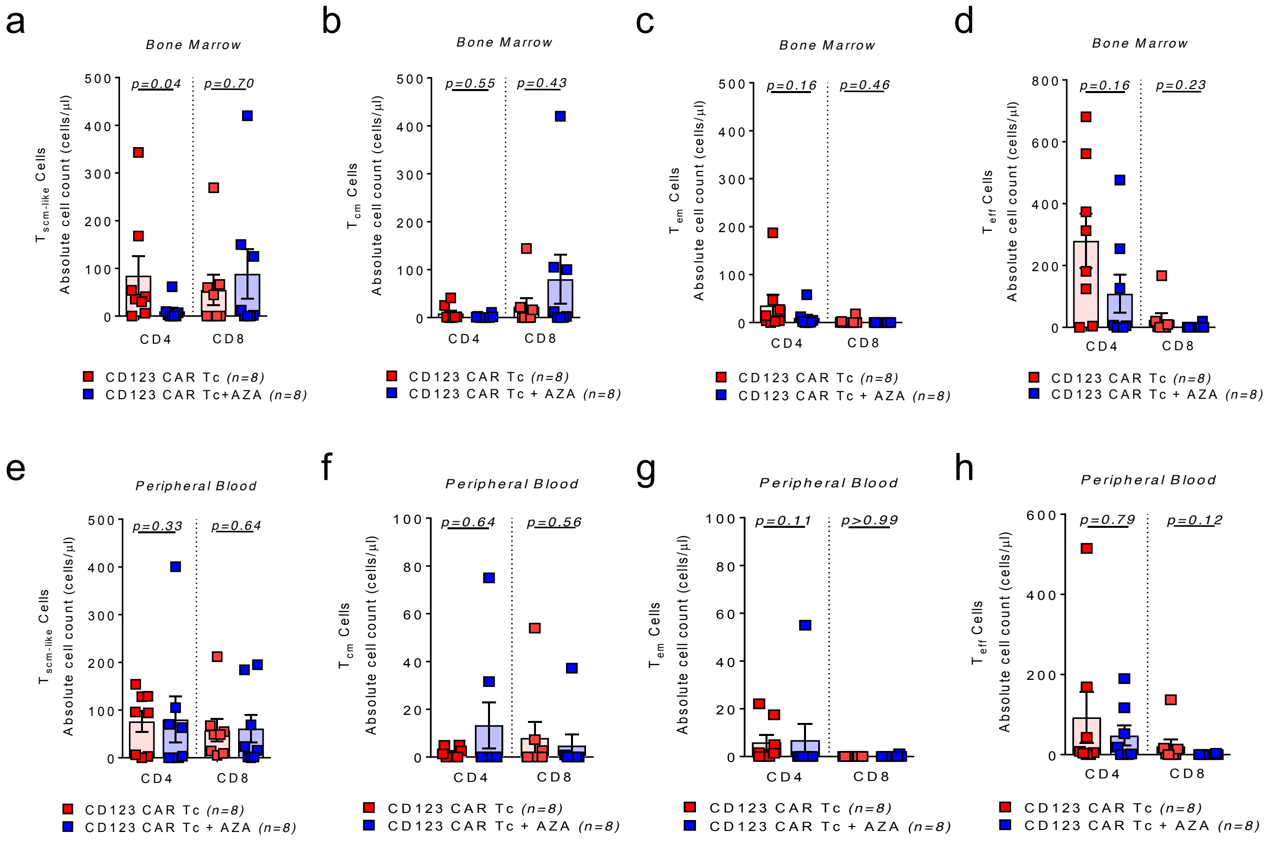

Supplementary Figure 9: Analysis of residual $CD4^+$ and $CD8^+$ T cell subsets in the bone marrow and peripheral blood of MOLM-13 AML xenograft mice.

Scatter plot graphs depicting **(a)** T stem cell-like ($T_{scm\text{-}like}$), **(b)** central memory (T_{cm}), **(c)** effector memory (T_{em}), and **(d)** terminally differentiated effectors (T_{eff}) cells from residual $CD4^+$ and $CD8^+$ anti-CD123 CAR T cells in the bone marrow of mice treated with anti-CD123 CAR T cells only versus the mice treated with AZA and anti-CD123 CAR T cells. Scatter plot graphs depicting **(e)** T stem cell-like ($T_{scm\text{-}like}$), **(f)** central memory (T_{cm}), **(g)** effector memory (T_{em}), and **(h)** terminally differentiated effectors (T_{eff}) cells from residual $CD4^+$ and $CD8^+$ anti-CD123 CAR T cells in the peripheral blood of mice treated with anti-CD123 CAR T cells only versus the mice treated with AZA and anti-CD123 CAR T cells. All data were pooled from 2 independent experiments and presented as mean absolute cell count ± SEM. *P*-values were calculated using unpaired Student's *t*-test (Mann-Whitney).

Supplementary Figure 10

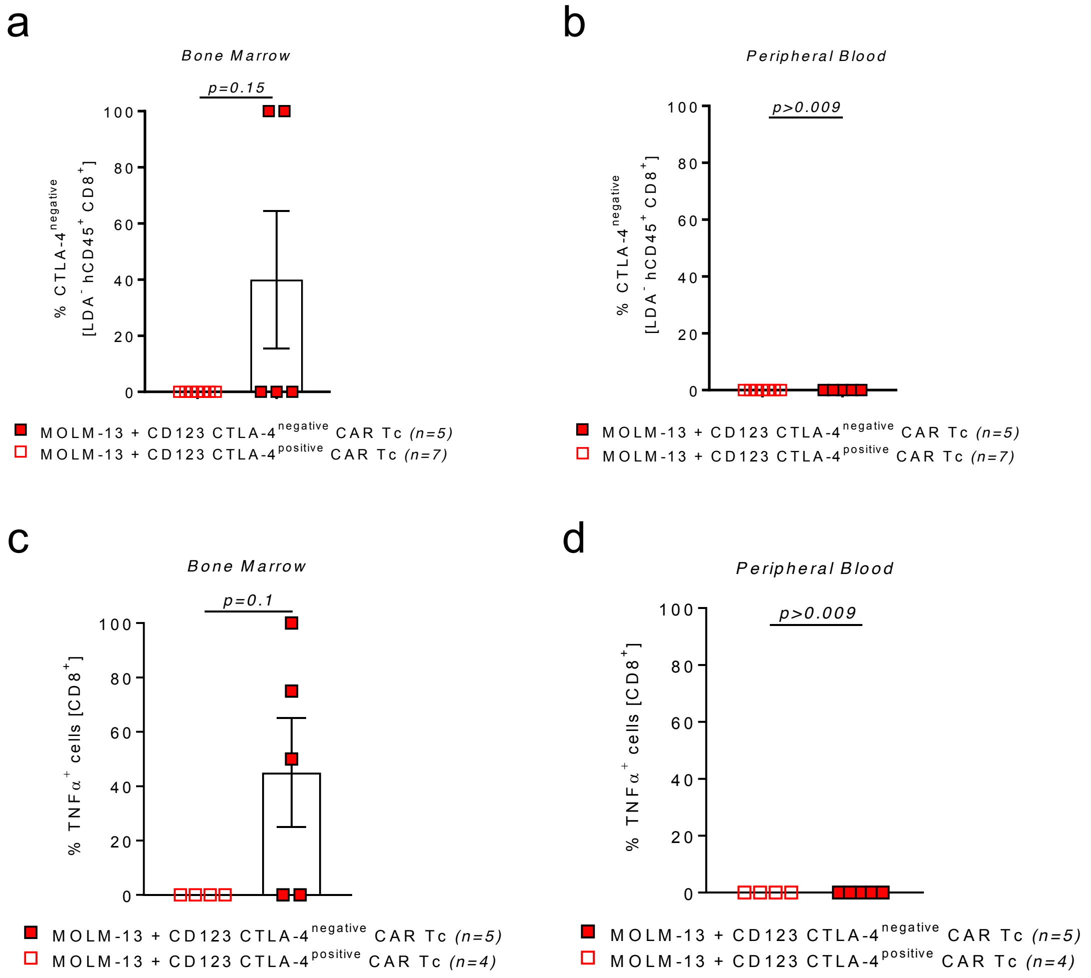

Supplementary Figure 10: Analysis of CTLA-4^{negative} and TNF expression on residual CD8^{+} T cells in the bone marrow and peripheral blood of MOLM-13 AML xenograft mice treated with CTLA-4^{negative} or CTLA-4^{positive} anti-CD123 CAR T cells.

Scatter plot graphs depicting the CTLA-4^{negative} expression of residual CD8^{+} T cells in the **(a)** bone marrow and **(b)** peripheral blood or mice treated with CTLA-4^{negative} or CTLA-4^{positive} anti-CD123 CAR T cells. Scatter plot graphs depicting the TNF expression of residual CD8^{+} T cells in the **(c)** bone marrow and **(d)** peripheral blood or mice treated with CTLA-4^{negative} or CTLA-4^{positive} anti-CD123 CAR T cells. All data were pooled from 2 independent experiments and presented as mean ± SEM. *P*-values were calculated using unpaired Student's *t*-test (Mann-Whitney).

Supplementary Figure 11

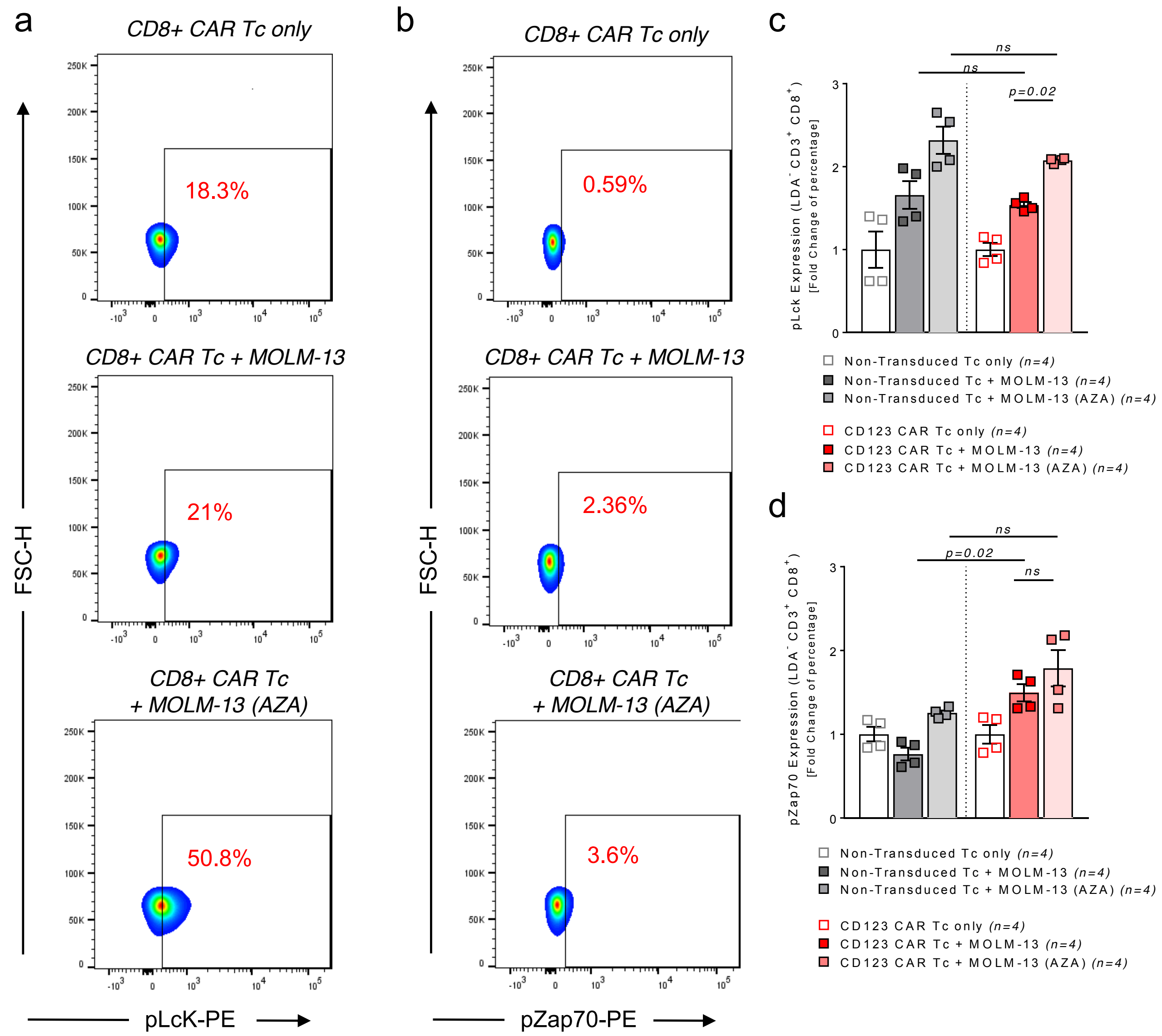

Supplementary Figure 11: Assessment of the phosphorylation of intracellular Lck and Zap70 in CD8$^+$ anti-CD123 CAR T cells in the presence of MOLM-13 AML cells.

(a) Representative flow cytometry plot depicting the phosphorylated level of LcK (pLck) in CD8$^+$ anti-CD123 CAR T cells that have been exposed for 96h to media only, naive MOLM-13 cells, or MOLM-13 cells pre-treated with 1μM AZA.

(b) Representative flow cytometry plot depicting the phosphorylated level of Zap70 (pZap70) in CD8$^+$ anti-CD123 CAR T cells that have been exposed for 96h to media only, naive MOLM-13 cells, or MOLM-13 cells pre-treated with 1μM AZA.

(c) Scatter plot depicting the fold change in percentage expression of pLcK in CD4$^+$ anti-CD123 CAR T cells. Data were pooled from 4 independent experiments.

(d) Scatter plot depicting the fold change in percentage expression of pZap70 in CD4$^+$ anti-CD123 CAR T cells. Data were pooled from 4 independent experiments. All graphed data are represented as mean ± SEM. *P*-values were unpaired Student's *t*-test (Mann-Whitney).

Suppl. Table 1: AML Patient Characteristics (SAHMRI, Adelaide, Australia)

Patient	Cytogenetics	Risk Group
1	Normal	Intermediate
2	Normal	Intermediate
3	Normal	Intermediate
4	Normal	Intermediate
5	Monosomy 7q	Poor
6	Normal	Intermediate
7	Normal	Intermediate
8	Trisomy 8	Intermediate
9	Normal	Intermediate
10	Normal	Intermediate
11	t(5,10); tri21	Intermediate
12	Trisomy 8, trisomy 19, 11q- and marker chromosome X 3	Poor
13	Normal	Intermediate
14	Del9q; trisomy21	Intermediate
15	Normal	Intermediate
16	Normal	Intermediate
17	Normal	Intermediate
18	Normal	Intermediate
19	Normal	Intermediate
20	Normal	Intermediate
21	11q23 rearranged, trisomy 21	Intermediate
22	Del6q	Intermediate
23	Normal	Intermediate
24	Normal	Intermediate
25	Flt3-ITD^{+}	Poor
26	Trisomy 8	Intermediate
27	Flt3-ITD^{+}	Poor
28	Flt3-ITD^{+}	Poor
29	Normal	Intermediate
30	Normal	Intermediate
31	Del5q; Monosomy 7	Poor
32	Trisomy 11	Intermediate

*Blast counts (%) for patients were not available in the database.

Suppl. Table 2: AML Patient Characteristics (University Medical Clinic, Freiburg, Germany)

Patient	Cytogenetics	% Blast Count PB	% Blast Count BM	Blast phenotype
1	V617F (JAK2)	94	85	CD34$^+$ CD117-
2	Normal	0	0.3	CD34$^+$ CD117-
3	21q22/RUNX1 mutation	12	71	CD34$^+$ CD117-
4	ASXL-1, DNMT3A, IDH1, PHF6, RUNX1 mutations	90	75	CD34$^+$ CD117-
5	5q31/5q33 (EGR1); KMT2A 11q23 rearrangement; t(8;21) RUNX1 mutation	4	43	CD34$^+$
6	NPM1 mutation	13	Not available	CD117$^+$
7	Monosomy 7; t(8;21)	50	74	CD34$^+$
8	Normal	77	93	CD117$^+$
9	IDH2, IKZF1, NRAS, TET-2 mutations	>95	80	CD34$^+$
10	Normal	Not available	Not available	Not available
11	CBL, TP53 mutations	35	2.5	CD34$^+$ CD117$^+$
12	PTPN11 (exon 13) mutation	13	Not available	CD34$^+$ CD117$^+$

Suppl. Table 3: Antibodies for flow cytometry

Antibody	Clone	Catalogue number	Fluorochrome	Vendor
Anti-human CD3	SK7	344824	Pacific Blue	Biolegend
Anti-human CD3	UCHT1	560835	PerCP-Cy5.5	BD Bioscience
Anti-human CD3	OKT3	317333	PeCy7	Biolegend
Anti-human CD3	HIT3a	300312	APC	Biolegend
Anti-human CD3	HIT3a	300306	FITC	Biolegend
Anti-human CD4	SK3	11-0047-42	FITC	eBioscience
Anti-human CD4	OKT4	317436	BV650	Biolegend
Anti-human CD95	DX2	555674	PE	BD Bioscience
Anti-human CD8	RPA-T8	555369	APC	BD Bioscience
Anti-human CD8	BW135/80	130-113-162	Pacific Blue	Miltenyi Biotec
Anti-human CD8	RPA-T8	563677	BV711	BD Bioscience
Anti-human CD45RO	UCHL1	25-0427-42	PeCy7	eBioscience
7-Aminoactinomycin D (7-AAD)	N/A	559925	PerCP-Cy5.5	BD Bioscience
Anti-human CD27	0323	47-0279-42	APC-ef780	eBioscience
Anti-human CD45RA	HI100	304138	BV711	Biolegend
Anti-human CD45RA	HI100	560675	PeCy7	BD Bioscience
Anti-human CD45	2D1	347463	FITC	BD Bioscience
Anti-human CD45	2D1	560178	APC-H7	BD Bioscience
Anti-human CD123	7G3	558714	PerCP-Cy5.5	BD Bioscience
Anti-human CD123	7G3	560826	PeCy7	BD Bioscience
Anti-human CD279 (PD-1)	EH12.2H7	329904	FITC	Biolegend
Anti-human CD279 (PD-1)	EH12.1	560795	PE	BD Bioscience
Anti-human CD152 (CTLA-4)	BN13	563931	BV786	BD Bioscience
Anti-human CD152 (CTLA-4)	L3D10	349908	APC	Biolegend
Anti-human CD152 (CTLA-4)	14D3	11-1529-42	FITC	BD Bioscience
Anti-human CD336 (TIM-3)	7D3	565564	BV650	BD Bioscience

Anti-human CD223 (LAG-3)	T47-530	565716	Alexa Flour 647	BD Bioscience
Live Dead Aqua	N/A	555516	V500/Amcyan	Invitrogen/Thermo Fischer Scientific
Anti-human Lin-Cocktail (CD3, CD14, CD16, CD19, CD20, CD56)	UCHT1;HCD14;3G8;HIB19:2H7:HCD56	348805	Pacific Blue	Biolegend
Anti-human CD38	LS198-4-3	A99022	ECD	Beckman Coulter
Anti-human CD34	581	561440	Alexa Fluor 700	BD Bioscience
Anti-human CD13	WM15	561599	PeCy7	BD Bioscience
Anti-human CD33	WM53	561157	V450	BD Bioscience
Anti-human CD19	HIB19	302234	BV421	Biolegend
Anti-human CD11c	3.9	301610	PeCy5	Biolegend
Anti-human CD304	12C2	354504	PE	Biolegend
Anti-human CD14	TuK4	MHCD1417	PE Texas Red	Life Technologies
Anti-human HLA-DR	TU36	MHLDR17	PE Texas Red	Life Technolgies
Anti-human CD117 (c-kit)	104D2	332785	PE	BD Biosciences
Anti-human CD107a	H4A3	555800	FITC	BD Bioscience
Streptavidin-Conjugated PE	N/A	349023	PE	BD Bioscience
Pierce Biotinylated recombinant Protein-L	N/A	21189	N/A	Thermo Fischer Scientific
Anti-human TNFα	Mab11	502909	PE	Biolegend
Anti-human IFN-γ	4S.B3	502512	APC	Biolegend

Supplementary Materials and Methods

Primary Healthy Donor (HD) and AML cells

Primary cells were maintained in RPMI-1640 supplemented with 20% fetal calf serum (FCS), 2mM L-glutamine, 100U/ml penicillin/streptomycin, and human stem cell factor (5ng/mL).

Tumor cell lines

The human leukemia cell lines MOLM-13, KG1a, and SUPB15 were purchased from ATCC (American Type Culture Collection, Manassas, Virginia, USA) and cultured in RPMI-1640 supplemented with 10% FCS, 2mM L-glutamine, 100U/ml penicillin/streptomycin. MOLM-13 cells were transduced with a lentiviral vector encoding the firefly luciferase (ffluc)-green fluorescent protein (GFP) transgene to enable detection by bioluminescence imaging (ffLuc). These cells were kindly provided by Max Jakob Kappenstein and Prof. Dr. Nikolas von Bubnoff, Freiburg, Germany.

Flow cytometric analysis of CD123-expression on primary bone marrow mononuclear cells

Cell surface expression of CD123 was analyzed on primary AML and healthy donor cells using conjugated mouse anti-human CD123 mAb. Cells were washed with 1x PBS supplemented with 2mM EDTA, 2% FCS, and 5% sodium azide, resuspended in 100µl, and stained with 15µl/test of human anti-CD123 PerCPCy5.5 (BD Biosciences) for 30minutes at 4°C. Cells were also stained with: Live dead Aqua-V500, CD13-PeCy7, CD33-V450, CD34-AF700, CD38-ECD, CD90-BV650, Lin- cocktail (CD3, CD14, CD16, CD19, CD20, CD56)-PB, and CD45RA-PeCy7 (BD Biosciences or Beckman Coulter). Unstained and fluorescence minus one (FMO) controls were used to identify gating boundaries.

Affinity of the CSL362 anti-CD123 monoclonal antibody

The affinity of the anti-CD123 antibody that was the basis for the scFv fragment that we used for the anti-CD123 CAR T cells was previously characterized for its affinity against wild-type (WT) IL-3Rα. The binding affinity was found to be high at: 4.0±1.1 K_D (nM)).[1, 2] The binding affinity of the CSL362 mAb is comparable or higher than the binding affinity of other antibodies/single chains used to generate CD123 directed CAR T cells published by others [3].

CAR construction and generation of CAR Lentivirus

A codon optimized single chain fragment variant (scFv) comprising the V_H and V_L segments of the humanized, and affinity-matured antibody of 7G3, CSL362, was synthesized and developed.[1] The scFv was fused to a CAR backbone comprising a short IgG4-Fc hinge spacer, a CD28 transmembrane, CD28 followed by an OX4O costimulatory moiety, and the CD3ζ signaling domain. The anti-CD123 CAR lentivirus was produced in HEK-293T cells. Briefly, 293T cells were plated one day prior to transfection and cultured in hi-glucose Dulbecco's minimum essential medium (DMEM) supplemented with 10% fetal calf serum (FCS) and 1% penecillin/streptomycin to achieve 60-80% confluence on the day of transfection. On the day of transfection, 5.5μg each of the anti-CD123 lentiviral DNA, pMDL-pRRE, pRSV-REV, and PMD2.G packaging plasmid DNA were added to serum-free media (Opti-MEM) and Lipofectamine 3000. The mixture was added to the HEK-293T cells following 30min incubation at RT. Cell culture media was replaced after 16 hours and cultured for a further 48 hours. The viral supernatant was harvested, centrifuged, and filtered through a 0.45µm membrane filter. The viral supernatant was concentrated by ultracentrifugation, resuspended in 1/150th of the original culture volume with cold sterile 1x phosphate-buffered saline (PBS) and stored in single use aliquots at -80°C until use.

Preparation of HD-derived CAR modified T cells

T cells were isolated from healthy donor peripheral blood mononuclear cells (PBMCs) using the human pan T cell isolation kit (Miltenyi Biotec). Purified $CD3^+$ T cells were stimulated and cultured with human CD3/CD28 dynabeads (Gibco Biosciences) two days prior to lentiviral transduction. Lentiviral gene-transfer was performed at a moiety of infection (MOI) range of 5-10. For the NTD T cells, lentiviral-gene transfer was not performed. After 7 days, CD3/CD28 dynabeads were removed from the culture and T cells successfully transduced with the CD123 CAR were determined by staining with biotinylated recombinant Protein-L (Pierce, Thermo Fischer), streptavidin-PE, and 7-AAD viability dye (BD Biosciences, San Diego, CA). Successfully transduced CD123 CAR T cells were purified (sort purity >95%) using flow sorting. Purified anti-CD123 CAR T cells were then expanded in culture with recombinant human 100U/ml interleukin (IL)-2 (Peprotech, Rocky Hill, NJ) for 10 days.

In Vitro T cell Subset Phenotypic Analysis

Anti-CD123 CAR T cells were harvested prior to and post lentiviral transduction and phenotypically analyzed. Cells were washed twice with 1x PBS supplemented with 2mM EDTA, 2%FCS, and 5% sodium azide, resuspended in 100µl, and stained with live dead aqua viability dye-V500, CD3-PerCPCy5.5, CD8-APC, CD27-APC-ef780, CD45RO-PeCy7 (BD Biosciences) for 30 minutes on ice, in the dark. Cells were washed twice and resuspended in a final volume of 200µl prior to flow cytometric analysis. Unstained and fluorescence minus one (FMO) controls were used to identify gating boundaries.

In Vivo T cell Subset Phenotypic Analysis

Bone marrow from the hind legs, and peripheral blood mononuclear cells following cardiac puncture were isolated from MOLM-13 xenograft mice treated with PBS, NTD T cells, CD123 CAR T cells only, azacytidine only, or dual treated. Cells were washed thrice with 1x PBS, trypan blue counted, and equally distributed. Cells were blocked with human FcR (Miltenyi Biotec) for 20 minutes. Cells were subsequently stained for residual leukemia cells, residual CAR T cells and its phenotypic subsets, and exhaustion expression on the residual CAR T cells (Supplementary Table 3). Cells were stained on ice, in the dark for 45 minutes. Unstained and fluorescence minus one (FMO) controls were used to identify gating boundaries.

Quantification of absolute cell numbers in bone marrow samples

Bone marrow from hind legs and hip bones were flushed in a fixed volume of PBS (20ml). Cells from the BM of each mouse were counted based on the flushing volume and equally distributed in the FACS tubes for staining. A fixed number of bead events were acquired during FACS analysis along with a fixed volume for acquisition (150ul). Absolute cell counts were calculated according to the formula provided by the CountBright^{TM} Absolute counting beads manufacturer's protocol (Invitrogen, Germany).

T cell phenotypic exhaustion profiling

Anti-CD123 CAR T cells were harvested at serial time-points during the expansion period and analyzed for surface expression of TIM-3, CTLA-4, LAG-3, and PD-1. Briefly, CAR T cells were harvested, CD3/CD28 dynabeads removed, and stained for CTLA-4-BV786, CD8-BV711, TIM-3-BV650, CD3-PerCPCy5.5, PD-1-PE, LAG-3-AlexaFluor 647 (BD Biosciences), and live dead aqua fixable viability stain (Life technologies) prior to flow cytometric analysis. Unstained and fluorescence minus one (FMO) controls were used to identify gating boundaries.

In vitro CAR T cell Functional Analysis

T cell Degranulation. Degranulation assays were performed as previously described [4]. In brief, anti-CD123 CAR T cells and KG1a were incubated at ratios 1:1, 2:1, 5:1, and

10:1 for 4 hours at 37°C with FITC-CD107a (clone H4A3, BD Biosciences) and the protein transport inhibitor monensin (BD GlogiStop). SUPB15 (CD123-) cells were used as a control. Following incubation, cells were stained with CD3-PerCPCy5.5, CD8-APC (BD Biosciences), and live dead aqua fixable dead cell stain (Life Technologies) to determine the percentage of $CD107^+$ CD4 and CD8 CAR T cells by flow cytometry. 1µg/ml Staphylococcus aureus, Enterotoxin type B (SEB) (Merck Millipore) was used as positive control of degranulation. Negative controls received RPMI-1640 culture medium (supplemented with 10% FCS) or RPMI-1640 media with anti-CD123 CAR T cells only.

CellTrace Violet Proliferation Assay. Anti-CD123 CAR T cells were labeled with CellTrace Violet (Life Technologies) according to the manufacturer's instructions. KG1a or SUPB15 cells were irradiated at a dose of 100 Gy. T cells were incubated at a ratio of 1:1 with irradiated target cells for 120 hours. Cells were then harvested, stained for CD3-PerCPCy5.5, CD8-BV711 and Live dead far red fixable viability stain (Invitrogen) prior to flow cytometric analysis.

Secretory Cytokine Measurement. Anti-CD123 CAR T cells (effectors) and KG1a cells (targets) were co-cultured at a E:T ratio of 10:1 at 37°C for 24 hours. For controls, SUPB15 cells were used as CD123- targets. The supernatant was harvested and stored in single use aliquots at -80°C until use. The supernatant was analyzed using the human 30-plex milliplex kit according to the manufacturer's protocol (Merck Millipore).

Epithelial Tissue Damage Histological Scoring

Mice were transplanted as described in the MOLM-13 $AML^{FLT3\ ITD}$ xenograft model. Samples from small intestine, colon, and liver were collected 28 days following T cell infusion. Samples were prepared, cut into 3µm sections, and stained with Hematoxylin & Eosin. The presence of epithelial tissue damage was determined and scored by an experienced pathologist (K.A) blinded to the treatment groups. Tissue damage severity was determined according to a previously described histopathology scoring system [5].

Pharmaceutical Drugs

5'-Azacytidine (Sigma Aldrich, Munich, Germany) was reconstituted in sterile dimethylsulfoxide (DMSO, Sigma Aldrich, Munich, Germany) prior to dilution in sterile dH_2O and used in *in vitro* and *in vivo* experiments.

Optimization of Azacitidine concentration *in vitro*

In human plasma, C_{max} values of AZA are 3-11 μM in order to observe substantial immunomodulatory and, especially, anti-leukemic effects [6, 7]. In our *in vitro* studies, preliminary dose escalation studies for the cell lines demonstrated no further enhanced immunomodulatory effects beyond 1uM. An immediate (by 12 hours following addition of AZA to cells) and significant decrease in cell viability was observed in all AML cell lines with concentrations higher than 1uM. For the purposes of these studies, 1uM AZA was therefore used in all *in vitro* experiments since the focus was aimed at the immunomodulatory effects of AZA and not anti-leukemic activity.

Optimization of Azacitidine administration *in vivo*

The dose and schedule of AZA administration were chosen based on previously published data. The minimum dose with therapeutic benefit/immunomodulatory effects was 2 mg/kg.[8] The maximum tolerated dose reported was 5mg/kg in a preclinical model of AML using immunocompromised mice.[9] Since the aim of the study was not to use AZA for anti-leukemic purposes, the concentration of AZA used was 2.5mg/kg with the same schedule of administration as the study conducted with AML xenografts.[9] In preliminary experiments, no significant anti-leukemic effects were observed. All *in vivo* experiments involving AZA, herein, followed this concentration and dosing schedule.

Supplementary References:

1. Busfield SJ, Biondo M, Wong M, Ramshaw HS, Lee EM, Ghosh S, Braley H, Panousis C, Roberts AW, He SZ, Thomas D, Fabri L, Vairo G, Lock RB, Lopez AF, Nash AD. Targeting of acute myeloid leukemia in vitro and in vivo with an anti-CD123 mAb engineered for optimal ADCC. *Leukemia* **28**, 2213-2221 (2014).

2. Broughton SE, Hercus TR, Hardy MP, McClure BJ, Nero TL, Dottore M, Huynh H, Braley H, Barry EF, Kan WL, Dhagat U, Scotney P, Hartman D, Busfield SJ, Owczarek CM, Nash AD, Wilson NJ, Parker MW, Lopez AF. Dual mechanism of interleukin-3 receptor blockade by an anti-cancer antibody. *Cell Rep* **8**, 410-419 (2014).

3. Mardiros A, Dos Santos, C., McDonald, T., Brown CE, Wang X, Budde LE, Hoffman L, Aguilar B, Chang WC, Bretzlaff W, Chang B, Jonnalagadda M, Starr R, Ostberg JR, Jensen MC, Bhatia R, Forman SJ. T cells expressing CD123-specific chimeric antigen receptors exhibit specific cytolytic effector functions and antitumor effects against human acute myeloid leukemia. *Blood* **122**, 3138-3148 (2013).

4. Betts MR, Koup RA. Detection of T-cell degranulation: CD107a and b. *Methods Cell Biol* **75**, 497-512 (2004).

5. Kaplan DH, Anderson, B.E., McNiff, J.M., Jain, D., Shlomchik, M.J., Shlomchik, W.D. Target antigens determine graft-versus-host disease phenotype. *J Immunol* **173**, 5467-5475 (2004).

6. Marcucci G, Silverman L, Eller M, Lintz L, Beach CL. Bioavailability of azacitidine subcutaneous versus intravenous in patients with the myelodysplastic syndromes. *J Clin Pharmacol* **45**, 597-602 (2005).

7. Hollenbach PW, Nguyen AN, Brady H, Williams M, Ning Y, Richard N, Krushel L, Aukerman SL, Heise C, MacBeth KJ. A comparison of azacitidine and decitabine activities in acute myeloid leukemia cell lines. *PLoS One* **5**, e9001 (2010).

8. Müller F, Cunningham T, Stookey S, Tai CH, Burkett S, Jailwala P, Stetler Stevenson M, Cam MC, Wayne AS, Pastan I. 5-Azacytidine prevents relapse and produces long-term complete remissions in leukemia xenografts treated with Moxetumomab pasudotox. *Proc Natl Acad Sci U S A* **115**, E1867-E1875 (2018).

9. Sutherland MK, Yu C, Anderson M, Zeng W, van Rooijen N, Sievers EL, Grewal IS, Law CL. 5-azacytidine enhances the anti-leukemic activity of lintuzumab (SGN-33) in preclinical models of acute myeloid leukemia. *MAbs* **4**, 440-448 (2010).

Main Text References

1. Zeiser R, Vago, L. Mechanisms of immune escape after allogeneic hematopoietic cell transplantation. *Blood* **133**, 1290-1297 (2019).

2. Stone RM, Mandrekar, S.J., Sanford BL, Laumann K, Geyer S, Bloomfield CD, Thiede C, Prior TW, Döhner K, Marcucci G, Lo-Coco F, Klisovic RB, Wei A, Sierra J, Sanz MA, Brandwein JM, de Witte T, Niederwieser D, Appelbaum FR, Medeiros BC, Tallman MS, Krauter J, Schlenk RF, Ganser A, Serve H, Ehninger G, Amadori S, Larson RA, Döhner H. Midostaurin plus Chemotherapy for Acute Myeloid Leukemia with a FLT3 Mutation. *N Eng J Med* **377**, 454-464 (2017).

3. Döhner H, Estey, E., Grimwade, D., Amadori S, Appelbaum FR, Büchner T, et al. Diagnosis and management of AML in adults: 2017 ELN recommendations from an international expert panel. *Blood* **129**, 424-447 (2017).

4. Mathew NR, Baumgartner, F., Braun, L., David O´Sullivan, Thomas S, Waterhouse M, Müller TA, Hanke K, Taromi S, Apostolova P, Illert AL, Melchinger W, Duquesne S, Schmitt-Graeff A, Osswald L, Yan K-L., Weber A, Tugues S, Spath S, Pfeifer D, Follo M, Claus R, Lübbert M, Rummelt C, Bertz H, Wäsch R, Haag J, Schmidts A, Schultheiss M, Bettinger M, Thimme R, Ullrich E, Tanriver Y, Vuong GL, Arnold R, Hemmati P, Wolf D, Ditschkowski M, Jilg C, Wilhelm K, Leiber C, Gerull S, Halter J, Lengerke C, Pabst T, Schroeder T, Kobbe G, Rösler W, Doostkam S, Meckel S, Stabla K, Metzelder SK, Halbach S, Brummer T, Hu Z, Dengjel J, Hackanson B, Schmid C, Holtick U, Scheid C, Spyridonidis A, Stölzel F, Ordemann F, Müller LP, Sicre-de-Fontbrune F, Ihorst G, Kuball J, Ehlert JE, Feger D, Wagner EV, Cahn JY, Schnell J, Kuchenbauer F, Bunjes D, Chakraverty R, Richardson S, Gill S, Kröger N, Ayuk F, Vago L, Ciceri F, Müller AM, Kondo T, Teshima T, Klaeger S, Kuster B, Kim D, Weisdorf D, van der Velden W, Dörfel D, Bethge W, Hilgendorf I, Hochhaus A, Andrieux G, Börries M, Busch H, Magenau J, Reddy P, Labopin M, H. Antin J, Henden AS, Hill GR, Kennedy GA, Bar M, Sarma A, McLornan D, Mufti G, Oran B, Rezvani K, Sha O, Negrin RS, Nagler A, Prinz M, Burchert A, Neubauer A, Beelen

D, Mackensen A, von Bubnoff N, Herr W, Becher B, Socié G, Caligiuri MA, Ruggiero E, Bonini C, Häcker G, Duyster J, Finke J, Pearce E, Blazar BR, Zeiser R. Sorafenib promotes graft-versus-leukemia activity in mice and humans through IL-15 production in FLT3-ITD mutant leukemia cells. *Nature medicine* **24**, 282-291 (2018).

5. Park JH, Rivière, I., Gonen, M., Wang X, Sénéchal B, Curran KJ, Sauter C, Wang Y, Santomasso B, Mead E, Roshal M, Maslak P, Davila M, Brentjens RJ, Sadelain M. Long-Term Follow-up of CD19 CAR Therapy in Acute Lymphoblastic Leukemia. *N Eng J Med* **378**, 449-459 (2018).

6. Gardner RA, Finney, O., Annesley, C., et al. Intent-to-treat leukemia remission by CD19 CAR T cells of defined formulation and dose in children and young adults. *Blood* **129**, 3322-3331 (2017).

7. Maude SL, Frey, N., Shaw, P.A., Aplenc, R., Barrett DM, Bunin NJ, Chew A, Gonzalez VE, Zheng Z, Lacey SF, Mahnke YD, Melenhorst JJ, Rheingold SR, Shen A, Teachey DT, Levine BL, June CH, Porter DL, Grupp SA. Chimeric antigen receptor T cells for sustained remissions in leukemia. *N Eng J Med* **371**, 1507-1517 (2014).

8. Jordan CT. Targeting myeloid leukemia stem cells. *Sci Transl Med* **31**, 31ps21 (2010).

9. Muñoz L, Nomdedéu, J.F., López O, Carnicer MJ, Bellido M, Aventín A, Brunet S, Sierra J. Interleukin-3 receptor alpha chain (CD123) is widely expressed in hematologic malignancies. *Haematologica* **86**, 1261-1269 (2001).

10. Mardiros A, Dos Santos C, McDonald T, Brown CE, Wang X, Budde LE, Hoffman L, Aguilar B, Chang WC, Bretzlaff W, Chang B, Jonnalagadda M, Starr R, Ostberg JR, Jensen MC, Bhatia R, Forman SJ. T cells expressing CD123-specific chimeric antigen receptors exhibit specific cytolytic effector functions and antitumor effects against human acute myeloid leukemia. *Blood* **122**, 3138-3148 (2013).

11. Fan M, Li, M., Gao L, Geng S, Wang J, Wang Y, Yan Z, Yu L. Chimeric antigen receptors for adoptive T cell therapy in acute myeloid leukemia. *J Hematol Oncol* **10**, 151 (2017).

12. Mardiana S, Gill, S. CAR T Cells for Acute Myeloid Leukemia: State of the Art and Future Directions. *Front Oncol* **10**, 697 (2020).

13. Busfield SJ, Biondo M, Wong M, Ramshaw HS, Lee EM, Ghosh S, Braley H, Panousis C, Roberts AW, He SZ, Thomas D, Fabri L, Vairo G, Lock RB, Lopez AF, Nash AD. Targeting of acute myeloid leukemia in vitro and in vivo with an anti-CD123 mAb engineered for optimal ADCC. *Leukemia* **28**, 2213-2221 (2014).

14. Goodyear O, Agathanggelou, A., Novitzky-Basso I, Siddique S, McSkeane T, Ryan G, et al. Induction of a CD8+ T-cell response to the MAGE cancer testis antigen by combined treatment with azacitidine and sodium valproate in patients with acute myeloid leukemia and myelodysplasia. *Blood* **116**, 1908-1918 (2010).

15. Chiappinelli KB, Strissel, P.L., Desrichard A, Li H, Henke C, Akman B, Hein A, Rote NS, Cope LM, Snyder A, Makarov V, Budhu S, Slamon DJ, Wolchok JD, Pardoll DM, Beckmann MW, Zahnow CA, Merghoub T, Chan TA, Baylin SB, Strick R. Inhibiting DNA Methylation Causes an Interferon Response in Cancer via dsRNA Including Endogenous Retroviruses. *Cell* **162**, 974-986 (2015).

16. Craddock C, Quek, L., Goardon N, Freeman S, Siddique S, Raghavan M, Aztberger A, Schuh A, Grimwade D, Ivey A, Virgo P, Hills R, McSkeane T, Arrazi J, Knapper S, Brookes

C, Davies B, Price A, Wall K, Griffiths M, Cavenagh J, Majeti R, Weissman I, Burnett A, Vyas P. Azacitidine fails to eradicate leukemic stem/progenitor cell populations in patients with acute myeloid leukemia and myelodysplasia. *Leukemia* **27**, 1028-1036 (2013).

17. Jin S, Cojocari D, Purkal JJ, Popovic R, Talaty NN, Xiao Y, Solomon LR, Boghaert ER, Leverson JD, Phillips DC. 5-Azacitidine Induces NOXA to Prime AML Cells for Venetoclax-mediated Apoptosis. *Clin Cancer Res* **26**, 3371-3383 (2020).

18. Jilg S, Hauch RT, Kauschinger J, Buschhorn L, Odinius TO, Dill V, Müller-Thomas C, Herold T, Prodinger PM, Schmidt B, Hempel D, Bassermann F, Peschel C, Götze KS, Höckendorf U, Haferlach T, Jost PJ. Venetoclax with azacitidine targets refractory MDS but spares healthy hematopoiesis at tailored dose. *Exp Hematol Oncol* **8**, 9 (2019).

19. DiNardo C, Stein EM, de Botton S, Roboz GJ, Altman JK, Mims AS, Swords R, Collins RH, Mannis GN, Pollyea DA, Donnellan W, Fathi AT, Pigneux A, Erba HP, Prince GT, Stein AS, Uy GL, Foran JM, Traer E, Stuart RK, Arellano ML, Slack JL, Sekeres MA, Willekens C, Choe S, Wang H, Zhang V, Yen KE, Kapsalis SM, Yang H, Dai D, Fan B, Goldwasser M, Liu H, Agresta S, Wu B, Attar EC, Tallman MS, Stone RM, Kantarjian HM. Durable Remissions with Ivosidenib in IDH1-Mutated Relapsed or Refractory AML. *N Eng J Med* **378**, 2386-2398 (2018).

20. DiNardo CD, Wei, A.H. How I treat acute myeloid leukemia in the era of new drugs. *Blood* **135**, 85-96 (2020).

21. Daver N, Garcia-Manero, G., Basu S, Boddu PC, Alfayez M, Cortes JE, Konopleva M, Ravandi-Kashani F, Jabbour E, Kadia T, Nogueras-Gonzalez GM, Ning J, Pemmaraju N, DiNardo CD, Andreeff M, Pierce SA, Gordon T, Kornblau SM, Flores W, Alhamal Z, Bueso-Ramos C, Jorgensen JL, Patel KP, Blando J, Allison JP, Sharma P, Kantarjian H. Efficacy, Safety, and Biomarkers of Response to Azacitidine and Nivolumab in Relapsed/Refractory Acute Myeloid Leukemia: A Non-randomized, Open-label, Phase 2 Study. *Cancer Discov* **3**, 370-383 (2019).

22. Yi JS, Cox MA, Zajac AJ. T-cell exhaustion: characteristics, causes and conversion. *Immunology* **129**, 474-481 (2010).

23. Croft M. The role of TNF superfamily members in T-cell function and diseases. *Nat Rev Immunol* **4**, 271–285. (2009).

24. Zeiser R, Nguyen, V.H., Beilhack, A., Buess, M., Schulz, S., Baker, J., Contag, C.H., Negrin, R.S. Inhibition of CD4+CD25+ regulatory T cell function by calcineurin dependent interleukin-2 production. *Blood* **108**, 390-399 (2006).

25. Rongvaux A, Willinger T, Martinek J, Strowig T, Gearty SV, Teichmann LL, et al. . Development and function of human innate immune cells in a humanized mouse model. *Nat Biotechnol* **32**, 364-372 (2014).

26. Saito Y, Ellegast, J.M., Rafiei A, Song Y, Kull D, Heikenwalder M, Rongvaux A, Halene S, Flavell RA, Manz MG. Peripheral blood CD34+ cells efficiently engraft human cytokine knock-in mice. *Blood* **128**, 1829-1833 (2014).

27. Gill S, Tasian, S.K., Ruella M, Shestova O, Li Y, Porter DL, Carroll M, Danet-Desnoyers G, Scholler J, Grupp SA, June CH, Kalos M. Preclinical targeting of human acute myeloid

leukemia and myeloablation using chimeric antigen receptor-modified T cells. *Blood* **123**, 2343-2354 (2014).

28. Jordan CT, Upchurch, D., Szilvassy SJ, Guzman ML, Howard DS, Pettigrew AL, Meyerrose T, Rossi R, Grimes B, Rizzieri DA, Luger SM, Phillips GL. The interleukin-3 receptor alpha chain is a unique marker for human acute myelogenous leukemia stem cells. *Leukemia* **14**, 1777-1784 (2000).

29. Issa JP. DNA methylation as a therapeutic target in cancer. *Clin Cancer Res* **13**, 1634-1637 (2007).

30. Stübig T, Badbaran A, Luetkens T, Hildebrandt Y, Atanackovic D, Binder TM, Fehse B, Kröger N. 5-azacytidine promotes an inhibitory T-cell phenotype and impairs immune mediated antileukemic activity. *Mediators Inflamm*, 418292 (2014).

31. Zeiser R, Blazar, B.R. Acute Graft-versus-host disease - Biologic process, prevention, and therapy. *N Eng J Med* **377**, 2167-2179 (2017).

32. Zeiser R, von Bubnoff, N, Butler J, Mohty M, Niederwieser D, Or R, Szer J, Wagner EM, Zuckerman T, Mahuzier B, Xu J, Wilke C, Gandhi KK, Socié G, for the REACH2 Trial Group. Ruxolitinib for Glucocorticoid-Refractory Acute Graft-versus-Host Disease. *N Eng J Med* **382**, 1800-1810 (2020).

33. Finelli C, Follo MY, Stanzani M, Parisi S, Clissa C, Mongiorgi S, Barraco M, Cocco L. Clinical Impact of Hypomethylating Agents in the Treatment of Myelodysplastic Syndromes. *Curr Pharm Des* **22**, 2349-2357 (2016).

34. Guntermann C, Alexander, D.R. CTLA-4 suppresses proximal TCR signaling in resting human CD4(+) T cells by inhibiting ZAP-70 Tyr(319) phosphorylation: a potential role for tyrosine phosphatases. *J Immunol* **168**, 4420-4429 (2002).

35. Orlando EJ, Han X, Tribouley C, Wood PA, Leary RJ, Riester M, et al. Genetic mechanisms of target antigen loss in CAR19 therapy of acute lymphoblastic leukemia. *Nature medicine* **24**, 1504–1506 (2018).

36. Shen C, Zhang, Z., Zhang Y. Chimeric Antigen Receptor T Cell Exhaustion during Treatment for Hematological Malignancies. *Biomed Res Int*, 8765028 (2020).

37. Gang AO, Frøsig, T.M., Brimnes MK, Lyngaa R, Treppendahl MB, Grønbæk K, Dufva IH, Straten PT, Hadrup SR. 5-Azacytidine treatment sensitizes tumor cells to T-cell mediated cytotoxicity and modulates NK cells in patients with myeloid malignancies. *Blood Cancer J* **4**, e197 (2014).

38. Hill GR, Teshima, T., Gerbitz, A., Pan, L., Cooke, K.R., Brinson, Y.S., Crawford, J.M., Ferrara, J.L. Differential roles of IL-1 and TNF-alpha on graft-versus-host disease and graft versus leukemia. *The Journal of clinical investigation* **104**, 459-467 (1999).

39. Walunas TL, Lenschow, D.J., Bakker, C.Y., Linsley, P.S., Freeman, G.J., Green, J.M., Thompson, C.B., Bluestone, J.A. CTLA-4 can function as a negative regulator of T cell activation. *Immunity* **5**, 405-413 (1994).

40. Wherry EJ, Kurachi M. Molecular and cellular insights into T cell exhaustion. *Nat Rev Immunol* **15**, 486-499 (2015).

41. Amezquita RA, Kaech, S,M. Immunology: The chronicles of T-cell exhaustion. *Nature* **543**, 190-191 (2017).

42. Yang H, Bueso-Ramos, C., DiNardo C, Estecio MR, Davanlou M, Geng QR, Fang Z, Nguyen M, Pierce S, Wei Y, Parmar S, Cortes J, Kantarjian H, Garcia-Manero G. Expression of PD-L1, PD-L2, PD-1 and CTLA4 in myelodysplastic syndromes is enhanced by treatment with hypomethylating agents. *Leukemia* **28**, 1280-1288 (2014).

43. Roulois D, Loo Yau, H., Singhania R, Wang Y, Danesh A, Shen SY, Han H, Liang G, Jones PA, Pugh TJ, O'Brien C, De Carvalho DD. DNA-Demethylating Agents Target Colorectal Cancer Cells by Inducing Viral Mimicry by Endogenous Transcripts. *Cell* **162**, 961-973 (2015).

44. Togami K, Pastika T, Stephansky J, Ghandi M, Christie AL, Jones KL, Johnson CA, Lindsay RW, Brooks CL, Letai A, Craig JW, Pozdnyakova O, Weinstock DM, Montero J, Aster JC, Johannessen CM, Lane AA. DNA methyltransferase inhibition overcomes diphthamide pathway deficiencies underlying CD123-targeted treatment resistance. *The Journal of clinical investigation* **129**, 5005-5019 (2019).

45. Salter AI, Ivey, R.G., Kennedy JJ, Voillet V, Rajan A, Alderman EJ, Voytovich UJ, Lin C, Sommermeyer D, Liu L, Whiteaker JR, Gottardo R, Paulovich AG, Riddell SR. Phosphoproteomic analysis of chimeric antigen receptor signaling reveals kinetic and quantitative differences that affect cell function. *Sci Signal* **544**, (2018).

46. Ramello MC, Benzaïd, I., Kuenzi BM, Lienlaf-Moreno M, Kandell WM, Santiago DN, Pabón-Saldaña M, Darville L, Fang B, Rix U, Yoder S, Berglund A, Koomen JM, Haura EB, Abate-Daga D. An immunoproteomic approach to characterize the CAR interactome and signalosome. *Sci Signal* **568**, eaap9777 (2019).

47. Gudipati V, Rydzek, J., Doel-Perez I, Gonçalves VDR, Scharf L, Königsberger S, Lobner E, Kunert R, Einsele H, Stockinger H, Hudecek M, Huppa JB. Inefficient CAR-proximal signaling blunts antigen sensitivity. *Nat Immunol* **8**, 848-856 (2020).

48. Hartl FA, Beck-Garcìa E, Woessner NM, Flachsmann LJ, Cárdenas RMV, Brandl SM, Taromi S, Fiala GJ, Morath A, Mishra P, Yousefi OS, Zimmermann J, Hoefflin N, Köhn M, Wöhrl BM, Zeiser R, Schweimer K, Günther S, Schamel WW, Minguet S. . Noncanonical binding of Lck to CD3ε promotes TCR signaling and CAR function. *Nat Immunol* **8**, 902-913 (2020).

49. Bôle-Richard E, Fredon M, Biichlé S, Anna F, Certoux JM, Renosi F, Tsé F, Molimard C, Valmary-Degano S, Jenvrin A, Warda W, Pallandre JR, Bonnefoy F, Poussard M, Deschamps M, Petrella T, Roumier C, Macintyre E, Féger F, Brissot E, Mohty M, HoWangYin KY, Langlade-Demoyen P, Loustau M, Caumartin J, Godet Y, Binda D, Pagadoy M, Deconinck E, Daguindau E, Saas P, Ferrand C, Angelot-Delettre F, Adotévi O, Garnache-Ottou F. . CD28/4-1BB CD123 CAR T cells in blastic plasmacytoid dendritic cell neoplasm. *Leukemia* **34**, 3228-3241 (2020).

50. Jiang YL, Li Q, Yuan T, Jiang YY, Deng Q. Case Report of Anti-CD123 Chimeric Antigen Receptor T-Cell Therapy Followed by Radiotherapy for a Recurrence of Blastic Plasmacytoid Dendritic Cell Neoplasm After Allogeneic Hematopoietic Stem Cell Transplantation. *Onco Targets Ther* **13**, 3425-3430 (2020).

51. Baroni ML, Sanchez Martinez D, Gutierrez Aguera F, Roca Ho H, Castella M, Zanetti SR, Velasco Hernandez T, Diaz de la Guardia R, Castaño J, Anguita E, Vives S, Nomdedeu J,

Lapillone H, Bras AE, van der Velden VHJ, Junca J, Marin P, Bataller A, Esteve J, Vick B, Jeremias I, Lopez A, Sorigue M, Bueno C, Menendez P. 41BB-based and CD28-based CD123-redirected T-cells ablate human normal hematopoiesis in vivo. *J Immunother Cancer* **8**, e000845 (2020).

52. Drent E, Themeli, M., Poels R, de Jong-Korlaar R, Yuan H, de Bruijn J, Martens ACM, Zweegman S, van de Donk NWCJ, Groen RWJ, Lokhorst HM, Mutis T. A Rational Strategy for Reducing On-Target Off-Tumor Effects of CD38-Chimeric Antigen Receptors by Affinity Optimization. *Mol Ther* **25**, 1946-1958 (2017).

53. Ghosh A, Smith M, James SE, Davila ML, Velardi E, Argyropoulos KV, Gunset G, Perna F, Kreines FM, Levy ER, Lieberman S, Jay HV, Tuckett AZ, Zakrzewski JL, Tan L, Young LF, Takvorian K, Dudakov JA, Jenq RR, Hanash AM, Motta AC, Murphy GF, Liu C, Schietinger A, Sadelain M, van den Brink MR. Donor CD19 CAR T cells exert potent graft-versus-lymphoma activity with diminished graft-versus-host activity. *Nature medicine* **23**, 242-249 (2017).

54. Schroeder T, Czibere, A., Platzbecker U, Bug G, Uharek L, Luft T, Giagounidis A, Zohren F, Bruns I, Wolschke C, Rieger K, Fenk R, Germing U, Haas R, Kröger N, Kobbe G. Azacitidine and donor lymphocyte infusions as first salvage therapy for relapse of AML or MDS after allogeneic stem cell transplantation. *Leukemia* **27**, 1229-1235 (2013).

55. Steinmann J, Bertz, H., Wäsch, R., Marks, R., Zeiser, R., Bogatyreva, L., Finke, J., Lübbert, M. 5-Azacytidine and DLI can induce long-term remissions in AML patients relapsed after allograft. *Bone Marrow Transplant* **50**, 690-695 (2015).

4.4 Additional Unpublished Methods

RNA Isolation & Microarray Analysis. HL-60 cells that were previously cultured in the absence (D0) or presence of AZA (D1, D4, D8) were harvested and RNA was isolated using the RNeasy Mini Kit. This was prepared by the working group of AG Miething. RNA quality and quantity were assessed using a spectrophotometer at wavelengths of 260 and 280nm. RNA was further processed by the working group of Dr. Dietmar Pfeifer (Genomic lab of the University Medical Center Freiburg). The RNA quality was additionally assessed using the Agilent 2100 Bioanalyser. Samples with an RNA integrity number (RIN) greater than 8 were then transcribed into complementary deoxyribonucleic acid (cDNA) and processed using the Ambion WT Expression kit, according to manufacturer's protocol. The cDNA was fragmented, labelled with the Affymetrix Terminal labelling kit, and hybridised to the Affymetrix Clariom S Mouse arrays. The arrays were scanned with the Affymetrix GeneChip Scanner 3000 7G. All initial analysis of differential gene pathways was performed by Prof. Dr. Melanie Borries, Dr. Geoffroy Andrieux (Institute of Medical Bioinformatics and Systems Medicine, University of Freiburg), and Prof. Dr. Cornelius Miething.

Western Blotting. HL-60 and MOLM-13 that were previously cultured in the absence (Day 0) or presence of AZA (Day 4 and Day 8) were lysed for 20mins at 4°C using a ratio-immunoprecipitation assay buffer (Santa Cruz Biotechnology, Heidelberg, Germany) supplemented with Phosphatase Inhibitor Cocktail 2 (Sigma-Aldrich, Germany). The cells were then centrifuged at 10,000 rpm for 10mins at 4°C. The supernatant was gently removed and stored at -80°C until protein quantification. The protein concentration was determined using Pierce™ BCA Protein Assay Kit (Life Technologies, Germany), following the manufacturer's protocol. For SDS-PAGE, 15μg of protein from each sample were mixed with NuPAGE LDS sample buffer and NuPAGE sample reducing agent and heat-denaturised for 10mins at 75°C. Samples were loaded onto a 4-12% sodium dodecyl sulphate-polyacrylamide electrophoresis gel (NuPAGE, Invitrogen, Germany) and separated in 1x MES SDS running buffer using the XCell SureLock Mini-Cell Electropheoresis System at 90-140V. For protein transfer, a hybond polyvinylidene fluoride (PVDF) membrane (Amersham Biosciences, Germany) was prepared and activated in methanol for 30s following by a wash in ddH_2O and NuPAGE transfer buffer. Proteins were transferred in NuPAGE transfer buffer using the XCell II Blot Module. The membrane was incubated with blocking buffer (5% BSA in 1x tris buffer saline containing 0.1% tween-20) for 2h at RT followed by incubation with primary antibodies (pIRF7, IRF7, pSTAT1, STAT1, HLA-

DR, and β-actin) (Cell Signaling Technology, USA or Santa Cruz Biotechnology, USA) diluted 1:1000 in blocking buffer overnight at 4^{o}C. Membranes were washed 3x with TBS-T at RT, then incubated with anti-rabbit IgG, HRP-linked antibody (secondary antibody) for 2h at RT. WesternBright Sirius Chemiluminescent Detection Kit (Advansta, USA) was used as the chemoluminescent substrate. The signals from the blot are captured using the ChemoCam Imager 3.2 (Intas Science Imaging Instruments GmbH, Germany) and quantified using LabImage 1D software of ImageJ.

4.5 Additional Unpublished Results

4.5.1 Azacitidine increases key immunogenic markers in AML

Several studies have previously demonstrated increased tumour cell immunogenicity following AZA treatment, prolonging survival in some patients with high-risk MDS and AML (Issa, 2007). To validate the results from published data, the AML cell line HL-60, was exposed to 1μM AZA for 8 days. HL60 cells cultured in media without AZA were used as a control. HL-60 cells were isolated 1, 4, and 8 days following AZA exposure and RNA isolation was performed followed by a microarray-based analysis to assess the differential gene expression of key immunogenic markers between cells isolated on d1,4, and 8, versus d0. This work was performed in collaboration with the working group of AG Miething and Dr. Desiree Redhaber.

The selective clustering of genes associated with the "antigen processing and presentation" as well as "cytokines" and "interleukins" annotation identified multiple genes that were significantly upregulated when the cells were treated for 4 and 8 days with AZA compared to cells cultured in the absence of AZA or 24h following AZA treatment *(Figure 4.2 A, B)*. Concordant with published data, the analysis verified that genes associated with MHC processing and presentation (HLA-DR molecules) were upregulated in the AZA treated cells compared to the cells treated in media only. Furthermore, the signal transducer and activator of transcription 1 (STAT1), the interferon regulatory factor 7 (IRF7), and several cytokines were also found to be upregulated in the treated groups compared to the non-treated control. Total STAT1, phosphorylated STAT1 (pSTAT1), total IRF7, phosphorylated IRF7 (pIRF7), and the human leukocyte antigen DR isotype (HLA-DR) were also found to be significantly upregulated via western blot on the protein level of HL-60 and MOLM-13 cells at day 4 and day 8 following AZA treatment compared to the non-treated control (d0) *(Figure 4.2 C-E, Figure 4.3)*.

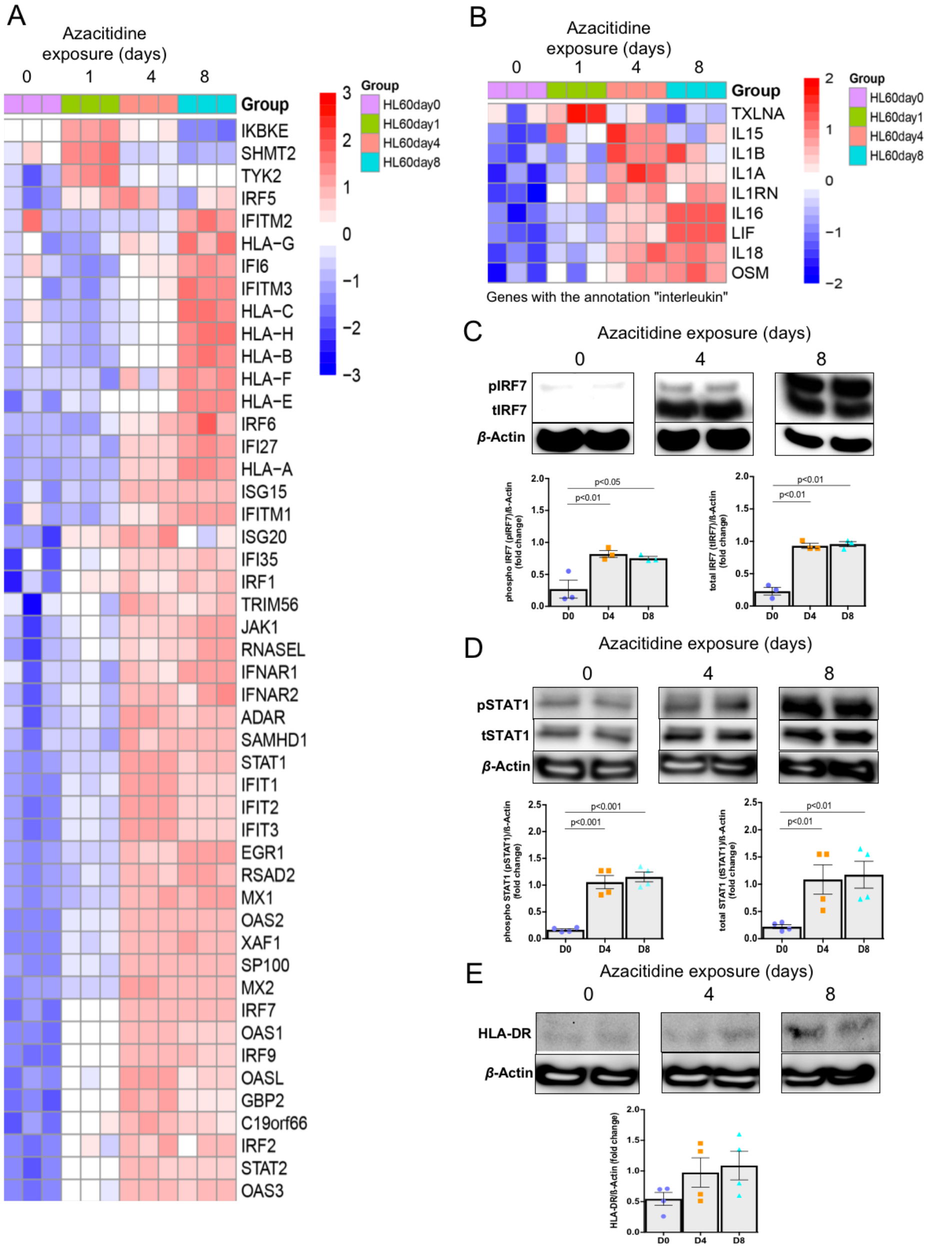

Figure 4.2. Azacitidine treatment leads to re-activation of key immunogenic markers on human HL60 cells.

(A) The heatmap represents the expression of antigen processing and presentation associated genes in human HL-60 cells in the absence (day 0) or presence (1, 4, and 8 days) of 1µM AZA in culture. **(B)** The heatmap represents the expression of cytokines in human HL-60 cells that are upregulated following culture with 1µM AZA for 1,4, and 8 days compared to cell treated in the absence of AZA. **(C)** Western blot analysis shows the amount of phosphorylated IRF7 (pIRF7) and total IRF7 (tIRF7) in HL-60 cells in response to 1µM AZA. The blot is representative for three independent experiments *(n=3)*. The ratio of pIRF7/β-actin and tIRF7/β-actin at D0, D4, and D8 is normalised to D0. **(D)** Western blot analysis shows the amount of phosphorylated STAT1 (pSTAT1) and total STAT1 (tSTAT1) in HL60 cells in response to 1µM AZA. The blot is representative for four independent experiments *(n=4)*. The ratio of pSTAT1/β-actin and tSTAT1/β-actin at D0, D4, and D8 is normalised to D0. **(E)** Western blot analysis shows the amount of HLA-DR in HL-60 cells in response to 1µM AZA. The blot is representative for four independent experiments *(n=4)*. The ratio of HLA-DR/β-actin at D0, D4, and D8 is normalised to D0.

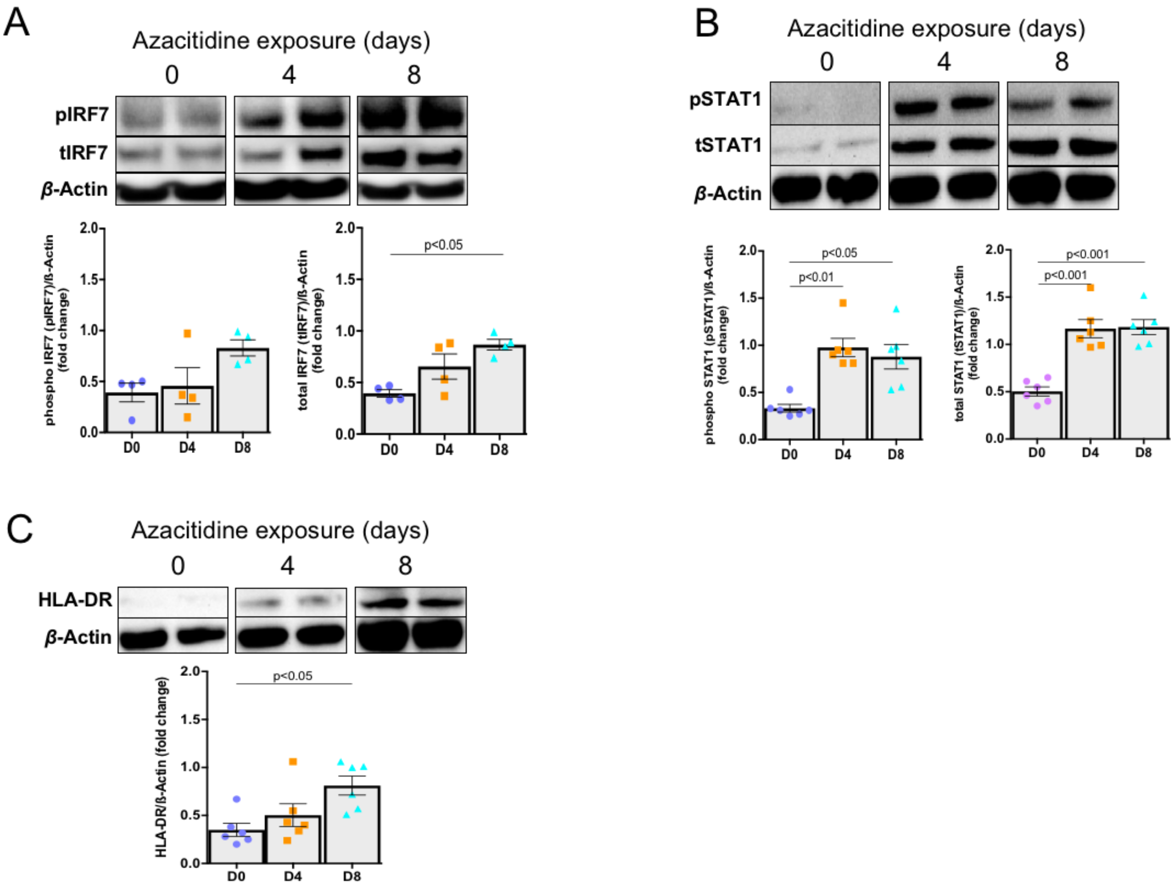

Figure 4.3. Evidence of immunogenic markers upregulated at the protein level on MOLM-13 AML cells in response to Azacitidine.

(A) Western blot analysis shows the amount of phosphorylated IRF7 (pIRF7) and total IRF7 (tIRF7) in MOLM-13 cells in response to 1µM AZA. The blot is representative for four independent experiments *(n=4)*. The ratio of pIRF7/β-actin and tIRF7/β-actin at D0, D4, and D8 is normalised to D0. **(B)** Western blot analysis shows the amount of phosphorylated STAT1 (pSTAT1) and total STAT1 (tSTAT1) in MOLM-13 cells in response to 1µM AZA. The blot is representative for six independent experiments *(n=6)*. The ratio of pSTAT1/β-actin and tSTAT1/β-actin at D0, D4, and D8 is normalised to D0. **(C)** Western blot analysis shows the amount of HLA-DR in MOLM-13 cells in response to 1µM AZA. The blot is representative for six independent experiments *(n=6)*. The ratio of HLA-DR/β-actin at D0, D4, and D8 is normalised to D0.

4.5.2 CTLA-4^{negative} CAR T cells are associated with lower levels of regulatory T (T$_{reg}$) cells *in vivo*

The CTLA-4 expression pathway and T$_{regs}$ are essential for immune homeostasis. In certain cases, upregulation of CTLA-4 and T$_{regs}$ serves an immunoregulatory function, suppressing the T cell response, when required, to avoid autoimmune responses. In the context of anti-tumour responses, increased CTLA-4 expression and/or increased numbers of T$_{regs}$ are undesirable and hampers the anti-tumour activity of T cells against the leukaemic cells (Walker, 2013)(N. Daver, Garcia-Manero, et al., 2019).

To investigate whether CTLA-4^{positive} CAR T cells are associated with increased T$_{regs}$, BM and PB CD4^{+} T cells were analysed for T$_{regs}$ in mice that were treated with CTLA-4^{positive} and CTLA-4^{negative} CD123 CAR T cells.

MOLM-13 AML xenograft mice were injected with either CTLA-4^{positive} or CTLA-4^{negative} CAR T cells on day 7 following confirmation of leukaemia engraftment. Analysis of the BM showed that mice injected with CTLA-4^{positive} CAR T cells remained CTLA-4^{positive} at day 28 following infusion *(Manuscript Figure 7)* and this was indeed associated with a high percentage (>60%) of CD4^{+} T$_{reg}$ cells *(Figure 4.4 A).*

In contrast, mice that were injected with CTLA-4^{negative} CAR T cells revealed more than 80% remaining CTLA-4^{negative} in the BM 28 days following infusion *(Manuscript Figure 7).* This was associated with low levels of (< 20%) CD4^{+} T$_{reg}$ cells *(Figure 4.4 A).* In the PB, the same trend was observed. Mice that were injected with CTLA-4^{positive} CAR T cells revealed a significantly higher percentage of T$_{regs}$ compared to mice injected with CTLA-4^{negative} CAR T cells (97% vs. 18%) *(Figure 4.4 B).*

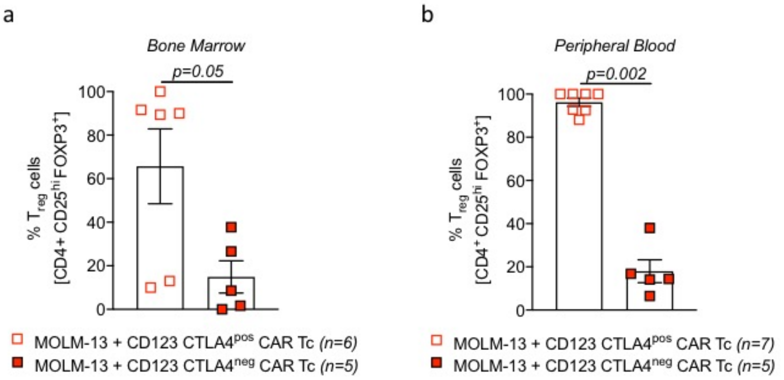

Figure 4.4. Analysis of regulatory CD4^{+} T cells in the BM and PB of MOLM-13 AML xenograft mice treated with CTLA-4^{negative} or CTLA-4^{positive} CD123 CAR T cells.
Scatter plot graphs depicting the expression of CD4^{+} T$_{reg}$ in the **(A)** BM and **(B)** PB of mice treated with CTLA-4^{negative} or CTLA-4^{positive} CD123 CAR T cells. All data were pooled from 2 independent experiments and presented as mean ± SEM. *P*-values were calculated using unpaired Student's *t*-test (Mann-Whitney).

4.5.3 Direct application of Azacitidine does not promote an inhibitory effect on the CAR T cells *in vitro*

Since AZA is ineffective at eradicating AML LSCs alone, several small studies have trialled simultaneous applications of AZA with DLI in AML patients. Due to the broad mechanism of action, these studies hypothesised that AZA may impact the quality or extent of the T cell anti-tumour response. One such study reported immunosuppressive properties in mice (Sánchez-Abarca et al., 2010) which prompted a more comprehensive study investigating the impact of AZA and DLI on T cell response in AML patients.

CD4^{+} T cells rely on epigenetic mechanisms to regulate lineage commitment (Wilson et al., 2009). It has previously been documented that the master regulator of T$_{regs}$, FOXP3, is strongly regulated by methylation. Furthermore, memory function and IFN-γ production in CD8^{+} T cells has also been reported to be controlled by methylation (Lal et al., 2009) (Chappell et al., 2006) (Kersh, 2006).

Although the data so far demonstrates that treatment with AZA at the indicated concentrations did not promote an inhibitory CAR T cell phenotype both *in vitro* and *in vivo,* it was important to confirm that AZA does not directly impact the CAR T cells. To answer this question, CD123 CAR T cells generated from 4 different HD's were co-cultured for 96h in the absence or presence (1μM or 5μM) of AZA. The data demonstrated that AZA did not have a direct impact on $CD4^+$ or $CD8^+$ T cell polarisation. Furthermore, no differences were seen in the levels of $CD4^+$ and $CD8^+$ CAR T cells regardless of AZA concentration *(Figure 4.5 A).*

Within the $CD4^+$ T cell compartment, no significant increase was observed in the percentage of T_{regs} between $CD4^+$ CAR T cells cultured in 1μM AZA and $CD4^+$ CAR T cells cultured in media only. A significant increase in the percentage of T_{regs} was, however, observed in the $CD4^+$ CAR T cells cultured in 5μM AZA compared to $CD4^+$ CAR T cells cultured in media only *(Figure 4.5 B).* Co-culture of CAR T cells with 5μM AZA led to significant decreases in PD-$1^{negative}$TIM-$3^{negative}$ $CD8^+$ CAR T cells compared to CAR T cells cultured with 1μM AZA or media only *(Figure 4.5 C).* The data suggests that AZA may directly increase immunosuppressive T cell responses at higher concentrations. However, at the concentrations that this study was carried out with, AZA does not seem to promote inhibitory CAR T cells.

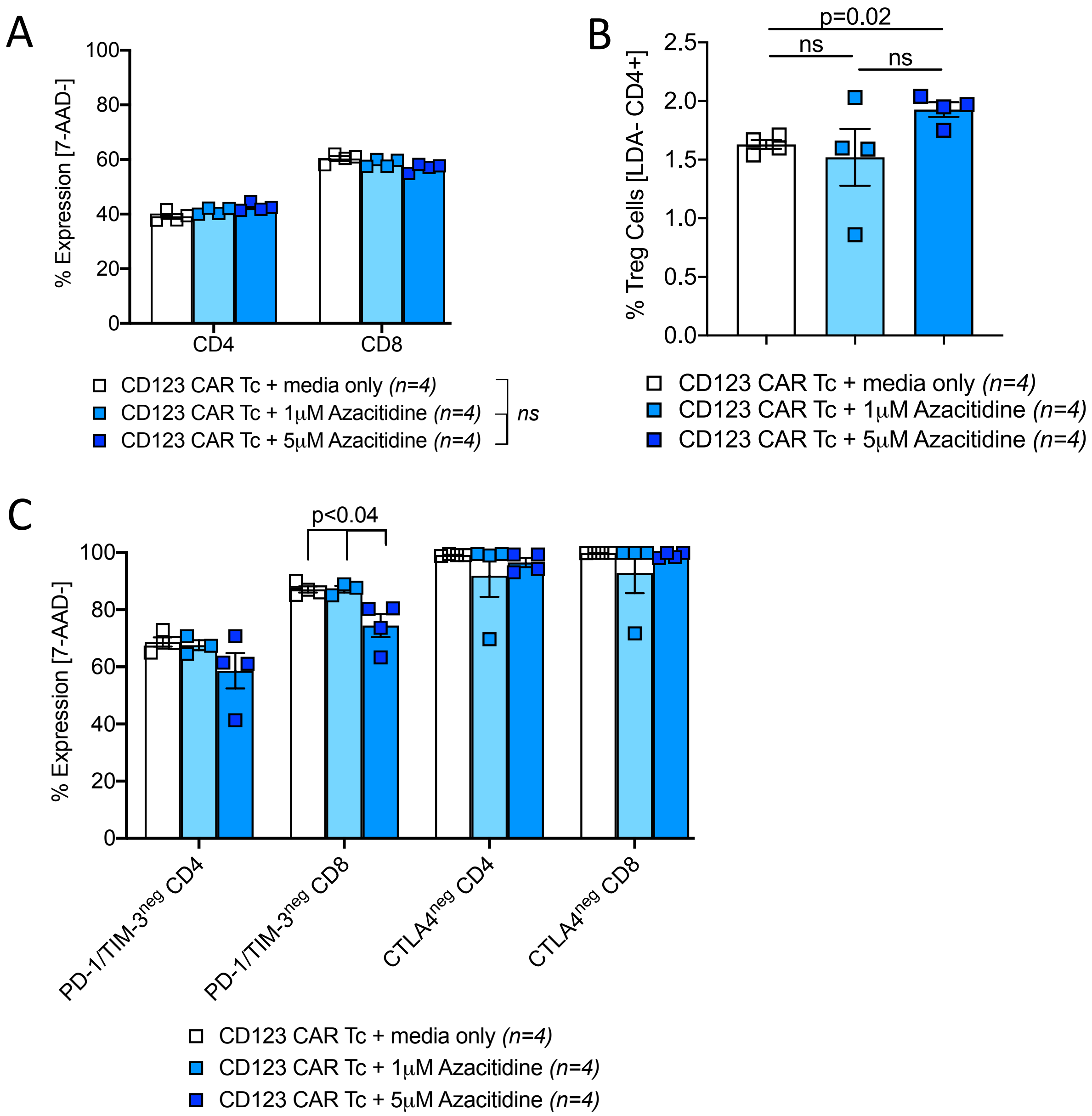

Figure 4.5. Exogenous application of Azacitidine does not promote inhibitory CD123 CAR T cells *in vitro*.

Scatter plot graphs depicting the expression of **(A)** CD4$^+$ and CD8$^+$ CAR T cells in the presence or absence of AZA following a 96h co-culture. **(B)** CD4$^+$ CAR T cells were further analysed for presence of T$_{regs}$ in the presence or absence of AZA following a 96h co-culture. **(C)** CD4$^+$ and CD8$^+$ CAR T cells were analysed for PD-1^{negative} TIM-3^{negative} and CTLA-4^{negative} expression following a 96h co-culture in the presence or absence of AZA. Data was graphed from experiments using CAR T cells generated from 4 HD's and presented as mean ± SEM. *P*-values were calculated using 1-way ANOVA.

Chapter 5

CONCLUSION & FUTURE PERSPECTIVES

5.1 Thesis Discussion & Future Perspectives

AML is an aggressive disease that incorporates a diverse landscape of genetic and epigenetic mutations. The therapeutic platform for which to effectively treat AML, has remained largely unchanged for many decades. Consequently, very few AML patients are able to achieve a durable remission following a first attempt with therapeutic intervention. Recent advances in research has proven that immunotherapeutic strategies have the capability to eradicate chemotherapy-resistant leukaemic clones thereby providing long-term disease control. Allo-hSCT is one of the oldest and most successful forms of immunotherapeutic strategies for post-remission therapy in AML. However, the vast majority of older patients are ineligible for allo-hSCT due to frailty and lack of suitable donors and, in some cases, relapse following allo-hSCT also occurs (Lichtenegger et al., 2017). Therefore, alternative immunotherapeutic strategies are urgently required.

The adoptive transfer of gene modified T cells (CAR T cells) is a rapidly evolving field of cancer immunotherapy. Although encouraging clinical data have been reported for AML by targeting various different antigens, the potential bench-to-bedside translation to date, has been much less inspiring. Currently, a major focus of CAR T cells for AML is to prevent on-target, off-tumour toxicities while ensuring anti-leukaemic efficacy and long-term activity remain intact.

The central aim of this thesis was to develop novel third generation CAR T cells to enhance the immunotherapeutic platform for the treatment of AML. In the work described in this thesis, several third-generation anti-CD123 CAR T cells were developed and characterised (Chapter 3). The anti-CD123-CD28-OX40-SF CAR demonstrated superior and robust performance following various functional testing *in vitro* and was therefore tested for anti-leukaemic efficacy *in vivo*. While no off-tumour toxicities were observed, the anti-CD123-CD28-OX40-SF CAR T cells demonstrated modest cytolytic capacity of AML cells in xenograft mouse models. As a consequence, incomplete eradication of the leukaemia was observed.

Combination therapy with the HMA, AZA, was therefore explored with the aim of boosting CAR T cell efficacy and longevity (Chapter 4). In this context, it was hypothesised that AZA would boost tumour cell visibility by upregulating the target antigen, CD123. Indeed, the work in this thesis identified that pre-treatment of AML cells with AZA increased the target antigen on the AML cell surface. Consequently, these anti-CD123 CAR T cells were found to eradicate AML *in vivo* and demonstrated a survival advantage over CAR T cell monotherapy.

Numerous mechanisms could be responsible for this increased tumour recognition. As this is the first study to observe such findings, the underlying mechanisms have not been reported on within the literature at present. My data, as shown in chapter 4 revealed a novel finding that pre-treatment of AML cells with AZA also increased intracellular retention of CTLA-4 in $CD4^+$ anti-CD123 CAR T cells. This suggested that besides increasing tumour cell visibility, priming of AML cells with AZA also induced T cell reactivity.

Under normal circumstances, CTLA-4 is known to be expressed following activation of T cells. CTLA-4 has a greater affinity for the CD80 and CD86 ligands present on the target cells. In turn, the expression of CD28 is reduced (Rotte et al., 2018). The loss of co-stimulation through CD28 leads to cessation of cell proliferation and cytokine production thereby increasing the number of immunosuppressive T_{reg} cells. This, therefore, restricts the extent and strength of the immune response to the malignant cells (Condomines et al., 2015) (Yoon et al., 2018). In cancer, the malignant cells use this mechanism to escape immune surveillance (Yoon et al., 2018).

In this case, pre-treatment of AML cells with AZA seemed to prevent or delay this process. It remains unclear what changes to the AML cells, beyond epigenetic modifications, occur following AZA treatment that could be formally correlated with the induced immune response. Therefore, future studies are warranted to further characterise the events occurring at the immunological synapse between CAR T cells and AZA-primed AML cells to provide further mechanistic insight.

The data presented in this thesis sought to elucidate how increased intracellular retention of CTLA-4 in the CAR T cells following exposure to AZA-primed AML cells contributed to increased T cell responses. It is known that sustained surface expression of CTLA-4 effectively blocks the formation of Zap-70 containing micro-clusters in T cells (Schneider et al., 2008). In this project, intracellular retention of CTLA-4 was associated with continued and sustained phosphorylation of Lck and Zap-70. As a result, this allowed the CAR T cells to be more efficacious, providing enhanced anti-leukaemic activity (duration and response) against AML.

Until recently, it was unclear whether CAR to antigen ligation activates CAR T cells using entirely conserved endogenous TCR signal transduction mechanisms. However, recently it was suggested that CARs are capable of recapitulating canonical T cell activation and function. How CAR design specifically influences these signalling events is an area of active investigation at present (Lindner et al., 2020) .

Following antigen recognition by the TCR, the immediate downstream consequences are initiated by LcK. In turn, LcK phosphorylates the tyrosines in immune-receptor tyrosine-based activation motifs (ITAMs). Additionally, LcK facilitates CD4 or CD8 co-receptor recruitment to strengthen the antigen:TCR interaction thereby creating a positive feedback loop to recruit additional LcK (Nika et al., 2010)(Casas et al., 2014)(Jiang et al., 2011).

The phosphorylation of the 10 ITAMs within the TCR complex serve as recruitment and activation sites for Zap70 further activating downstream signalling proteins (Love & Hayes, 2010)(Jiang et al., 2011) . In contrast to the signalling events that occur in TCRs, CARs contain only 3 ITAMs (6 if they dimerise) and function through co-receptor independent phosphorylation of CD3 ITAMs (Lindner et al., 2020).

It has been shown that the choice of co-stimulatory domain can greatly influence CD3ζ ITAM phosphorylation. While ITAM phosphorylation occurs in the same position upon ligation of antigen and the CAR T cells, the intensity of phosphorylation is greater in CD28-containing compared to 4-1BB-containing CAR T cells. This phenomenon was likely due to the proline-rich region of CD28 with which LcK associates (Salter et al., 2018)(Ramello et al., 2019).

Mutations to CD28 demonstrated a significant decrease in phosphorylation of CD3ζ upon CAR ligation (Salter et al., 2018). This suggested that CD28 in CARs act in a similar fashion to co-receptors in the TCR complex, and recruit LcK to potentiate a positive feedback loop. These observations are all based on early responses to CAR and target cell ligation. The role of Lck and its impact on long-term CAR T cell efficacy as well as its influence on T_{reg} induction or resistance is currently an area of active research (Kofler et al., 2011) (Suryadevara et al., 2019).

Following phosphorylation, Zap-70 is recruited and docks via the dual SH2 domains and consequently phosphorylates a number of downstream substrates. Recruitment and phosphorylation of Zap-70 is usually mediated 24h following stimulation. However, it should be noted that other factors such as CAR density and affinity and/or T cell phenotype can affect this process. It remains elusive, at present, how CARs recruit proximal signalling molecules and should be further interrogated in future studies (Drent et al., 2019)(Karlsson et al., 2015).

A recent study (Gudipati et al., 2020) showed that while the CAR outperformed the TCR with regards to antigen binding at the immunological synapse, antigen sensitivity was compromised. The investigators could show that CAR-proximal signalling was significantly attenuated due to inefficient recruitment of Zap-70 and therefore resulted in reduced concomitant activation and subsequent release of pro-inflammatory cytokines. Cycling of Zap-70 is integral to the signal amplification and the initiation of downstream signalling cascades (Katz et al., 2017). Inefficient Lck-mediated ITAM phosphorylation and Zap-70 activation therefore contribute to decreased CAR T cell responsiveness to low antigen levels.

It may therefore be a possibility that the reduced cytolytic capacity of the CAR T cells over time could be a result of this. However, future studies are required to quantitatively investigate the differences in Lck and Zap-70 membrane recruitment, phosphorylation, and synaptic turnover in antigen engaged CAR T cells over a prolonged period of time. Furthermore, comparison should be made to CAR T cells engaged to AZA-primed AML antigens. This would allow for better elucidation on how AZA can indirectly maintain antigen sensitivity by the CAR T cells.

While increased CD123 expression on the AML cells following AZA administration is hypothesized to be the main reason for increased efficacy of the CD123 CAR T cells, the epigenetic changes to the AML cells that allows for this effect to be seen has not been explored extensively in this project. As a follow up to the data presented here, the project would benefit from detailed methylome studies. This may help clarify whether CD123, the ligands on the AML cell that bind CTLA-4 on the CAR T cell, and other loci that regulate or enhance an interferon response by the AML cells could be responsible or, at least, contribute to the increased and long-term efficacy seen by the CD123 CAR T cells.

5.2 Conclusion

In conclusion, data presented in this thesis demonstrate, for the first time, that anti-leukaemic functions of the third generation anti-CD123 CAR T cells characterised here can be enhanced with prior treatment of primary AML cells with AZA. This thesis provides evidence that the LAA, CD123, can be augmented with treatment of AML cells with AZA. Further investigation identified that AZA primed AML cells induced a CTLA-4^{negative} CAR T cell population which may be responsible for enhanced leukaemia control. Additionally, these CTLA-4^{negative} CAR T cells were able to demonstrate increased signalling events immediately downstream of CAR ligation.

Based on the findings observed in this thesis, prolonged proximal CAR signalling events beyond early responses to CAR ligation may be imperative for long term and enhanced CAR efficacy. The novel findings presented in this thesis pave the way for exploring the therapeutic efficacy of AZA and anti-CD123 CAR T cells in a world first clinical trial for AML patients who are treatment refractory and/or ineligible for allo-hSCT.

Chapter 6

APPENDIX

6.1. CAR Construct Full DNA Sequences

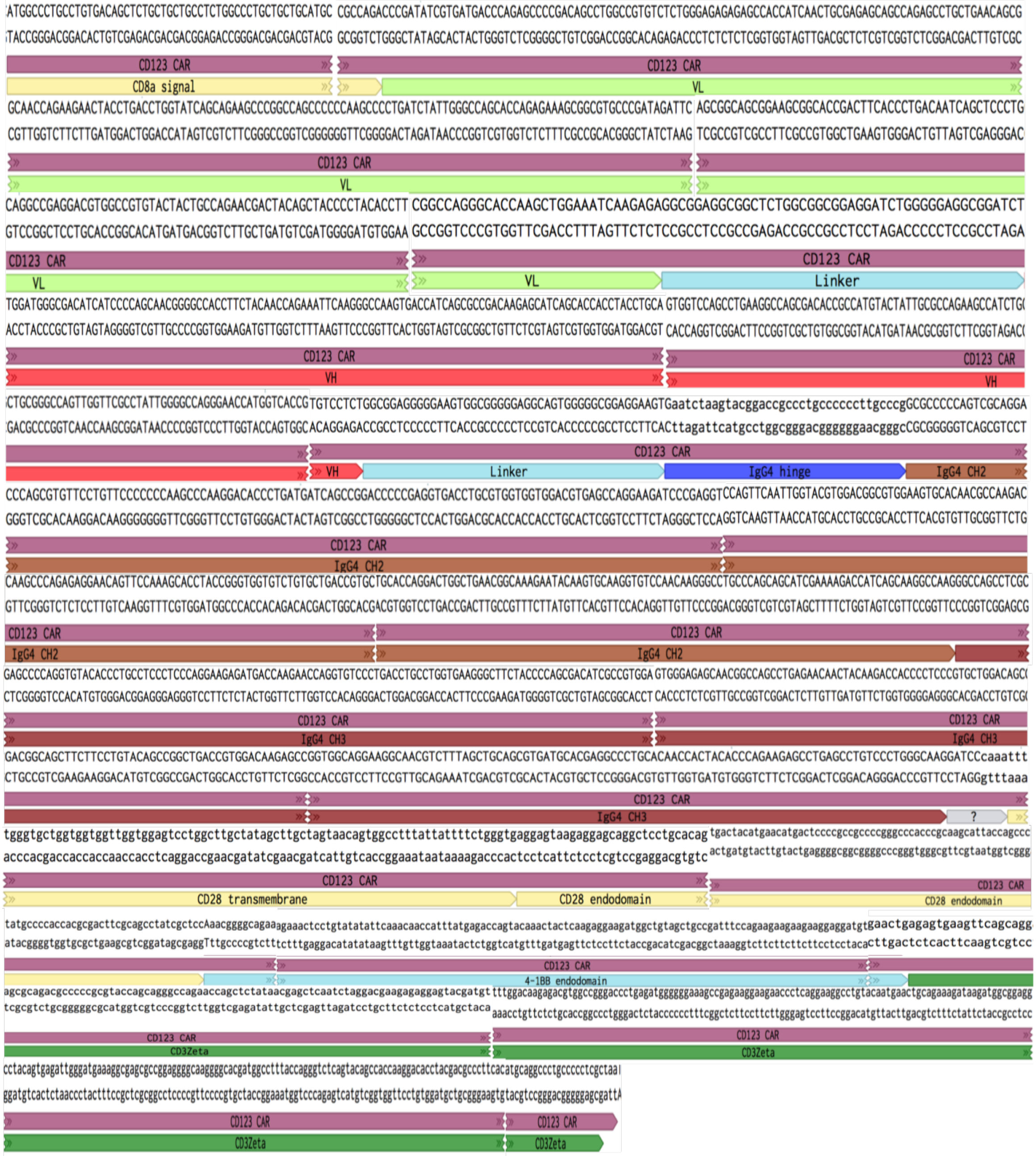
CD123 CAR
CD8a signal
VL
Linker
VH
IgG4 hinge
IgG4 CH2
IgG4 CH3
?
CD28 transmembrane
CD28 endodomain
4-1BB endodomain
CD3Zeta

Figure 6.1. Schematic representation of the anti-CD123 (CSL362) CD28-41BB-LF CAR DNA sequence. The DNA sequence first includes the scFv, a linker sequence, the IgG4 extended hinge, the CD28 and 4-1BB co-stimulatory signalling domains, and finally the CD3ζ.

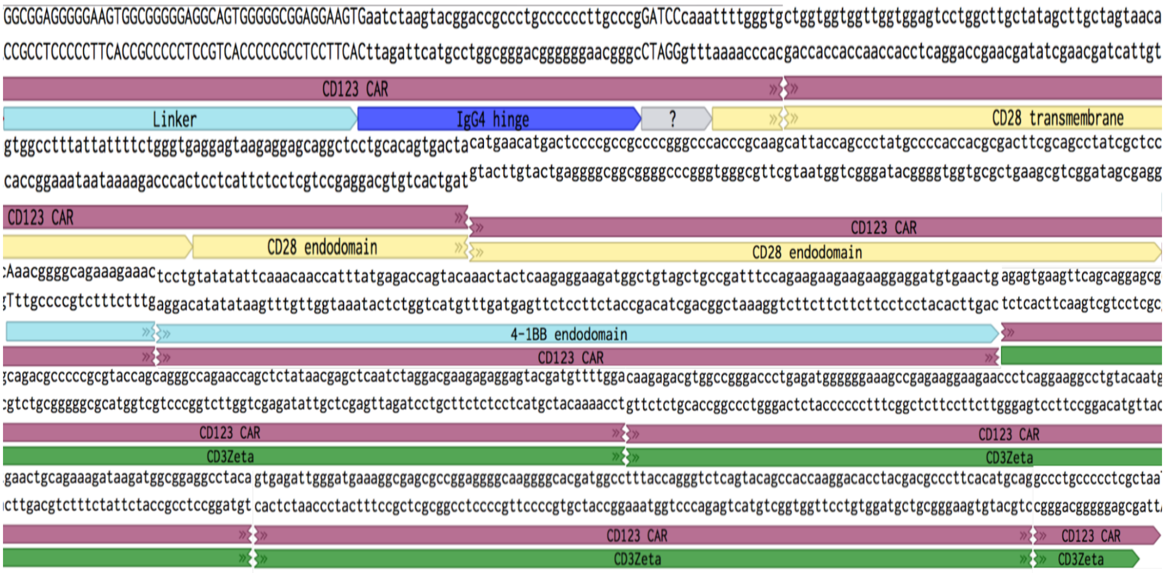
CD123 CAR
Linker
IgG4 hinge
?
CD28 transmembrane
CD123 CAR
CD123 CAR
CD28 endodomain
CD28 endodomain
4-1BB endodomain
CD123 CAR
CD123 CAR
CD123 CAR
CD3Zeta
CD3Zeta
CD123 CAR
CD123 CAR
CD3Zeta
CD3Zeta

Figure 6.2. Schematic representation of the anti-CD123 (CSL362) CD28-41BB-SF CAR DNA sequence. The DNA sequence first includes the scFv (not shown, but represented in Figure 6.1), a linker sequence, the IgG4 (short) hinge, the CD28 and 4-1BB co-stimulatory signalling domains, and finally the CD3ζ.

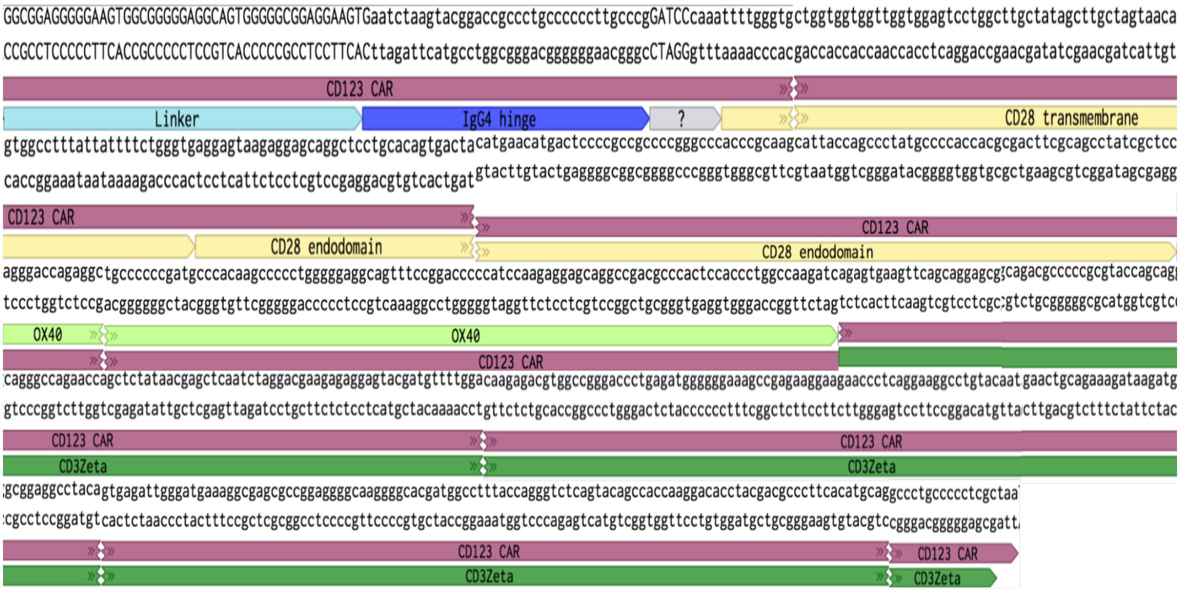
CD123 CAR
Linker
IgG4 hinge
?
CD28 transmembrane
CD123 CAR
CD123 CAR
CD28 endodomain
CD28 endodomain
OX40
OX40
CD123 CAR
CD123 CAR
CD123 CAR
CD3Zeta
CD3Zeta
CD123 CAR
CD123 CAR
CD3Zeta
CD3Zeta

Figure 6.3. Schematic representation of the anti-CD123 (CSL362) CD28-OX40-SF CAR DNA sequence. The DNA sequence first includes the scFv (not shown, but represented in Figure 6.1), a linker sequence, the IgG4 (short) hinge, the CD28 and OX40 co-stimulatory signalling domains, and finally the CD3ζ.

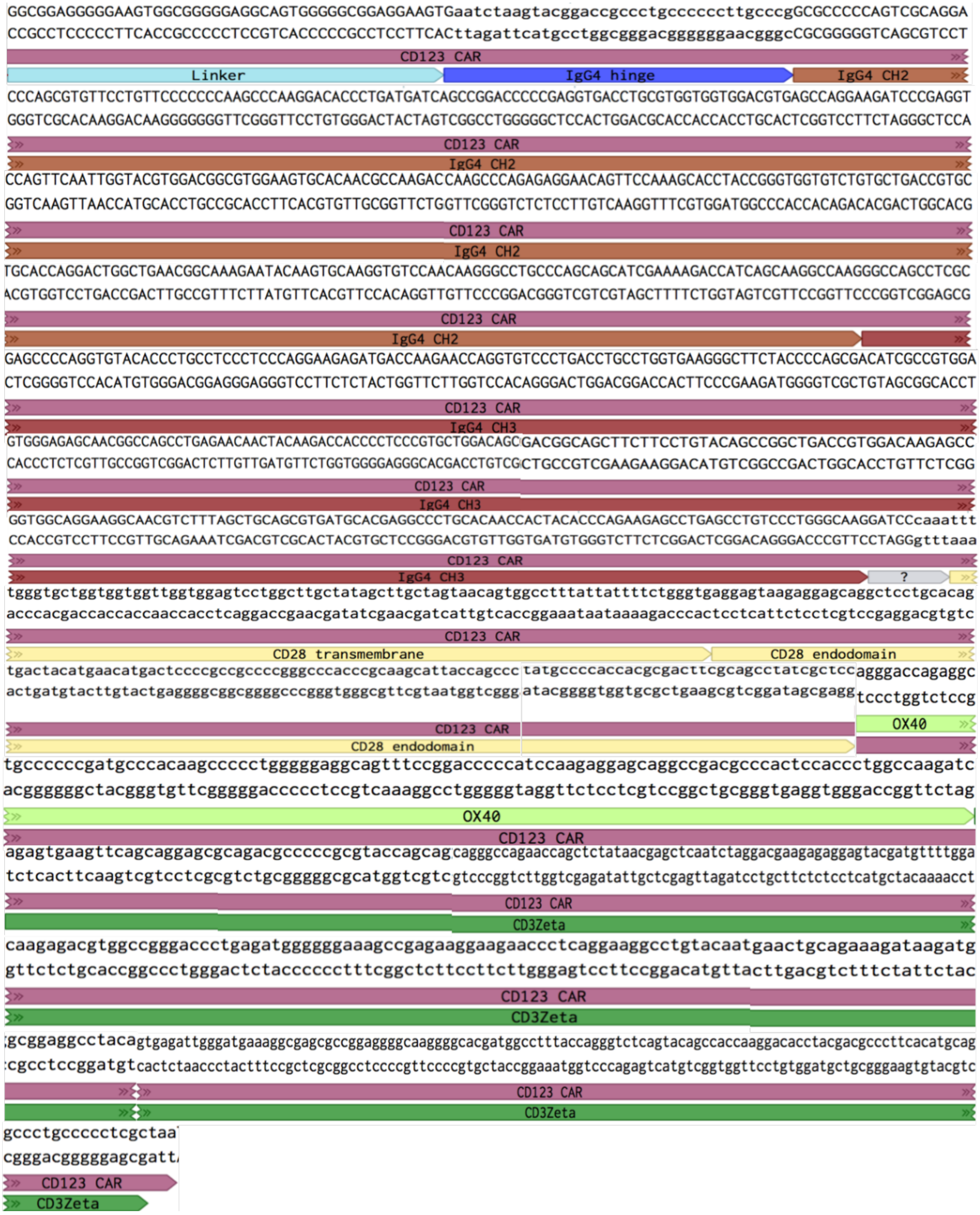
CD123 CAR
Linker
IgG4 hinge
IgG4 CH2
IgG4 CH3
?
CD28 transmembrane
CD28 endodomain
OX40
CD3Zeta

Figure 6.4. Schematic representation of the anti-CD123 (CSL362) CD28-OX40-LF CAR DNA sequence. The DNA sequence first includes the scFv (not shown, but represented in Figure 6.1), a linker sequence, the IgG4 extended hinge, the CD28 and OX40 co-stimulatory signalling domains, and finally the CD3ζ.

6.2. List of All Consumables & Reagents

Table 6.2.1: Supplier details of specialised reagents, reagent kits, and consumables

Product	Supplier	Catalogue No.
Ampicillin, Ready-made solution 100mg/mL	Sigma Aldrich	A5354-10mL
Aqua ad injectabilia	Braun	8609255
5-Azacytidine	Sigma Aldrich/Merck Millipore	A2385-100MG
BD compensation beads (FACS)	BD Bioscience	552843
BD CS&T beads	BD Bioscience	656505
Biotin-conjugated Protein-L 1mg	Genscript/Assay Matrix	M00097
Bovine Serum Albumin (BSA)	Sigma Aldrich	A7030-100G
β-mercaptoethanol	Sigma Aldrich GIBCO	M6250 31350
Celltrace Violet Cell Proliferation Stain Kit	Life technologies, Thermo Fischer Scientific	C34557
WesternBright Chemiluminescent Substrate Quantum	Biozym Scientific GmbH	541015
Countbright Beads 5mL	Life technologies	C36950
Dimethyl-sulphoxide (DMSO)	Roth Sigma-Aldrich	A994.2 D2438
D-Luciferin Firefly Potassium Salt	Biosynth	FL08608/L-8220
Dnase 1 grade II 100mg	Roche Applied Science (Sigma Aldrich)	10104159001
Dulbecco's Phosphate Buffered Saline (DPBS) (without $CaCl_2$ and $MgCl_2$)	Sigma Aldrich	D8537-500mL
Dulbecco's Modified Eagle's Medium (DMEM-high glucose)	Sigma Aldrich	D6429-6x500ML
Dynabeads, Human T-activator CD3/CD28	Life technologies	11131D

Eosin	Thermo Fisher Scientific	6766009
Ethanol	J.T Baker	9401-33
Fetal Bovine Serum (FBS)	Sigma Aldrich	12003C-500ml
Forene (isoflurane)	Abbott Laboratories	5260:B506
Formaldehyde (4%, pH6.9)	Merck	100496
Haematoxylin	Dako	S3301
Hanks Balanced Salt Solution (HBSS) with $NaHCO_3$, without $CaCl_2$ & $MgSO_4$	Sigma Aldrich	H9394-100mL
Hexadimethrine bromide (Polybrene)	Sigma Aldrich	107689-10G
Hi-speed Plasmid Midi Kit (25)	Qiagen	12643
Human FcR Blocking Reagent	Miltenyi Biotec	130-059-901
Human IL3RA/CD123 Protein (His & Fc Tag) 20µg	Sinobiological/Jomar life research	10518-H03H-20
Human recombinant IL-2 (10µg)	Peprotech/Lonza	200-02
Human Pan T-cell Isolation Kit	Miltenyi Biotec	130-096-535
Lenti-X Concentrator	Clontech/Scientifix	631231
L-glutamine-Penicillin-Streptomycin Solution	Sigma Aldrich GIBCO	G6784 15140
Live/Dead Fixable Aqua Dead Cell stain kit	Life technologies	L34957
Live/Dead Fixable Far Red Dead cell stain kit	Life technologies	L10120
Lipofectamine 3000 transfection reagent 0.1mL	Life technologies	L3000-001
LS columns (25)	Miltenyi Biotec	130-042-401
Lymphoprep	Stemcell technologies	7861
MACs Seperation buffer	Miltenyi Biotec	130-091-221
MES Running Buffer Concentrate	Thermo Fisher Scientific	NP002
Methocult Opti	Stem Cell Technologies	H3404
Millipore Milliplex Human	Abacus, Merck	MPHCYTMAG6

Cytokine/Chemokine pre-mixed 30-plex kit	Millipore	0KPX30
Neomycin sulfate	Gibco/Thermo Fisher	21810031
NuPage Antioxidant	Thermo Fisher Scientific	NP0005
NuPage Bis-Tris Gels, variable sizes	Thermo Fisher Scientific	NP0332BOX, NP0335BOX
NuPage LDS Buffer	Thermo Fisher Scientific	NP0007
NuPage Sample Reducing Agent	Thermo Fisher Scientific	NP0009
PageRuler™ Prestained Protein Ladder, 10-180kDa	Thermo Fisher Scientific	26616
Opti-MEM Reduced Serum Medium 100mL	Thermo Fisher Scientific	31985062
Penicillin/Streptomycin	GIBCO	15140
Pierce recombinant Protein-L, Biotinylated, 0.5mg	Thermo Fisher Scientific	29997
Poly-D-lysine solution	Merck Millipore	A-003-E
Polyvinylidene difluoride (PVDF) transfer membrane	GE Healthcare	RPN303F
Protein transport inhibitor monensin (BD GolgiStop)	BD Bioscience	554724
Purified Mouse IgG1-κ Isotype Control	BD Bioscience	554121
QiAzol Lysis Reagent	Qiagen	79306
Recombinant Human Stem Cell Factor (SCF)	Peprotech	300-07
Retronectin Recombinant Human Fibronectin Fragment	Takara/Scientifix	T100B
RIPA Lysis Buffer	Santa Cruz	sc-24948
RPMI-1640 Medium	Sigma Aldrich	R0883-500mL
Staphylococcus aureus, Enterotoxin Type B (SEB)	Merck Millipore	324798-500µg

Syringe filter unit 0.45µM, PVDF membrane	Merck Millipore	SLGV033RS
Thinwall Polypropylene Tube, 14mL, 14x95mm	Beckman Coulter	331374
Thinwall Open-Top Ultraclear Tubes, 38.5mL, 25x89mm	Beckman Coulter	344058
Transfer Buffer	Thermo Fisher Scientific	NP0006-1
Triton X-100	Merck Millipore	1086431000
Trypan Blue Solution (0.4%)	Thermo Fisher Scientific	15250-061
Trypsin-EDTA 0.05% (1x)	Gibco	25-300-054
Tween 20	Sigma Aldrich	P7949
UltraComp eBeads Compensation Beads	eBioscience	01-2222-42
24 well non-tissue culture treated plates	VWR International	FAL351147
CD34 Ultrapure Microbead kit	Miltenyi Biotec	130-100-453
2-Propanol	Roth	AE73.1

Table 6.2.2: Supplier details of general consumables used

Product	Supplier
Cannulae, Sterile (18-27 gauge)	B. Braun
Cell Culture Flasks (T25-T175)	Sarstedt
Cell Culture Plates (6-48 wells)	Sarstedt
Cell Culture Plates (96 wells), round and flat bottom	BD Falcon
Conical tubes (15mL, 50mL)	Greiner bio-one
Centrifuge tube-15mL, 50mL	Greiner bio-one
Cover glass for microscope slides	Lagenbrinck
Cryogenic vials (2mL)	Corning
CELLSTAR Easy strainer (70µM, 100µM)	Greiner bio-one
Eppendorfs tubes, sterile (1.5mL, 2mL)	Eppendorf
Insulin syringes, U-100 0.5mL, sterile	B. Braun
Microscope slides	Langenbrinck

Parafilm M	American National Can
Pipette tips with filter, sterile (10, 20, 200, and 1000µL)	Biozym
Pipette tips without filter, sterile, (10, 20, 200, and 1000µL)	Corning
Polypropylene Round bottom tubes (5mL)	Corning
Polystyrene Round bottom tubes (5mL)	Corning
Polystyrol-tube (FACS)	BD Falcon
Roti Histo Kit	Carl Roth GmbH
Safe-lock tubes (1.5mL, 2mL)	Eppendorf
Scalpels, disposable	Feather
Stripette serological pipettes (5mL, 10mL, 25mL)	Corning
Syringe filter unit 0.22µM	Pall Corporation
Syringes Luer Lock (5mL, 10mL, 20mL)	Braun
Syringes Luer Solo 20mL	Braun

Table 6.2.3: Fluorochrome-conjugated flow cytometry antibodies

Antibody	**Clone**	**Catalogue number**	**Flourochrome**	**Vendor**
Anti-human CD3	SK7	344824	Pacific Blue	Biolegend
Anti-human CD3	UCHT1	560835	PerCP-Cy5.5	BD Bioscience
Anti-human CD3	OKT3	317333	PeCy7	Biolegend
Anti-human CD3	HIT3a	300312	APC	Biolegend
Anti-human CD3	HIT3a	300306	FITC	Biolegend
Anti-human CD4	SK3	11-0047-42	FITC	eBioscience
Anti-human CD95	DX2	555674	PE	BD Bioscience
Anti-human CD8	RPA-T8	555369	APC	BD Bioscience
Anti-human CD8	BW135/80	130-113-162	Pacific Blue	Miltenyi Biotec
Anti-human CD8	RPA-T8	563677	BV711	BD Bioscience
Anti-human CD45RO	UCHL1	25-0427-42	PeCy7	eBioscience
7-Aminoactinomycin D (7-AAD)	N/A	559925	PerCP-Cy5.5	BD Bioscience
Anti-human CD27	0323	47-0279-42	APC-ef780	eBioscience
Anti-human CD45RA	HI100	304138	BV711	Biolegend
Anti-human CD45RA	HI100	560675	PeCy7	BD Bioscience
Anti-human CD45	2D1	347463	FITC	BD Bioscience
Anti-human CD45	2D1	560178	APC-H7	BD Bioscience

Anti-human CD123	7G3	558714	PerCP-Cy5.5	BD Bioscience
Anti-human CD123	7G3	560826	PeCy7	BD Bioscience
Anti-human CD279 (PD-1)	EH12.2H7	329904	FITC	Biolegend
Anti-human CD279 (PD-1)	EH12.1	560795	PE	BD Bioscience
Anti-human CD152 (CTLA-4)	BN13	563931	BV786	BD Bioscience
Anti-human CD152 (CTLA-4)	L3D10	349908	APC	Biolegend
Anti-human CD152 (CTLA-4)	14D3	11-1529-42	FITC	BD Bioscience
Anti-human CD336 (TIM-3)	7D3	565564	BV650	BD Bioscience
Anti-human CD223 (LAG-3)	T47-530	565716	Alexa Flour 647	BD Bioscience
Live Dead Aqua	N/A	555516	V500/Amcyan	Invitrogen/Thermo Fischer Scientific
Anti-human Lin-Cocktail (CD3, CD14, CD16, CD19, CD20, CD56)	UCHT1; HCD14;3G8;HIB19:2H7:HCD56	348805	Pacific Blue	Biolegend
Anti-human CD38	LS198-4-3	A99022	ECD	Beckman Coulter
Anti-human CD34	581	561440	Alexa Fluor 700	BD Bioscience
Anti-human CD13	WM15	561599	PeCy7	BD Bioscience
Anti-human CD33	WM53	561157	V450	BD Bioscience
Anti-human CD127	HIL-7R-M21	560823	BV421	BD Bioscience
Anti-human FOXP3	236A/E7	17-4777-42	APC	eBioscience
Anti-human CD25	2A3	341009	PE	BD Bioscience
Anti-human CD90	5E10	562686	BV650	BD Bioscience
Anti-human CLL-1	50C1	562569	FITC	BD Bioscience
Anti-human CD107a	H4A3	555800	FITC	BD Bioscience
Streptavidin-Conjugated PE	N/A	349023	PE	BD Bioscience
Pierce Biotinylated recombinant Protein-L	N/A	21189	N/A	Thermo Fischer Scientific
Anti-human TNF	Mab11	502909	PE	Biolegend
Anti-human IFN-γ	4S.B3	502512	APC	Biolegend
Anti-human IgG (Fc-		12-4998-82	PE	eBioscience

gamma specific)				

Table 6.2.4: Supplier details of reagents and kits used for CD123 CAR T cell cloning

Reagent	Supplier	Catalogue No.
CutSmart Digestion Buffer	New England Biolabs (NEB)	B7204S
XbaI Restriction enzyme	New England Biolabs (NEB)	R0145T
AatII Restriction enzyme	New England Biolabs (NEB)	R0117L
EcoRV-HF Restriction enzyme	New England Biolabs (NEB)	R3195T
BamHI Restriction enzyme	New England Biolabs (NEB)	R0136T
SacI-HF Restriction enzyme	New England Biolabs (NEB)	R3156S
Gel Loading dye (6X)	New England Biolabs (NEB)	B7024S
Gel red dye	Biotium	41003
1kb DNA ladder	New England Biolabs (NEB)	N3200S
PureLink PCR Purification kit	Invitrogen/Thermofisher	K3100-01
DNA Polymerase I, Large (Klenow) Fragment	New England Biolabs (NEB)	M0212S
dNTPs	New England Biolabs (NEB)	0447S
EDTA	Sigma	E-5134
Antarctic Phosphatase and Buffer	New England Biolabs (NEB)	M0289S
T4 DNA ligase	New England Biolabs (NEB)	M0202S
T4 DNA Ligase Reaction Buffer	New England Biolabs (NEB)	B0202S
DH5-α E.Coli competent cells	New England Biolabs (NEB)	C2987I
S.O.C medium	ThermoFisher Scientific	15544-034
PureLink Quick Plasmid Miniprep kit	Invitrogen/ThermoFisher	K2100-10
Qiagen Plasmid Midiprep kit	Qiagen	12143
Kanamycin	Sigma	K4000

6.3 Solutions, Buffers, and Cell Culture Media

Table 6.3.1: Recipes of all solutions, buffers, and cell culture media used

Name	Recipe
Adherent Cell Line Culture Media (HEK-293T)	500mL DMEM +50mL FCS (final conc. 10%) +5mL L-glutamine-Pen-Strep (final conc. 1%) +50µM β-mercaptoethanol (final conc.1:1000) *Media was sterile-filtered (0.22µM), stored at 4°C and preheated to 37°C in a water bath prior to use.*
Cell Thaw Media	50mL RPMI-1640 +5mL FCS (final conc. 10%) +0.02mg/mL DNase1
Erythrocyte lysis (Erylysis) buffer	500mL ddH_20 + 40.13g NH_4Cl +0.5g $KHCO_3$ +1.0mL 0.5M EDTA
FACS buffer	500mL 1xPBS + 10mL FCS (final conc. 2%) +2.1mL 5% sodium azide (final conc. 0.02%) +375mg EDTA (Titriplex III)
FACS buffer (CAR T cell staining)	500mL 1x PBS
Freeze Mix	9mL FCS (final conc. 90%) 1mL DMSO (final conc. 10%) *Solution made fresh each time for freezing cells*
Human T lymphocyte Culture Media	500mL RPMI-1640 +100mL FCS (final conc. 20%) +5mL L-glutamine-Pen-Strep (final conc. 1%) +50µM β-mercaptoethanol (final conc.1:1000) *Media was sterile-filtered (0.22µM), stored at 4°C and preheated to 37°C in a water bath prior to use.*

Non-Adherent Cell line culture Media (KG1a, MOLM-13, SUPB15, HL-60, ML-2, Jurkat)	500mL RPMI-1640 +50mL FCS (final conc. 10%) +5mL L-glutamine-Pen-Strep (final conc. 1%) +50µM β-mercaptoethanol (final conc.1:1000) *Media was sterile-filtered (0.22µM), stored at 4°C and preheated to 37°C in a water bath prior to use.*
PBS (10x)	80g NaCl 2g KH_2PO4 2g KCl 11.5g Na_2HPO_4 pH 7.4
RIPA Lysis Buffer	50mL 1x RIPA +500µL PMSF+10µL Sodium orthovanadate +500µL Protease Inhibitor +500µL Phosphatase Inhibitor Cocktail (P5726 Sigma-Aldrich)
Retronectin Blocking Buffer	50mL 1xPBS +1g BSA (final conc. 2%) *Solution was filter sterilized (0.22µM) and stored at 4°C up to 2 weeks*
TAE (50x)	242g Tris in 500mL H_2O 100mL 0.5M EDTA 57.1mL blacial acetic acid fill up to 1L with H_2O
TBS (10x)	+60.5g Tris Ultra pure +87.6g NaCl Dissolve in ddH20 Adjust pH 7.6 with HCl Fill up to 1L
Transfection Media (HEK-293T)	500mL high-glucose DMEM +50mL FCS (final conc. 10%) *Media was sterile-filtered (0.22µM), stored at 4°C and preheated to 37°C in a water bath prior to use.*

6.4 General Laboratory Techniques

6.4.1 Cryopreservation of Cells

Cells (Cell lines and Patient PBMCs) were pelleted and re-suspended in 1-2mL of Freeze Mix per $5x10^6$-$1x10^7$ cells and quickly transferred to pre-cooled cryo-ampoules (Nalgene/Corning). The cryo-ampoules were frozen to -80°C using a 'Mr Frosty' container (Nalgene) for a minimum of 6h. Samples were then transferred and stored in liquid nitrogen (-175 to -196°C). Samples were stored until use if not required in the immediate future.

6.4.2 Thawing of Cells

Cells were removed from liquid nitrogen and thawed rapidly in a 37°C water bath. In a laminar flow hood, the cell suspension was quickly transferred drop-wise to a 50mL Falcon tube containing 5mL of thaw media (pre-warmed). With continuous mixing, approximately 20mL of thaw media was added drop-wise to dilute the DMSO. The sample volume was topped up to 30mL with thaw media and cells were pelleted by centrifugation at 400 *x g* for 10mins at room temperature. The supernatant was aspirated and the procedure was repeated to remove any residual DMSO before culturing.

6.4.3 Lymphoprep Isolation of Peripheral Blood Mononuclear cells (PBMNCs)

PB or BM aspirates (40-60mL) from patients with AML or HD were collected in lithium heparin tubes. All samples were collected with informed consent in accordance with the Institutional Ethics approved protocols and with reference to the Declaration of Helsinki. In Adelaide, lymphoprep Isolation of PBMNCs was performed by transferring a maximum of 15mL of blood into a 50mL polypropylene conical tube (Falcon tube). The blood volume was brought to 35mL with HBSS and underlain with 15mL of lymphoprep solution. Tubes were centrifuged at 300 *x g* for 30min with no brake. The interface containing the PBMNCs (opaque layer) was then carefully transferred to a new 50mL Falcon tube using a transfer pipette and topped up to 50mL with HBSS. Cells were washed twice with HBSS and centrifuged at 1400rpm, 10mins @ RT. A cell count was performed as described in 2.3.4 and cells were frozen down at a concentration of $5x10^6$-$5x10^7$ as described in 2.3.1. In Germany, isolation of PBMNCs was performed by transferring a maximum of 15mL of blood into a 50mL Falcon tube. The blood volume was brought to 35mL with 1x PBS and overlain with 15mL of Pancoll solution. Tubes were centrifuged at 400 *x g* for 30min with no brake. The interface containing the PBMNCs (opaque layer) was then carefully transferred to a new

50mL Falcon tube using a transfer pipette and topped up to 5mL with 1x PBS. Cells were washed twice with HBSS and centrifuged at 1400rpm, 10mins @ RT. A cell count was performed as described in 2.3.4 and cells were frozen down at a concentration of $5x10^6$-$5x10^7$ as described in 2.3.1.

6.4.4 Cell Counts and Viability

Patient PBMNC cell concentration was determined by diluting the cell suspension in white cell fluid (WCF). Viability of patient PBMNCs and cell lines was determined by diluting the cell samples with trypan blue solution (usually 1:10). 15uL of the suspension was transferred to a hemocytometer counting chamber (Neubauer Improved, Assistant, Germany) and cell concentration and viability was calculated accordingly as shown below.

Number of Viable Cells/mL:

(Average cell count from each set of 16 squares) x 10^4 x dilution factor

= total cells/mL

E.g. $((25 + 39)/2) \times 10^4 \times 10 = 3.2\times10^6$ *cells/mL*

6.5 Maintenance & Culture of Cell lines

6.5.1 Cell Line Specifications

KG1a cells were originally derived from bone marrow of a 59-year-old Caucasian male with promyeloblast AML and obtained from the American Type Tissue Culture Collection CLL-246.1 (ATCC, Manassas, VA).

Jurkat T-cells were derived from the peripheral blood of a 14-year-old male with acute T lymphocyte leukemia and obtained from the American Type Tissue Culture Collection CLL-246.1 (ATCC, Manassas, VA).

HEK-293T cells are epithelial cells that were originally derived from the embryonic kidney of a fetus and obtained from the American Type Tissue Culture Collection CRL-3216 (ATCC, Manassas, VA).

SUPB15 cells were originally derived from the bone marrow of an 8-year-old Caucasian male with B-lymphoblastic leukaemia and kindly provided by Prof. Deborah White, SAHMRI, Adelaide, SA.

MOLM-13 cells were established from the peripheral blood of a 20-year-old Caucasian man with Flt-3 ITD AML. MOLM-13 cells were transfected with the firefly luciferase reporter gene which also included a GFP reporter gene in the vector (kindly provided by Prof. Dr. Nikolas von Bubnoff, University of Freiburg, Freiburg, Germany). The resultant MOLM-13 luciferase+ cells were selected and cultured in (1mg/ml) neomycin. Luciferase expression was confirmed by regular BLI screening.

HL60 cells were established from the peripheral blood of a 36-year-old Caucasian female with promyelocytic AML. The cells were kindly provided by Prof. Dr. Robert Zeiser, University of Freiburg, Freiburg, Germany.

ML-2 cells originated from the peripheral blood of a 26-year-old Caucasian man with AML and were kindly provided by Prof. Dr. Robert Zeiser, University of Freiburg, Freiburg, Germany.

6.5.2 Culture of General Cell lines

All tissue culture techniques were performed under sterile conditions in a Class two 'biohazard' laminar flow hood (Nuaire, In vitro Technologies, Model #S480-400E). Adherent cell lines (HEK-293T) were maintained at a cell density between $5x10^5$-$1x10^6$ cells/mL in $75cm^2$ tissue culture flasks. Suspension cell lines (KG1a, SUPB-15, MOLM-13, Jurkat, HL60, ML-2) were maintained at a cell density between $1x10^5$ and $1x10^6$ cells/mL in $25cm^2$, $75cm^2$ or $175cm^2$ tissue flasks (Falcon, Sigma Aldrich). Media was pre-warmed to 37°C prior to use. Cultures were incubated in a 37°C/5% CO_2 incubator. Cell cultures were checked every 2-3 days for contamination, counted and re-cultured at the above concentrations. For adherent cell lines, cells were rinsed twice with room temperature 1x PBS and trypsinized at 37°C for 2-5mins with 0.25% trypsin. Cell aggregates were separated by pipetting and suspending in fresh media devoid of trypsin. Cells were centrifuged at 400 *x g*, 4°C for 10mins and re-cultured in the above concentrations in fresh media. All cell lines were regularly checked for mycoplasma.

6.6 Instruments & Equipment

Table 6.6.1: List of instruments and equipment used

Instrument	Supplier
Autoclave	Vakulal S 3000
Centrifuges:	
Sorvall WX80 Ultra series ultracentrifuge	Thermo Fischer Scientific
Multifuge X3R	Thermo Fischer Scientific
Multifuge X1R	Thermo Fischer Scientific
Multifuge IS-R	Thermo Fischer Scientific
Microcentrifuge 5424R	Eppendorf
Coverstainer, H&E automated stainer	Dako
ECL Chemocam Imager	Intas Imaging
Electric pipettor, pipetboy	Integra Bioscience
CANTO II, LSR Fortessa Cytometers	BD Biosciences
Haemocytometer	Neubauer
Ice Machine	Ziegra

Incubator	Heraeus
LaminAir 2448, Laminar flow hood	Heraeus
Lamina flow hood, Nuaire #S480-400E	In Vitro Technologies
Microtome	Leica
Nanodrop 1000	Peqlab
Nitrogen tank	Air Liquide
Refrigerator, 4°C	Liebherr
RS-2000 X-ray Irradiator	Rad Source Technologies
Surgical Dissection kit	Aesculap
Vortex	Heidolph Reax 2000
Water bath	Lauda MGW C20
Weighing Scale	Sartorius CL420
-20°C freezer	Siemens
-80°C freezer	Heraeus

6.7 Data Analysis Software

Table 6.7.1: List of software programs used

Name	Application	Developer
Diva v8.0.1	Flow cytometry acquisition	BD Biosciences
Flowjo v10	Flow cytometry analysis	Tree Star, Inc.
Image J	Western Blotting Analysis/quantification	National Institute of Health
Lab Image 1D v4.1	Western Blotting Acquisition	Intas Science Imaging GmbH
Microsoft Office Profession Plus 2010	Word processor, presentation, spreadsheets	Microsoft, Inc.
Prism v7.01 and v8	Graphical and statistical analyses	GraphPad Software, Inc.
Tierbase 4D v12.6	Mouse strain management and ordering	4D Deutschland, GmbH

REFERENCES

Aigner, M., Feulner, J., Schaffer, S., Kischel, R., Kufer, P., Schneider, K., Henn, A., Rattel, B., Friedrich, M., Baeuerle, P. A., Mackensen, A., & Krause, S. W. (2013). T lymphocytes can be effectively recruited for ex vivo and in vivo lysis of AML blasts by a novel CD33/CD3-bispecific BiTE antibody construct. *Leukemia*, *27*(5), 1107–1115. https://doi.org/10.1038/leu.2012.341

Alfei, F., Kanev, K., Hofmann, M., Wu, M., Ghoneim, H. E., Roelli, P., Utzschneider, D. T., von Hoesslin, M., Cullen, J. G., Fan, Y., Eisenberg, V., Wohlleber, D., Steiger, K., Merkler, D., Delorenzi, M., Knolle, P. A., Cohen, C. J., Thimme, R., Youngblood, B., & Zehn, D. (2019). TOX reinforces the phenotype and longevity of exhausted T cells in chronic viral infection. *Nature*, *571*(7764), 265–269. https://doi.org/10.1038/s41586-019-1326-9

Algarra, I., Collado, A., & Garrido, F. (1997). Altered MHC class I antigens in tumors. *International Journal of Clinical & Laboratory Research*, *27*(2–4), 95–102. https://doi.org/10.1007/BF02912442

Al-Hussaini, M., Rettig, M. P., Ritchey, J. K., Karpova, D., Uy, G. L., Eissenberg, L. G., Gao, F., Eades, W. C., Bonvini, E., Chichili, G. R., Moore, P. A., Johnson, S., Collins, L., & DiPersio, J. F. (2016). Targeting CD123 in acute myeloid leukemia using a T-cell–directed dual-affinity retargeting platform. *Blood*, *127*(1), 122–131. https://doi.org/10.1182/blood-2014-05-575704

Al-Mawali, A., Pinto, A. D., & Al-Zadjali, S. (2017). CD34+CD38-CD123+ Cells Are Present in Virtually All Acute Myeloid Leukaemia Blasts: A Promising Single Unique Phenotype for Minimal Residual Disease Detection. *Acta Haematologica*, *138*(3), 175–181. https://doi.org/10.1159/000480448

Anderson, A. C., Joller, N., & Kuchroo, V. K. (2016). Lag-3, Tim-3, and TIGIT: Co-inhibitory Receptors with Specialized Functions in Immune Regulation. *Immunity*, *44*(5), 989–1004. https://doi.org/10.1016/j.immuni.2016.05.001

Annibali, O., Crescenzi, A., Tomarchio, V., Pagano, A., Bianchi, A., Grifoni, A., & Avvisati, G. (2018). PD-1 /PD-L1 checkpoint in hematological malignancies. *Leukemia Research*, *67*, 45–55. https://doi.org/10.1016/j.leukres.2018.01.014

Arcangeli, S., Rotiroti, M. C., Bardelli, M., Simonelli, L., Magnani, C. F., Biondi, A., Biagi, E., Tettamanti, S., & Varani, L. (2017). Balance of Anti-CD123 Chimeric Antigen Receptor Binding Affinity and Density for the Targeting of Acute Myeloid Leukemia. *Molecular Therapy*, *25*(8), 1933–1945. https://doi.org/10.1016/j.ymthe.2017.04.017

Australian Institute of Health and Welfare. (2017). *Cancer in Australia, 2017*.

Baeuerle, P. A., & Reinhardt, C. (2009). Bispecific T-Cell Engaging Antibodies for Cancer Therapy: Figure 1. *Cancer Research*, *69*(12), 4941–4944. https://doi.org/10.1158/0008-5472.CAN-09-0547

Baumeister, S. H., Murad, J., Werner, L., Daley, H., Trebeden-Negre, H., Gicobi, J. K., Schmucker, A., Reder, J., Sentman, C. L., Gilham, D. E., Lehmann, F. F., Galinsky, I., DiPietro, H., Cummings, K., Munshi, N. C., Stone, R. M., Neuberg, D. S., Soiffer, R., Dranoff, G., … Nikiforow, S. (2019). Phase I Trial of Autologous CAR T Cells Targeting NKG2D Ligands in Patients with AML/MDS and Multiple Myeloma. *Cancer Immunology Research*, *7*(1), 100–112. https://doi.org/10.1158/2326-6066.CIR-18-0307

Bengsch, B., Ohtani, T., Khan, O., Setty, M., Manne, S., O'Brien, S., Gherardini, P. F., Herati, R. S., Huang, A. C., Chang, K.-M., Newell, E. W., Bovenschen, N., Pe'er, D., Albelda, S. M., & Wherry, E. J. (2018). Epigenomic-Guided Mass Cytometry Profiling Reveals Disease-Specific Features of Exhausted CD8 T Cells. *Immunity*, *48*(5), 1029-1045.e5. https://doi.org/10.1016/j.immuni.2018.04.026

Betts, M. R., & Koup, R. A. (2004). Detection of T-cell degranulation: CD107a and b. *Methods in Cell Biology*, *75*, 497–512. https://doi.org/10.1016/s0091-679x(04)75020-7

Blank, C., Gajewski, T. F., & Mackensen, A. (2005). Interaction of PD-L1 on tumor cells with PD-1 on tumor-specific T cells as a mechanism of immune evasion: Implications for tumor immunotherapy. *Cancer Immunology, Immunotherapy*, *54*(4), 307–314. https://doi.org/10.1007/s00262-004-0593-x

Bleakley, M., & Riddell, S. R. (2004). Molecules and mechanisms of the graft-versus-leukaemia effect. *Nature Reviews Cancer*, *4*(5), 371–380. https://doi.org/10.1038/nrc1365

Bôle-Richard, E., Fredon, M., Biichlé, S., Anna, F., Certoux, J.-M., Renosi, F., Tsé, F., Molimard, C., Valmary-Degano, S., Jenvrin, A., Warda, W., Pallandre, J.-R., Bonnefoy, F., Poussard, M., Deschamps, M., Petrella, T., Roumier, C., Macintyre, E., Féger, F., … Garnache-Ottou, F. (2020). CD28/4-1BB CD123 CAR T cells in blastic plasmacytoid dendritic cell neoplasm. *Leukemia*, *34*(12), 3228–3241. https://doi.org/10.1038/s41375-020-0777-1

Bonifant, C. L., Jackson, H. J., Brentjens, R. J., & Curran, K. J. (2016). Toxicity and management in CAR T-cell therapy. *Molecular Therapy - Oncolytics*, *3*, 16011. https://doi.org/10.1038/mto.2016.11

Bose, P., Rahmani, M., & Grant, S. (2012). Coordinate PI3K pathway and Bcl-2 family disruption in AML. *Oncotarget*, *3*(12), 1499–1500. https://doi.org/10.18632/oncotarget.809

Bross, P. F., Beitz, J., Chen, G., Chen, X. H., Duffy, E., Kieffer, L., Roy, S., Sridhara, R., Rahman, A., Williams, G., & Pazdur, R. (2001). Approval summary: Gemtuzumab ozogamicin in relapsed acute myeloid leukemia. *Clinical Cancer Research: An Official Journal of the American Association for Cancer Research*, *7*(6), 1490–1496.

Brudno, J. N., & Kochenderfer, J. N. (2016). Toxicities of chimeric antigen receptor T cells: Recognition and management. *Blood*, *127*(26), 3321–3330. https://doi.org/10.1182/blood-2016-04-703751

Brunner, A. M., Li, S., Fathi, A. T., Wadleigh, M., Ho, V. T., Collier, K., Connolly, C., Ballen, K. K., Cutler, C. S., Dey, B. R., El-Jawahri, A., Nikiforow, S., McAfee, S. L., Koreth, J., Deangelo, D. J., Alyea, E. P., Antin, J. H., Spitzer, T. R., Stone, R. M., … Chen, Y.-B. (2016). Haematopoietic cell transplantation with and without sorafenib maintenance for patients with *FLT3* -ITD acute myeloid leukaemia in first complete remission. *British Journal of Haematology*, *175*(3), 496–504. https://doi.org/10.1111/bjh.14260

Bu, J. Y., Shaw, A. S., & Chan, A. C. (1995). Analysis of the interaction of ZAP-70 and syk protein-tyrosine kinases with the T-cell antigen receptor by plasmon resonance. *Proceedings of the National Academy of Sciences of the United States of America*, *92*(11), 5106–5110. https://doi.org/10.1073/pnas.92.11.5106

Burnet, F. M. (1970). The Concept of Immunological Surveillance. In R. S. Schwartz (Ed.), *Progress in Tumor Research* (Vol. 13, pp. 1–27). S. Karger AG. https://doi.org/10.1159/000386035

Burnett, A. K., Russell, N. H., Hills, R. K., Kell, J., Freeman, S., Kjeldsen, L., Hunter, A. E., Yin, J., Craddock, C. F., Dufva, I. H., Wheatley, K., & Milligan, D. (2012). Addition of Gemtuzumab Ozogamicin to Induction Chemotherapy Improves Survival in Older Patients With Acute Myeloid Leukemia. *Journal of Clinical Oncology*, *30*(32), 3924–3931. https://doi.org/10.1200/JCO.2012.42.2964

Busfield, S. J., Biondo, M., Wong, M., Ramshaw, H. S., Lee, E. M., Martin, K., Ghosh, S., Braley, H., Tomasetig, V., Panousis, C., Vairo, G., Roberts, A. W., He, S. Z., Sprigg, N., Thomas, D., DeWitte, M., Lock, R. B., Lopez, A. F., & Nash, A. (2012). CSL362: A Monoclonal Antibody to Human Interleukin-3 Receptor (CD123), Optimized for NK Cell-Mediated Cytotoxicity of AML Stem Cells. *Blood*, *120*(21), 3598–3598. https://doi.org/10.1182/blood.V120.21.3598.3598

Calabrò, L., Danielli, R., Sigalotti, L., & Maio, M. (2010). Clinical Studies With Anti–CTLA-4 Antibodies in Non-melanoma Indications. *Seminars in Oncology*, *37*(5), 460–467. https://doi.org/10.1053/j.seminoncol.2010.09.006

Carpenito, C., Milone, M. C., Hassan, R., Simonet, J. C., Lakhal, M., Suhoski, M. M., Varela-Rohena, A., Haines, K. M., Heitjan, D. F., Albelda, S. M., Carroll, R. G., Riley, J. L., Pastan, I., & June, C. H. (2009). Control of large, established tumor xenografts with genetically retargeted human T cells containing CD28 and CD137 domains. *Proceedings of the National Academy of Sciences*, *106*(9), 3360–3365. https://doi.org/10.1073/pnas.0813101106

Caruso, H. G., Hurton, L. V., Najjar, A., Rushworth, D., Ang, S., Olivares, S., Mi, T., Switzer, K., Singh, H., Huls, H., Lee, D. A., Heimberger, A. B., Champlin, R. E., & Cooper, L. J. N. (2015). Tuning Sensitivity of CAR to EGFR Density Limits Recognition of Normal Tissue While Maintaining Potent

Antitumor Activity. *Cancer Research*, *75*(17), 3505–3518. https://doi.org/10.1158/0008-5472.CAN-15-0139

Casas, J., Brzostek, J., Zarnitsyna, V. I., Hong, J., Wei, Q., Hoerter, J. A. H., Fu, G., Ampudia, J., Zamoyska, R., Zhu, C., & Gascoigne, N. R. J. (2014). Ligand-engaged TCR is triggered by Lck not associated with CD8 coreceptor. *Nature Communications*, *5*(1), 5624. https://doi.org/10.1038/ncomms6624

Castaigne, S., Pautas, C., Terré, C., Renneville, A., Gardin, C., Suarez, F., Caillot, D., Berthon, C., Rousselot, P., Preudhomme, C., Morisset, L., Celli Lebras, K., Chevret, S., & Dombret, H. (2014). Final Analysis of the ALFA 0701 Study. *Blood*, *124*(21), 376–376. https://doi.org/10.1182/blood.V124.21.376.376

Chabner, B. A., & Oliverio, V. T. (1975). Drug Interactions in Cancer Chemotherapy. In J. R. Gillette & J. R. Mitchell (Eds.), *Concepts in Biochemical Pharmacology* (pp. 325–342). Springer Berlin Heidelberg. https://doi.org/10.1007/978-3-642-46314-3_13

Chappell, C., Beard, C., Altman, J., Jaenisch, R., & Jacob, J. (2006). DNA Methylation by DNA Methyltransferase 1 Is Critical for Effector CD8 T Cell Expansion. *The Journal of Immunology*, *176*(8), 4562–4572. https://doi.org/10.4049/jimmunol.176.8.4562

Cheever, M. A., Allison, J. P., Ferris, A. S., Finn, O. J., Hastings, B. M., Hecht, T. T., Mellman, I., Prindiville, S. A., Viner, J. L., Weiner, L. M., & Matrisian, L. M. (2009). The Prioritization of Cancer Antigens: A National Cancer Institute Pilot Project for the Acceleration of Translational Research. *Clinical Cancer Research*, *15*(17), 5323–5337. https://doi.org/10.1158/1078-0432.CCR-09-0737

Cheson, B. D., Bennett, J. M., Kopecky, K. J., Büchner, T., Willman, C. L., Estey, E. H., Schiffer, C. A., Doehner, H., Tallman, M. S., Lister, T. A., Lo-Coco, F., Willemze, R., Biondi, A., Hiddemann, W., Larson, R. A., Löwenberg, B., Sanz, M. A., Head, D. R., Ohno, R., & Bloomfield, C. D. (2003). Revised Recommendations of the International Working Group for Diagnosis, Standardization of Response Criteria, Treatment Outcomes, and Reporting Standards for Therapeutic Trials in Acute Myeloid Leukemia. *Journal of Clinical Oncology*, *21*(24), 4642–4649. https://doi.org/10.1200/JCO.2003.04.036

Collins, A. V., Brodie, D. W., Gilbert, R. J. C., Iaboni, A., Manso-Sancho, R., Walse, B., Stuart, D. I., van der Merwe, P. A., & Davis, S. J. (2002). The interaction properties of costimulatory molecules revisited. *Immunity*, *17*(2), 201–210. https://doi.org/10.1016/s1074-7613(02)00362-x

Colmone, A., Amorim, M., Pontier, A. L., Wang, S., Jablonski, E., & Sipkins, D. A. (2008). Leukemic Cells Create Bone Marrow Niches That Disrupt the Behavior of Normal Hematopoietic Progenitor Cells. *Science*, *322*(5909), 1861–1865. https://doi.org/10.1126/science.1164390

Condomines, M., Arnason, J., Benjamin, R., Gunset, G., Plotkin, J., & Sadelain, M. (2015). Tumor-

Targeted Human T Cells Expressing CD28-Based Chimeric Antigen Receptors Circumvent CTLA-4 Inhibition. *PLOS ONE*, *10*(6), e0130518. https://doi.org/10.1371/journal.pone.0130518

Cortes, J. E., Khaled, S., Martinelli, G., Perl, A. E., Ganguly, S., Russell, N., Krämer, A., Dombret, H., Hogge, D., Jonas, B. A., Leung, A. Y.-H., Mehta, P., Montesinos, P., Radsak, M., Sica, S., Arunachalam, M., Holmes, M., Kobayashi, K., Namuyinga, R., … Levis, M. J. (2019). Quizartinib versus salvage chemotherapy in relapsed or refractory FLT3-ITD acute myeloid leukaemia (QuANTUM-R): A multicentre, randomised, controlled, open-label, phase 3 trial. *The Lancet Oncology*, *20*(7), 984–997. https://doi.org/10.1016/S1470-2045(19)30150-0

Cortes, J., Perl, A. E., Döhner, H., Kantarjian, H., Martinelli, G., Kovacsovics, T., Rousselot, P., Steffen, B., Dombret, H., Estey, E., Strickland, S., Altman, J. K., Baldus, C. D., Burnett, A., Krämer, A., Russell, N., Shah, N. P., Smith, C. C., Wang, E. S., … Levis, M. (2018). Quizartinib, an FLT3 inhibitor, as monotherapy in patients with relapsed or refractory acute myeloid leukaemia: An open-label, multicentre, single-arm, phase 2 trial. *The Lancet Oncology*, *19*(7), 889–903. https://doi.org/10.1016/S1470-2045(18)30240-7

Courtney, A. H., Lo, W.-L., & Weiss, A. (2018). TCR Signaling: Mechanisms of Initiation and Propagation. *Trends in Biochemical Sciences*, *43*(2), 108–123. https://doi.org/10.1016/j.tibs.2017.11.008

Craddock, C., Quek, L., Goardon, N., Freeman, S., Siddique, S., Raghavan, M., Aztberger, A., Schuh, A., Grimwade, D., Ivey, A., Virgo, P., Hills, R., McSkeane, T., Arrazi, J., Knapper, S., Brookes, C., Davies, B., Price, A., Wall, K., … Vyas, P. (2013). Azacitidine fails to eradicate leukemic stem/progenitor cell populations in patients with acute myeloid leukemia and myelodysplasia. *Leukemia*, *27*(5), 1028–1036. https://doi.org/10.1038/leu.2012.312

Croft, M., So, T., Duan, W., & Soroosh, P. (2009). The significance of OX40 and OX40L to T-cell biology and immune disease. *Immunological Reviews*, *229*(1), 173–191. https://doi.org/10.1111/j.1600-065X.2009.00766.x

Curran, K. J., Seinstra, B. A., Nikhamin, Y., Yeh, R., Usachenko, Y., van Leeuwen, D. G., Purdon, T., Pegram, H. J., & Brentjens, R. J. (2015). Enhancing Antitumor Efficacy of Chimeric Antigen Receptor T Cells Through Constitutive CD40L Expression. *Molecular Therapy*, *23*(4), 769–778. https://doi.org/10.1038/mt.2015.4

Daver, N., Basu, S., Garcia-Manero, G., Cortes, J., Ravandi, F., Kornblau, S., Konopleva, M., Andreeff, M., Borthakur, G., Jain, N., Wierda, W., Verstovsek, S., Ruvolo, P., Kadia, T., Matthews, J., Flores, W., Yang, H., Bueso-Ramos, C., Somani, N., … Sharma, P. (2016). Abstract 3205: Defining the immune checkpoint landscape of acute myeloid leukemia (AML). *Immunology*, 3205–3205. https://doi.org/10.1158/1538-7445.AM2016-3205

Daver, N., Cortes, J., Ravandi, F., Patel, K. P., Burger, J. A., Konopleva, M., & Kantarjian, H. (2015). Secondary mutations as mediators of resistance to targeted therapy in leukemia. *Blood*, *125*(21), 3236–3245. https://doi.org/10.1182/blood-2014-10-605808

Daver, N. G., Erba, H. P., Papadantonakis, N., De Angelo, D. J., Wang, E. S., Konopleva, M., Sloss, C. M., Culm-Merdek, K., Zweilder-Mckay, P. A., & Kantarjian, H. M. (2018). *A phase I, First-in-human study evaluating the safety and preliminary antileukemia activity of IMGN632, a novel CD123-tergeting antibody-drug conjugate, in patients with relapsed/refractory acute myeloid leukemia and other CD123-positive hematologic malignancies. 132*, 27.

Daver, N., Garcia-Manero, G., Basu, S., Boddu, P. C., Alfayez, M., Cortes, J. E., Konopleva, M., Ravandi-Kashani, F., Jabbour, E., Kadia, T., Nogueras-Gonzalez, G. M., Ning, J., Pemmaraju, N., DiNardo, C. D., Andreeff, M., Pierce, S. A., Gordon, T., Kornblau, S. M., Flores, W., … Kantarjian, H. (2019). Efficacy, Safety, and Biomarkers of Response to Azacitidine and Nivolumab in Relapsed/Refractory Acute Myeloid Leukemia: A Nonrandomized, Open-Label, Phase II Study. *Cancer Discovery*, *9*(3), 370–383. https://doi.org/10.1158/2159-8290.CD-18-0774

Daver, N., Schlenk, R. F., Russell, N. H., & Levis, M. J. (2019). Targeting FLT3 mutations in AML: Review of current knowledge and evidence. *Leukemia*, *33*(2), 299–312. https://doi.org/10.1038/s41375-018-0357-9

Davids, M. S., Kim, H. T., Bachireddy, P., Costello, C., Liguori, R., Savell, A., Lukez, A. P., Avigan, D., Chen, Y.-B., McSweeney, P., LeBoeuf, N. R., Rooney, M. S., Bowden, M., Zhou, C. W., Granter, S. R., Hornick, J. L., Rodig, S. J., Hirakawa, M., Severgnini, M., … Soiffer, R. J. (2016). Ipilimumab for Patients with Relapse after Allogeneic Transplantation. *New England Journal of Medicine*, *375*(2), 143–153. https://doi.org/10.1056/NEJMoa1601202

Davila, M. L., Riviere, I., Wang, X., Bartido, S., Park, J., Curran, K., Chung, S. S., Stefanski, J., Borquez-Ojeda, O., Olszewska, M., Qu, J., Wasielewska, T., He, Q., Fink, M., Shinglot, H., Youssif, M., Satter, M., Wang, Y., Hosey, J., … Brentjens, R. (2014). Efficacy and Toxicity Management of 19-28z CAR T Cell Therapy in B Cell Acute Lymphoblastic Leukemia. *Science Translational Medicine*, *6*(224), 224ra25-224ra25. https://doi.org/10.1126/scitranslmed.3008226

del Campo, A. B., Carretero, J., Aptsiauri, N., & Garrido, F. (2012). Targeting HLA class I expression to increase tumor immunogenicity. *Tissue Antigens*, *79*(3), 147–154. https://doi.org/10.1111/j.1399-0039.2011.01831.x

DiNardo, C. D., Pratz, K., Pullarkat, V., Jonas, B. A., Arellano, M., Becker, P. S., Frankfurt, O., Konopleva, M., Wei, A. H., Kantarjian, H. M., Xu, T., Hong, W.-J., Chyla, B., Potluri, J., Pollyea, D. A., & Letai, A. (2019). Venetoclax combined with decitabine or azacitidine in treatment-naive, elderly patients with acute myeloid leukemia. *Blood*, *133*(1), 7–17. https://doi.org/10.1182/blood-2018-08-868752

Döhner, H., Dolnik, A., Tang, L., Seymour, J. F., Minden, M. D., Stone, R. M., Del Castillo, T. B., Al-Ali, H. K., Santini, V., Vyas, P., Beach, C. L., MacBeth, K. J., Skikne, B. S., Songer, S., Tu, N., Bullinger, L., & Dombret, H. (2018). Cytogenetics and gene mutations influence survival in older patients with acute myeloid leukemia treated with azacitidine or conventional care. *Leukemia*, *32*(12), 2546–2557. https://doi.org/10.1038/s41375-018-0257-z

Döhner, H., Estey, E., Grimwade, D., Amadori, S., Appelbaum, F. R., Büchner, T., Dombret, H., Ebert, B. L., Fenaux, P., Larson, R. A., Levine, R. L., Lo-Coco, F., Naoe, T., Niederwieser, D., Ossenkoppele, G. J., Sanz, M., Sierra, J., Tallman, M. S., Tien, H.-F., … Bloomfield, C. D. (2017). Diagnosis and management of AML in adults: 2017 ELN recommendations from an international expert panel. *Blood*, *129*(4), 424–447. https://doi.org/10.1182/blood-2016-08-733196

Döhner, H., Estey, E. H., Amadori, S., Appelbaum, F. R., Büchner, T., Burnett, A. K., Dombret, H., Fenaux, P., Grimwade, D., Larson, R. A., Lo-Coco, F., Naoe, T., Niederwieser, D., Ossenkoppele, G. J., Sanz, M. A., Sierra, J., Tallman, M. S., Löwenberg, B., & Bloomfield, C. D. (2010). Diagnosis and management of acute myeloid leukemia in adults: Recommendations from an international expert panel, on behalf of the European LeukemiaNet. *Blood*, *115*(3), 453–474. https://doi.org/10.1182/blood-2009-07-235358

Döhner, H., Weisdorf, D. J., & Bloomfield, C. D. (2015). Acute Myeloid Leukemia. *New England Journal of Medicine*, *373*(12), 1136–1152. https://doi.org/10.1056/NEJMra1406184

Dombret, H., Seymour, J. F., Butrym, A., Wierzbowska, A., Selleslag, D., Jang, J. H., Kumar, R., Cavenagh, J., Schuh, A. C., Candoni, A., Récher, C., Sandhu, I., Bernal del Castillo, T., Al-Ali, H. K., Martinelli, G., Falantes, J., Noppeney, R., Stone, R. M., Minden, M. D., … Döhner, H. (2015). International phase 3 study of azacitidine vs conventional care regimens in older patients with newly diagnosed AML with >30% blasts. *Blood*, *126*(3), 291–299. https://doi.org/10.1182/blood-2015-01-621664

Dong, H., Strome, S. E., Salomao, D. R., Tamura, H., Hirano, F., Flies, D. B., Roche, P. C., Lu, J., Zhu, G., Tamada, K., Lennon, V. A., Celis, E., & Chen, L. (2002). Tumor-associated B7-H1 promotes T-cell apoptosis: A potential mechanism of immune evasion. *Nature Medicine*, *8*(8), 793–800. https://doi.org/10.1038/nm730

Drent, E., Poels, R., Ruiter, R., van de Donk, N. W. C. J., Zweegman, S., Yuan, H., de Bruijn, J., Sadelain, M., Lokhorst, H. M., Groen, R. W. J., Mutis, T., & Themeli, M. (2019). Combined CD28 and 4-1BB Costimulation Potentiates Affinity-tuned Chimeric Antigen Receptor–engineered T Cells. *Clinical Cancer Research*, *25*(13), 4014–4025. https://doi.org/10.1158/1078-0432.CCR-18-2559

Drent, E., Themeli, M., Poels, R., de Jong-Korlaar, R., Yuan, H., de Bruijn, J., Martens, A. C. M., Zweegman, S., van de Donk, N. W. C. J., Groen, R. W. J., Lokhorst, H. M., & Mutis, T. (2017). A Rational Strategy for Reducing On-Target Off-Tumor Effects of CD38-Chimeric Antigen Receptors by Affinity Optimization. *Molecular Therapy*, *25*(8), 1946–1958. https://doi.org/10.1016/j.ymthe.2017.04.024

Duchmann, M., & Itzykson, R. (2019). Clinical update on hypomethylating agents. *International*

Journal of Hematology, *110*(2), 161–169. https://doi.org/10.1007/s12185-019-02651-9

Dull, T., Zufferey, R., Kelly, M., Mandel, R. J., Nguyen, M., Trono, D., & Naldini, L. (1998). A third-generation lentivirus vector with a conditional packaging system. *Journal of Virology*, *72*(11), 8463–8471. https://doi.org/10.1128/JVI.72.11.8463-8471.1998

Enblad, G., Karlsson, H., Gammelgård, G., Wenthe, J., Lövgren, T., Amini, R. M., Wikstrom, K. I., Essand, M., Savoldo, B., Hallböök, H., Höglund, M., Dotti, G., Brenner, M. K., Hagberg, H., & Loskog, A. (2018). A Phase I/IIa Trial Using CD19-Targeted Third-Generation CAR T Cells for Lymphoma and Leukemia. *Clinical Cancer Research*, *24*(24), 6185–6194. https://doi.org/10.1158/1078-0432.CCR-18-0426

Eshhar, Z., Waks, T., Gross, G., & Schindler, D. G. (1993). Specific activation and targeting of cytotoxic lymphocytes through chimeric single chains consisting of antibody-binding domains and the gamma or zeta subunits of the immunoglobulin and T-cell receptors. *Proceedings of the National Academy of Sciences of the United States of America*, *90*(2), 720–724. https://doi.org/10.1073/pnas.90.2.720

Estey, E. (2016). Acute myeloid leukemia: 2016 Update on risk-stratification and management: Acute Myeloid Leukemia. *American Journal of Hematology*, *91*(8), 824–846. https://doi.org/10.1002/ajh.24439

Estey, E. H. (2012). Acute myeloid leukemia: 2012 update on diagnosis, risk stratification, and management. *American Journal of Hematology*, *87*(1), 89–99. https://doi.org/10.1002/ajh.22246

Fathi, A. T., Borate, U., DeAngelo, D. J., O'Brien, M. M., Trippett, T., Shah, B. D., Hale, G. A., Foran, J. M., Silverman, L. B., Tibes, R., Cramer, S., Pauly, M., Kim, S., Kostic, A., Huang, X., Pan, Y., & Chen, R. (2015). A Phase 1 Study of Denintuzumab Mafodotin (SGN-CD19A) in Adults with Relapsed or Refractory B-Lineage Acute Leukemia (B-ALL) and Highly Aggressive Lymphoma. *Blood*, *126*(23), 1328–1328. https://doi.org/10.1182/blood.V126.23.1328.1328

Fenaux, P., Mufti, G. J., Hellstrom-Lindberg, E., Santini, V., Finelli, C., Giagounidis, A., Schoch, R., Gattermann, N., Sanz, G., List, A., Gore, S. D., Seymour, J. F., Bennett, J. M., Byrd, J., Backstrom, J., Zimmerman, L., McKenzie, D., Beach, C., Silverman, L. R., & International Vidaza High-Risk MDS Survival Study Group. (2009). Efficacy of azacitidine compared with that of conventional care regimens in the treatment of higher-risk myelodysplastic syndromes: A randomised, open-label, phase III study. *The Lancet. Oncology*, *10*(3), 223–232. https://doi.org/10.1016/S1470-2045(09)70003-8

Fenaux, P., Mufti, G. J., Hellström-Lindberg, E., Santini, V., Gattermann, N., Germing, U., Sanz, G., List, A. F., Gore, S., Seymour, J. F., Dombret, H., Backstrom, J., Zimmerman, L., McKenzie, D., Beach, C. L., & Silverman, L. R. (2010). Azacitidine prolongs overall survival compared with conventional care regimens in elderly patients with low bone marrow blast count acute myeloid leukemia. *Journal of Clinical Oncology: Official Journal of the American Society of Clinical Oncology*, *28*(4), 562–569. https://doi.org/10.1200/JCO.2009.23.8329

Finney, H. M., Akbar, A. N., & Lawson, A. D. G. (2004). Activation of resting human primary T cells with chimeric receptors: Costimulation from CD28, inducible costimulator, CD134, and CD137 in series with signals from the TCR zeta chain. *Journal of Immunology (Baltimore, Md.: 1950)*, *172*(1), 104–113. https://doi.org/10.4049/jimmunol.172.1.104

Finney, H. M., Lawson, A. D., Bebbington, C. R., & Weir, A. N. (1998). Chimeric receptors providing both primary and costimulatory signaling in T cells from a single gene product. *Journal of Immunology (Baltimore, Md.: 1950)*, *161*(6), 2791–2797.

Fos, C., Salles, A., Lang, V., Carrette, F., Audebert, S., Pastor, S., Ghiotto, M., Olive, D., Bismuth, G., & Nunès, J. A. (2008). ICOS ligation recruits the p50alpha PI3K regulatory subunit to the immunological synapse. *Journal of Immunology (Baltimore, Md.: 1950)*, *181*(3), 1969–1977. https://doi.org/10.4049/jimmunol.181.3.1969

Franke, T. F., Hornik, C. P., Segev, L., Shostak, G. A., & Sugimoto, C. (2003). PI3K/Akt and apoptosis: Size matters. *Oncogene*, *22*(56), 8983–8998. https://doi.org/10.1038/sj.onc.1207115

Fröhling, S., Scholl, C., Gilliland, D. G., & Levine, R. L. (2005). Genetics of Myeloid Malignancies: Pathogenetic and Clinical Implications. *Journal of Clinical Oncology*, *23*(26), 6285–6295. https://doi.org/10.1200/JCO.2005.05.010

Gagliani, N., Vesely, M. C. A., Iseppon, A., Brockmann, L., Xu, H., Palm, N. W., de Zoete, M. R., Licona-Limón, P., Paiva, R. S., Ching, T., Weaver, C., Zi, X., Pan, X., Fan, R., Garmire, L. X., Cotton, M. J., Drier, Y., Bernstein, B., Geginat, J., … Flavell, R. A. (2015). Th17 cells transdifferentiate into regulatory T cells during resolution of inflammation. *Nature*, *523*(7559), 221–225. https://doi.org/10.1038/nature14452

Garcia-Manero, G., Daver, N. G., Montalban-Bravo, G., Jabbour, E. J., DiNardo, C. D., Kornblau, S. M., Bose, P., Alvarado, Y., Ohanian, M., Borthakur, G., Cortes, J. E., Naqvi, K., Pemmaraju, N., Huang, X., Nogueras-Gonzalez, G. M., Bueso-Ramos, C. E., Gasior, Y., Bayer, V. R., Pierce, S., … Kantarjian, H. M. (2016). A Phase II Study Evaluating the Combination of Nivolumab (Nivo) or Ipilimumab (Ipi) with Azacitidine in Pts with Previously Treated or Untreated Myelodysplastic Syndromes (MDS). *Blood*, *128*(22), 344–344. https://doi.org/10.1182/blood.V128.22.344.344

Gattinoni, L., Lugli, E., Ji, Y., Pos, Z., Paulos, C. M., Quigley, M. F., Almeida, J. R., Gostick, E., Yu, Z., Carpenito, C., Wang, E., Douek, D. C., Price, D. A., June, C. H., Marincola, F. M., Roederer, M., & Restifo, N. P. (2011). A human memory T cell subset with stem cell-like properties. *Nature Medicine*, *17*(10), 1290–1297. https://doi.org/10.1038/nm.2446

Giannopoulos, K. (2019). Targeting Immune Signaling Checkpoints in Acute Myeloid Leukemia. *Journal of Clinical Medicine*, *8*(2), 236. https://doi.org/10.3390/jcm8020236

Gill, S., & June, C. H. (2015). Going viral: Chimeric antigen receptor T-cell therapy for hematological malignancies. *Immunological Reviews*, *263*(1), 68–89. https://doi.org/10.1111/imr.12243

Gill, S., Tasian, S. K., Ruella, M., Shestova, O., Li, Y., Porter, D. L., Carroll, M., Danet-Desnoyers, G., Scholler, J., Grupp, S. A., June, C. H., & Kalos, M. (2014). Preclinical targeting of human acute myeloid leukemia and myeloablation using chimeric antigen receptor–modified T cells. *Blood*, *123*(15), 2343–2354. https://doi.org/10.1182/blood-2013-09-529537

Goodyear, O., Agathanggelou, A., Novitzky-Basso, I., Siddique, S., McSkeane, T., Ryan, G., Vyas, P., Cavenagh, J., Stankovic, T., Moss, P., & Craddock, C. (2010). Induction of a CD8+ T-cell response to the MAGE cancer testis antigen by combined treatment with azacitidine and sodium valproate in patients with acute myeloid leukemia and myelodysplasia. *Blood*, *116*(11), 1908–1918. https://doi.org/10.1182/blood-2009-11-249474

Gorcea, C. M., Burthem, J., & Tholouli, E. (2018). ASP2215 in the treatment of relapsed/refractory acute myeloid leukemia with *FLT3* mutation: Background and design of the ADMIRAL trial. *Future Oncology*, *14*(20), 1995–2004. https://doi.org/10.2217/fon-2017-0582

Grada, Z., Hegde, M., Byrd, T., Shaffer, D. R., Ghazi, A., Brawley, V. S., Corder, A., Schönfeld, K., Koch, J., Dotti, G., Heslop, H. E., Gottschalk, S., Wels, W. S., Baker, M. L., & Ahmed, N. (2013). TanCAR: A Novel Bispecific Chimeric Antigen Receptor for Cancer Immunotherapy. *Molecular Therapy - Nucleic Acids*, *2*, e105. https://doi.org/10.1038/mtna.2013.32

Grimwade, D., & Freeman, S. D. (2014). Defining minimal residual disease in acute myeloid leukemia: Which platforms are ready for “prime time”? *Blood*, *124*(23), 3345–3355. https://doi.org/10.1182/blood-2014-05-577593

Grupp, S. A., Kalos, M., Barrett, D., Aplenc, R., Porter, D. L., Rheingold, S. R., Teachey, D. T., Chew, A., Hauck, B., Wright, J. F., Milone, M. C., Levine, B. L., & June, C. H. (2013). Chimeric Antigen Receptor–Modified T Cells for Acute Lymphoid Leukemia. *New England Journal of Medicine*, *368*(16), 1509–1518. https://doi.org/10.1056/NEJMoa1215134

Gudipati, V., Rydzek, J., Doel-Perez, I., Gonçalves, V. D. R., Scharf, L., Königsberger, S., Lobner, E., Kunert, R., Einsele, H., Stockinger, H., Hudecek, M., & Huppa, J. B. (2020). Inefficient CAR-proximal signaling blunts antigen sensitivity. *Nature Immunology*, *21*(8), 848–856. https://doi.org/10.1038/s41590-020-0719-0

Guedan, S., Chen, X., Madar, A., Carpenito, C., McGettigan, S. E., Frigault, M. J., Lee, J., Posey, A. D., Scholler, J., Scholler, N., Bonneau, R., & June, C. H. (2014). ICOS-based chimeric antigen receptors program bipolar TH17/TH1 cells. *Blood*, *124*(7), 1070–1080. https://doi.org/10.1182/blood-2013-10-535245

Guest, R. D., Hawkins, R. E., Kirillova, N., Cheadle, E. J., Arnold, J., O??Neill, A., Irlam, J., Chester, K. A., Kemshead, J. T., Shaw, D. M., Embleton, M. J., Stern, P. L., & Gilham, D. E. (2005). The Role of Extracellular Spacer Regions in the Optimal Design of Chimeric Immune Receptors: Evaluation of Four Different scFvs and Antigens. *Journal of Immunotherapy*, *28*(3), 203–211. https://doi.org/10.1097/01.cji.0000161397.96582.59

Han, Y., Dong, Y., Yang, Q., Xu, W., Jiang, S., Yu, Z., Yu, K., & Zhang, S. (2018). Acute Myeloid Leukemia Cells Express ICOS Ligand to Promote the Expansion of Regulatory T Cells. *Frontiers in*

Immunology, *9*, 2227. https://doi.org/10.3389/fimmu.2018.02227

Hanahan, D., & Weinberg, R. A. (2011). Hallmarks of Cancer: The Next Generation. *Cell*, *144*(5), 646–674. https://doi.org/10.1016/j.cell.2011.02.013

Harada, Y., Ohgai, D., Watanabe, R., Okano, K., Koiwai, O., Tanabe, K., Toma, H., Altman, A., & Abe, R. (2003). A single amino acid alteration in cytoplasmic domain determines IL-2 promoter activation by ligation of CD28 but not inducible costimulator (ICOS). *The Journal of Experimental Medicine*, *197*(2), 257–262. https://doi.org/10.1084/jem.20021305

Harrington, K. H., Gudgeon, C. J., Laszlo, G. S., Newhall, K. J., Sinclair, A. M., Frankel, S. R., Kischel, R., Chen, G., & Walter, R. B. (2015). The Broad Anti-AML Activity of the CD33/CD3 BiTE Antibody Construct, AMG 330, Is Impacted by Disease Stage and Risk. *PLOS ONE*, *10*(8), e0135945. https://doi.org/10.1371/journal.pone.0135945

Hedrick, S. M., Cohen, D. I., Nielsen, E. A., & Davis, M. M. (2005). Isolation of cDNA clones encoding T cell-specific membrane-associated proteins. 1984. *Journal of Immunology (Baltimore, Md.: 1950)*, *175*(5), 2771–2775.

Herzog, E., Busfield, S., Biondo, M., Vairo, G., DeWitte, M., Pragst, I., Dickneite, G., Nash, A., & Zollner, S. (2012). Pharmacodynamic Activity and Preclinical Safety of CSL362, a Novel Humanised, Affinity Matured Monoclonal Antibody Against Human Interleukin 3 Receptor. *Blood*, *120*(21), 1524–1524. https://doi.org/10.1182/blood.V120.21.1524.1524

Ho, T.-C., LaMere, M., Stevens, B. M., Ashton, J. M., Myers, J. R., O'Dwyer, K. M., Liesveld, J. L., Mendler, J. H., Guzman, M., Morrissette, J. D., Zhao, J., Wang, E. S., Wetzler, M., Jordan, C. T., & Becker, M. W. (2016). Evolution of acute myelogenous leukemia stem cell properties after treatment and progression. *Blood*, *128*(13), 1671–1678. https://doi.org/10.1182/blood-2016-02-695312

Hodi, F. S., O'Day, S. J., McDermott, D. F., Weber, R. W., Sosman, J. A., Haanen, J. B., Gonzalez, R., Robert, C., Schadendorf, D., Hassel, J. C., Akerley, W., van den Eertwegh, A. J. M., Lutzky, J., Lorigan, P., Vaubel, J. M., Linette, G. P., Hogg, D., Ottensmeier, C. H., Lebbé, C., … Urba, W. J. (2010). Improved Survival with Ipilimumab in Patients with Metastatic Melanoma. *New England Journal of Medicine*, *363*(8), 711–723. https://doi.org/10.1056/NEJMoa1003466

Hofmann, S., Schubert, M.-L., Wang, L., He, B., Neuber, B., Dreger, P., Müller-Tidow, C., & Schmitt, M. (2019). Chimeric Antigen Receptor (CAR) T Cell Therapy in Acute Myeloid Leukemia (AML). *Journal of Clinical Medicine*, *8*(2), 200. https://doi.org/10.3390/jcm8020200

Hombach, A. A., & Abken, H. (2011). Costimulation by chimeric antigen receptors revisited the T cell antitumor response benefits from combined CD28-OX40 signalling. *International Journal of Cancer*, *129*(12), 2935–2944. https://doi.org/10.1002/ijc.25960

Hombach, A. A., Heiders, J., Foppe, M., Chmielewski, M., & Abken, H. (2012). OX40 costimulation by a chimeric antigen receptor abrogates CD28 and IL-2 induced IL-10 secretion by redirected CD4 $^{+}$ T cells. *OncoImmunology*, *1*(4), 458–466. https://doi.org/10.4161/onci.19855

Hombach, A. A., Rappl, G., & Abken, H. (2013). Arming cytokine-induced killer cells with chimeric antigen receptors: CD28 outperforms combined CD28-OX40 "super-stimulation." *Molecular Therapy: The Journal of the American Society of Gene Therapy*, *21*(12), 2268–2277.

https://doi.org/10.1038/mt.2013.192

Huang, S., Chen, Z., Yu, J. F., Young, D., Bashey, A., Ho, A. D., & Law, P. (1999). Correlation Between IL&hyphen;3 Receptor Expression and Growth Potential of Human CD34 &plus; Hematopoietic Cells from Different Tissues. *Stem Cells*, *17*(5), 265–272. https://doi.org/10.1002/stem.170265

Huard, B., Gaulard, P., Faure, F., Hercend, T., & Triebel, F. (1994). Cellular expression and tissue distribution of the human LAG-3-encoded protein, an MHC class II ligand. *Immunogenetics*, *39*(3). https://doi.org/10.1007/BF00241263

Hudecek, M., Lupo-Stanghellini, M.-T., Kosasih, P. L., Sommermeyer, D., Jensen, M. C., Rader, C., & Riddell, S. R. (2013). Receptor affinity and extracellular domain modifications affect tumor recognition by ROR1-specific chimeric antigen receptor T cells. *Clinical Cancer Research: An Official Journal of the American Association for Cancer Research*, *19*(12), 3153–3164. https://doi.org/10.1158/1078-0432.CCR-13-0330

Hudecek, M., Sommermeyer, D., Kosasih, P. L., Silva-Benedict, A., Liu, L., Rader, C., Jensen, M. C., & Riddell, S. R. (2015). The nonsignaling extracellular spacer domain of chimeric antigen receptors is decisive for in vivo antitumor activity. *Cancer Immunology Research*, *3*(2), 125–135. https://doi.org/10.1158/2326-6066.CIR-14-0127

Hughes, A., Clarson, J., Tang, C., Vidovic, L., White, D. L., Hughes, T. P., & Yong, A. S. M. (2017). CML patients with deep molecular responses to TKI have restored immune effectors and decreased PD-1 and immune suppressors. *Blood*, *129*(9), 1166–1176. https://doi.org/10.1182/blood-2016-10-745992

Huntly, B. J. P., & Gilliland, D. G. (2005). Leukaemia stem cells and the evolution of cancer-stem-cell research. *Nature Reviews Cancer*, *5*(4), 311–321. https://doi.org/10.1038/nrc1592

Il-Hoan, O., & Kyung-rim, K. (2010). Multiple Niches for Hematopoietic Stem Cell Regulations. *STEM CELLS*, N/A-N/A. https://doi.org/10.1002/stem.453

Imai, C., Mihara, K., Andreansky, M., Nicholson, I. C., Pui, C.-H., Geiger, T. L., & Campana, D. (2004). Chimeric receptors with 4-1BB signaling capacity provoke potent cytotoxicity against acute lymphoblastic leukemia. *Leukemia*, *18*(4), 676–684. https://doi.org/10.1038/sj.leu.2403302

Issa, J.-P. J. (2007). DNA Methylation as a Therapeutic Target in Cancer: Fig. 1. *Clinical Cancer Research*, *13*(6), 1634–1637. https://doi.org/10.1158/1078-0432.CCR-06-2076

Jagannathan-Bogdan, M., & Zon, L. I. (2013). Hematopoiesis. *Development*, *140*(12), 2463–2467. https://doi.org/10.1242/dev.083147

James, S. E., Greenberg, P. D., Jensen, M. C., Lin, Y., Wang, J., Till, B. G., Raubitschek, A. A., Forman, S. J., & Press, O. W. (2008). Antigen sensitivity of CD22-specific chimeric TCR is modulated by target epitope distance from the cell membrane. *Journal of Immunology (Baltimore, Md.: 1950)*, *180*(10), 7028–7038. https://doi.org/10.4049/jimmunol.180.10.7028

Jamieson, C. H. M., Ailles, L. E., Dylla, S. J., Muijtjens, M., Jones, C., Zehnder, J. L., Gotlib, J., Li, K., Manz, M. G., Keating, A., Sawyers, C. L., & Weissman, I. L. (2004). Granulocyte–Macrophage

Progenitors as Candidate Leukemic Stem Cells in Blast-Crisis CML. *New England Journal of Medicine*, *351*(7), 657–667. https://doi.org/10.1056/NEJMoa040258

Jenq, R. R., & van den Brink, M. R. M. (2010). Allogeneic haematopoietic stem cell transplantation: Individualized stem cell and immune therapy of cancer. *Nature Reviews Cancer*, *10*(3), 213–221. https://doi.org/10.1038/nrc2804

Jiang, N., Huang, J., Edwards, L. J., Liu, B., Zhang, Y., Beal, C. D., Evavold, B. D., & Zhu, C. (2011). Two-stage cooperative T cell receptor-peptide major histocompatibility complex-CD8 trimolecular interactions amplify antigen discrimination. *Immunity*, *34*(1), 13–23. https://doi.org/10.1016/j.immuni.2010.12.017

Jilg, S., Hauch, R. T., Kauschinger, J., Buschhorn, L., Odinius, T. O., Dill, V., Müller-Thomas, C., Herold, T., Prodinger, P. M., Schmidt, B., Hempel, D., Bassermann, F., Peschel, C., Götze, K. S., Höckendorf, U., Haferlach, T., & Jost, P. J. (2019). Venetoclax with azacitidine targets refractory MDS but spares healthy hematopoiesis at tailored dose. *Experimental Hematology & Oncology*, *8*, 9. https://doi.org/10.1186/s40164-019-0133-1

Jin, S., Cojocari, D., Purkal, J. J., Popovic, R., Talaty, N. N., Xiao, Y., Solomon, L. R., Boghaert, E. R., Leverson, J. D., & Phillips, D. C. (2020). 5-Azacitidine Induces NOXA to Prime AML Cells for Venetoclax-Mediated Apoptosis. *Clinical Cancer Research*, *26*(13), 3371–3383. https://doi.org/10.1158/1078-0432.CCR-19-1900

Jordan, C., Upchurch, D., Szilvassy, S., Guzman, M., Howard, D., Pettigrew, A., Meyerrose, T., Rossi, R., Grimes, B., Rizzieri, D., Luger, S., & Phillips, G. (2000). The interleukin-3 receptor alpha chain is a unique marker for human acute myelogenous leukemia stem cells. *Leukemia*, *14*(10), 1777–1784. https://doi.org/10.1038/sj.leu.2401903

June, C. H., & Sadelain, M. (2018). Chimeric Antigen Receptor Therapy. *New England Journal of Medicine*, *379*(1), 64–73. https://doi.org/10.1056/NEJMra1706169

Karlsson, H., Svensson, E., Gigg, C., Jarvius, M., Olsson-Strömberg, U., Savoldo, B., Dotti, G., & Loskog, A. (2015). Evaluation of Intracellular Signaling Downstream Chimeric Antigen Receptors. *PLOS ONE*, *10*(12), e0144787. https://doi.org/10.1371/journal.pone.0144787

Kashio, Y., Nakamura, K., Abedin, M. J., Seki, M., Nishi, N., Yoshida, N., Nakamura, T., & Hirashima, M. (2003). Galectin-9 Induces Apoptosis Through the Calcium-Calpain-Caspase-1 Pathway. *The Journal of Immunology*, *170*(7), 3631–3636. https://doi.org/10.4049/jimmunol.170.7.3631

Katherine D Cummins, Noelle Frey, Anne Marie Nelson, Aliza Schmidt, Selina Luger, Randi E. Isaacs, Simon F Lacey, Elizabeth Hexner, J. Joseph Melenhorst, Carl H June, David L Porter, Saar I Gill. (2017). *Treating Relapsed / Refractory (RR) AML with Biodegradable Anti-CD123 CAR Modified T Cells. 130*, 1359. https://doi.org/10.1182/blood.V130.Suppl_1.1359.1359

Katz, Z. B., Novotná, L., Blount, A., & Lillemeier, B. F. (2017). A cycle of Zap70 kinase activation and release from the TCR amplifies and disperses antigenic stimuli. *Nature Immunology*, *18*(1), 86–95. https://doi.org/10.1038/ni.3631

Kelly, L. M., & Gilliland, D. G. (2002). G ENETICS OF M YELOID L EUKEMIAS. *Annual Review of Genomics and Human Genetics*, *3*(1), 179–198.

https://doi.org/10.1146/annurev.genom.3.032802.115046

Kenderian, S. S., Porter, D. L., & Gill, S. (2017). Chimeric Antigen Receptor T Cells and Hematopoietic Cell Transplantation: How Not to Put the CART Before the Horse. *Biology of Blood and Marrow Transplantation: Journal of the American Society for Blood and Marrow Transplantation*, *23*(2), 235–246. https://doi.org/10.1016/j.bbmt.2016.09.002

Kersh, E. N. (2006). Impaired memory CD8 T cell development in the absence of methyl-CpG-binding domain protein 2. *Journal of Immunology (Baltimore, Md.: 1950)*, *177*(6), 3821–3826. https://doi.org/10.4049/jimmunol.177.6.3821

Khan, O., Giles, J. R., McDonald, S., Manne, S., Ngiow, S. F., Patel, K. P., Werner, M. T., Huang, A. C., Alexander, K. A., Wu, J. E., Attanasio, J., Yan, P., George, S. M., Bengsch, B., Staupe, R. P., Donahue, G., Xu, W., Amaravadi, R. K., Xu, X., … Wherry, E. J. (2019). TOX transcriptionally and epigenetically programs CD8+ T cell exhaustion. *Nature*, *571*(7764), 211–218. https://doi.org/10.1038/s41586-019-1325-x

Kihara, R., Nagata, Y., Kiyoi, H., Kato, T., Yamamoto, E., Suzuki, K., Chen, F., Asou, N., Ohtake, S., Miyawaki, S., Miyazaki, Y., Sakura, T., Ozawa, Y., Usui, N., Kanamori, H., Kiguchi, T., Imai, K., Uike, N., Kimura, F., … Naoe, T. (2014). Comprehensive analysis of genetic alterations and their prognostic impacts in adult acute myeloid leukemia patients. *Leukemia*, *28*(8), 1586–1595. https://doi.org/10.1038/leu.2014.55

Kim, H. P., Gerhard, B., Harasym, T. O., Mayer, L. D., & Hogge, D. E. (2011). Liposomal encapsulation of a synergistic molar ratio of cytarabine and daunorubicin enhances selective toxicity for acute myeloid leukemia progenitors as compared to analogous normal hematopoietic cells. *Experimental Hematology*, *39*(7), 741–750. https://doi.org/10.1016/j.exphem.2011.04.001

Kim, M. Y., Yu, K.-R., Kenderian, S. S., Ruella, M., Chen, S., Shin, T.-H., Aljanahi, A. A., Schreeder, D., Klichinsky, M., Shestova, O., Kozlowski, M. S., Cummins, K. D., Shan, X., Shestov, M., Bagg, A., Morrissette, J. J. D., Sekhri, P., Lazzarotto, C. R., Calvo, K. R., … Gill, S. (2018). Genetic Inactivation of CD33 in Hematopoietic Stem Cells to Enable CAR T Cell Immunotherapy for Acute Myeloid Leukemia. *Cell*, *173*(6), 1439-1453.e19. https://doi.org/10.1016/j.cell.2018.05.013

Kinter, A. L., Godbout, E. J., McNally, J. P., Sereti, I., Roby, G. A., O'Shea, M. A., & Fauci, A. S. (2008). The common gamma-chain cytokines IL-2, IL-7, IL-15, and IL-21 induce the expression of programmed death-1 and its ligands. *Journal of Immunology (Baltimore, Md.: 1950)*, *181*(10), 6738–6746. https://doi.org/10.4049/jimmunol.181.10.6738

Kisielow, M., Kisielow, J., Capoferri-Sollami, G., & Karjalainen, K. (2005). Expression of lymphocyte activation gene 3 (LAG-3) on B cells is induced by T cells. *European Journal of Immunology*, *35*(7), 2081–2088. https://doi.org/10.1002/eji.200526090

Kline, J., Liu, H., Michael, T., Artz, A. S., Godfrey, J., Curran, E. K., Stock, W., Smith, S. M., & Bishop, M. R. (2018). Pembrolizumab for the Treatment of Disease Relapse Following Allogeneic Hematopoietic Cell Transplantation. *Blood*, *132*(Supplement 1), 3415–3415. https://doi.org/10.1182/blood-2018-99-115108

Kloss, C. C., Condomines, M., Cartellieri, M., Bachmann, M., & Sadelain, M. (2013). Combinatorial antigen recognition with balanced signaling promotes selective tumor eradication by engineered

T cells. *Nature Biotechnology*, *31*(1), 71–75. https://doi.org/10.1038/nbt.2459

Kochenderfer, J. N., Dudley, M. E., Feldman, S. A., Wilson, W. H., Spaner, D. E., Maric, I., Stetler-Stevenson, M., Phan, G. Q., Hughes, M. S., Sherry, R. M., Yang, J. C., Kammula, U. S., Devillier, L., Carpenter, R., Nathan, D.-A. N., Morgan, R. A., Laurencot, C., & Rosenberg, S. A. (2012). B-cell depletion and remissions of malignancy along with cytokine-associated toxicity in a clinical trial of anti-CD19 chimeric-antigen-receptor–transduced T cells. *Blood*, *119*(12), 2709–2720. https://doi.org/10.1182/blood-2011-10-384388

Kochenderfer, J. N., Dudley, M. E., Kassim, S. H., Somerville, R. P. T., Carpenter, R. O., Stetler-Stevenson, M., Yang, J. C., Phan, G. Q., Hughes, M. S., Sherry, R. M., Raffeld, M., Feldman, S., Lu, L., Li, Y. F., Ngo, L. T., Goy, A., Feldman, T., Spaner, D. E., Wang, M. L., … Rosenberg, S. A. (2015). Chemotherapy-refractory diffuse large B-cell lymphoma and indolent B-cell malignancies can be effectively treated with autologous T cells expressing an anti-CD19 chimeric antigen receptor. *Journal of Clinical Oncology: Official Journal of the American Society of Clinical Oncology*, *33*(6), 540–549. https://doi.org/10.1200/JCO.2014.56.2025

Kochenderfer, J. N., Wilson, W. H., Janik, J. E., Dudley, M. E., Stetler-Stevenson, M., Feldman, S. A., Maric, I., Raffeld, M., Nathan, D.-A. N., Lanier, B. J., Morgan, R. A., & Rosenberg, S. A. (2010). Eradication of B-lineage cells and regression of lymphoma in a patient treated with autologous T cells genetically engineered to recognize CD19. *Blood*, *116*(20), 4099–4102. https://doi.org/10.1182/blood-2010-04-281931

Kofler, D. M., Chmielewski, M., Rappl, G., Hombach, A., Riet, T., Schmidt, A., Hombach, A. A., Wendtner, C.-M., & Abken, H. (2011). CD28 Costimulation Impairs the Efficacy of a Redirected T-cell Antitumor Attack in the Presence of Regulatory T cells Which Can Be Overcome by Preventing Lck Activation. *Molecular Therapy*, *19*(4), 760–767. https://doi.org/10.1038/mt.2011.9

Kohlmann, A., Nadarajah, N., Alpermann, T., Grossmann, V., Schindela, S., Dicker, F., Roller, A., Kern, W., Haferlach, C., Schnittger, S., & Haferlach, T. (2014). Monitoring of residual disease by next-generation deep-sequencing of RUNX1 mutations can identify acute myeloid leukemia patients with resistant disease. *Leukemia*, *28*(1), 129–137. https://doi.org/10.1038/leu.2013.239

Kolb, H.-J. (2008). Graft-versus-leukemia effects of transplantation and donor lymphocytes. *Blood*, *112*(12), 4371–4383. https://doi.org/10.1182/blood-2008-03-077974

Kong, Y., Zhang, J., Claxton, D. F., Ehmann, W. C., Rybka, W. B., Zhu, L., Zeng, H., Schell, T. D., & Zheng, H. (2015). PD-1(hi)TIM-3(+) T cells associate with and predict leukemia relapse in AML patients post allogeneic stem cell transplantation. *Blood Cancer Journal*, *5*, e330. https://doi.org/10.1038/bcj.2015.58

Konopleva, M., Pollyea, D. A., Potluri, J., Chyla, B., Hogdal, L., Busman, T., McKeegan, E., Salem, A. H., Zhu, M., Ricker, J. L., Blum, W., DiNardo, C. D., Kadia, T., Dunbar, M., Kirby, R., Falotico, N., Leverson, J., Humerickhouse, R., Mabry, M., … Letai, A. (2016). Efficacy and Biological Correlates of Response in a Phase II Study of Venetoclax Monotherapy in Patients with Acute Myelogenous Leukemia. *Cancer Discovery*, *6*(10), 1106–1117. https://doi.org/10.1158/2159-8290.CD-16-0313

Korin, Y. D., & Zack, J. A. (1998). Progression to the G1b phase of the cell cycle is required for completion of human immunodeficiency virus type 1 reverse transcription in T cells. *Journal of Virology*, *72*(4), 3161–3168. https://doi.org/10.1128/JVI.72.4.3161-3168.1998

Kovtun, Y., Jones, G. E., Adams, S., Harvey, L., Audette, C. A., Wilhelm, A., Bai, C., Rui, L., Laleau, R., Liu, F., Ab, O., Setiady, Y., Yoder, N. C., Goldmacher, V. S., Chari, R. V. J., Pinkas, J., & Chittenden, T. (2018). A CD123-targeting antibody-drug conjugate, IMGN632, designed to eradicate AML while sparing normal bone marrow cells. *Blood Advances*, *2*(8), 848–858. https://doi.org/10.1182/bloodadvances.2018017517

Kowolik, C. M., Topp, M. S., Gonzalez, S., Pfeiffer, T., Olivares, S., Gonzalez, N., Smith, D. D., Forman, S. J., Jensen, M. C., & Cooper, L. J. N. (2006). CD28 costimulation provided through a CD19-specific chimeric antigen receptor enhances in vivo persistence and antitumor efficacy of adoptively transferred T cells. *Cancer Research*, *66*(22), 10995–11004. https://doi.org/10.1158/0008-5472.CAN-06-0160

Krystal, W. M., Walker, R., Fishkin, N., Audette, C., Kovtun, Y., & Romanelli, A. (2015). IMGN779, a CD33-Targeted Antibody-Drug Conjugate (ADC) with a Novel DNA-Alkylating Effector Molecule, Induces DNA Damage, Cell Cycle Arrest, and Apoptosis in AML Cells. *Blood*, *126*(23), 1366–1366. https://doi.org/10.1182/blood.V126.23.1366.1366

LaBelle, J. L., Hanke, C. A., Blazar, B. R., & Truitt, R. L. (2002). Negative effect of CTLA-4 on induction of T-cell immunity in vivo to B7-1+, but not B7-2+, murine myelogenous leukemia. *Blood*, *99*(6), 2146–2153. https://doi.org/10.1182/blood.V99.6.2146

Lal, G., Zhang, N., van der Touw, W., Ding, Y., Ju, W., Bottinger, E. P., Reid, S. P., Levy, D. E., & Bromberg, J. S. (2009). Epigenetic regulation of Foxp3 expression in regulatory T cells by DNA methylation. *Journal of Immunology (Baltimore, Md.: 1950)*, *182*(1), 259–273. https://doi.org/10.4049/jimmunol.182.1.259

Lamers, C. H. J., Sleijfer, S., Vulto, A. G., Kruit, W. H. J., Kliffen, M., Debets, R., Gratama, J. W., Stoter, G., & Oosterwijk, E. (2006). Treatment of Metastatic Renal Cell Carcinoma With Autologous T-Lymphocytes Genetically Retargeted Against Carbonic Anhydrase IX: First Clinical Experience. *Journal of Clinical Oncology*, *24*(13), e20–e22. https://doi.org/10.1200/JCO.2006.05.9964

Lancet, J. E., Uy, G. L., Cortes, J. E., Newell, L. F., Lin, T. L., Ritchie, E. K., Stuart, R. K., Strickland, S. A., Hogge, D., Solomon, S. R., Stone, R. M., Bixby, D. L., Kolitz, J. E., Schiller, G. J., Wieduwilt, M. J., Ryan, D. H., Hoering, A., Banerjee, K., Chiarella, M., … Medeiros, B. C. (2018). CPX-351 (cytarabine and daunorubicin) Liposome for Injection Versus Conventional Cytarabine Plus Daunorubicin in Older Patients With Newly Diagnosed Secondary Acute Myeloid Leukemia. *Journal of Clinical Oncology*, *36*(26), 2684–2692. https://doi.org/10.1200/JCO.2017.77.6112

Larson, R. A., Sievers, E. L., Stadtmauer, E. A., Löwenberg, B., Estey, E. H., Dombret, H., Theobald, M., Voliotis, D., Bennett, J. M., Richie, M., Leopold, L. H., Berger, M. S., Sherman, M. L., Loken, M. R., van Dongen, J. J. M., Bernstein, I. D., Appelbaum, F. R., & Mylotarg Study Group. (2005). Final report of the efficacy and safety of gemtuzumab ozogamicin (Mylotarg) in patients with CD33-positive acute myeloid leukemia in first recurrence. *Cancer*, *104*(7), 1442–1452. https://doi.org/10.1002/cncr.21326

Laszlo, G. S., Estey, E. H., & Walter, R. B. (2014). The past and future of CD33 as therapeutic target in acute myeloid leukemia. *Blood Reviews*, *28*(4), 143–153. https://doi.org/10.1016/j.blre.2014.04.001

Laurent, S., Palmisano, G. L., Martelli, A. M., Kato, T., Tazzari, P. L., Pierri, I., Clavio, M., Dozin, B., Balbi, G., Megna, M., Morabito, A., Lamparelli, T., Bacigalupo, A., Gobbi, M., & Pistillo, M. P. (2007). CTLA-4 expressed by chemoresistant, as well as untreated, myeloid leukaemia cells can be targeted with ligands to induce apoptosis. *British Journal of Haematology*, *136*(4), 597–608. https://doi.org/10.1111/j.1365-2141.2006.06472.x

Lee, D. W., Kochenderfer, J. N., Stetler-Stevenson, M., Cui, Y. K., Delbrook, C., Feldman, S. A., Fry, T. J., Orentas, R., Sabatino, M., Shah, N. N., Steinberg, S. M., Stroncek, D., Tschernia, N., Yuan, C., Zhang, H., Zhang, L., Rosenberg, S. A., Wayne, A. S., & Mackall, C. L. (2015). T cells expressing CD19 chimeric antigen receptors for acute lymphoblastic leukaemia in children and young adults: A phase 1 dose-escalation trial. *The Lancet*, *385*(9967), 517–528. https://doi.org/10.1016/S0140-6736(14)61403-3

Lee, D. W., Santomasso, B. D., Locke, F. L., Ghobadi, A., Turtle, C. J., Brudno, J. N., Maus, M. V., Park, J. H., Mead, E., Pavletic, S., Go, W. Y., Eldjerou, L., Gardner, R. A., Frey, N., Curran, K. J., Peggs, K., Pasquini, M., DiPersio, J. F., van den Brink, M. R. M., … Neelapu, S. S. (2019). ASTCT Consensus Grading for Cytokine Release Syndrome and Neurologic Toxicity Associated with Immune Effector Cells. *Biology of Blood and Marrow Transplantation: Journal of the American Society for Blood and Marrow Transplantation*, *25*(4), 625–638. https://doi.org/10.1016/j.bbmt.2018.12.758

Lee DW, Gardner R, Porter DL, et al. Current concepts in the diagnosis and management of cytokine release syndrome. Blood. 2014;124(2):188-195. (2015). *Blood*, *126*(8), 1048–1048. https://doi.org/10.1182/blood-2015-07-656918

Lee, E. M., Yee, D., Busfield, S., Vairo, G., & Lock, R. B. (2012). *A neutralizing antibody (CSL362) against the interleukin-3 receptor alpha with CSL362 augments the efficacy of a cytabarine/daunorubicin induction-type therapy in preclinical xenograft models of acute myelogenous leukemia*. *120*, 3599.

Lemos, N. E., Farias, M. G., Kubaski, F., Scotti, L., Onsten, T. G. H., Brondani, L. de A., Wagner, S. C., & Sekine, L. (2018). Quantification of peripheral blood CD34+ cells prior to stem cell harvesting by leukapheresis: A single center experience. *Hematology, Transfusion and Cell Therapy*, *40*(3), 213–218. https://doi.org/10.1016/j.htct.2018.01.002

Letourneur, F., & Klausner, R. D. (1992). Activation of T cells by a tyrosine kinase activation domain in the cytoplasmic tail of CD3 epsilon. *Science (New York, N.Y.)*, *255*(5040), 79–82. https://doi.org/10.1126/science.1532456

Lichtenegger, F. S., Krupka, C., Haubner, S., Köhnke, T., & Subklewe, M. (2017). Recent developments in immunotherapy of acute myeloid leukemia. *Journal of Hematology & Oncology*, *10*(1), 142. https://doi.org/10.1186/s13045-017-0505-0

Lindner, S. E., Johnson, S. M., Brown, C. E., & Wang, L. D. (2020). Chimeric antigen receptor signaling: Functional consequences and design implications. *Science Advances*, *6*(21), eaaz3223. https://doi.org/10.1126/sciadv.aaz3223

Lindsley, R. C., Mar, B. G., Mazzola, E., Grauman, P. V., Shareef, S., Allen, S. L., Pigneux, A., Wetzler, M., Stuart, R. K., Erba, H. P., Damon, L. E., Powell, B. L., Lindeman, N., Steensma, D. P., Wadleigh, M., DeAngelo, D. J., Neuberg, D., Stone, R. M., & Ebert, B. L. (2015). Acute myeloid leukemia ontogeny is defined by distinct somatic mutations. *Blood*, *125*(9), 1367–1376. https://doi.org/10.1182/blood-2014-11-610543

Linsley, P. S., Bradshaw, J., Greene, J., Peach, R., Bennett, K. L., & Mittler, R. S. (1996). Intracellular trafficking of CTLA-4 and focal localization towards sites of TCR engagement. *Immunity*, *4*(6), 535–543. https://doi.org/10.1016/s1074-7613(00)80480-x

Liu, X., Zhang, N., & Shi, H. (2017). Driving better and safer HER2-specific CARs for cancer therapy. *Oncotarget*, *8*(37), 62730–62741. https://doi.org/10.18632/oncotarget.17528

Lonez, C., Verma, B., Hendlisz, A., Aftimos, P., Awada, A., Van Den Neste, E., Catala, G., Machiels, J.-P. H., Piette, F., Brayer, J. B., Sallman, D. A., Kerre, T., Odunsi, K., Davila, M. L., Gilham, D. E., & Lehmann, F. F. (2017). Study protocol for THINK: A multinational open-label phase I study to assess the safety and clinical activity of multiple administrations of NKR-2 in patients with different metastatic tumour types. *BMJ Open*, *7*(11), e017075. https://doi.org/10.1136/bmjopen-2017-017075

Loskog, A., Giandomenico, V., Rossig, C., Pule, M., Dotti, G., & Brenner, M. K. (2006). Addition of the CD28 signaling domain to chimeric T-cell receptors enhances chimeric T-cell resistance to T regulatory cells. *Leukemia*, *20*(10), 1819–1828. https://doi.org/10.1038/sj.leu.2404366

Love, P. E., & Hayes, S. M. (2010). ITAM-mediated signaling by the T-cell antigen receptor. *Cold Spring Harbor Perspectives in Biology*, *2*(6), a002485. https://doi.org/10.1101/cshperspect.a002485

Malissen, M., Minard, K., Mjolsness, S., Kronenberg, M., Goverman, J., Hunkapiller, T., Prystowsky, M. B., Yoshikai, Y., Fitch, F., & Mak, T. W. (1984). Mouse T cell antigen receptor: Structure and organization of constant and joining gene segments encoding the beta polypeptide. *Cell*, *37*(3), 1101–1110. https://doi.org/10.1016/0092-8674(84)90444-6

Mani, R., Goswami, S., Gopalakrishnan, B., Ramaswamy, R., Wasmuth, R., Tran, M., Mo, X., Gordon, A., Bucci, D., Lucas, D. M., Mims, A., Brooks, C., Dorrance, A., Walker, A., Blum, W., Byrd, J. C., Lozanski, G., Vasu, S., & Muthusamy, N. (2018). The interleukin-3 receptor CD123 targeted SL-401 mediates potent cytotoxic activity against CD34 $^+$ CD123 $^+$ cells from acute myeloid leukemia/myelodysplastic syndrome patients and healthy donors. *Haematologica*, *103*(8), 1288–1297. https://doi.org/10.3324/haematol.2018.188193

Manz, M. G., Miyamoto, T., Akashi, K., & Weissman, I. L. (2002). Prospective isolation of human clonogenic common myeloid progenitors. *Proceedings of the National Academy of Sciences*, *99*(18), 11872–11877. https://doi.org/10.1073/pnas.172384399

Marco Vitale, Giuseppe Pelusi, Beatrice Taroni, Giuliana Gobbi, Cristina Micheloni, Rita Rezzani, Francesco Donato, Xinhui Wang and Soldano Ferrone. (2005). *HLA Class I Antigen Down-Regulation in Primary Ovary Carcinoma Lesions: Association with Disease Stage*. *11*(1), 67–72.

Marcucci, G., Haferlach, T., & Döhner, H. (2011). Molecular Genetics of Adult Acute Myeloid Leukemia: Prognostic and Therapeutic Implications. *Journal of Clinical Oncology*, *29*(5), 475–486. https://doi.org/10.1200/JCO.2010.30.2554

Mardiros, A., Dos Santos, C., McDonald, T., Brown, C. E., Wang, X., Budde, L. E., Hoffman, L., Aguilar, B., Chang, W.-C., Bretzlaff, W., Chang, B., Jonnalagadda, M., Starr, R., Ostberg, J. R., Jensen, M. C., Bhatia, R., & Forman, S. J. (2013). T cells expressing CD123-specific chimeric antigen receptors exhibit specific cytolytic effector functions and antitumor effects against human acute myeloid leukemia. *Blood*, *122*(18), 3138–3148. https://doi.org/10.1182/blood-2012-12-474056

Mátrai, J., Chuah, M. K. L., & VandenDriessche, T. (2010). Recent advances in lentiviral vector development and applications. *Molecular Therapy: The Journal of the American Society of Gene Therapy*, *18*(3), 477–490. https://doi.org/10.1038/mt.2009.319

Maude, S. L., Frey, N., Shaw, P. A., Aplenc, R., Barrett, D. M., Bunin, N. J., Chew, A., Gonzalez, V. E., Zheng, Z., Lacey, S. F., Mahnke, Y. D., Melenhorst, J. J., Rheingold, S. R., Shen, A., Teachey, D. T., Levine, B. L., June, C. H., Porter, D. L., & Grupp, S. A. (2014). Chimeric Antigen Receptor T Cells for Sustained Remissions in Leukemia. *New England Journal of Medicine*, *371*(16), 1507–1517. https://doi.org/10.1056/NEJMoa1407222

Maude, S. L., Teachey, D. T., Porter, D. L., & Grupp, S. A. (2015). CD19-targeted chimeric antigen receptor T-cell therapy for acute lymphoblastic leukemia. *Blood*, *125*(26), 4017–4023. https://doi.org/10.1182/blood-2014-12-580068

Maurice, M., Verhoeyen, E., Salmon, P., Trono, D., Russell, S. J., & Cosset, F.-L. (2002). Efficient gene transfer into human primary blood lymphocytes by surface-engineered lentiviral vectors that display a T cell–activating polypeptide. *Blood*, *99*(7), 2342–2350. https://doi.org/10.1182/blood.V99.7.2342

Medeiros, B. C., Othus, M., Fang, M., Roulston, D., & Appelbaum, F. R. (2010). Prognostic impact of monosomal karyotype in young adult and elderly acute myeloid leukemia: The Southwest Oncology Group (SWOG) experience. *Blood*, *116*(13), 2224–2228. https://doi.org/10.1182/blood-2010-02-270330

Merten, O.-W., Charrier, S., Laroudie, N., Fauchille, S., Dugué, C., Jenny, C., Audit, M., Zanta-Boussif, M.-A., Chautard, H., Radrizzani, M., Vallanti, G., Naldini, L., Noguiez-Hellin, P., & Galy, A. (2011). Large-scale manufacture and characterization of a lentiviral vector produced for clinical ex vivo gene therapy application. *Human Gene Therapy*, *22*(3), 343–356. https://doi.org/10.1089/hum.2010.060

Milone, M. C., Fish, J. D., Carpenito, C., Carroll, R. G., Binder, G. K., Teachey, D., Samanta, M., Lakhal, M., Gloss, B., Danet-Desnoyers, G., Campana, D., Riley, J. L., Grupp, S. A., & June, C. H. (2009). Chimeric Receptors Containing CD137 Signal Transduction Domains Mediate Enhanced Survival of T Cells and Increased Antileukemic Efficacy In Vivo. *Molecular Therapy*, *17*(8), 1453–1464. https://doi.org/10.1038/mt.2009.83

Montini, E., Cesana, D., Schmidt, M., Sanvito, F., Bartholomae, C. C., Ranzani, M., Benedicenti, F., Sergi, L. S., Ambrosi, A., Ponzoni, M., Doglioni, C., Di Serio, C., von Kalle, C., & Naldini, L. (2009). The genotoxic potential of retroviral vectors is strongly modulated by vector design and integration site selection in a mouse model of HSC gene therapy. *The Journal of Clinical Investigation*, *119*(4), 964–975. https://doi.org/10.1172/JCI37630

Movahedi, K., Guilliams, M., Van den Bossche, J., Van den Bergh, R., Gysemans, C., Beschin, A., De Baetselier, P., & Van Ginderachter, J. A. (2008). Identification of discrete tumor-induced myeloid-derived suppressor cell subpopulations with distinct T cell–suppressive activity. *Blood*, *111*(8), 4233–4244. https://doi.org/10.1182/blood-2007-07-099226

Mrózek, K., Marcucci, G., Nicolet, D., Maharry, K. S., Becker, H., Whitman, S. P., Metzeler, K. H., Schwind, S., Wu, Y.-Z., Kohlschmidt, J., Pettenati, M. J., Heerema, N. A., Block, A. W., Patil, S. R., Baer, M. R., Kolitz, J. E., Moore, J. O., Carroll, A. J., Stone, R. M., … Bloomfield, C. D. (2012). Prognostic Significance of the European LeukemiaNet Standardized System for Reporting Cytogenetic and Molecular Alterations in Adults With Acute Myeloid Leukemia. *Journal of Clinical Oncology*, *30*(36), 4515–4523. https://doi.org/10.1200/JCO.2012.43.4738

Murphy, K. M., & Reiner, S. L. (2002). The lineage decisions of helper T cells. *Nature Reviews Immunology*, *2*(12), 933–944. https://doi.org/10.1038/nri954

Murthy, H., Iqbal, M., Chavez, J. C., & Kharfan-Dabaja, M. A. (2019). Cytokine Release Syndrome: Current Perspectives. *ImmunoTargets and Therapy*, *Volume 8*, 43–52. https://doi.org/10.2147/ITT.S202015

Nabhan, C., Rundhaugen, L., Jatoi, M., Riley, M. B., Boehlke, L., Peterson, L. C., & Tallman, M. S. (2004). Gemtuzumab ozogamicin (MylotargTM) is infrequently associated with sinusoidal obstructive syndrome/veno-occlusive disease. *Annals of Oncology*, *15*(8), 1231–1236. https://doi.org/10.1093/annonc/mdh324

Nagorsen, D., Bargou, R., Rüttinger, D., Kufer, P., Baeuerle, P. A., & Zugmaier, G. (2009). Immunotherapy of lymphoma and leukemia with T-cell engaging BiTE antibody blinatumomab. *Leukemia & Lymphoma*, *50*(6), 886–891. https://doi.org/10.1080/10428190902943077

Nassereddine, S., Lap, C. J., & Tabbara, I. A. (2018). Evaluating ivosidenib for the treatment of relapsed/refractory AML: Design, development, and place in therapy. *OncoTargets and Therapy*, *Volume 12*, 303–308. https://doi.org/10.2147/OTT.S182443

Neelapu, S. S., Tummala, S., Kebriaei, P., Wierda, W., Gutierrez, C., Locke, F. L., Komanduri, K. V., Lin, Y., Jain, N., Daver, N., Westin, J., Gulbis, A. M., Loghin, M. E., de Groot, J. F., Adkins, S., Davis, S. E., Rezvani, K., Hwu, P., & Shpall, E. J. (2018). Chimeric antigen receptor T-cell therapy—Assessment and management of toxicities. *Nature Reviews. Clinical Oncology*, *15*(1), 47–62. https://doi.org/10.1038/nrclinonc.2017.148

Nika, K., Soldani, C., Salek, M., Paster, W., Gray, A., Etzensperger, R., Fugger, L., Polzella, P., Cerundolo, V., Dushek, O., Höfer, T., Viola, A., & Acuto, O. (2010). Constitutively active Lck kinase in T cells drives antigen receptor signal transduction. *Immunity*, *32*(6), 766–777. https://doi.org/10.1016/j.immuni.2010.05.011

Nikiforow, S., Murad, J., Daley, H., Negre, H., Reder, J., Sentman, C. L., Lehmann, F., Snykers, S., Allen, R., Galinsky, I., Munshi, N. C., Stone, R. M., Soiffer, R., Ritz, J., & Baumeister, S. H. C. (2016). A first-in-human phase I trial of NKG2D chimeric antigen receptor-T cells in AML/MDS and multiple myeloma. *Journal of Clinical Oncology*, *34*(15_suppl), TPS3102–TPS3102. https://doi.org/10.1200/JCO.2016.34.15_suppl.TPS3102

Noll, J. E., Williams, S. A., Purton, L. E., & Zannettino, A. C. W. (2012). Tug of war in the haematopoietic stem cell niche: Do myeloma plasma cells compete for the HSC niche? *Blood Cancer Journal*, *2*(9), e91–e91. https://doi.org/10.1038/bcj.2012.38

Nosaka, T. (1999). STAT5 as a molecular regulator of proliferation, differentiation and apoptosis in hematopoietic cells. *The EMBO Journal*, *18*(17), 4754–4765. https://doi.org/10.1093/emboj/18.17.4754

Ostrand-Rosenberg, S., & Fenselau, C. (2018). Myeloid-Derived Suppressor Cells: Immune-

Suppressive Cells That Impair Antitumor Immunity and Are Sculpted by Their Environment. *The Journal of Immunology*, *200*(2), 422–431. https://doi.org/10.4049/jimmunol.1701019

Pan, R., Hogdal, L. J., Benito, J. M., Bucci, D., Han, L., Borthakur, G., Cortes, J., DeAngelo, D. J., Debose, L., Mu, H., Döhner, H., Gaidzik, V. I., Galinsky, I., Golfman, L. S., Haferlach, T., Harutyunyan, K. G., Hu, J., Leverson, J. D., Marcucci, G., … Letai, A. G. (2014). Selective BCL-2 Inhibition by ABT-199 Causes On-Target Cell Death in Acute Myeloid Leukemia. *Cancer Discovery*, *4*(3), 362–375. https://doi.org/10.1158/2159-8290.CD-13-0609

Parkhurst, M. R., Yang, J. C., Langan, R. C., Dudley, M. E., Nathan, D.-A. N., Feldman, S. A., Davis, J. L., Morgan, R. A., Merino, M. J., Sherry, R. M., Hughes, M. S., Kammula, U. S., Phan, G. Q., Lim, R. M., Wank, S. A., Restifo, N. P., Robbins, P. F., Laurencot, C. M., & Rosenberg, S. A. (2011). T Cells Targeting Carcinoembryonic Antigen Can Mediate Regression of Metastatic Colorectal Cancer but Induce Severe Transient Colitis. *Molecular Therapy*, *19*(3), 620–626. https://doi.org/10.1038/mt.2010.272

Paulos, C. M., Carpenito, C., Plesa, G., Suhoski, M. M., Varela-Rohena, A., Golovina, T. N., Carroll, R. G., Riley, J. L., & June, C. H. (2010). The inducible costimulator (ICOS) is critical for the development of human T(H)17 cells. *Science Translational Medicine*, *2*(55), 55ra78. https://doi.org/10.1126/scitranslmed.3000448

Peinert, S., Prince, H. M., Guru, P. M., Kershaw, M. H., Smyth, M. J., Trapani, J. A., Gambell, P., Harrison, S., Scott, A. M., Smyth, F. E., Darcy, P. K., Tainton, K., Neeson, P., Ritchie, D. S., & Hönemann, D. (2010). Gene-modified T cells as immunotherapy for multiple myeloma and acute myeloid leukemia expressing the Lewis Y antigen. *Gene Therapy*, *17*(5), 678–686. https://doi.org/10.1038/gt.2010.21

Perl, A. E., Altman, J. K., Cortes, J., Smith, C., Litzow, M., Baer, M. R., Claxton, D., Erba, H. P., Gill, S., Goldberg, S., Jurcic, J. G., Larson, R. A., Liu, C., Ritchie, E., Schiller, G., Spira, A. I., Strickland, S. A., Tibes, R., Ustun, C., … Levis, M. (2017). Selective inhibition of FLT3 by gilteritinib in relapsed or refractory acute myeloid leukaemia: A multicentre, first-in-human, open-label, phase 1–2 study. *The Lancet Oncology*, *18*(8), 1061–1075. https://doi.org/10.1016/S1470-2045(17)30416-3

Perl, A. E., Martinelli, G., Cortes, J. E., Neubauer, A., Berman, E., Paolini, S., Montesinos, P., Baer, M. R., Larson, R. A., Ustun, C., Fabbiano, F., Erba, H. P., Di Stasi, A., Stuart, R., Olin, R., Kasner, M., Ciceri, F., Chou, W.-C., Podoltsev, N., … Levis, M. J. (2019). Gilteritinib or Chemotherapy for Relapsed or Refractory *FLT3* -Mutated AML. *New England Journal of Medicine*, *381*(18), 1728–1740. https://doi.org/10.1056/NEJMoa1902688

Petersdorf, S., Kopecky, K., Stuart, R. K., Larson, R. A., Nevill, T. J., Stenke, L., Slovak, M. L., Tallman, M. S., Willman, C. L., Erba, H., & Appelbaum, F. R. (2009). Preliminary Results of Southwest Oncology Group Study S0106: An International Intergroup Phase 3 Randomized Trial Comparing the Addition of Gemtuzumab Ozogamicin to Standard Induction Therapy Versus Standard Induction Therapy Followed by a Second Randomization to Post-Consolidation Gemtuzumab Ozogamicin Versus No Additional Therapy for Previously Untreated Acute Myeloid Leukemia. *Blood*, *114*(22), 790–790. https://doi.org/10.1182/blood.V114.22.790.790

Pistello, M., Vannucci, L., Ravani, A., Bonci, F., Chiuppesi, F., del Santo, B., Freer, G., & Bendinelli, M. (2007). Streamlined design of a self-inactivating feline immunodeficiency virus vector for transducing ex vivo dendritic cells and T lymphocytes. *Genetic Vaccines and Therapy*, *5*, 8. https://doi.org/10.1186/1479-0556-5-8

Pizzitola, I., Anjos-Afonso, F., Rouault-Pierre, K., Lassailly, F., Tettamanti, S., Spinelli, O., Biondi, A., Biagi, E., & Bonnet, D. (2014). Chimeric antigen receptors against CD33/CD123 antigens efficiently target primary acute myeloid leukemia cells in vivo. *Leukemia*, *28*(8), 1596–1605. https://doi.org/10.1038/leu.2014.62

Porter, D. L., Levine, B. L., Kalos, M., Bagg, A., & June, C. H. (2011). Chimeric Antigen Receptor–Modified T Cells in Chronic Lymphoid Leukemia. *New England Journal of Medicine*, *365*(8), 725–733. https://doi.org/10.1056/NEJMoa1103849

Priceman, S. J., Forman, S. J., & Brown, C. E. (2015). Smart CARs engineered for cancer immunotherapy. *Current Opinion in Oncology*, *27*(6), 466–474. https://doi.org/10.1097/CCO.0000000000000232

Pulè, M. A., Straathof, K. C., Dotti, G., Heslop, H. E., Rooney, C. M., & Brenner, M. K. (2005). A chimeric T cell antigen receptor that augments cytokine release and supports clonal expansion of primary human T cells. *Molecular Therapy: The Journal of the American Society of Gene Therapy*, *12*(5), 933–941. https://doi.org/10.1016/j.ymthe.2005.04.016

Ram, R., Amit, O., Zuckerman, T., Gurion, R., Raanani, P., Bar-On, Y., Avivi, I., & Wolach, O. (2019). Venetoclax in patients with acute myeloid leukemia refractory to hypomethylating agents-a multicenter historical prospective study. *Annals of Hematology*, *98*(8), 1927–1932. https://doi.org/10.1007/s00277-019-03719-6

Ramello, M. C., Benzaïd, I., Kuenzi, B. M., Lienlaf-Moreno, M., Kandell, W. M., Santiago, D. N., Pabón-Saldaña, M., Darville, L., Fang, B., Rix, U., Yoder, S., Berglund, A., Koomen, J. M., Haura, E. B., & Abate-Daga, D. (2019). An immunoproteomic approach to characterize the CAR interactome and signalosome. *Science Signaling*, *12*(568). https://doi.org/10.1126/scisignal.aap9777

Ramos, C. A., Rouce, R., Robertson, C. S., Reyna, A., Narala, N., Vyas, G., Mehta, B., Zhang, H., Dakhova, O., Carrum, G., Kamble, R. T., Gee, A. P., Mei, Z., Wu, M.-F., Liu, H., Grilley, B., Rooney, C. M., Heslop, H. E., Brenner, M. K., … Dotti, G. (2018). In Vivo Fate and Activity of Second- versus Third-Generation CD19-Specific CAR-T Cells in B Cell Non-Hodgkin’s Lymphomas. *Molecular Therapy: The Journal of the American Society of Gene Therapy*, *26*(12), 2727–2737. https://doi.org/10.1016/j.ymthe.2018.09.009

Reya, T., Morrison, S. J., Clarke, M. F., & Weissman, I. L. (2001). Stem cells, cancer, and cancer stem cells. *Nature*, *414*(6859), 105–111. https://doi.org/10.1038/35102167

Riccioni, R., Diverio, D., Riti, V., Buffolino, S., Mariani, G., Boe, A., Cedrone, M., Ottone, T., Foà, R., & Testa, U. (2009). Interleukin (IL)-3/granulocyte macrophage-colony stimulating factor/IL-5 receptor alpha and beta chains are preferentially expressed in acute myeloid leukaemias with mutated FMS-related tyrosine kinase 3 receptor. *British Journal of Haematology*, *144*(3), 376–387. https://doi.org/10.1111/j.1365-2141.2008.07491.x

Riccioni, R., Pelosi, E., Riti, V., Castelli, G., Lo-Coco, F., & Testa, U. (2011). Immunophenotypic features of acute myeloid leukaemia patients exhibiting high FLT3 expression not associated with mutations: Acute Myeloid Leukaemia with High FLT3 Expression. *British Journal of Haematology*, *153*(1), 33–42. https://doi.org/10.1111/j.1365-2141.2011.08577.x
Riether, C., Schürch, C. M., & Ochsenbein, A. F. (2015). Regulation of hematopoietic and leukemic stem cells by the immune system. *Cell Death & Differentiation*, *22*(2), 187–198.

https://doi.org/10.1038/cdd.2014.89

Ritchie, D. S., Neeson, P. J., Khot, A., Peinert, S., Tai, T., Tainton, K., Chen, K., Shin, M., Wall, D. M., Hönemann, D., Gambell, P., Westerman, D. A., Haurat, J., Westwood, J. A., Scott, A. M., Kravets, L., Dickinson, M., Trapani, J. A., Smyth, M. J., … Prince, H. M. (2013). Persistence and Efficacy of Second Generation CAR T Cell Against the LeY Antigen in Acute Myeloid Leukemia. *Molecular Therapy*, *21*(11), 2122–2129. https://doi.org/10.1038/mt.2013.154

Rivière, I., Brose, K., & Mulligan, R. C. (1995). Effects of retroviral vector design on expression of human adenosine deaminase in murine bone marrow transplant recipients engrafted with genetically modified cells. *Proceedings of the National Academy of Sciences of the United States of America*, *92*(15), 6733–6737. https://doi.org/10.1073/pnas.92.15.6733

Robert, C., Thomas, L., Bondarenko, I., O'Day, S., Weber, J., Garbe, C., Lebbe, C., Baurain, J.-F., Testori, A., Grob, J.-J., Davidson, N., Richards, J., Maio, M., Hauschild, A., Miller, W. H., Gascon, P., Lotem, M., Harmankaya, K., Ibrahim, R., … Wolchok, J. D. (2011). Ipilimumab plus Dacarbazine for Previously Untreated Metastatic Melanoma. *New England Journal of Medicine*, *364*(26), 2517–2526. https://doi.org/10.1056/NEJMoa1104621

Röllig, C., Kramer, M., Schliemann, C., Mikesch, J.-H., Steffen, B., Krämer, A., Noppeney, R., Schäfer-Eckart, K., Krause, S. W., Hänel, M., Herbst, R., Kunzmann, V., Einsele, H., Jost, E., Brümmendorf, T. H., Scholl, S., Hochhaus, A., Neubauer, A., Sohlbach, K., … Bornhäuser, M. (2020). Does time from diagnosis to treatment affect the prognosis of patients with newly diagnosed acute myeloid leukemia? *Blood*, *136*(7), 823–830. https://doi.org/10.1182/blood.2019004583

Rollins-Raval, M., Pillai, R., Warita, K., Mitsuhashi-Warita, T., Mehta, R., Boyiadzis, M., Djokic, M., Kant, J. A., & Roth, C. G. (2013). CD123 Immunohistochemical Expression in Acute Myeloid Leukemia is Associated With Underlying FLT3-ITD and NPM1 Mutations. *Applied Immunohistochemistry & Molecular Morphology*, *21*(3), 212–217. https://doi.org/10.1097/PAI.0b013e318261a342

Rosenberg, S. A. (2001). Progress in human tumour immunology and immunotherapy. *Nature*, *411*(6835), 380–384. https://doi.org/10.1038/35077246

Rotte, A., Jin, J. Y., & Lemaire, V. (2018). Mechanistic overview of immune checkpoints to support the rational design of their combinations in cancer immunotherapy. *Annals of Oncology*, *29*(1), 71–83. https://doi.org/10.1093/annonc/mdx686

Rowshanravan, B., Halliday, N., & Sansom, D. M. (2018). CTLA-4: A moving target in immunotherapy. *Blood*, *131*(1), 58–67. https://doi.org/10.1182/blood-2017-06-741033

Ruella, M., Barrett, D. M., Kenderian, S. S., Shestova, O., Hofmann, T. J., Perazzelli, J., Klichinsky, M., Aikawa, V., Nazimuddin, F., Kozlowski, M., Scholler, J., Lacey, S. F., Melenhorst, J. J., Morrissette, J. J. D., Christian, D. A., Hunter, C. A., Kalos, M., Porter, D. L., June, C. H., … Gill, S. (2016). Dual CD19 and CD123 targeting prevents antigen-loss relapses after CD19-directed immunotherapies. *Journal of Clinical Investigation*, *126*(10), 3814–3826. https://doi.org/10.1172/JCI87366

Sadelain, M., Brentjens, R., & Rivière, I. (2013). The Basic Principles of Chimeric Antigen Receptor Design. *Cancer Discovery*, *3*(4), 388–398. https://doi.org/10.1158/2159-8290.CD-12-0548

Sage, P. T., Paterson, A. M., Lovitch, S. B., & Sharpe, A. H. (2014). The Coinhibitory Receptor CTLA-4 Controls B Cell Responses by Modulating T Follicular Helper, T Follicular Regulatory, and T Regulatory Cells. *Immunity*, *41*(6), 1026–1039. https://doi.org/10.1016/j.immuni.2014.12.005

Saito, T., & Germain, R. N. (1987). Predictable acquisition of a new MHC recognition specificity following expression of a transfected T-cell receptor beta-chain gene. *Nature*, *329*(6136), 256–259. https://doi.org/10.1038/329256a0

Sakuishi, K., Apetoh, L., Sullivan, J. M., Blazar, B. R., Kuchroo, V. K., & Anderson, A. C. (2010). Targeting Tim-3 and PD-1 pathways to reverse T cell exhaustion and restore anti-tumor immunity. *Journal of Experimental Medicine*, *207*(10), 2187–2194. https://doi.org/10.1084/jem.20100643

Salik, B., Smyth, M. J., & Nakamura, K. (2020). Targeting immune checkpoints in hematological malignancies. *Journal of Hematology & Oncology*, *13*(1), 111. https://doi.org/10.1186/s13045-020-00947-6

Salter, A. I., Ivey, R. G., Kennedy, J. J., Voillet, V., Rajan, A., Alderman, E. J., Voytovich, U. J., Lin, C., Sommermeyer, D., Liu, L., Whiteaker, J. R., Gottardo, R., Paulovich, A. G., & Riddell, S. R. (2018). Phosphoproteomic analysis of chimeric antigen receptor signaling reveals kinetic and quantitative differences that affect cell function. *Science Signaling*, *11*(544). https://doi.org/10.1126/scisignal.aat6753

Sánchez-Abarca, L. I., Gutierrez-Cosio, S., Santamaría, C., Caballero-Velazquez, T., Blanco, B., Herrero-Sánchez, C., García, J. L., Carrancio, S., Hernández-Campo, P., González, F. J., Flores, T., Ciudad, L., Ballestar, E., Del Cañizo, C., San Miguel, J. F., & Pérez-Simon, J. A. (2010). Immunomodulatory effect of 5-azacytidine (5-azaC): Potential role in the transplantation setting. *Blood*, *115*(1), 107–121. https://doi.org/10.1182/blood-2009-03-210393

Sato, N., Caux, C., Kitamura, T., Watanabe, Y., Arai, K., Banchereau, J., & Miyajima, A. (1993). Expression and factor-dependent modulation of the interleukin-3 receptor subunits on human hematopoietic cells. *Blood*, *82*(3), 752–761.

Savoldo, B., Ramos, C. A., Liu, E., Mims, M. P., Keating, M. J., Carrum, G., Kamble, R. T., Bollard, C. M., Gee, A. P., Mei, Z., Liu, H., Grilley, B., Rooney, C. M., Heslop, H. E., Brenner, M. K., & Dotti, G. (2011). CD28 costimulation improves expansion and persistence of chimeric antigen receptor–modified T cells in lymphoma patients. *Journal of Clinical Investigation*, *121*(5), 1822–1826. https://doi.org/10.1172/JCI46110

Saygin, C., & Carraway, H. E. (2017). Emerging therapies for acute myeloid leukemia. *Journal of Hematology & Oncology*, *10*(1), 93. https://doi.org/10.1186/s13045-017-0463-6

Schmidt-Wolf, I. G., Negrin, R. S., Kiem, H. P., Blume, K. G., & Weissman, I. L. (1991). Use of a SCID mouse/human lymphoma model to evaluate cytokine-induced killer cells with potent antitumor cell activity. *Journal of Experimental Medicine*, *174*(1), 139–149. https://doi.org/10.1084/jem.174.1.139

Schneider, H., Smith, X., Liu, H., Bismuth, G., & Rudd, C. E. (2008). CTLA-4 disrupts ZAP70 microcluster formation with reduced T cell/APC dwell times and calcium mobilization. *European Journal of Immunology*, *38*(1), 40–47. https://doi.org/10.1002/eji.200737423

Schuster, S. J., Bishop, M. R., Tam, C. S., Waller, E. K., Borchmann, P., McGuirk, J. P., Jäger, U., Jaglowski, S., Andreadis, C., Westin, J. R., Fleury, I., Bachanova, V., Foley, S. R., Ho, P. J., Mielke, S., Magenau, J. M., Holte, H., Pantano, S., Pacaud, L. B., … Maziarz, R. T. (2019). Tisagenlecleucel in Adult Relapsed or Refractory Diffuse Large B-Cell Lymphoma. *New England Journal of Medicine*, *380*(1), 45–56. https://doi.org/10.1056/NEJMoa1804980

Sen, D. R., Kaminski, J., Barnitz, R. A., Kurachi, M., Gerdemann, U., Yates, K. B., Tsao, H.-W., Godec, J., LaFleur, M. W., Brown, F. D., Tonnerre, P., Chung, R. T., Tully, D. C., Allen, T. M., Frahm, N., Lauer, G. M., Wherry, E. J., Yosef, N., & Haining, W. N. (2016). The epigenetic landscape of T cell exhaustion. *Science*, *354*(6316), 1165–1169. https://doi.org/10.1126/science.aae0491

Seshadri, M., & Qu, C.-K. (2016). Microenvironmental regulation of hematopoietic stem cells and its implications in leukemogenesis: *Current Opinion in Hematology*, *23*(4), 339–345. https://doi.org/10.1097/MOH.0000000000000251

Seymour, J. F., Döhner, H., Butrym, A., Wierzbowska, A., Selleslag, D., Jang, J. H., Kumar, R., Cavenagh, J., Schuh, A. C., Candoni, A., Récher, C., Sandhu, I., Del Castillo, T. B., Al-Ali, H. K., Falantes, J., Stone, R. M., Minden, M. D., Weaver, J., Songer, S., … Dombret, H. (2017). Azacitidine improves clinical outcomes in older patients with acute myeloid leukaemia with myelodysplasia-related changes compared with conventional care regimens. *BMC Cancer*, *17*(1), 852. https://doi.org/10.1186/s12885-017-3803-6

Shapiro, M., Herishanu, Y., Katz, B.-Z., Dezorella, N., Sun, C., Kay, S., Polliack, A., Avivi, I., Wiestner, A., & Perry, C. (2017). Lymphocyte activation gene 3: A novel therapeutic target in chronic lymphocytic leukemia. *Haematologica*, *102*(5), 874–882. https://doi.org/10.3324/haematol.2016.148965

Sharpe, M., & Mount, N. (2015). Genetically modified T cells in cancer therapy: Opportunities and challenges. *Disease Models & Mechanisms*, *8*(4), 337–350. https://doi.org/10.1242/dmm.018036

Sheppard, S., Ferry, A., Guedes, J., & Guerra, N. (2018). The Paradoxical Role of NKG2D in Cancer Immunity. *Frontiers in Immunology*, *9*, 1808. https://doi.org/10.3389/fimmu.2018.01808

Sill, H., Olipitz, W., Zebisch, A., Schulz, E., & Wölfler, A. (2011). Therapy-related myeloid neoplasms: Pathobiology and clinical characteristics: Therapy-related myeloid neoplasms. *British Journal of Pharmacology*, *162*(4), 792–805. https://doi.org/10.1111/j.1476-5381.2010.01100.x

Singh, N., Frey, N. V., Grupp, S. A., & Maude, S. L. (2016). CAR T Cell Therapy in Acute Lymphoblastic Leukemia and Potential for Chronic Lymphocytic Leukemia. *Current Treatment Options in Oncology*, *17*(6), 28. https://doi.org/10.1007/s11864-016-0406-4

Śledzińska, A., Menger, L., Bergerhoff, K., Peggs, K. S., & Quezada, S. A. (2015). Negative immune checkpoints on T lymphocytes and their relevance to cancer immunotherapy. *Molecular Oncology*, *9*(10), 1936–1965. https://doi.org/10.1016/j.molonc.2015.10.008

Sommermeyer, D., Hudecek, M., Kosasih, P. L., Gogishvili, T., Maloney, D. G., Turtle, C. J., & Riddell, S. R. (2016). Chimeric antigen receptor-modified T cells derived from defined CD8+ and CD4+ subsets confer superior antitumor reactivity in vivo. *Leukemia*, *30*(2), 492–500. https://doi.org/10.1038/leu.2015.247

Song, D.-G., Ye, Q., Carpenito, C., Poussin, M., Wang, L.-P., Ji, C., Figini, M., June, C. H., Coukos, G., & Powell, D. J. (2011). *In Vivo* Persistence, Tumor Localization, and Antitumor Activity of CAR-Engineered T Cells Is Enhanced by Costimulatory Signaling through CD137 (4-1BB). *Cancer Research*, *71*(13), 4617–4627. https://doi.org/10.1158/0008-5472.CAN-11-0422

Srivastava, S., & Riddell, S. R. (2015). Engineering CAR-T cells: Design concepts. *Trends in Immunology*, *36*(8), 494–502. https://doi.org/10.1016/j.it.2015.06.004

Stamper, C. C., Zhang, Y., Tobin, J. F., Erbe, D. V., Ikemizu, S., Davis, S. J., Stahl, M. L., Seehra, J., Somers, W. S., & Mosyak, L. (2001). Crystal structure of the B7-1/CTLA-4 complex that inhibits human immune responses. *Nature*, *410*(6828), 608–611. https://doi.org/10.1038/35069118

Stein, E. M. (2015). IDH2 inhibition in AML: Finally progress? *Best Practice & Research Clinical Haematology*, *28*(2–3), 112–115. https://doi.org/10.1016/j.beha.2015.10.016

Stein, E. M., DiNardo, C. D., Pollyea, D. A., Fathi, A. T., Roboz, G. J., Altman, J. K., Stone, R. M., DeAngelo, D. J., Levine, R. L., Flinn, I. W., Kantarjian, H. M., Collins, R., Patel, M. R., Frankel, A. E., Stein, A., Sekeres, M. A., Swords, R. T., Medeiros, B. C., Willekens, C., … Tallman, M. S. (2017). Enasidenib in mutant IDH2 relapsed or refractory acute myeloid leukemia. *Blood*, *130*(6), 722–731. https://doi.org/10.1182/blood-2017-04-779405

Sterner, R. M., Sakemura, R., Cox, M. J., Yang, N., Khadka, R. H., Forsman, C. L., Hansen, M. J., Jin, F., Ayasoufi, K., Hefazi, M., Schick, K. J., Walters, D. K., Ahmed, O., Chappell, D., Sahmoud, T., Durrant, C., Nevala, W. K., Patnaik, M. M., Pease, L. R., … Kenderian, S. S. (2019). GM-CSF inhibition reduces cytokine release syndrome and neuroinflammation but enhances CAR-T cell function in xenografts. *Blood*, *133*(7), 697–709. https://doi.org/10.1182/blood-2018-10-881722

Stojanovic, A., Fiegler, N., Brunner-Weinzierl, M., & Cerwenka, A. (2014). CTLA-4 Is Expressed by Activated Mouse NK Cells and Inhibits NK Cell IFN-γ Production in Response to Mature Dendritic Cells. *The Journal of Immunology*, *192*(9), 4184–4191. https://doi.org/10.4049/jimmunol.1302091

Stone, R. M., Mandrekar, S. J., Sanford, B. L., Laumann, K., Geyer, S., Bloomfield, C. D., Thiede, C., Prior, T. W., Döhner, K., Marcucci, G., Lo-Coco, F., Klisovic, R. B., Wei, A., Sierra, J., Sanz, M. A., Brandwein, J. M., de Witte, T., Niederwieser, D., Appelbaum, F. R., … Döhner, H. (2017). Midostaurin plus Chemotherapy for Acute Myeloid Leukemia with a *FLT3* Mutation. *New England Journal of Medicine*, *377*(5), 454–464. https://doi.org/10.1056/NEJMoa1614359

Stone, R. M., Manley, P. W., Larson, R. A., & Capdeville, R. (2018). Midostaurin: Its odyssey from discovery to approval for treating acute myeloid leukemia and advanced systemic mastocytosis. *Blood Advances*, *2*(4), 444–453. https://doi.org/10.1182/bloodadvances.2017011080

Suryadevara, C. M., Desai, R., Farber, S. H., Choi, B. D., Swartz, A. M., Shen, S. H., Gedeon, P. C., Snyder, D. J., Herndon, J. E., Healy, P., Reap, E. A., Archer, G. E., Fecci, P. E., Sampson, J. H., & Sanchez-Perez, L. (2019). Preventing Lck Activation in CAR T Cells Confers Treg Resistance but Requires 4-1BB Signaling for Them to Persist and Treat Solid Tumors in Nonlymphodepleted Hosts. *Clinical Cancer Research*, *25*(1), 358–368. https://doi.org/10.1158/1078-0432.CCR-18-1211

Sutherland, M. K., Yu, C., Anderson, M., Zeng, W., van Rooijen, N., Sievers, E. L., Grewal, I. S., & Law, C.-L. (2010). 5-Azacytidine enhances the anti-leukemic activity of lintuzumab (SGN-33) in preclinical models of acute myeloid leukemia. *MAbs*, *2*(4), 440–448. https://doi.org/10.4161/mabs.12203

Tammana, S., Huang, X., Wong, M., Milone, M. C., Ma, L., Levine, B. L., June, C. H., Wagner, J. E., Blazar, B. R., & Zhou, X. (2010). 4-1BB and CD28 signaling plays a synergistic role in redirecting umbilical cord blood T cells against B-cell malignancies. *Human Gene Therapy*, *21*(1), 75–86. https://doi.org/10.1089/hum.2009.122

Tardi, P., Johnstone, S., Harasym, N., Xie, S., Harasym, T., Zisman, N., Harvie, P., Bermudes, D., & Mayer, L. (2009). In vivo maintenance of synergistic cytarabine:daunorubicin ratios greatly enhances therapeutic efficacy. *Leukemia Research*, *33*(1), 129–139. https://doi.org/10.1016/j.leukres.2008.06.028

Teague, R. M., & Kline, J. (2013). Immune evasion in acute myeloid leukemia: Current concepts and future directions. *Journal for ImmunoTherapy of Cancer*, *1*(1), 13. https://doi.org/10.1186/2051-1426-1-13

Testa, U., Pelosi, E., & Frankel, A. (2014). CD 123 is a membrane biomarker and a therapeutic target in hematologic malignancies. *Biomarker Research*, *2*(1), 4. https://doi.org/10.1186/2050-7771-2-4

Testa, U., Riccioni, R., Biffoni, M., Diverio, D., Lo-Coco, F., Foà, R., Peschle, C., & Frankel, A. E. (2005). Diphtheria toxin fused to variant human interleukin-3 induces cytotoxicity of blasts from patients with acute myeloid leukemia according to the level of interleukin-3 receptor expression. *Blood*, *106*(7), 2527–2529. https://doi.org/10.1182/blood-2005-02-0540

Testa, U., Riccioni, R., Diverio, D., Rossini, A., Lo Coco, F., & Peschle, C. (2004). Interleukin-3 receptor in acute leukemia. *Leukemia*, *18*(2), 219–226. https://doi.org/10.1038/sj.leu.2403224

Tettamanti, S., Marin, V., Pizzitola, I., Magnani, C. F., Giordano Attianese, G. M. P., Cribioli, E., Maltese, F., Galimberti, S., Lopez, A. F., Biondi, A., Bonnet, D., & Biagi, E. (2013). Targeting of acute myeloid leukaemia by cytokine-induced killer cells redirected with a novel CD123-specific chimeric antigen receptor. *British Journal of Haematology*, *161*(3), 389–401. https://doi.org/10.1111/bjh.12282

Tiscornia, G., Singer, O., & Verma, I. M. (2006). Production and purification of lentiviral vectors. *Nature Protocols*, *1*(1), 241–245. https://doi.org/10.1038/nprot.2006.37

Toffalori, C., Zito, L., Gambacorta, V., Riba, M., Oliveira, G., Bucci, G., Barcella, M., Spinelli, O., Greco, R., Crucitti, L., Cieri, N., Noviello, M., Manfredi, F., Montaldo, E., Ostuni, R., Naldini, M. M., Gentner, B., Waterhouse, M., Zeiser, R., … Vago, L. (2019). Immune signature drives leukemia escape and relapse after hematopoietic cell transplantation. *Nature Medicine*, *25*(4), 603–611. https://doi.org/10.1038/s41591-019-0400-z

Topalian, S. L., Drake, C. G., & Pardoll, D. M. (2015). Immune checkpoint blockade: A common denominator approach to cancer therapy. *Cancer Cell*, *27*(4), 450–461. https://doi.org/10.1016/j.ccell.2015.03.001

Triebel, F., Jitsukawa, S., Baixeras, E., Roman-Roman, S., Genevee, C., Viegas-Pequignot, E., & Hercend, T. (1990). LAG-3, a novel lymphocyte activation gene closely related to CD4. *Journal of*

Experimental Medicine, *171*(5), 1393–1405. https://doi.org/10.1084/jem.171.5.1393

Turtle, C. J., Hanafi, L.-A., Berger, C., Gooley, T. A., Cherian, S., Hudecek, M., Sommermeyer, D., Melville, K., Pender, B., Budiarto, T. M., Robinson, E., Steevens, N. N., Chaney, C., Soma, L., Chen, X., Yeung, C., Wood, B., Li, D., Cao, J., … Maloney, D. G. (2016). CD19 CAR–T cells of defined CD4+:CD8+ composition in adult B cell ALL patients. *Journal of Clinical Investigation*, *126*(6), 2123–2138. https://doi.org/10.1172/JCI85309

Tuthill, M. & Hatzimichael. (2010). Hematopoietic stem cell transplantation. *Stem Cells and Cloning: Advances and Applications*, 105. https://doi.org/10.2147/SCCAA.S6815

Vago, L., Perna, S. K., Zanussi, M., Mazzi, B., Barlassina, C., Stanghellini, M. T. L., Perrelli, N. F., Cosentino, C., Torri, F., Angius, A., Forno, B., Casucci, M., Bernardi, M., Peccatori, J., Corti, C., Bondanza, A., Ferrari, M., Rossini, S., Roncarolo, M. G., … Fleischhauer, K. (2009). Loss of Mismatched HLA in Leukemia after Stem-Cell Transplantation. *New England Journal of Medicine*, *361*(5), 478–488. https://doi.org/10.1056/NEJMoa0811036

Vibhakar, R., Juan, G., Traganos, F., Darzynkiewicz, Z., & Finger, L. R. (1997). Activation-Induced Expression of Human Programmed Death-1 Gene in T-Lymphocytes. *Experimental Cell Research*, *232*(1), 25–28. https://doi.org/10.1006/excr.1997.3493

Villalobos, I. B., Takahashi, Y., Akatsuka, Y., Muramatsu, H., Nishio, N., Hama, A., Yagasaki, H., Saji, H., Kato, M., Ogawa, S., & Kojima, S. (2010). Relapse of leukemia with loss of mismatched HLA resulting from uniparental disomy after haploidentical hematopoietic stem cell transplantation. *Blood*, *115*(15), 3158–3161. https://doi.org/10.1182/blood-2009-11-254284

Walker, L. S. K. (2013). Treg and CTLA-4: Two intertwining pathways to immune tolerance. *Journal of Autoimmunity*, *45*, 49–57. https://doi.org/10.1016/j.jaut.2013.06.006

Wang, Q., Wang, Y., Lv, H., Han, Q., Fan, H., Guo, B., Wang, L., & Han, W. (2015). Treatment of CD33-directed Chimeric Antigen Receptor-modified T Cells in One Patient With Relapsed and Refractory Acute Myeloid Leukemia. *Molecular Therapy*, *23*(1), 184–191. https://doi.org/10.1038/mt.2014.164

Watanabe, N., Bajgain, P., Sukumaran, S., Ansari, S., Heslop, H. E., Rooney, C. M., Brenner, M. K., Leen, A. M., & Vera, J. F. (2016). Fine-tuning the CAR spacer improves T-cell potency. *OncoImmunology*, *5*(12), e1253656. https://doi.org/10.1080/2162402X.2016.1253656

Wei, A. H., Strickland, S. A., Hou, J.-Z., Fiedler, W., Lin, T. L., Walter, R. B., Enjeti, A., Tiong, I. S., Savona, M., Lee, S., Chyla, B., Popovic, R., Salem, A. H., Agarwal, S., Xu, T., Fakouhi, K. M., Humerickhouse, R., Hong, W.-J., Hayslip, J., & Roboz, G. J. (2019). Venetoclax Combined With Low-Dose Cytarabine for Previously Untreated Patients With Acute Myeloid Leukemia: Results From a Phase Ib/II Study. *Journal of Clinical Oncology*, *37*(15), 1277–1284. https://doi.org/10.1200/JCO.18.01600

Wherry, E. J., Ha, S.-J., Kaech, S. M., Haining, W. N., Sarkar, S., Kalia, V., Subramaniam, S., Blattman, J. N., Barber, D. L., & Ahmed, R. (2007). Molecular signature of CD8+ T cell exhaustion during chronic viral infection. *Immunity*, *27*(4), 670–684. https://doi.org/10.1016/j.immuni.2007.09.006

Whiteman, K. R., Noordhuis, P., Walker, R., Watkins, K., Kovtun, Y., Harvey, L., Wilhelm, A., Johnson, H., Schuurhuis, G. J., Ossenkoppele, G. J., & Lutz, R. J. (2014). The Antibody-Drug Conjugate (ADC) IMGN779 Is Highly Active in Vitro and in Vivo Against Acute Myeloid Leukemia (AML) with FLT3-ITD Mutations. *Blood*, *124*(21), 2321–2321. https://doi.org/10.1182/blood.V124.21.2321.2321

Wilkie, S., van Schalkwyk, M. C. I., Hobbs, S., Davies, D. M., van der Stegen, S. J. C., Pereira, A. C. P., Burbridge, S. E., Box, C., Eccles, S. A., & Maher, J. (2012). Dual Targeting of ErbB2 and MUC1 in Breast Cancer Using Chimeric Antigen Receptors Engineered to Provide Complementary Signaling. *Journal of Clinical Immunology*, *32*(5), 1059–1070. https://doi.org/10.1007/s10875-012-9689-9

Williams, P., Basu, S., Garcia-Manero, G., Hourigan, C. S., Oetjen, K. A., Cortes, J. E., Ravandi, F., Jabbour, E. J., Al-Hamal, Z., Konopleva, M., Ning, J., Xiao, L., Hidalgo Lopez, J., Kornblau, S. M., Andreeff, M., Flores, W., Bueso-Ramos, C., Blando, J., Galera, P., … Daver, N. G. (2019). The distribution of T-cell subsets and the expression of immune checkpoint receptors and ligands in patients with newly diagnosed and relapsed acute myeloid leukemia. *Cancer*, *125*(9), 1470–1481. https://doi.org/10.1002/cncr.31896

Wilson, C. B., Rowell, E., & Sekimata, M. (2009). Epigenetic control of T-helper-cell differentiation. *Nature Reviews. Immunology*, *9*(2), 91–105. https://doi.org/10.1038/nri2487

Workman, C. J., Rice, D. S., Dugger, K. J., Kurschner, C., & Vignali, D. A. A. (2002). Phenotypic analysis of the murine CD4-related glycoprotein, CD223 (LAG-3). *European Journal of Immunology*, *32*(8), 2255–2263. https://doi.org/10.1002/1521-4141(200208)32:8<2255::AID-IMMU2255>3.0.CO;2-A

Xie, L. H., Biondo, M., Busfield, S. J., Arruda, A., Yang, X., Vairo, G., & Minden, M. D. (2017). CD123 target validation and preclinical evaluation of ADCC activity of anti-CD123 antibody CSL362 in combination with NKs from AML patients in remission. *Blood Cancer Journal*, *7*(6), e567. https://doi.org/10.1038/bcj.2017.52

Xue, T., & Budde, L. E. (2020). Immunotherapies Targeting CD123 for Blastic Plasmacytoid Dendritic Cell Neoplasm. *Hematology/Oncology Clinics of North America*, *34*(3), 575–587. https://doi.org/10.1016/j.hoc.2020.01.006

Yalcintepe, L., Frankel, A. E., & Hogge, D. E. (2006). Expression of interleukin-3 receptor subunits on defined subpopulations of acute myeloid leukemia blasts predicts the cytotoxicity of diphtheria toxin interleukin-3 fusion protein against malignant progenitors that engraft in immunodeficient mice. *Blood*, *108*(10), 3530–3537. https://doi.org/10.1182/blood-2006-04-013813

Yamazaki, T., Akiba, H., Iwai, H., Matsuda, H., Aoki, M., Tanno, Y., Shin, T., Tsuchiya, H., Pardoll, D. M., Okumura, K., Azuma, M., & Yagita, H. (2002). Expression of Programmed Death 1 Ligands by Murine T Cells and APC. *The Journal of Immunology*, *169*(10), 5538–5545. https://doi.org/10.4049/jimmunol.169.10.5538

Yip, A., & Webster, R. M. (2018). The market for chimeric antigen receptor T cell therapies. *Nature Reviews Drug Discovery*, *17*(3), 161–162. https://doi.org/10.1038/nrd.2017.266

Yoon, D., Osborn, M., Tolar, J., & Kim, C. (2018). Incorporation of Immune Checkpoint Blockade into Chimeric Antigen Receptor T Cells (CAR-Ts): Combination or Built-In CAR-T. *International*

Journal of Molecular Sciences, *19*(2), 340. https://doi.org/10.3390/ijms19020340

Yu, S., Li, A., Liu, Q., Li, T., Yuan, X., Han, X., & Wu, K. (2017). Chimeric antigen receptor T cells: A novel therapy for solid tumors. *Journal of Hematology & Oncology*, *10*(1), 78. https://doi.org/10.1186/s13045-017-0444-9

Zah, E., Lin, M.-Y., Silva-Benedict, A., Jensen, M. C., & Chen, Y. Y. (2016). T Cells Expressing CD19/CD20 Bispecific Chimeric Antigen Receptors Prevent Antigen Escape by Malignant B Cells. *Cancer Immunology Research*, *4*(6), 498–508. https://doi.org/10.1158/2326-6066.CIR-15-0231

Zeidner JF, Vincent BG, Ivanova A, Foster M, Coombs CC, Jamieson K, Van Deventer H, Scibilia R, Blanchard L, Cassiopeia F, Gallagher S, Matson M, Pepin K, Vaught L, Vogler N, Gojo I, Luznik L, Serody JS. (2017). *Phase II Study of High Dose Cytarabine Followed By Pembrolizumab in Relapsed/Refractory Acute Myeloid Leukemia (AML)*. *130*, 1349. https://doi.org/10.1182/blood.V130.Suppl_1.1349.1349

Zhang, C., Liu, J., Zhong, J. F., & Zhang, X. (2017). Engineering CAR-T cells. *Biomarker Research*, *5*(1), 22. https://doi.org/10.1186/s40364-017-0102-y

Zhao, Z., Condomines, M., van der Stegen, S. J. C., Perna, F., Kloss, C. C., Gunset, G., Plotkin, J., & Sadelain, M. (2015). Structural Design of Engineered Costimulation Determines Tumor Rejection Kinetics and Persistence of CAR T Cells. *Cancer Cell*, *28*(4), 415–428. https://doi.org/10.1016/j.ccell.2015.09.004

Zhu, C., Anderson, A. C., Schubart, A., Xiong, H., Imitola, J., Khoury, S. J., Zheng, X. X., Strom, T. B., & Kuchroo, V. K. (2005). The Tim-3 ligand galectin-9 negatively regulates T helper type 1 immunity. *Nature Immunology*, *6*(12), 1245–1252. https://doi.org/10.1038/ni1271

ABBREVIATIONS

(p)IRF7	Phosphorylated-Interferon Regulatory Factor 7
(p)STAT1	Phosphorylated- Signal Transducer and Activator of Transcription 1
2HG	2-Hydroxyglutarate
AKT/PKB	Protein Kinase B
allo-hSCT	Allogeneic Stem Cell Transplantation
AML	Acute Myeloid Leukaemia
APC	Antigen Presenting Cells
ASXL1	Additional Sex Comb-Like 1
AZA	Azacitidine/Azacytidine
B-ALL	B Cell Acute Lymphoblastic Leukaemia
Bcl-2	B-cell Lymphoma 2
BiTE	Bi-Specific T Cell Engager
BM	Bone Marrow
BMMNC	Bone Marrow Mononuclear Cells
BPDCN	Blastic Plasmacytoid Dendritic Cell Neoplasm
BSA	Bovine Serum Albumin
BSH	Biosafety Hood
C/EBPα	CCAAT/Enhancer-Binding Protein Alpha
CAR	Chimeric Antigen Receptor
CB	Cord Blood
cCR	Composite Complete Remission
cDNA	Complementary Deoxyribonucleic Acid
CEA	Carcinoembryonic Antigen
CFU-L	Colony Forming Units- Leukaemia

CHOP	Children's Hopsital of Pensylvannia
CIK	Cytokine Induced Killer
CLL	Chronic Lymphocytic Leukaemia
CLP	Common Lymphoid Progenitor
CM	Central Memory
CMP	Common Myeloid Progenitor
CR	Complete Remission
CRi	Complete Remission with Incomplete Count Recovery
CRS	Cytokine Release Syndrome
CTLA-4	Cytotoxic T Lymphocyte Antigen-4
CXCL12	C-X-C Motif Chemokine Ligand 12
DEC	Decitibine
DLI	Donor Lymphocyte Infusion
DNA	Deoxyribonucleic Acid
DNMT	DNA Methyltransferase
DNMT3A	DNA Methyltransferase 3A
dNTP	Deoxyribose Nucleoside Triphosphate
DOT1L	DOT-1 like Histone H3K79 Methyltransferase
E	Erythrocytes
E:T	Effector to Target
E. coli	Escherichia Coli
EDTA	Ethylenediaminetetraacetic Acid
EFS	Event Free Survival
ELN	European LeukemiaNet
EM	Effector Memory
Env	Encapsulation

EZH2	Enhancer of Zeste Homolog 2
Fab	Anti-fragment Antigen Binding Fragment
FCS	Foetal Calf Serum
FDA	Food and Drug Administration
FISH	Fluorescence *In Situ* Hybridisation
FLT3	FMS-like Tyrosine Kinase 3
FMO	Fluorescence Minus One
FOXP3	Forkhead Box P3
FSC-(H)	Forward Side Scatter (Height)
G	Granulocytes
Gal-9	Galectin-9
GFP	Green Fluorescent Protein
GM-CSF	Granulocyte Macrophage-Colony Stimulating Factor
GM-CSFR	Granulocyte Macrophage-Colony Stimulating Factor Receptor
GMP	Granulocyte-Macrophage Progenitor
GO	Gemtuzumab Ozogamicin
Grb-2	Growth Factor Receptor-bound Protein 2
GVHD	Graft-Versus-Host-Disease
GvL	Graft-Versus-Leukaemia
HD	Healthy Donor
HER2	Human Epidermal Growth Factor Receptor 2
HIV	Human Immunodeficiency Virus
HLA	Human Leukocyte Antigen
HLA-DR	Human Leukocyte Antigen DR Isotype
HMAs	Hypomethylating Agents
HOX	Homeobox

HPC	Haematopoietic Progenitor Cell
HSC	Haematopoietic Stem Cells
iCasp9	Inducible Caspase 9
ICOS	Inducible T Cell Co-Stimulator
IDH1/2	Isocitrate Dehydrogenase 1/2
IDO	Indolamine 2,3, Dioxygenase
IFN-γ	Interferon Gamma
Ig	Immunoglobulin
IL	Interleukin
IL-3R	Interleukin-3 Receptor
IRF(7)	Interferon Regulatory Factor (7)
ICOSL	Inducible T Cell Co-Stimulator Ligand
ITAMs	Immune-receptor Tyrosine-based Activation Motifs
ITD	Internal Tandem Duplication
JAK2	Janus Kinase 2
JM	Juxtamembrane
LAA	Leukaemia Associated Antigen
LAG-3	Lymphocyte-Activation Gene-3
LAMP-1/CD107a	Lysosomal-Associated Membrane Protein 1
LB	Luria Broth
LDA	Live Dead Aqua
LeY	Lewis Y
LF	Long Fragment
LIC	Leukaemia-Initiating Cells
LSC	Leukaemic Stem Cells
LTR	Long Terminal Repeat

M	Monocytes
mAb	Monoclonal Antibody
MDACC	MD Anderson Cancer Centre
MDM2	Mouse Double Minute 2 Homologue
MDS	Myelodysplastic Syndrome
MDSC	Myeloid Derived Suppressor Cells
MEP	Megakaryocyte-Erythrocyte Progenitor
MHC	Major Histocompatibility Complex
MIP1α/β	Macrophage Inflammatory Protein 1 alpha/beta
MLFS	Morphologic Leukaemia Free State
MLL	Mixed Lineage Leukaemia
MOI	Multiplicity of Infection
MPP	Multipotent Progenitors/Transient-amplifying Multipotent Cells
MRD	Minimal Residual Disease
mRNA	Messenger Ribonucleic Acid
MSKCC	Memorial Sloan Kettering Cancer Centre
NCI	National Cancer Institute
NGS	Next Generation Sequencing
NHL	Non-Hodgkins Lymphoma
NK	Natural Killer Cell
NKG2D	Transmembrane Natural Killer Group 2D
NKG2DL	Transmembrane Natural Killer Group 2D Ligand
NPM1	Nucleophosmin 1
NTD	Non-Transduced
OPP	Oligo-Potent Lineage-Restricted Progenitors
ORR	Overall Response Rate

OS	Overall Survival
P	Platelets
PB	Peripheral Blood
PBMC	Peripheral Blood Mononuclear Cells
PCR	Polymerase Chain Reaction
PD-1	Programmed Cell Death-1
PD-L1	Programmed Death-Ligand 1
pDCs	Plasmacytoid dendritic cells
PGE_2	Prostaglandin E_2
PI3K-Akt	Phosphatidylinositol 3-Kinase/Protein Kinase-B
PML-RARA	Promyelocytic Leukaemic/Retinoic Acid Receptor Alpha
PMSF	phenylmethylsulfonyl fluoride
PTD	Partial Tandem Duplication
PTEN	Phosphatase and Tensin Homologue
PTPN1	Tyrosine-Protein Phosphatase Non-Receptor Type 1
PVDF	Polyvinylidene Fluoride
qPCR	Quantitative Polymerase Chain Reaction
r/r	Relapsed/Refractory
RAD21	Double Strand Break Repair Protein 21
Ras-MAPK	Ras-Mitogen Activated Protein Kinase
RetroNectin	Recombinant Human Fibronectin Fragment
Rev	Reverse Transcriptase
RFS	Relapse Free Survival
RIN	RNA Integrity Number
RIPA	Radioimmunoprecipitation Assay Buffer

RNA	Ribonucleic Acid
RT	Room Temperature
RUNX1/RUNX1T1	Runt-related Transcription Factor 1/ RUNX1 Translocation Partner 1
SACRB	South Australian Cancer Research Biobank
scFv	Single-Chain Fragment Variable
SEB	Staphylococcus aureus, Enterotoxin Type B
SEM	Standard Error of the Mean
SF	Short Fragment
SPECT	Single Photon Emission Tomography Imaging
SSC-(A)	Side Scatter (Area)
STAG2	Stromal Antigen-2
STAT	Signal Transducer and Activator of Transcription
TAA	Tumour-Associated Antigen
TCR	T Cell Receptor
TDEM	Terminally Differentiated Effector Memory
T_{eff}	T Effector Cell
TET2	Tet Methylcytosine Dioxygenase 2
TGF-β	Transforming Growth Factor Beta
T_h	T Helper Cell
TIM-3	T Cell Immunoglobulin Doman and Mucin Doman 3
TKD	Tyrosine Kinase Domain
TKI	Tyrosine Kinase Inhibitors
TM	Transmembrane Domain
T_{mem}	T Memory Cell
TNF	Tumour Necrosis Factor

TNFR	Tumour Necrosis Factor Receptor
TOX	Thymocyte Selection-Associated High Mobility Group Box Factor
TP	Tumour Suppressor
TRAF	Tumour Necrosis Factor Receptor-Associated Factor
T_{reg}	T Regulatory Cell
TRUCK	CAR T Cell Redirected for Universal Cytokine Killing
UPENN	University of Pennsylvania
WCF	White Cell Fluid
WHO	World Health Organisation
WT	Wildtype
α-KG	Alpha Ketoglutaric Acid

LIST OF TABLES

TABLE 1. 1. CLINICAL SIGNIFICANCE OF FREQUENT AND RECURRENT GENE MUTATIONS IN AML. ... 12
TABLE 1. 2. ELN CURRENT RISK STRATIFICATION OF MOLECULAR, GENETIC AND CYTOGENETIC ALTERATIONS. ... 14

TABLE 2. 1. HD AND AML IMMUNE PHENOTYPING STAINING PANEL ... 46
TABLE 2. 2. PATIENT CHARACTERISTICS OF THE PRIMARY AML BM SAMPLES. ... 47
TABLE 2. 3. COMPARISON OF CD123 EXPRESSION ON BLASTS AND STEM CELLS IN POOR RISK CYTOGENETIC AML PATIENTS. ... 52

TABLE 3. 1. HEALTHY DONOR T CELL ISOLATION PURITY CHECK STAINING PANEL ... 72
TABLE 3. 2. SERIAL TIME POINTS FOR IMMUNOPHENOTYPIC EXHAUSTION ANALYSIS OF CAR T CELLS. ... 76

TABLE 6.2.1: SUPPLIER DETAILS OF SPECIALISED REAGENTS, REAGENT KITS, AND CONSUMABLES ... 214
TABLE 6.2.2: SUPPLIER DETAILS OF GENERAL CONSUMABLES USED ... 217
TABLE 6.2.3: FLUOROCHROME-CONJUGATED FLOW CYTOMETRY ANTIBODIES ... 218
TABLE 6.2.4: SUPPLIER DETAILS OF REAGENTS AND KITS USED FOR CD123 CAR T CELL CLONING ... 220

TABLE 6.3.1: RECIPES OF ALL SOLUTIONS, BUFFERS, AND CELL CULTURE MEDIA USED ... 221

TABLE 6.6.1: LIST OF INSTRUMENTS AND EQUIPMENT USED ... 226

TABLE 6.7.1: LIST OF SOFTWARE PROGRAMS USED ... 227

LIST OF FIGURES

FIGURE 1. 1. THE ABERRANT TRANSFORMATION OF HAEMATOPOIETIC STEM CELLS TO LEUKAEMIC STEM CELLS. 8
FIGURE 1. 2. FUNCTIONAL CATEGORIES OF GENES FREQUENTLY MUTATED IN ACUTE MYELOID LEUKAEMIA. 11
FIGURE 1. 3. THE DIFFERENCE BETWEEN ENDOGENOUS TCR AND CAR T CELL STRUCTURE. 28
FIGURE 1. 4. CHIMERIC ANTIGEN RECEPTORS CURRENTLY UNDER ACTIVE INVESTIGATION. 30
FIGURE 1. 5. POTENTIAL TARGETABLE ANTIGENS FOR CAR T CELL THERAPY IN AML. ANTIGENS ARE EITHER RECENTLY IDENTIFIED AND/OR UNDER INVESTIGATION PRE-CLINICALLY AND CLINICALLY. 36

FIGURE 2. 1. REPRESENTATIVE FLOW CYTOMETRY GATING STRATEGY USED TO EVALUATE CD123 EXPRESSION ON AML AND HD STEM AND PROGENITOR CELLS. 49
FIGURE 2. 2. DIFFERENTIAL EXPRESSION OF CD123 IN AML PATIENTS COMPARED TO HD. 50
FIGURE 2. 3. DIFFERENTIAL EXPRESSION OF CD123 IN AML PATIENTS COMPARED TO HD ON BULK MYELOID CELLS. 51

FIGURE 3.1.THE ANTI-CD123 (CSL362) HUMANISED SCFV AMINO ACID SEQUENCE INCORPORATED INTO THE THIRD GENERATION CAR T CELL EXPRESSION CONSTRUCT. 62
FIGURE 3.2. SCHEMATIC REPRESENTATION OF THE PPHLV-A LENTIVIRAL EXPRESSION VECTOR. 63
FIGURE 3.3. THE ANTI-CD123 (CSL362) HUMANISED SCFV AMINO ACID SEQUENCE INCORPORATED INTO THE THIRD GENERATION CAR T CELL EXPRESSION CONSTRUCT. 63
FIGURE 3.4. EXEMPLAR SCHEMATIC REPRESENTATION OF THE CD28-OX40-LF CAR INTRODUCED INTO THE INTERMEDIATE PENTRY VECTOR VIA THE AATII AND XBAI RESTRICTION SITES. 66
FIGURE 3.5. SCHEMATIC REPRESENTATION OF THE ANTI-CD123 (CSL362) CD28-OX40 SF (TOP) OR LF (BOTTOM) CARS CLONED INTO THE PPHLV-A EXPRESSION VECTOR VIA THE ECORV RESTRICTION SITE. 67
FIGURE 3.6. SCHEMATIC REPRESENTATION OF THE ANTI-CD123 (CSL362) CD28-4-1BB SF (TOP) OR LF (BOTTOM) CARS CLONED INTO THE PPHLV-A EXPRESSION VECTOR VIA THE ECORV RESTRICTION SITE. 69
FIGURE 3.7. SUB-CLONING OF THE CD123–CD28-41BB CAR CONSTRUCT INTO THE PENTRY LENTIVIRAL EXPRESSION VECTOR. 80
FIGURE 3.8. CLONING OF THE CD123-CD28-OX40 SCFV CONSTRUCT INTO THE PPHLV-A LENTIVIRAL EXPRESSION VECTOR. 80
FIGURE 3.9. ESTABLISHMENT OF OPTIMAL CONDITIONS FOR EFFICIENT AND HIGH YIELD LENTIVIRUS PRODUCTION USING THE CD123-CD28-OX40-SF CAR PLASMID. 83
FIGURE 3.10. TRANSDUCTION EFFICIENCY OF PRIMARY T CELLS WITH FRESH OR CRYOPRESERVED VIRUS SUPERNATANT FROM THE CD123-CD28-OX40-SF CAR PLASMID. 84
FIGURE 3.11. CONFIRMATION OF OPTIMAL VIRUS CONCENTRATION METHODOLOGY TO GENERATE PRIMARY T CELLS HARBOURING THE CD123-CD28-OX40-SF CAR PLASMID WITH GOOD EFFICIENCY. 86
FIGURE 3.12. OPTIMAL CONDITIONS FOR PRIMARY T CELL TRANSDUCTIONS USING THE CD123-CD28-OX40-SF CAR PLASMID. 88
FIGURE 3.13. DETERMINING THE OPTIMAL VIRAL MULTIPLICITY OF INFECTION (MOI) FOR CONSISTENT DELIVERY OF CAR TRANSGENE INTO PRIMARY T CELLS. 89
FIGURE 3.14. GENERATION AND PRODUCTION OF CD123 CAR T CELLS. 90
FIGURE 3.15. DEGRANULATION OF CD123 CAR T CELLS HARBOURING CD28-OX40 CO-STIMULATORY MOTIFS IN THE PRESENCE OF CD123$^+$ AML CELLS. 92
FIGURE 3.16. DEGRANULATION OF CD123 CAR T CELLS HARBOURING CD28-4-1BB CO-STIMULATORY MOTIFS IN THE PRESENCE OF CD123$^+$ AML CELLS. 93

Figure 3.17. The proliferative capacity of CD123 CAR T cells harbouring CD28-OX40 co-stimulatory motifs in the presence of CD123$^+$ AML cells. 94
Figure 3.18. The proliferative capacity of CD123 CAR T cells harbouring CD28-4-1BB co-stimulatory motifs in the presence of CD123$^+$ AML cells. 95
Figure 3.19. The expression of immune exhaustion markers of the third generation CD123 CAR T cells in the absence or presence of CD123$^+$ AML cells. 97
Figure 3.20. The effect of the third generation CD123 CAR T cells to lyse the CD123$^+$ KG1a AML cell line. 99
Figure 3.21. In vitro cytokine production by CD123-CD28-OX40-SF CAR T cells following 24h co-culture with CD123$^+$ AML cells. 101
Figure 3.22. In vitro cytokine production by CD123-CD28-OX40-LF CAR T cells following 24h co-culture with CD123$^+$ AML cells. 102
Figure 3.23. In vitro cytokine production by CD123-CD28-4-1BB-SF CAR T cells following 24h co-culture with CD123$^+$ AML cells. 103
Figure 3.24. CD123-CD28-OX40-SF CAR T cells specifically target and lyse primary AML BMMNCs. 104
Figure 3.25. Effect of CD123-CD28-OX40-SF CAR T cells on leukaemic progenitor cell colony formation. 105

Figure 4. 1. Molecular and cellular mechansims of Azacitidine. 113
Figure 4. 2. Azacitidine treatment leads to re-activation of key immunogenic markers on human HL60 cells. 198
Figure 4. 3. Evidence of immunogenic markers upregulated at the protein level on MOLM-13 AML cells in response to Azacitidine. 199
Figure 4. 4. Analysis of regulatory CD4$^+$ T cells in the bone marrow and peripheral blood of MOLM-13 AML xenograft mice treated with CTLA-4^{negative} or CTLA-4^{positive} CD123 CAR T cells. 201
Figure 4. 5. Exogenous application of Azacitidine does not promote inhibitory CD123 CAR T cells in vitro. 203

Figure 6.1. Schematic representation of the anti-CD123 (CSL362) CD28-41BB-LF CAR DNA sequence. The DNA sequence first includes the ScFv, a linker sequence, the IgG4 extended hinge, the CD28 and 4-1BB co-stimulatory signalling domains, and finally the CD3ζ. 211
Figure 6.2. Schematic representation of the anti-CD123 (CSL362) CD28-41BB-SF CAR DNA sequence. The DNA sequence first includes the ScFv (not shown, but represented in Figure 6.1), a linker sequence, the IgG4 (short) hinge, the CD28 and 4-1BB co-stimulatory signalling domains, and finally the CD3ζ. 212
Figure 6.3. Schematic representation of the anti-CD123 (CSL362) CD28-OX40-SF CAR DNA sequence. The DNA sequence first includes the ScFv (not shown, but represented in Figure 6.1), a linker sequence, the IgG4 (short) hinge, the CD28 and OX40 co-stimulatory signalling domains, and finally the CD3ζ. 212
Figure 6.4. Schematic representation of the anti-CD123 (CSL362) CD28-OX40-LF CAR DNA sequence. The DNA sequence first includes the ScFv (not shown, but represented in Figure 6.1), a linker sequence, the IgG4 extended hinge, the CD28 and OX40 co-stimulatory signalling domains, and finally the CD3ζ. 213